Investigating the roles of neuropeptides in the development of the sea urchin, *Strongylocentrotus purpuratus*

Natalie Jane Wood

Centre for Life's Origins and Evolution
Research Department of Genetics, Evolution and Environment
University College London

Submitted for the Degree of Doctor of Philosophy

December 2020

Declaration of Ownership

I, Natalie Jane Wood, confirm that the work presented in this thesis is my own. Where information has been derived from other sources, I confirm that this have been indicated in the thesis.

Abstract

Neuropeptides are ancient signalling molecules that bind to receptors on target cells to induce a variety of growth, metabolic, reproductive and behavioural responses. At least 30 neuropeptide signalling systems were present in the common ancestor of bilaterians, and therefore neuropeptide signalling systems offer a good opportunity to characterise neuronal cell types and help determine the evolution of neuronal cell types and nervous systems. 38 neuropeptide precursor (NP) genes have so far been identified in the invertebrate deuterostome, the purple sea urchin, *Strongylocentrotus purpuratus*, but their function is largely unknown.

Here I molecularly characterise and investigate the roles of NP signalling systems in the *S. purpuratus* embryo and larva. I first present the spatio-temporal data for NP genes and G-protein coupled receptors (GPCRs) genes during the development of *S. purpuratus*. QPCR and transcriptome data have revealed that almost all of these NP genes are expressed in the late larval stage, when cells differentiate. ISH data of these NP genes has revealed at least nine distinct populations of peptidergic neurons and showed that the sea urchin larval nervous system is more neurochemically complex than previously thought. Interestingly, some NP genes are also expressed in the pre-gastrula phase of embryogenesis, before cells differentiate. These early expressing NP genes are expressed in undifferentiated ectodermal and endodermal cells, suggesting that these signalling molecules may have a novel developmental role as well as a neuronal role.

I also optimised CRISPR/Cas9 genome-editing in the sea urchin and used CRISPR/Cas9 and morpholino oligonucleotides to perturb the expression of an NP gene *Sp-Thyrotropin releasing hormone* (*Sp-TRH*) and its proven receptor. Here I show that the TRH neuropeptide signalling system acts as a local ectodermal cue, to regulate larval skeleton growth through VEGF and FGF signalling. This is the first study to investigate the roles of TRH signalling in a marine invertebrate larvae, which together with previous studies in adults reveals that the TRH signalling system is an ancient regulator of growth.

Statement of Impact

Nervous systems are essential for most animal life and the diversity of nervous systems that exist are hugely fascinating to study. The presence of a nervous system, in any form, allows an organism to interact and to sense and respond to an environment in an appropriate manner.

Investigating the molecular identity of the sea urchin larval nervous system is valuable to the study of evolutionary developmental biology for several reasons. I reveal the chemical complexity of these animals and embark upon understanding the function of each different neuronal type in the sea urchin. Moreover, by making comparisons with diverse nervous systems in other organisms we can begin to trace neuronal cell type evolution and set about understanding when different cell types emerged. Furthermore, these echinoderms are both invertebrates and deuterostomes and so they have shared characteristics of both groups of animals. Echinoderms can therefore help to provide insights into the evolutionary history of nervous systems in bilaterian animals.

Comparing the neurochemical complexity in a sea urchin larva to other organisms wonderfully illustrates how morphological distinct animals use many of the same genes for similar functions. In a wider context, research in sea urchin larvae, as well as other invertebrates, sheds more light on uncommon animals and with this increased awareness, research in sea urchin larvae fosters a greater appreciation for the marvel that is life on earth.

Acknowledgments

I consider myself extremely fortunate to have had the opportunity to pursue curiosity-driven research over the past few years. As with every PhD there were challenges along the way, but my passion for science has undoubtably grown and wherever I go in the future I will take that love of science with me.

There are many people who made my PhD research possible and contributed to my enjoyment of it. I would like to thank my primary supervisor Paola Oliveri for the valuable help, guidance and opportunities that she has given me. And for teaching me how to make proper Italian coffee! She is an inspiring female scientist and I have very much enjoyed working with her over the past few years. I would also like to thank my secondary supervisor Maurice Elphick for his invaluable neurobiology expertise and advice. I have very much enjoyed participating in yours and Paola's successful London Echinoderm (LEN) meeting's and watching it expand over the past few years – I hope to remain a part of this wonderful community! I am also very grateful to the BBSRC for funding my PhD research and to LiDo for organising a brilliant PhD program.

I would like to thank the past and current members of the Oliveri, Telford and Ziheng labs for their cherished friendships: Paschalia Kapli, Tomas Flouri, Xiyun Jiao, Daniel Leite, Johannes Girstmair, Jeff Thompson, Hugh Carter, Helen Robertson, Anna Czarkwiani, the board game enthusiast Steven Müller and my fun conference buddy Irepan Salvador-Martínez. In particular, I would like to thank my lovely office buddies and beautiful friends, Anne Zakrzewski and Laura Piovani. Thank you for the daily help, support and wonderfully amusing chit-chat. I thank Luis Alfonso Yañez Guerra, Nayeli Escudero Castelan and Dean Semmens for their help in Maurice's lab. I thank all the undergraduates and masters students for the chance to teach and help me become a better teacher, and for their friendship. I would like to thank our helpful lab technicians Wendy Hart, Farrell Mackenzie and Sheida Rezaee for their

assistance. I would also like to thank our collaborators in the Arnone lab, I really enjoyed working with you all, especially at our EDEN lab retreats.

I thank my friends and family who have let me waffle on about my beautiful larvae. I would like to thank my best friend Anna Haddelsey for listening to my practice talks, reading my work, and getting me through the final stages of thesis writing. Finally, I would like to thank my amazing mum and dad for their incredible encouragement and constant support throughout all my endeavours and my brother for his beautiful sense of humour that always makes me smile.

"Neurobiology in other phyla is so often more of the same – not so in Echinodermata" Cobb (1987) Neurobiology of the echinodermata In: Ali MA, editor. Invertebrate Nervous systems. New York: Plenum Press. 483-525

"If your car isn't showing wear, you're not pushing it hard enough" Josh Trin, Automobiles

Table of Contents:

Table of Tables:

Table of Figures:

Abbreviations

AbV – Aboral view

AO – apical organ

AV – aboral view

BR – body rod

DAPI – 4,6-Diamidino-2-phenylindole

DIC – Differential Interference contrast

DMSO – Dimethyl sulfoxide

DSB – double strand break

EdU – Ethynyl-2’ deoxyuridine

FASW – filtered artificial seawater

FISH – fluorescence *in situ* hybridization

GPCR – G protein coupled receptor

GRN – gene regulatory network

hpf – hours’ post fertilisation

IHC - immunohistochemistry

ISH – *in situ* hybridisation

LV – lateral view

MABT – maleic acid buffer

NP – neuropeptide precursor

NS – nervous system

OD – oral distal

OT – oral transverse

OV – oral view

PBS – phosphate buffered saline

PCR – polymerase chain reaction

PFA – paraformaldehyde

PO – post oral

QPCR – quantitative polymerase chain reaction

RT – room temperature

sgRNA – specific guide RNA

TF – transcription factor

Preface

As an evolutionary developmental biologist, I am intrigued by the huge diversity of organisms that exist on planet earth. My passion for biology came from my fascination with how single cells can develop into such complex and diverse organisms. Nervous systems are arguably one of the best characteristics of animals to illustrate this wonderful diversity. Hence my scientific interest focuses on understanding the **evolution and development of diverse nervous systems**. This field has already gripped the interest of many prominent researchers, leading to almost 2 million publications (Google Scholar). Whilst answering many questions, research has undoubtably revealed many more questions to be answered, making the present an exciting time to be working in this field.

I begin my research with the investigation of nervous system development in an invertebrate deuterostome, the purple sea urchin *Strongylocentrotus purpuratus*. Specifically, I focus on the characterisation and function of neuropeptide signalling molecules in the *S. purpuratus* embryo and larva.

In the introduction I begin by outlining what is known about neuropeptide signalling systems and the evolution and development of nervous systems. I discuss the benefits of using neuropeptide signalling systems to characterise nervous systems, particularly larval nervous systems. I consider the importance of using echinoderms for evolutionary developmental biology studies. Finally, I describe how these topics were incorporated into my research and I present the main aims of my PhD research.

Chapter 1 Introduction

1.1 Neuropeptides are ancient signalling molecules

Neuropeptides are ancient neuronal signalling molecules that are found throughout metazoans. There are many NP signalling systems present in bilaterian phyla and at least thirty of these were present in the urbilaterian common ancestor of the Bilateria (Elphick *et al.,* 2018) (Figure 1.1). Some neuropeptides have also been identified in non-bilaterian metazoans (Anctil, 2009; Roch and Sherwood, 2014). Interestingly, neuropeptide-like proteins have even been identified in placozoans, a group of animals with no neurons (Smith *et al.,* 2014; Srivastava *et al.,* 2008), suggesting that neuropeptides predate the origin of nervous systems. However, homologues of the majority of bilaterian neuropeptides and their receptors have not been found in non-bilaterians (Jékely, 2013; Krishnan and Schiöth, 2015; Srivastava *et al.,* 2008).

Neuropeptides often bind to rhodopsin-type and secretin-type G-protein coupled receptors (GPCRs) on target cells and induce a variety of growth, metabolic, reproductive and behavioural responses. They can act as neurohormones, neurotransmitters and neuromodulators (Figure 1.4) (Burrows, 1996). Examples of neuropeptides relevant to this PhD thesis are Thyrotropin-releasing hormone (TRH) and pedal peptides. Pedal-peptides were first discovered in the mollusc *Apylsia californica* for their role in regulating locomotor activity, specifically foot muscle activity and ciliary beating in foot epithelium (Hall and Lloyd, 1990; Willows *et al.,* 1997). Pedal-peptides have since been identified in other invertebrates, including other protostomes (nematodes and annelids) and deuterostomes (echinoderms) (Conzelmann *et al.,* 2013; Cornelia I., 1998; Lin *et al.,* 2017, 2018; Rowe and Elphick, 2012; Semmens *et al.,* 2016). However, pedal-peptide receptors have not yet been identified in any species. TRH has been well characterised in vertebrates and is involved in many physiological processes including growth, development, metabolism, body temperature and heart rate (Lovejoy, 2005). Sequencing of the sea urchin *S. purpuratus* genome led to the discovery of the first invertebrate TRH-type precursor (Figure 1.3) (Rowe and Elphick, 2012). Recently, the first functional study of TRH-type signalling in an invertebrate revealed that TRH-type neuropeptides have

a conserved role in the growth of the nematode, *Caenorhabditis elegans* (Sinay *et al.,* 2017b). TRH-type neuropeptides and TRH-type receptors have also been identified in most bilaterian phyla, indicating that this signalling system was present in Urbilateria (Figure 1.1).

G protein coupled receptors (GPCRs) are a large and diverse group of cell surface receptors, which bind extracellular molecules and activate intracellular responses. There are several classes of GPCRs, including the rhodopsin-type and secretin-type receptors which neuropeptides often bind. GPCRs consist of seven transmembrane domains, meaning they pass through the cell membrane seven times. As their name suggests, GPCRs interact with G proteins in the cell membrane. When a ligand binds, the GPCR undergoes a conformational change that alters the interaction between the GPCR and the G proteins. The inactive G protein heterodimers separate into active Gα and Gβψ subunits. The active G protein subunits can then initiate an extensive range of intracellular responses, which are responsible for inducing a huge variety of responses (O'Connor and Adams, 2010; Pfleger et al., 2019). For example, the mammalian TRH receptors couple Gαq/Gα11 proteins, and upon TRH binding the active Gαq/Gα11 proteins typically trigger the phospholipase C (PLC)/ protein kinase C (PKC) signalling pathway (Gershengorn and Osman, 1996; McCudden et al., 2005).

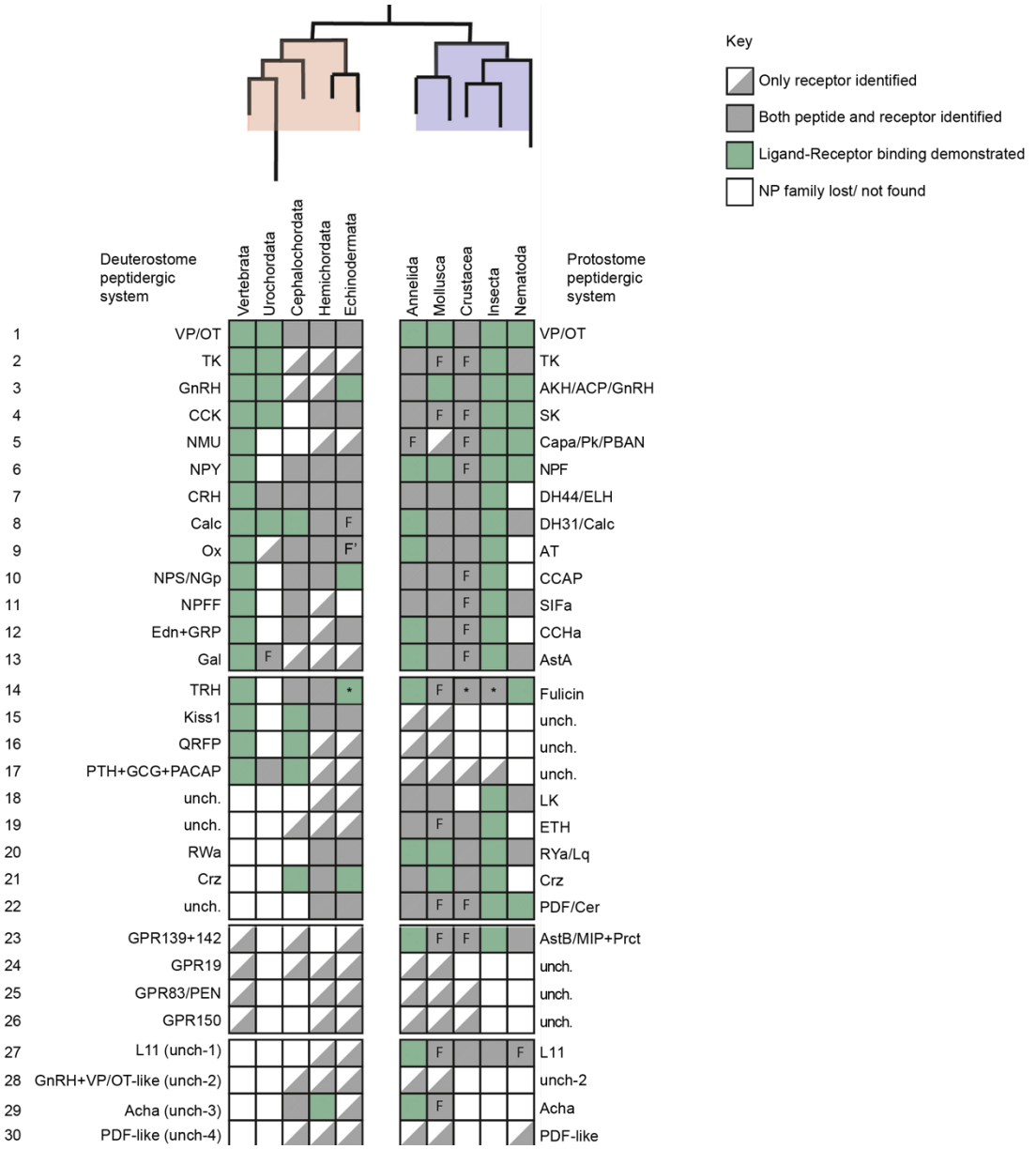

Figure 1.1 Ancestral bilaterian neuropeptide signalling systems

This figure is adapted from (Elphick *et al.,* 2018; Mirabeau and Joly, 2013). The occurrence of 30 bilaterian neuropeptide signalling systems in different taxa is shown, with deuterostomian phyla or sub-phyla (pink) shown on the left side, and protostomian phyla/classes shown on the right side (light blue). Abbreviated names of neuropeptide signalling systems are used (see appendix Table 8.1 for full names). Inclusion of an asterisk in a square indicates that additional peptide ligand and/or receptors were identified in this research. A full green square indicates that, for at least one member of that taxonomic group, binding between a peptide and its receptor has been demonstrated experimentally. Inclusion of the letter F in a grey square indicates that experimental insights into the physiological function(s) of the neuropeptide have been obtained. F' physiological function(s) have been reported since Elphick at al., 2018. Data supporting the conclusions shown here are from papers listed in Supplementary Table 1 in Elphick at al., 2018 and (Odekunle *et al.,* 2019).

TRH activating TRHR is the first step in the thyroid hormone (TH) signalling pathway. (See Figure 1.2 for a detailed description of the pathway). Mutations in genes encoding enzymes involved in TH synthesis are known to cause many defects in vertebrates, among which are skeletal defects (Bassett and Williams, 2016b). Currently, little is known about the TH signalling pathway present in invertebrates. Taylor and Heyland showed that exogenous thyroid hormones can accelerate skeletogenesis in the sea urchin larva (Taylor and Heyland, 2018). Furthermore, some genes encoding enzymes involved in TH synthesis have been found identified in invertebrates (Wu *et al.,* 2007). For example, a putative thyroid hormone receptor and thyroid peroxidase have been found in *S. purpuratus* (Heyland *et al.,* 2006; Sodergren *et al.,* 2006). Therefore, it has been hypothesised that marine invertebrates use both endogenous and exogenous sources of TH (Heyland, 2005; Taylor and Heyland, 2018). Further investigation is needed to determine if invertebrates have a functional TH signalling pathway.

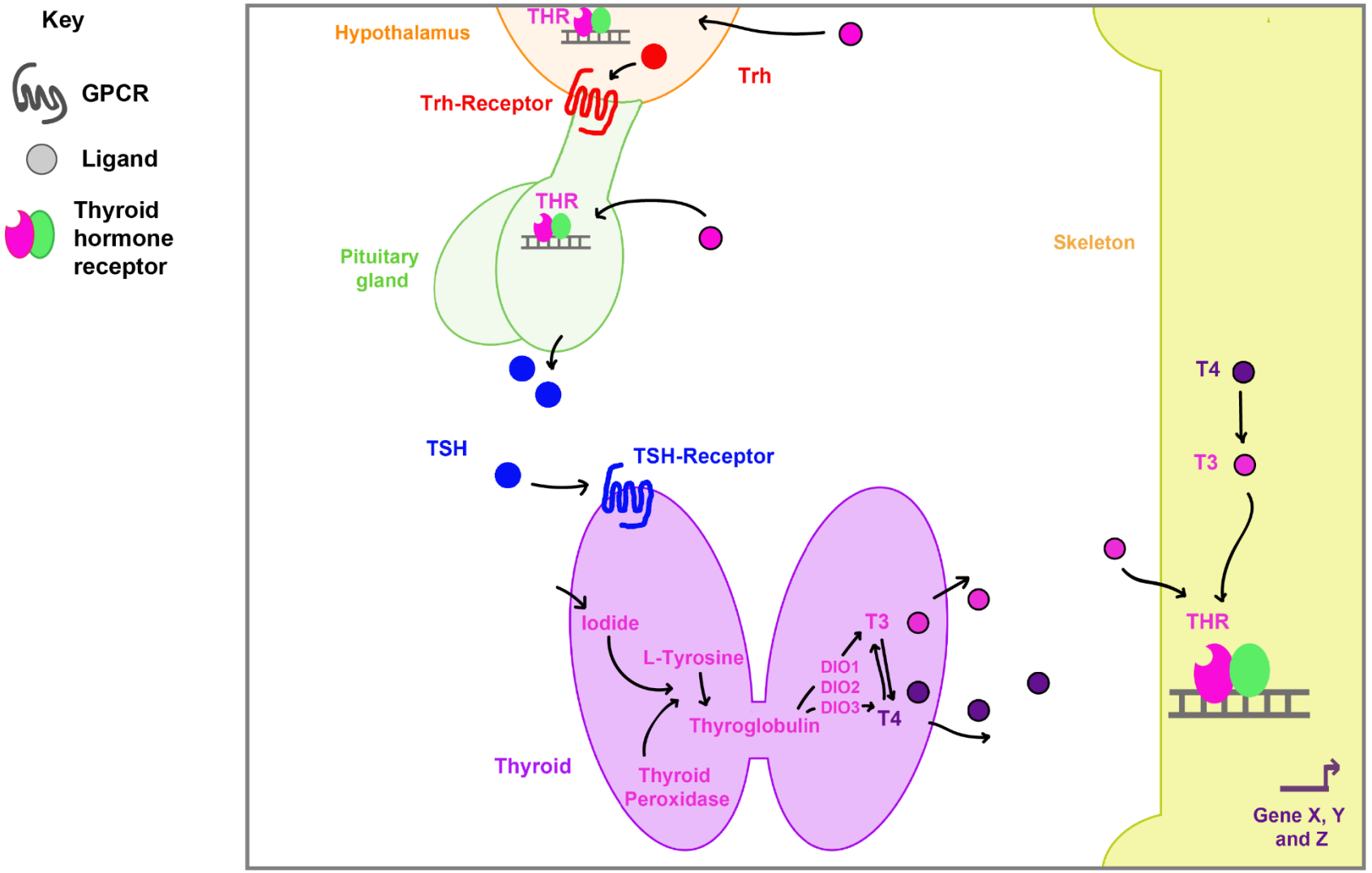
Key
GPCR
Ligand
Thyroid hormone receptor
Hypothalamus
THR
Trh
Trh-Receptor
THR
Pituitary gland
Skeleton
T4
T3
TSH
TSH-Receptor
Iodide
L-Tyrosine
Thyroglobulin
DIO1
DIO2
DIO3
T3
T4
THR
Thyroid
Thyroid Peroxidase
Gene X, Y and Z

Figure 1.2 An illustration of the thyroid hormone signalling pathway in mammals

1) TRH (red circle) is produced in the hypothalamus and binds to a TRH-Receptor (red) in the pituitary gland. 2) This stimulates the release of TSH (blue circle) which travels through via blood to the thyroid gland to bind to a TSH-Receptor (blue). 3) Iodide is taken into the thyroid gland by a sodium iodide cotransporter (SLC5A5). 4) A thyroid peroxidase causes the oxidation of iodide to the unstable iodine. 5) Iodine reacts with L-tyrosine residues on the protein thyroglobulin. 6) Iodothyronine deiodinases, which are peroxidase enzymes, catalyse the activation and inactivation of thyroxine (T4) and triiodothyronine (T3). 7) T3 (pink circle) and T4 (purple circle) are released into the blood and travel around body to exert their effects by binding to thyroid hormone receptors in target cells. 8) Thyroid hormone receptors also bind to genes encoding TRH and TSH to inhibit their transcription and, thus create a negative feedback loop to control the levels of thyroid hormones (Dale Abel *et al.,* 2001).

Neuropeptides are produced from larger neuropeptide precursor (NP) proteins (sometimes referred to as a prohormone). The NP proteins consist of a signal peptide at the N-terminal end, repetitive neuropeptide sequences (these can vary in number and sequence), and mono/di/tri-basic cleavage sites that surround these neuropeptide sequences (Figure 1.3) (Douglass *et al.,* 1984; Steiner, 1998). Mature neuropeptides are cleaved from the NP protein, post-translationally modified and transported out of the cell, via vesicles to bind to GPCRs on target cells. These cleaved neuropeptides can range in length from 3 to 30 amino acids in length. An example of a short peptide is the *H. sapiens* TRH, which is characterised by a QHP tripeptide sequence (Wilber *et al.,* 1992). Post-translational modifications such as N-terminal pyroglutamation and C-terminal amination (Eipper *et al.,* 1992) can also occur to alter the structure of the peptide, as exemplified by the mature TRH peptide – pyroGlu-His-Pro-amide (Figure 1.3). Once released, peptides travel a range of distances, from travelling to the next cell to travelling to cells on the opposite side of the organism (Figure 1.4). Mature neuropeptides acting as neurotransmitters are released from the neuron at a synapse to affect one or a few cells nearby. Alternatively, neuropeptides acting as neurohormones or neuromodulators are released from any part of the neuron and can affect local or widespread cells. The difference between neurohormones and neuromodulators is in the distance of target cells, with neurohormones generally exerting their effects on more distant targets (Figure 1.4). Signalling molecules have also been proposed to act by intracrine

signalling, where extracellular surface proteins act intracellularly either within target cells or within their cells of synthesis. They bind to receptors intracellularly and induce a signalling cascade (Re and Cook, 2006) (Figure 1.4).

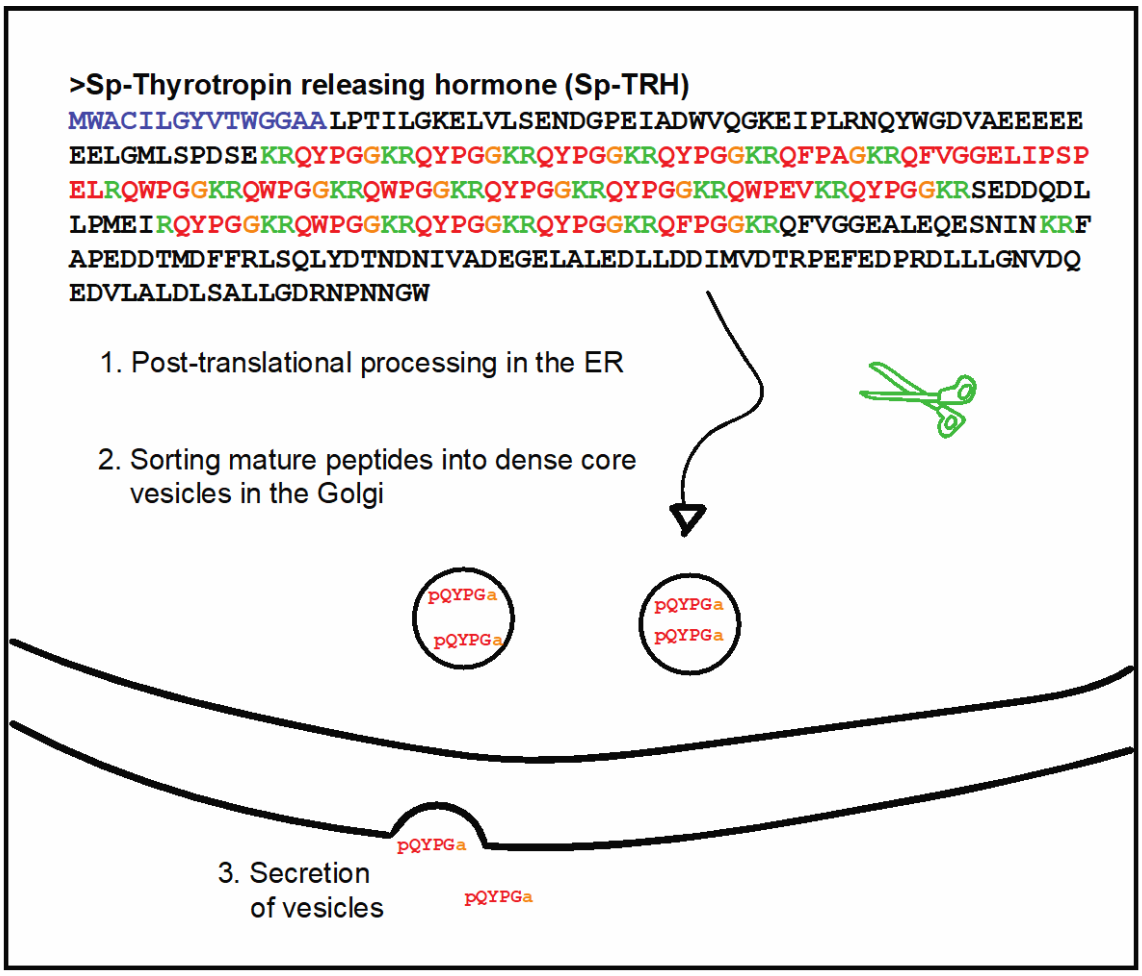

Figure 1.3 Processing of a neuropeptide precursor (NP) protein

Top) Sp-Thyrotropin-releasing hormone (Sp-TRH) neuropeptide precursor (NP) amino acid sequence with colour-coding parts. Signal peptide (blue), repetitive peptide sequences (red), C-terminal glycine residues that are putative substrates for amidation (orange) and mono/di-basic cleavage sites (green). Bottom) An illustration of mature TRH peptides cleaved, post-translational modified (conversion of N-terminal glutamine (Q) to pyroglutamate (pQ) and conversion of C-terminal glycine to an amide group (amidation)), sorted into dense core vesicles and secreted.

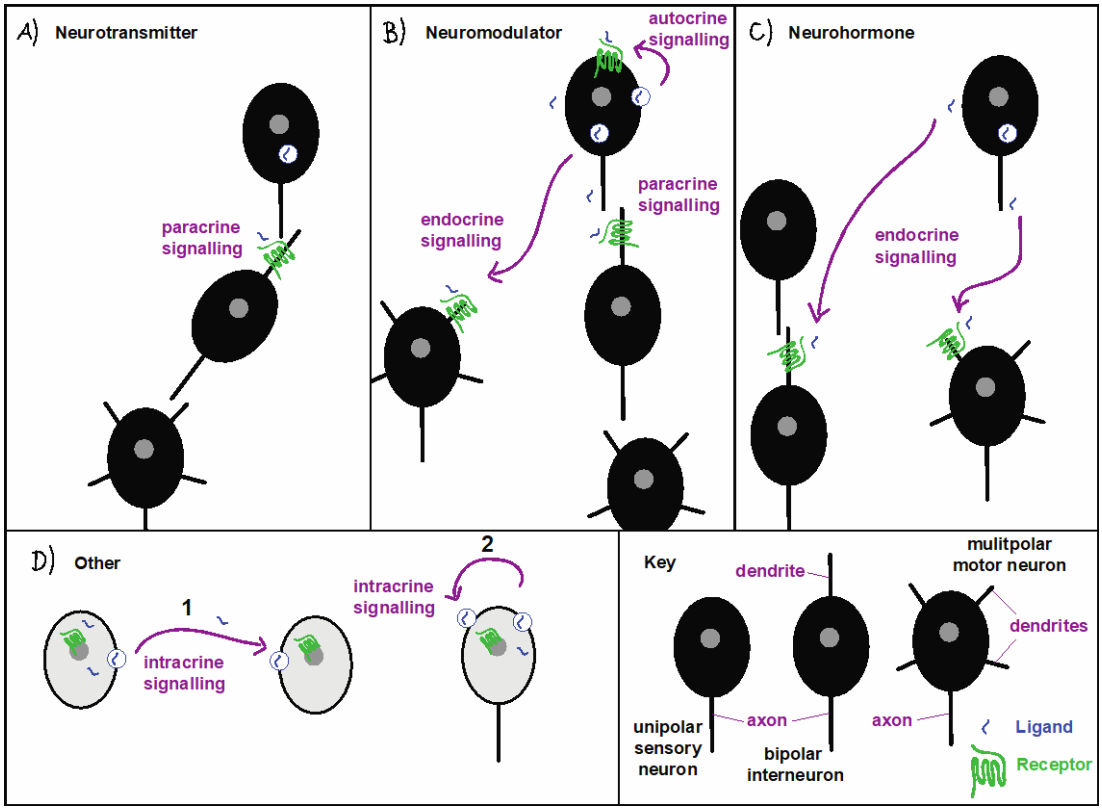

Figure 1.4 Peptidergic signalling

Peptidergic signalling occurs in a variety of ways. Neuropeptides can act as neurotransmitters, neuromodulators and neurohormones. A) Neurotransmitters are released at a synapse to affect one of few cells (paracrine signalling) nearby by changing their membrane potential. B) Neuromodulators are released from any part of the neuron and can affect local (autocrine or paracrine signalling) or widespread cells (endocrine signalling). C) Neurohormones are released from any part of the neuron into the haemolymph or equivalent and may therefore exert its effect of distant cells (endocrine signalling). D) Neuropeptide have been proposed to act by intracrine signalling where extracellular signalling proteins act intracellularly either within target cells (1) or within their cells of synthesis (2).

Neuropeptides have been functionally characterised in adult echinoderms, molluscs and crustaceans (See boxes with the letter F and F' in Figure 1-1). For example, Odekunle and collaborators recently showed that a vasopressin/oxytocin-type (VP/OT) neuropeptide triggers cardiac stomach eversion and changes in body posture in the starfish *Asterias rubens* (Odekunle *et al.,* 2019). VP/OT-type neuropeptides are known for their effects on social and reproductive physiology/behaviour, feeding and gut activity across bilaterian animals (Beets *et al.,* 2012; Johnson and Young, 2017;

Skinner *et al.,* 2019; Spetter and Hallschmid, 2017). Thus, VP/OT-type neuropeptides appear to have an evolutionarily ancient role in regulating feeding in animals.

Most functional studies focus on neuropeptide action in adults, when the animal and nervous system are large in terms of number of cells. Although studies have characterised neuropeptides in different larval nervous systems (Beer *et al.,* 2001; Byrne and Cisternas, 2006; Herget and Ryu, 2015; Mayorova *et al.,* 2016; Nakanishi *et al.,* 2018; Williams *et al.,* 2017), only a few studies have investigated the functions of neuropeptides in the larval nervous system (Conzelmann *et al.,* 2011; Lin and Chen, 2019; Thiel *et al.,* 2017, 2019; Verasztó *et al.,* 2017; Yan *et al.,* 2012). However, most of these functional studies do not explore the molecular mechanisms underpinning behavioural responses. The larval nervous system of indirect developers is often simpler and smaller in comparison to the adult nervous system. The larva therefore offers a unique opportunity to experimentally determine the molecular mechanism underpinning neuropeptide function(s) in a small tractable organism.

1.2 Nervous systems

Nervous systems enable organisms to sense environmental stimuli and coordinate growth, physiological and behavioural responses. The degree to which an animal can sense, detect and respond depends on the complexity of its nervous system. How do we define complexity? The number of cells, the number of cell types, the number of interactions? The term centralised is often used as a proxy for complexity. The more centralised, the more complex. The more decentralised, the less complex. However, according to Richter and colleagues the term centralised is problematic because the degree of centralisation is continuous (Richter *et al.,* 2010).

The term centralisation is used throughout the neuroscience community and is useful when establishing whether centralised structures are homologous or homoplastic. In this section, I discuss the diversity and origin of nervous system with respect to common structures of centralisation which apply to one or more of the following criteria: a) the location of the centralised structure and b) the shape of the centralised structure. The objective of this is to understand whether these specifically located or shaped centralised structures are homologous. A brain is the most prominent anterior condensation of neurons that also contains other cell types, including glial cell and pigment cells (Richter *et al.,* 2010). A brain is considered to be the most important part of the central nervous system of an animal. A nerve cord is a collection of plexuses and is the most prominent longitudinally extending condensed structure (Arendt *et al.,* 2016b; Richter *et al.,* 2010). A nerve cord is often connected to an anteriorly condensed structure including a brain, or nerve ring and so the nerve cord can integrate the bodies information with the anterior structure to direct responses. A nerve ring is a cluster of ganglia in the shape of a ring, which is often found towards the anterior of the animal. These centralised structures are present in adult nervous systems. Larval nervous systems of indirect developers often contain a centralised structured in the form of an apical organ, which is found anteriorly to detect environmental stimuli.

Placozoans and porifera, non-bilaterian metazoans, lack any kind of nervous system; whereas neuralia (bilaterians and cnidarians) and ctenophores do have a nervous

system (Figure 1.5). There are many challenges when thinking about the origin of these nervous systems. The first challenge is the uncertainty over the phylogenetic position of the phylum Ctenophora. If ctenophores are the sister group to neuralia, then there was likely a single origin of nervous systems, after porifera and placozoans diverged from the last common ancestor of all metazoans (Jékely *et al.,* 2015). However, if ctenophores are the sister group to all other metazoans, then either a) nervous systems evolved independently or b) there was a single origin in the metazoan ancestor and then nervous systems were subsequently lost in both placozoans and porifera. There is currently molecular and morphological data to support both homologous and convergent nervous systems (Jager *et al.,* 2011; Jékely *et al.,* 2015; Krishnan and Schiöth, 2015; Moroz *et al.,* 2014; Ryan, 2014; Ryan *et al.,* 2013).

The second challenge is the vast diversity of nervous system types that exist in different animal phyla, from the 'simple' nerve net of cnidarians, to the 'complex centralised' brain of vertebrates and cephalopods. When did 'centralised' structures, such as **nerve rings, nerve cords** and **brains** evolve? Have they evolved more than once? Should we even use the term 'centralised' to define a type of nervous system?

All bilaterian phyla have some degree of centralisation. Large brains are only found in vertebrates and cephalopods (a class of molluscs) (Figure 1.5) (Shigeno *et al.,* 2018; Yoshida *et al.,* 2015). There are other types of brains present in invertebrates including: a compound brain, a cycloneuralian brain, a compact brain, a commissural brain and a syncerebrum (Richter *et al.,* 2010) (illustrated on Figure 1.5 as a small centralised brain). These specific terms are usually restricted to a particular taxon. The absence of a large brain in ambulacraria (echinoderms and hemichordates) and in the remaining chordates and protostomes support the parsimonious hypothesis that large brains evolved convergently. There is some evidence for homology of brain subdivisions between vertebrates and invertebrate chordates and protostomes. Homology is thought to extend to invertebrate chordates but homology with non-chordate invertebrate is controversial (Arendt, 2005; Arendt *et al.,* 2008; De Velasco *et al.,* 2004; Hirth *et al.,* 2003; Holland, 2015; Holland *et al.,* 2013; Nielsen, 1999; Reichert and Simeone, 2001; Takahashi and Holland, 2004).

Nerve rings are also only present in few taxa, including ambulacraria, and protostomian nematodes (Figure 1.5) (Cobb, 1987; Hoekstra *et al.,* 2012; Mashanov *et al.,* 2006; Schafer, 2016). Some studies have claimed that some cnidarians also have a nerve ring (Koizumi *et al.,* 2015; Mackie, 2004; Marlow *et al.,* 2009). However, it seems unclear over whether this a true nerve ring (as defined earlier). Taken together, the most supported hypothesis is the convergent evolution of nerve rings and brains.

Nerve cords are the most common type of nervous system, with at least one present in almost all animal phyla (Figure 1.5) (Budelamnn, 1995; Cobb, 1987; Glover and Fritzsch, 2009; Lowe *et al.,* 2003; Niven *et al.,* 2008; Schafer, 2016; Smarandache-Wellmann, 2016; Swanson, 2012). Interestingly, the nerve cord of protostomian invertebrates is ventral, whilst it is dorsal in chordates. The different position of the nerve cord relative to the body axis has led to questions over the homology of these structures. Many co-expression studies show similar molecular patterning and therefore support the homology of vertebrate and protostome nerve cords (Arendt and Nübler-Jung, 1999; Denes *et al.,* 2007; Holland *et al.,* 2013; Reichert and Simeone, 2001). However, a recent study by Martin-Duran and colleagues looked at a larger and more diverse range of animal, and in so doing has revealed the limitation of molecular patterning. This study suggests that similarities in dorsal-ventral patterning likely evolved independently (Martin-Duran et al. 2018).

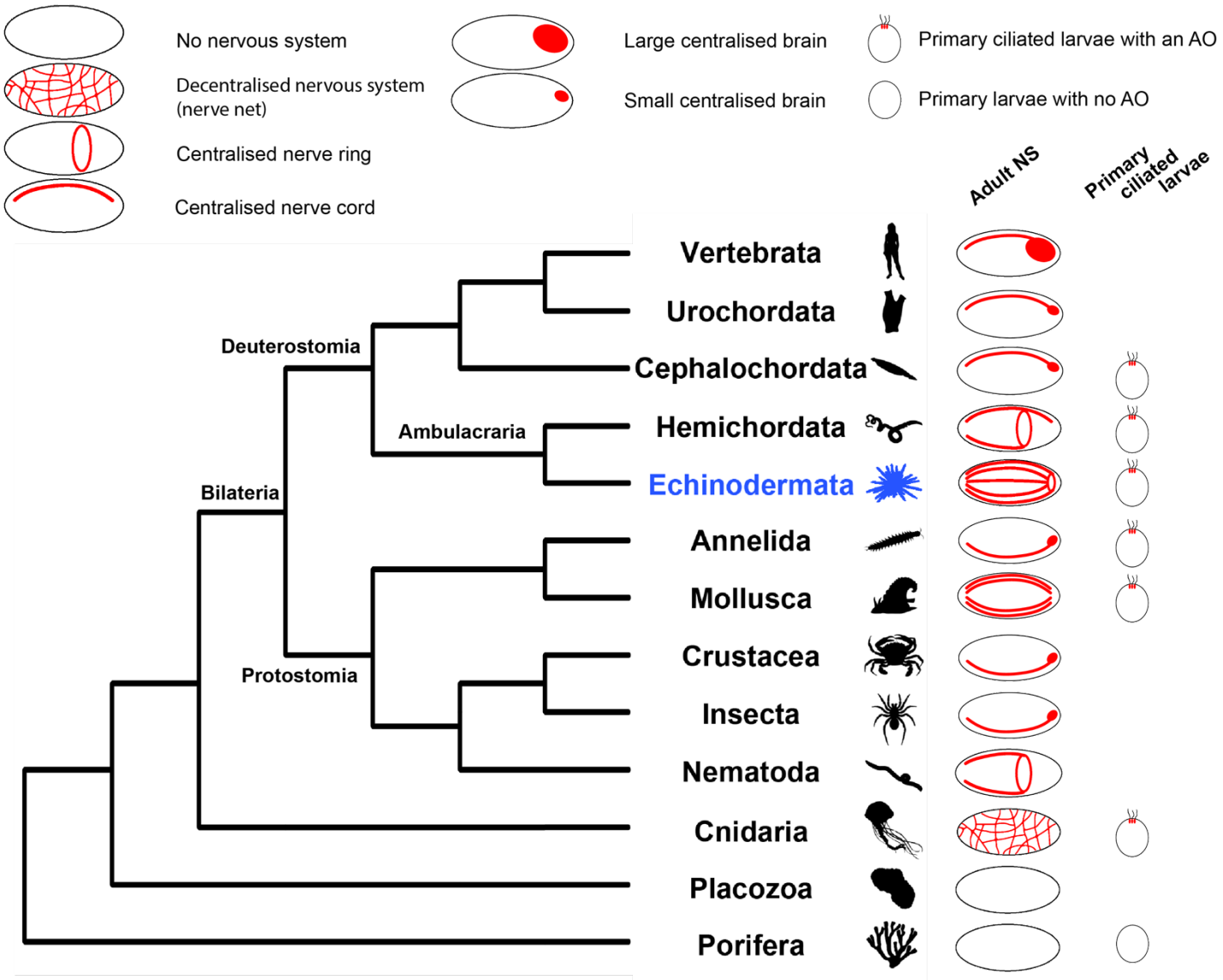
No nervous system
Decentralised nervous system (nerve net)
Centralised nerve ring
Centralised nerve cord
Large centralised brain
Small centralised brain
Primary ciliated larvae with an AO
Primary larvae with no AO
Adult NS
Primary ciliated larvae
Deuterostomia
Ambulacraria
Bilateria
Protostomia
Vertebrata
Urochordata
Cephalochordata
Hemichordata
Echinodermata
Annelida
Mollusca
Crustacea
Insecta
Nematoda
Cnidaria
Placozoa
Porifera

Figure 1.5 The diversity of centralised nervous systems across metazoans

A phylogenetic tree of metazoan animals (excluding Ctenophora and Xenacolemorpha, phyla with uncertain phylogenetic positions) highlighting the distribution of different types of centralised nervous systems present in deuterostomian phyla or sub-phyla, and protostomian phyla/classes. Some clades have more than one type of adult centralised nervous system. Vertebrates have a large brain and nerve cord. Larval urochordates and adult cephalochordates have a small brain and one dorsal nerve cord. Hemichordates, echinoderms and nematodes have multiple nerve cords and a nerve ring. Molluscs have a nerve ring and/or multiple nerve cords, with the exception of cephalopods (e.g. octopus) that also have large brain. Annelids, crustaceans and insects have a small brain and one ventral nerve cord. A decentralised nervous system (nerve net) is present in Cnidaria. No nervous system is present in Placozoa or Porifera. Primary ciliated larvae are found Porifera, Cnidaria, Lophotrochozoa (annelids, molluscs), Ambulacraria (echinoderms and hemichordates) and non-feeding amphioxus larvae (cephalochordates). Some Porifera have primary ciliated larvae, but they do not have an apical organ (Degnan *et al.,* 2015; Leys, 2015; Leys and Degnan, 2005).

The echinoderms (sea urchins, starfish, sea cucumbers, brittle stars and sea feathers), which are deuterostomian invertebrates, further complicate the question of nerve cord homology by having radial symmetry, with five nerve cords around a central circumoral nerve ring (Figure 1.6) (Cobb, 1987). Adult echinoderms are therefore considered to have a centralised, but not cephalised, nervous system (Richter *et al.,* 2010). Cephalisation is when the concentration of a nervous system is found at the anterior or head end of an animal. Echinoderms are unique because they are the only phyla with penta-radial symmetry. As a result, they are often excluded from discussions on nervous system evolution (Burke, 2011; Holland *et al.,* 2013; Nielsen, 1999). See Hinman and Burke 2018 for a summary of the frequent misunderstandings of echinoderm nervous systems (Hinman & Burke 2018).

Two distinct regions that run adjacent to one another make up each of the five radial nerve cords in adult echinoderms - a thicker oral ectoneural region and a thinner aboral hyponeural region (Figure 1.6). The ectoneural region have both sensory and motor functions, whilst the hyponeural region have motor functions. There is also a third apical, entoneural region, which has so far only been identified in asteroids and crinoids (Cobb, 1987). The ectonural and hyponeural regions of the nervous system were classically thought to be separated from one another by a basement membrane

of collagenous connective tissue (Cobb 1985). However, recent studies have shown that these two bands are connected by neurons (Figure 1.6) (Cobb 1985; Hoeskstra *et al.,* 2012). Furthermore, the hyponeural band has now been shown to have an ectodermal origin rather than a mesodermal origin (Mashanov *et al.,* 2007). These discoveries coupled with the identification of glial cells and chemical synapses (features also present in chordates) support the hypothesis that echinoderm radial nerve cords are homologous to the dorsal nerve cords of chordates (Díaz-Balzac *et al.,* 2016; Mashanov *et al.,* 2006, 2007, 2009; Mashanov and Zueva, 2018). Further studies involving molecular characterisation of nerve cords are needed to gain more insight into whether structures are homologous or analogous.

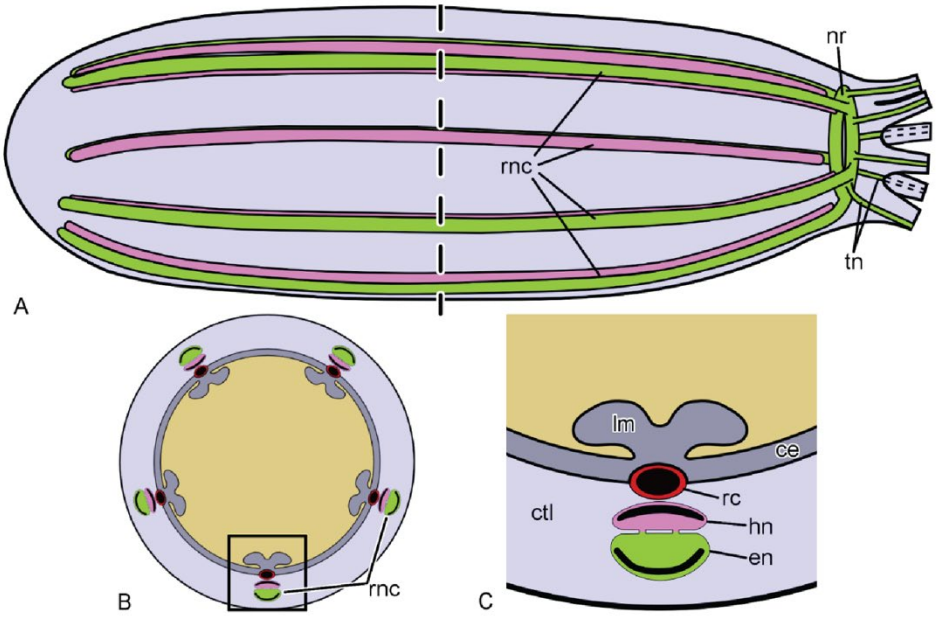

Figure 1.6 Diagrams of an adult sea cucumber nervous system

This figure is taken from Mashanov and colleagues 2009. The presence of two connected tissue types (pink and green) in the five radial nerve cords. A) A lateral view of an adult sea cucumber, oral end to the right. The dashed line corresponds to the cross section at the mid-body level shown in (B). C) A higher magnification of the boxed area in (B) showing the relationship between radial nerve cords and other radial organs. Abbreviated labels refer to the following: ce (coelomic epithelial lining of the body cavity, ctl (connective tissue layer of the body wall), en (ectoneural part of the radial nerve cord), hn (hyponeural part of the radial nerve cord, lm (longitudinal muscle band), nr (nerve ring), rc (radial canal of the water vascular system), rnc (radial nerve cord), tn (tentacular nerve) (Mashanov *et al.,* 2009).

Taken together, the diversity of animal nervous systems give many plausible hypotheses on the origin of nerve cords. Further work comparing morphological features and regulatory states of nerve cords from **all** extant taxa may provide more clarity on the possible homology of bilaterian nerve cords, as well as more clarity on what type of nervous system (a nerve net or nerve cord) was present in Urbilateria.

1.2.1 Larval nervous systems

Another challenge when discussing the origin of nervous systems is the presence of a ciliated larval stage as part of the life cycle of many marine animals. These ciliated larvae often contain a nervous system to sense environmental stimuli, swim and feed. Primary ciliated larvae are found in many phyla, including poriferans, cnidarians, lophotrochozoans (molluscs, annelids) and ambulacraria (hemichordates and echinoderms) (Figure 1.5) (Byrne and Cisternas, 2006; Degnan *et al.,* 2015; Leys, 2015; Leys and Degnan, 2005; Marlow *et al.,* 2014; Nielsen, 2015; Raff and Byrne, 2006). Thus, another widely debated question is the origin of larval nervous systems

The most prominent feature of larval nervous systems is the apical organ (AO) with associated ciliary tufts, which is present in the majority of ciliated larvae (Lacalli, 1994). The AO is characterised by the presence of flask-shaped serotonergic neurons bearing a cilium that extends from the embryo surface and axonal projections that extend to a central neurophile. In addition to serotonin, these ciliated sensory neurons can contain neuropeptides (Conzelmann *et al.,* 2011; Nezlin and Yushin, 2004; Temereva and Wanninger, 2012). AOs have been well characterised and most comparative and molecular biology studies support the homology of AOs across different larval nervous systems (Marlow *et al.,* 2014; Nielsen, 2015). Furthermore, the wide distribution across animal taxa has led to the hypothesis that the neuralian ancestor had a nervous system in the form of an AO (Jagersten, 1972; Marlow *et al.,* 2014). Some have further developed this idea to suggest that adult body plans, and therefore adult nervous systems, evolved from a larval-type ancestor (Nielsen, 2012).

In summary, the characterisation of adult and larval nervous systems supports the hypothesis that the common ancestor of neuralians had some sort of centralised nervous system. Coupled with the knowledge that at least 30 NP signalling systems

were present in the urbilaterian ancestor, this suggests that the urbilaterian was an animal capable of advanced physiological and behaviour responses. Furthermore, the conservation of larval AOs across neuralian taxa brings to attention the potential conservation of other larval nervous systems features (i.e. the decentralised nervous system of larvae), which should be studied in more depth.

1.3 Neuronal cell-types

Other prominent questions in the field of neurobiology are: when did neuronal cell types originate and what did they evolve from? A huge diversity of neuronal cell types make up a given nervous system and they have diverse molecular, morphological, connectional and functional properties (Masland, 2004; Richter *et al.,* 2010; Zeng and Sanes, 2017), which define the type and function of the nervous system. Terminally differentiated neuronal cells can be divided into two general morphological types: projection/principal cells and intrinsic/interneuron cells (Arendt *et al.,* 2008; Masland, 2004). Interneurons convey information between different types of neurons (Richter *et al.,* 2010). Projection cells can be further sub-divided into sensory neurons and motor neurons. Sensory neurons sense external stimuli, while motor neurons convey information to muscles to respond. While function defines these neuron types, structure can also be used to recognise types of neurons. There are three main types of morphologically distinct neurons, unipolar, bipolar, and multipolar neurons. All of these neurons have a cell body (also known as soma), but vary in the number of neurites extending from the cell body (Meinertzhagen, 2019; Richter et al., 2010) (Figure 1.7). In Drosophila and *C. elegans* the majority of neurons have been identified as unipolar or bipolar (Figure 1.7). In vertebrates, neurites are further divided into axons and dendrites, where dendrites typically receive signals (postsynaptic) and axons send signals (presynaptic). However, in invertebrates the terms axon and dendrite may not be as useful, with little distinction seen between these structures.

There are a huge diversity of sensory cells that can detect a wide range of stimuli and one well known example are photosensory cells. Photoreception has been particularly well studied in vertebrates and the invertebrate annelids revealing two major types of photoreceptors cells (PRCs), rhabdomeric and ciliary PRCs (Arendt *et al.,* 2004; Eakin, 1979; Erclik *et al.,* 2009). There are also additional supportive cells including glial cells, which are often referred to as the 'glue' of the nervous system. Glial cells and photoreceptors are found throughout the Bilateria (Arendt *et al.,* 2004; Eakin, 1979; Hartline, 2011; Richter *et al.,* 2010).

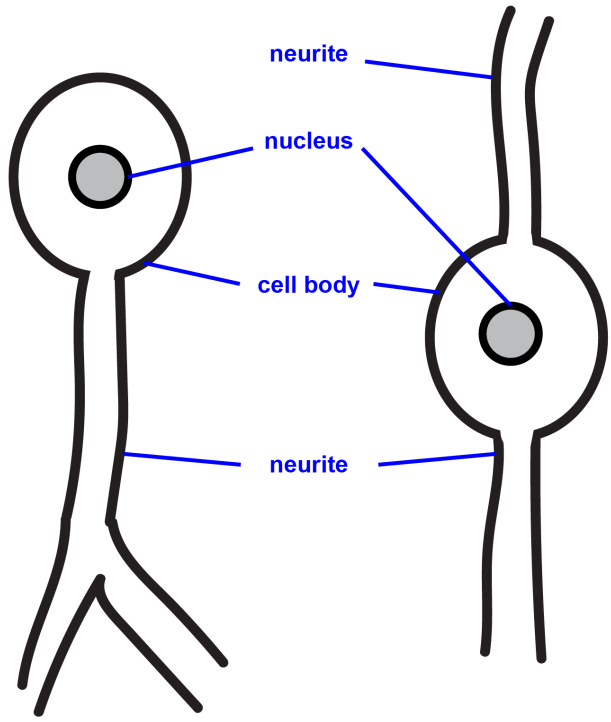

Figure 1.7 Terminally differentiated neuronal cells

Representative labelled illustrations of morphologically distinct neurons, a unipolar neuron and a bipolar neuron

While placozoans have no obvious neurons, they do have ciliated secretory cells (Smith *et al.,* 2014). These secretory cells express neuropeptide-type molecules (Nikitin, 2015; Senatore *et al.,* 2017). Senatore and colleagues found that when endomorphin-like peptides were applied to Trichoplax, ciliary beating was arrested (Senatore *et al.,* 2017). Furthermore, they found that this pausing behaviour propagates from animal to animal, suggesting that neuropeptide-type molecules may induce peptide secretion in other individuals to result in behavioural responses at a population level (Senatore *et al.,* 2017). The similarities between neuronal and secretory cells, coupled with the appearance of sensory secretory cells before nervous systems appear evolved supports the hypothesis that neuronal cells may have evolved from secretory-type cells (Moroz, 2009).

1.3.1 Molecular characterisation of neuronal cell types

An important component of identifying cell types is molecular characterisation. Neurotransmitters are most often used to identify neuronal cell types, although they typically only reveal large populations of cell types. An example can be seen in the early sea urchin pluteus larva where localisation of neurotransmitters reveals four populations of neuronal cells: serotonin-positive neurons in the apical organ cells, dopamine-positive neurons in the lower lip and post-oral cells, and GABA-positive neurons in the esophagus (Bisgrove and Burke, 1987) (Figure 1.12). More recently, the larger complement of neuropeptide signalling molecules has been used to further characterise nervous systems in many species (Beer *et al.,* 2001; Conzelmann *et al.,* 2013; Hansen *et al.,* 2002; Herget and Ryu, 2015; Mayorova *et al.,* 2016; Williams *et al.,* 2017). As well as neurotransmitters and neuropeptides, neurons can be molecularly identified by peptide processing, secretory machinery and neurite structural proteins.

Neurotransmitters and neuropeptides are synthesised by or derived from proteins that are encoded by genes that are categorised as **terminal differentiation or effector genes**. Thus, expression of unique combinations of these genes defines neuronal identity and functionality (Arendt, 2008; Hobert, 2016a) (Figure 1.8). Combinations of **terminal selector genes** (transcription factors) assign neuronal identity by directly regulating the expression of these downstream **terminal effector genes** (Figure 1.8). Two criteria have so far been established, to define transcription factors as terminal selector genes in *C. elegans*: a) the gene is present in the whole life of a neuron, and b) the gene directly binds to the effector gene (Hobert, 2010). Expression of unique combinations of terminal effector genes, as opposed to unique sets of genes, define neuronal types (Figure 1.8). Therefore, neurotransmitters and neuropeptides are often expressed in many cell types. Much work has been done in characterising the **regulatory states** (the specific combination of expressed terminal selector genes in a given time and space) of neuronal cells of the nematode *C. elegans* (Hobert, 2010, 2016b; Hobert *et al.,* 2010). One example is that sra-11, kal1-1, hen-1, unc-17 and ser-2 are among the genes that specify AIY interneurons by being

regulating by ceh-10 and ttx-3 transcription factors (Figure 1.8). However, less is known about neuronal regulatory states and neuronal identity in other species.

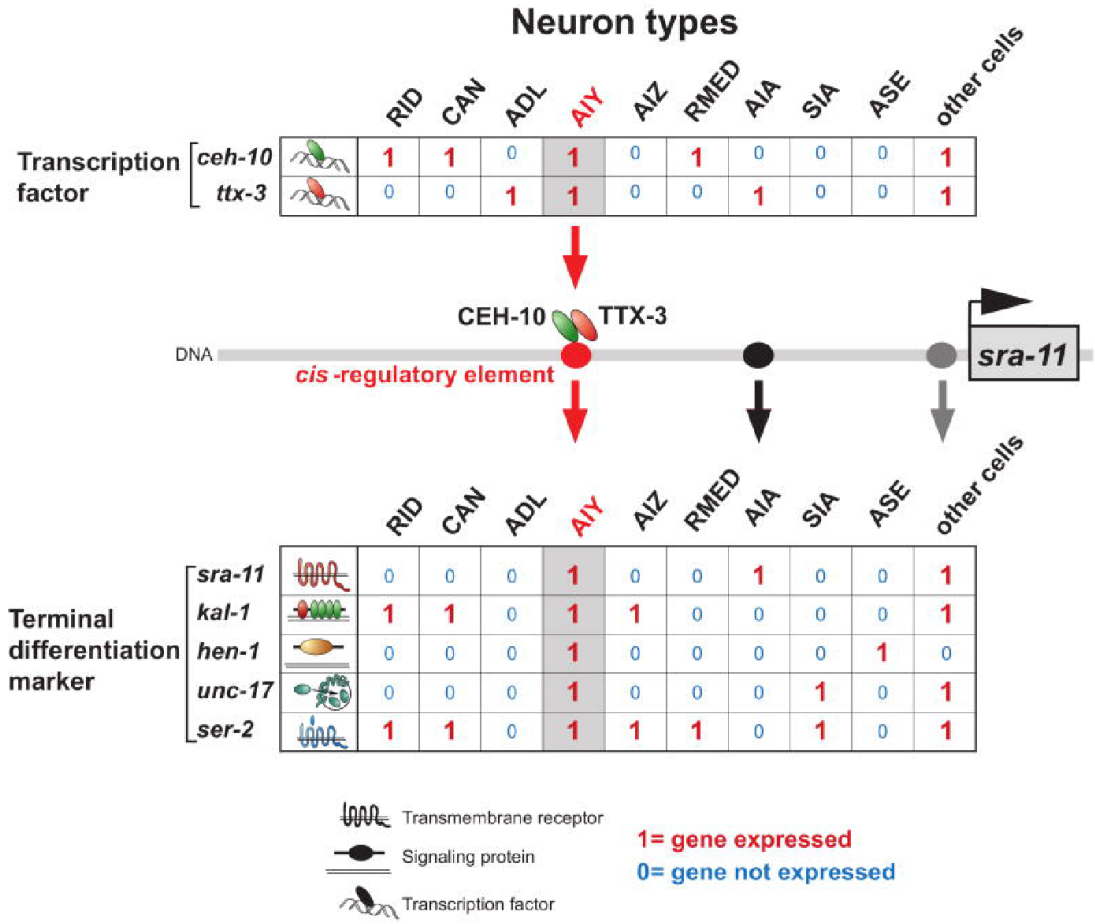

Figure 1.8 Control of neuronal identity

Figures taken from *Hobert et al.,* 2010 are showing different ways to illustrate a regulatory state. A) Combinatorial gene expression patterns (of both transcription factors and terminal differentiation markers) are unique identifiers of terminal neuron fate. An example Is shown for *C. elegans* AIY interneuron, two transcription factors ceh-10 and ttx-3 (top table) synergistically bind to a cis-regulatory element, the AIY motif (red circle), found in different terminal differentiation genes (sra-11, kal-1, hen-1, unc-17 and ser-2) (bottom table) that define the terminal identity of the AIY neuron type. Individual genes, such as sra-11 are also activated in other neuron types (AIA and other neuronal cells) through separate regulatory elements (black and grey circles) which may represent binding sites for other terminal selector genes. Other cell types such as ADL, do not express the sra-11 gene. (Hobert *et al.,* 2010).

The identification of **regulatory states** in time and space will reveal hierarchical interactions of regulatory genes and thus a **gene regulatory network (GRN)** for a given neuronal cell type. As Davidson and colleagues have stated, "in mechanistic terms, development proceeds as a progression of states of spatially defined regulatory gene expression" (Davidson *et al.,* 2002a). An example of a well-studied GRN is the GRN controlling formation of the larval sea urchin skeleton (Figure 1.9) (Davidson *et al.,* 2002a). A GRN can be viewed at different levels, from the whole to a particular regulatory state/sub-circuit. The "view from the genome", considered the functional genomics point of view, provides a summary of all inputs into a gene that occur in all cells at all times in the developmental process. The "view from the nuclei" contains interactions present in different cells over a particular time period. The "view from the nucleus" reveals a particular regulatory state at a specific time in a given nucleus. This view is considered the developmental biology point of view (Figure 1.9) (Davidson *et al.,* 2002a).

Building regulatory states and GRNs of individual neuronal cell types across bilaterian animals will provide the most comprehensive molecular characterisation. A more in-depth molecular characterisation coupled with morphological and functional characterisation will shed more light on the evolution of neuronal cell types and nervous systems as a whole. However, this will be an enormous challenge for scientists.

Finally, larval nervous systems with fewer neuronal cells, but with a diverse complement of neuronal cell types, offer a better opportunity to observe and compare the complete development and functions of animal nervous systems.

A) View from the genome

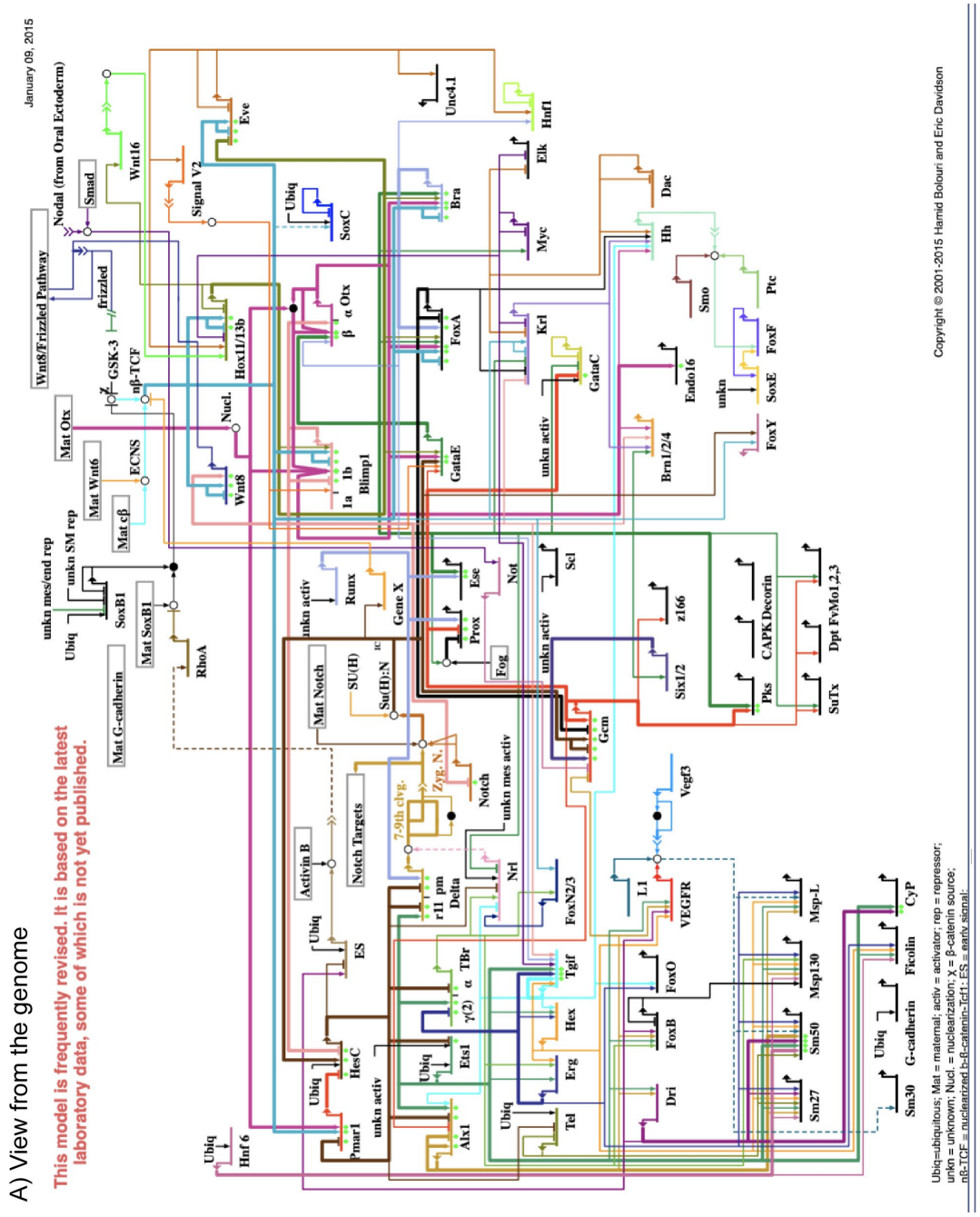

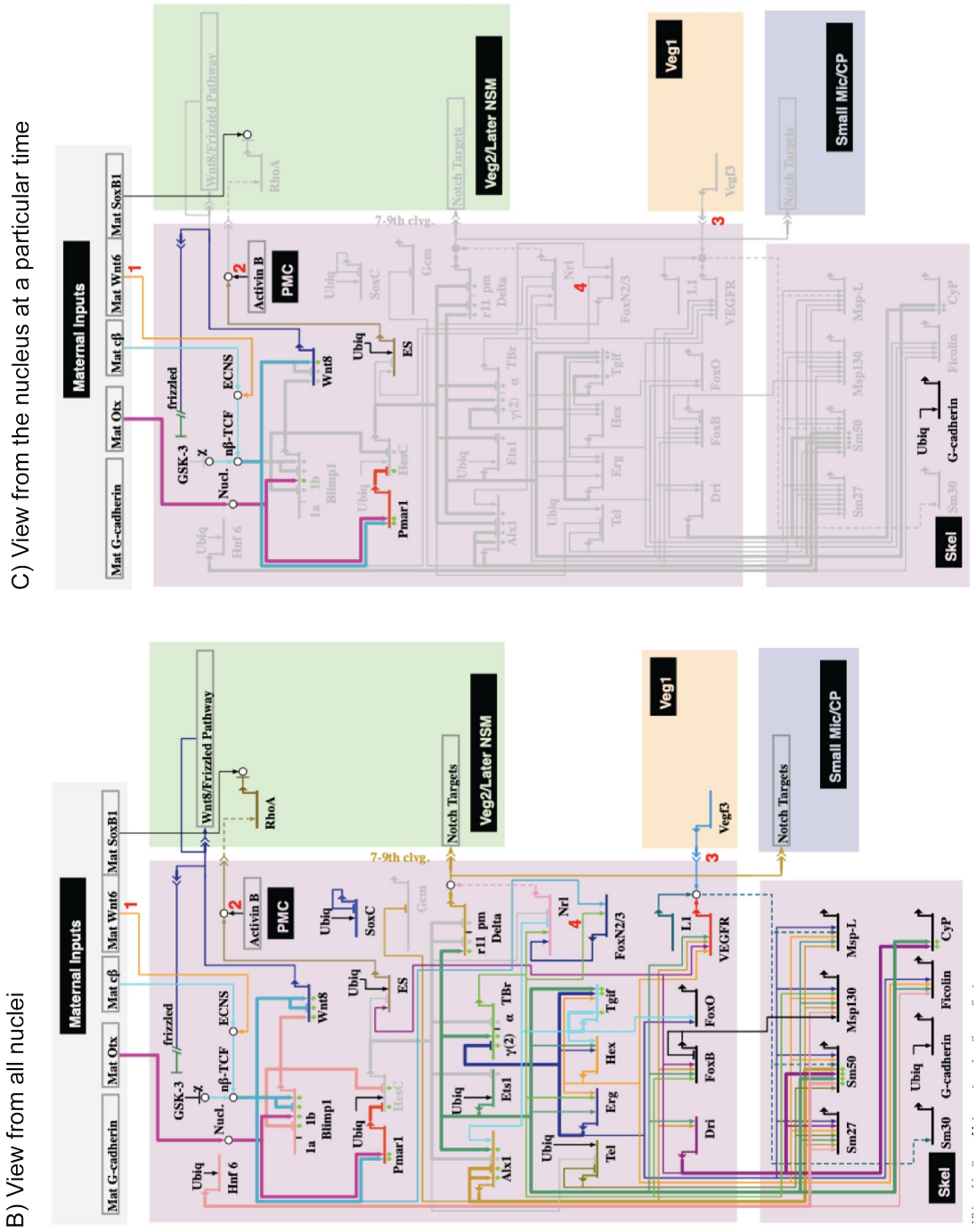

Figure 1.9 Different views of a gene regulatory network (GRN) model in BioTapestry

The endomesoderm GRN as seen using the A) view from the genome, B) view from the nuclei and C) view from the nucleus (http://www.echinobase.org/endomes/). Genes (nodes) are shown by horizontal lines with a bended arrow and positive or negative regulatory interactions (edges) are shown between different genes. Each gene and their regulatory interactions are colour coded. Dashed lines show possible interactions and sub-networks from various domains of the embryo are represented in different colour-coded blocks.

1.4 The sea urchin as a developmental model

Sea urchins are marine invertebrate deuterostomes found throughout oceans across the world. They have been used as a developmental model since the mid 19th century, when Oskar Hertwig first discovered pronuclear fusion in the sea urchin (Hertwig, 1876). Many prominent experiments then followed, including Hans Driesch's experiment, which illustrated that a complete embryo can develop from an isolated blastomere at 2 and 4-cell stage and therefore part of an egg has the ability to develop into a full organism (Driesch 1891). In 1902, Theodor Boveri demonstrated that a complete genome must be present in all blastomere nuclei for normal development to progress (Boveri 1902). By the late 20th century, Eric Davidson and colleagues used the sea urchin to progress ideas on how the genome can direct development (Britten and Davidson, 1969; Davidson, 1989; Davidson *et al.,* 1998, 2002a). In 2002, they published the first gene regulatory network for the specification of the sea urchin endomesoderm (Davidson *et al.,* 2002b). Since then, many publications have refined and expanded the endomesoderm GRN (one of the best examples is the skeletal GRN) (Oliveri *et al.,* 2008; Ransick *et al.,* 2002; Shashikant *et al.,* 2018).

The sea urchin is an excellent experimental system for developmental biology studies. It is an attractive model with millions of synchronous, easily accessible developing embryos (even in central London, if one has access to a marine aquarium!), with transparency and rapid development to larvae in two-three days. Furthermore, the cell-lineage is well known from the first cleavages to the pluteus larvae (Cameron *et al.,* 1987; Davidson *et al.,* 1998). Sequencing of the *S. purpuratus* genome and transcriptome studies were crucial steps to further utilise the sea urchin for developmental questions, including experimental validation of the most well-studied GRN (Sodergren *et al.,* 2006; Tu *et al.,* 2012, 2014a). There now exists an extensive range of tools and approaches, including: *in situ* hybridisation, immunohistochemistry, morpholino oligonucleotide gene knockdown, CRISPR/Cas9 knockouts, BAC-based reporter constructs, cis-regulatory analysis and ATAC-sequencing (Cameron *et al.,* 2009; Hamdoun and Foltz, 2019; Kudtarkar and Cameron, 2017; Samanta, 2006; Tu *et al.,* 2012, 2014a).

Taken together, the sea urchin really is a wonderful organism for developmental biology studies and to address questions related to the development of neuronal cells. Advances in research on other echinoderms make the whole phylum exemplary for evolutionary studies (Cary *et al.,* 2019; Dylus *et al.,* 2018; Mayorova *et al.,* 2016). Furthermore, these echinoderms are both invertebrates and deuterostomes and so they have shared characteristics of both groups of animals. Echinoderms can therefore bridge the gap and help provide insights into the evolutionary history of bilaterian animals.

1.4.1 Sea urchin development

Sea urchins (echinoids) are one of the five classes of the phylum Echinodermata. Echinoderms have direct development or indirect development through a planktonic larval stage. *S. purpuratus* is an indirect developer and so has a feeding larval stage before undergoing metamorphosis into a juvenile. These marine invertebrates use external fertilisation, where the gametes are released into the environment and the embryos develop externally. The eggs of *S. purpuratus* are approximately 80 μm in diameter and are immediately surrounded by a vitellin layer bonded to the plasma membrane. Surrounding the vitelline layer is a second extracellular matrix, the egg jelly layer (Vacquier and Moy, 1977). The sperm of *S. purpuratus* are much smaller in size. They have a conical head, containing the acrosomal vesicle (0.3 μm diameter) and the haploid nucleus, a single mitochondrion and a single long flagellum (Bernstein, 1962). Fusion of the egg and sperm initiates the formation of the fertilisation membrane and the hyaline layer to block polyspermy.

After fertilisation, development starts with a series of cleavage divisions that divides the egg into smaller nucleated cells. The sea urchin undergoes radial, holoblastic cleavage (Gilbert, 2000). Holoblastic cleavage is characterised by total cleavage that divides the whole egg, resulting in the equal blastomeres. Radial cleavage is the arrangement of blastomeres on the upper tier directly over those on the lower tier. Radial cleavage is typical of deuterostomes, in contrast to the spiral cleavage typically found in protostomes (Gilbert, 2000). The sea urchin blastomeres continue to divide and undergo equal and unequal cleavages (Gilbert, 2000). After eight cleavages, the

cells are organised into a true epithelium around a blastocoel to form a blastula stage embryo (Figure 1.10). Each blastomere develops a single cilium, and the ciliated blastula begins to rotate inside the fertilisation membrane. At hatching, enzymes digest the fertilisation membrane and releases the motile embryo into the external environment. *S. purpuratus* embryos grown at 15°C hatch from the fertilisation membrane around 15 hours post fertilisation (hpf). (From here on, any development timepoint referred to are cultures grown at 15°C, unless otherwise stated). Cell lineage tracing experiments reveal that major embryonic territories present at the blastula stage are specified at the 60-cell stage, but not irreversibly. Each of these territories is defined by a unique regulatory state that will give rise to one or more cell types (Cameron *et al.,* 1987; Davidson, 1989; Davidson *et al.,* 1998). At the hatched blastula stage the three germ layers specified at the 60-cell stage - ectoderm, endoderm and mesoderm – are divided into seven territories, as shown in Figure 1.10. The ectoderm, which gives rise to neurons and the larval skin, is divided into oral (yellow), aboral (green) and apical plate (orange) territories. The endoderm (blue), which gives rise to the gut, is specified by one territory. The mesoderm, is spilt into: a) skeletogenic mesoderm (red), also called primary mesenchyme cells (PMCs), giving rise to the skeleton, and b) non-skeletogenic mesoderm (light purple), also called secondary mesenchyme cells (SMCs), which give rise to pigment cells, immunocytes and muscle cells. There are also small micromeres at the vegetal pole that give rise to the coelomic pouches (dark purple). By the mesenchyme blastula stage (24 hpf), PMCs have migrated into the blastocoel, followed by the migration of SMCs and the invagination of endodermal cells to form the archenteron. The archenteron continues to elongate towards the oral ectoderm, where it forms the larval mouth. Simultaneously, the PMCs form calcium carbonate spicules, which eventually grow to form a bilaterially symmetrical elongated skeletons, which gives the pluteus larvae its characteristic pyramidal shape (Figure 1.10).

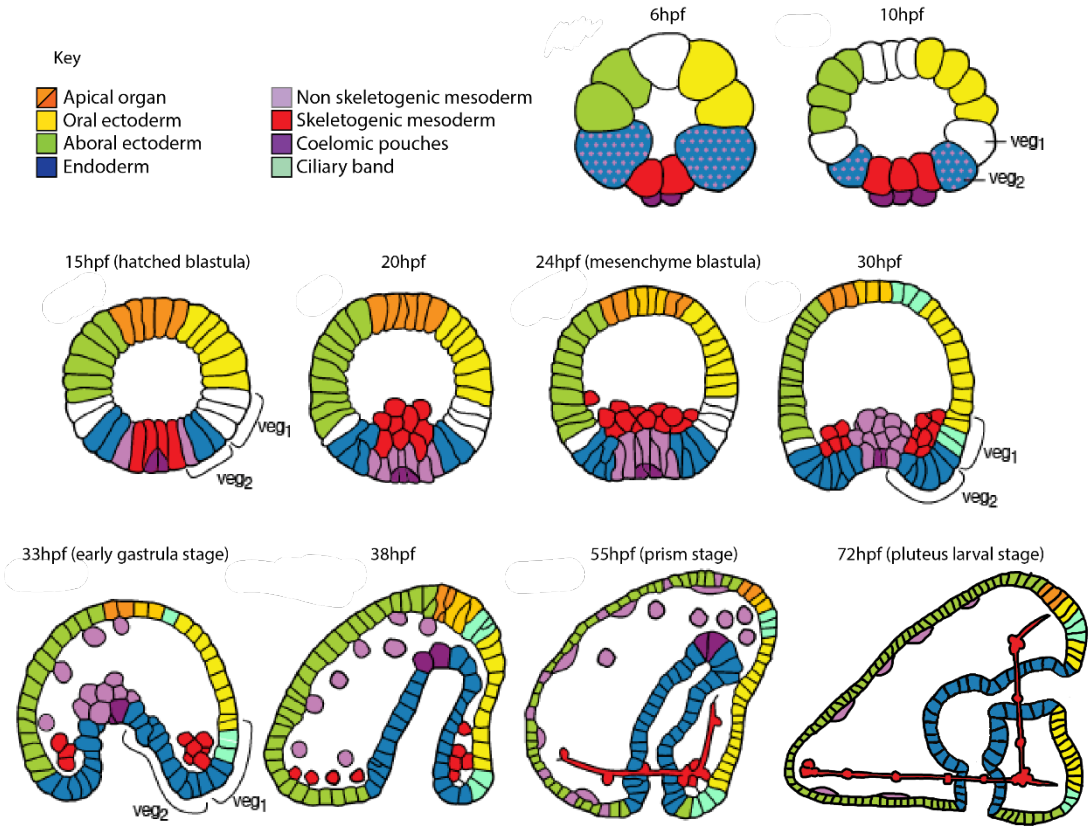

Figure 1.10 Representational drawing of *Strongylocentrotus purpuratus* developmental stages.

Developmental stages from early blastula stage at 6 hours post fertilisation (hpf) to pluteus larval stage at 72 hpf, when incubated at 15°C. Different colours depict different territories (a group of embryonic cells identified by the expression of specific genes) through development: the apical organ will give rise to sensory neurons, interneurons and supporting cells; the oral ectoderm will give rise to the larval mouth, oral epithelium, and several neurogenic structures including the oral hood and the ciliated band; the aboral ectoderm will give rise to the squamous epithelium that forms the wall of the late embryo and larvae, except from the oral and ciliated band regions; the vegetal plate will go onto form the non-skeletogenic mesodermal cells that will give rise to a pigment cells, immunocytes and muscle cells and endodermal cells that will give rise to foregut and midgut cells; the large micromeres will give rise to only the skeletal cells; and the small micromeres will give rise to only the coelomic pouches. For embryonic axes at different developmental stages see Figure 8.2.

Once the mouth has formed, the pluteus larva begins to feed on unicellular algae. In the ocean, the larvae continues to feed for several weeks (four to eight weeks) while the larval skeleton and other tissues grow in complexity to eventually form an 8 arm

plutei. During the larval life, the juvenile develops from the left coelomic pouch (Smith *et al.,* 2008). The larva becomes competent for metamorphosis when the juvenile is fully developed. The larva settles on the floor and environmental cues trigger metamorphosis. Cameron and colleagues have shown that a bacterial film can stimulate metamorphosis in the laboratory (Cameron and Hinegardner, 1974). The juvenile begins metamorphosis by pushing tube feet out of the side of larva, and then undergoes a drastic inside-out movement. The juvenile engulfs the larva and uses it as a food source until its gut has fully developed to form a mouth.

1.4.2 Sea urchin nervous system development

Neurogenic capacity in the sea urchin embryo is initially present throughout the entire ectoderm, but later it becomes restricted to the anterior neuroectoderm (ANE) and the ciliary band neuroectoderm (CBE). The neurogenic capacity of the embryo is restricted by Wnt-dependent pathways that regulate Nodal and bone morphogenetic protein (BMP) signalling (Angerer *et al.,* 2011). The ANE is first established, during cleavage stages, by balancing the opposing Wnt signalling and ANE regulatory genes (such as, *Sp-Six3*). The CBE is established later, during the mesenchyme blastula stage, by factors such as Lefty and Chordin that inhibit Nodal and BMP signalling. Moreover, the mechanisms that specify the ANE and CBE are connected by a double-repression mechanism, whereby Wnt signalling downregulates FoxQ2 expression (restricting its expression to the ANE), which then supresses Nodal signalling in ANE (Angerer et al., 2011).

The first neuronal precursor cells appear at the mesenchyme blastula stage (24 hpf): the serotonergic neuronal precursor cells in the apical plate (which will become the apical organ) and post oral neuronal precursor cells in the oral ectoderm (Bisgrove and Burke, 1987; Garner et al., 2016) (Figure 1.11). The nervous system of the larval sea urchin first appears at the late gastrula stage (48 hpf) when the first serotonergic neurons begin to differentiate (Figure 1.11). By the pluteus larval stage, 40-50 neurons are present across the apical organ, ciliary band, lateral ganglia, mouth and foregut (Bisgrove and Burke, 1987; Burke, 1978; Burke *et al.,* 2014; Garner *et al.,* 2016; Hinman and Burke, 2018; Mellott *et al.,* 2017; Wei *et al.,* 2011) (Figure 1.11;

Figure 1.12). These neurons have diverse functions including sensation and controlling muscle movement (Beer *et al.,* 2001; Burke *et al.,* 2014; Nakajima *et al.,* 2004b). As the larva develops, the nervous system continues to increase in size by expanding the number of neurons (Beer *et al.,* 2001; Bisgrove and Burke, 1987) (Figure 1.12A-C). The juvenile develops a nervous system from scratch, and so the larval nervous system is completely independent to that of the adult (Burke *et al.,* 2006b).

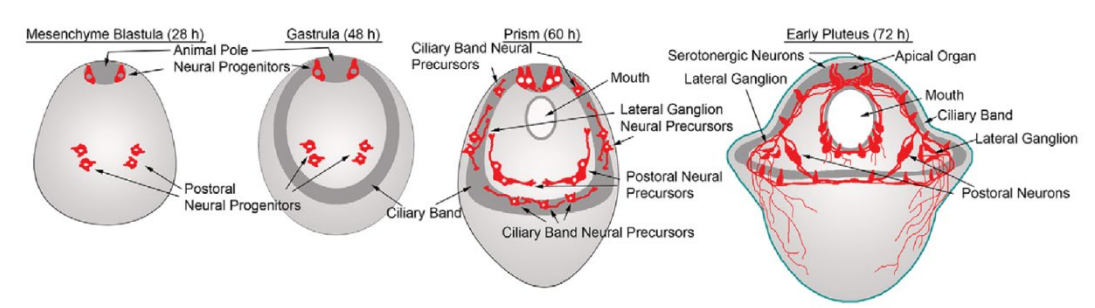

Figure 1.11 Neurogenesis in the sea urchin embryos

This figure is taken from Garner *et al.,* 2016. Diagram of sea urchin larval nervous system development from; the appearance of neuronal precursor cells at mesenchyme blastula stage (28 hpf), the onset of neuronal differentiation at gastrula stage (48 hpf), the increase of neuronal precursor cells at prism stage (60 hpf), the presence of many differentiated neurons in the pluteus larval stage (72 hpf) (Garner *et al.,* 2016).

1.4.2.1 Pluteus larval nervous system

The sea urchin larval nervous system has so far been characterised in terms of the pan-neuronal marker (synaptotagmin, a synaptic vesicle trafficking protein), end-products of terminal effector genes (neurotransmitters and neuropeptides) and some terminal selector genes (transcription factors). Synaptotagmin (SynB) is reported to be exclusively expressed in neurons and is thought to be a pan-neuronal marker (expressed in all neurons) of the sea urchin larval nervous system (Figure 1.12D) (Burke et al., 2006b, 2014; Nakajima et al., 2004b), while all other neuronal genes/proteins (studied so far) are localised to specific neurons (Figure 1.12). The expression patterns of serotonin, dopamine and GABA, some of the most common

neurotransmitters, have been well studied in *Strongylocentrotus droebachinesis* by Burke and colleagues (Bisgrove and Burke, 1987) (Figure 1.12). They revealed four populations of neurons in the four-arm pluteus larva (72 hpf), serotonin-positive neurons in apical organ cells, dopamine-positive neurons in lower lip and post-oral cells and GABA-positive neurons in the esophagus (Bisgrove and Burke, 1987) (Figure 1.12A-C). Adams and collaborators have reported that the post-oral dopaminergic neurons are involved in controlling arm length in response to food (Adams *et al.,* 2011).

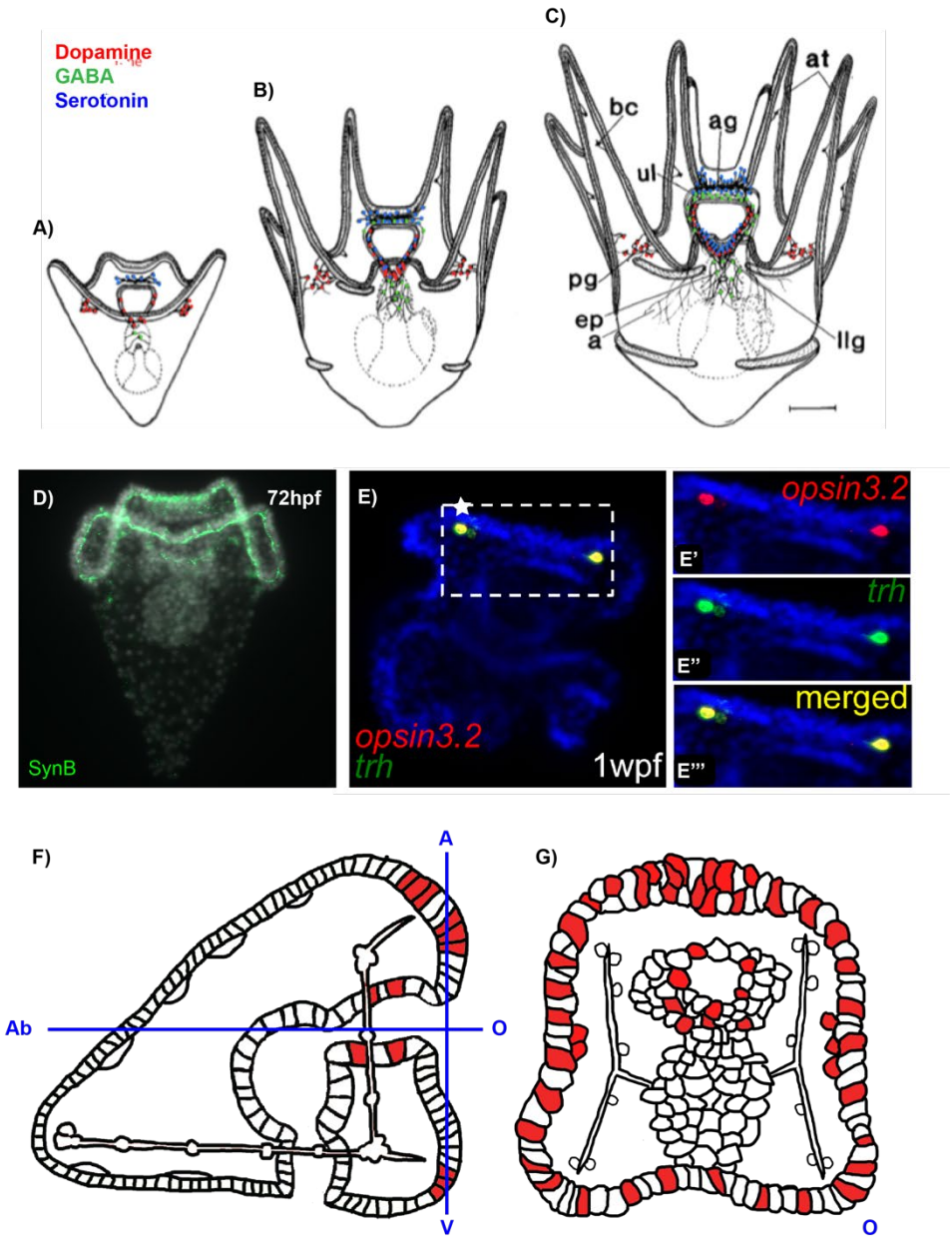

Figure 1.12 Markers of terminal effector gene expression in the sea urchin larval nervous system

Characterisation of sea urchin larval nervous systems using antibodies against neurotransmitters and Synaptotagmin (SynB), and *Sp-TRH* and Sp-Opsin3.2 fluorescent ISH. A-C) Distribution of dopamine-, GABA-, serotonin-positive cells during larval development in *S. droebachiensis*. D) Distribution of SynB (1E11) positive cells during early pluteus larval development in *S. purpuratus*. E) Fluorescent ISH of *Sp-TRH* and *Sp-Opsin3.2* co-expressed in photoreceptor oral-distal neurons of a one-week larvae. F-G) Cartoon summary of markers of terminal effector gene expression in the apical organ, ciliary band and mouth of a four-arm pluteus larval nervous system. Panel images A-C modified from (Bisgrove and Burke, 1987). Panel image E

taken from (Petrone, 2015). Abbreviations of embryonic axes shown in panel F are the following: A (Animal), V (Vegetal), O (Oral) and Ab (Aboral)

Additional types of neuronal cells have also been identified in the sea urchin. Potential ciliary photoreceptors have been identified by the expression of a GO opsin, *Sp-Opsin3.2* in two cells located either side of the apical organ (Petrone, 2015; Valero-gracia *et al.,* 2016) (Figure 1.12B). Further, co-expression of *Sp-Opsin3.2* and the SynB neuronal marker in ciliary band cells reveal that these larval photoreceptors are neuronal cells (Valencia *et al.,* 2019). Valero-gracia and collaborators refer to these cells as non-directional photoreceptors because they are not associated with pigment cells (Valero-gracia *et al.,* 2016). However, Valencia and collaborators argue that pigment cells nearby could be sufficient to enable directionality to the perception of light (Valencia *et al.,* 2019). Petrone and colleagues also revealed that these *Sp-Opsin3.2* photoreceptive neurons co-express the neuropeptide precursor *Sp-TRH* (Petrone, 2015) (Figure 1.12E).

1.4.2.2 Transcription factors

Many neuronal transcription factors (terminal selector genes) have also been identified in populations of neuronal precursor cells and neurons in the larval sea urchin nervous system (Figure 1.13).

Neuronal terminal selector genes belong to many different transcription factor families, including but not limited to: forkhead (*Sp-FoxG, Sp-FoxJ1*), sox (*Sp-SoxC, Sp-SoxB1*), homeobox (*Sp-Otp, Sp-Six3, Sp-Islet*), parahox (*Sp-Lox*), zinc finger (*Sp-sip1*) and bHLH genes (*Sp-NeuroD, Sp-Ngn*) (Burke *et al.,* 2006a; Di Bernardo *et al.,* 1999; Garner *et al.,* 2016; Mcclay *et al.,* 2018; Perillo *et al.,* 2018; Slota and Mcclay, 2018; Tu *et al.,* 2006; Wei *et al.,* 2009). In addition, the transcription factors *Sp-SoxB1*, *Sp-Six3* and *Sp-Nkx3.2* are also expressed in neurons identified within the larval foregut (Wei *et al.,* 2011). Interestingly, the neuron-associated genes *Sp-Islet, Sp-NeuroD, Sp-Ngn, Sp-Brn1/2/4, Sp-Mist,* and *Sp-Lox* are also expressed during the development of pancreatic-like endocrine cells found in the sea urchin gut. This reveals that subsets of sea urchin larval neurons have a similar regulatory state to endocrine cells in the gut (Annunziata *et al.,* 2014b; Perillo *et al.,* 2018).

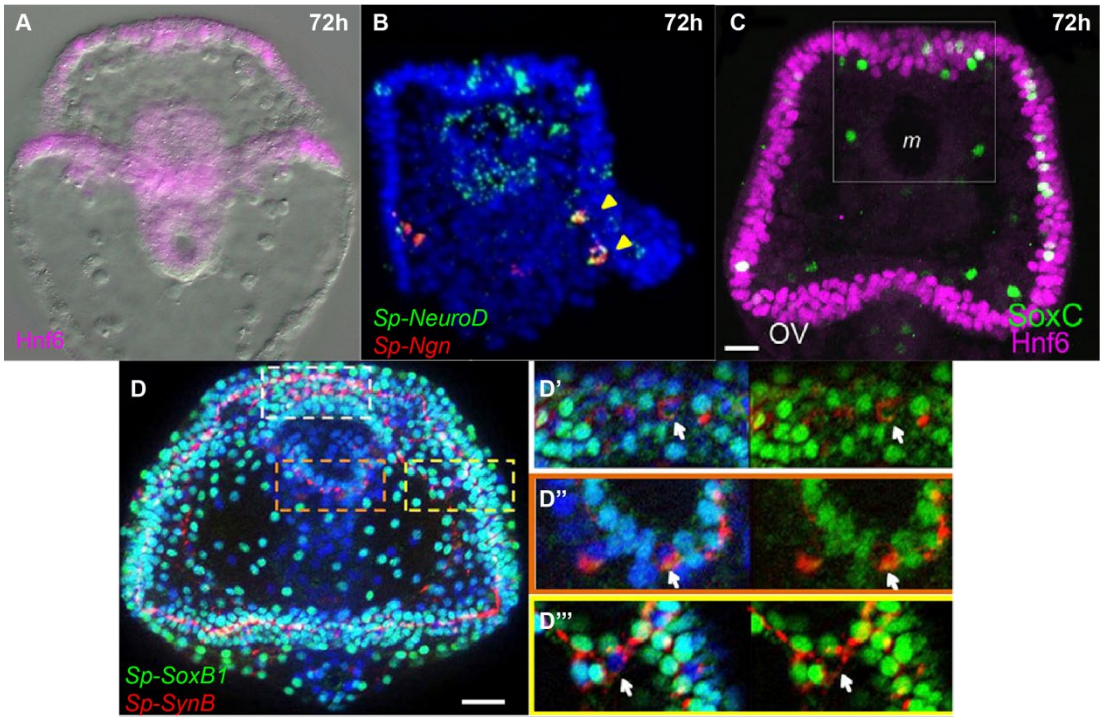

Figure 1.13 Terminal selector genes specifying the nervous system in the sea urchin

Localisation of transcription factor expression in sea urchin larval nervous systems using mRNA Fluorescence *in situ* hybridisation (FISH) (B) and immunohistochemistry (A, C-D). A) Localisation of Hnf6 antibody in ciliary band. B) Localisation of expression of the bHLH genes S*p-NeuroD* and *Sp-Ngn* in the apical organ, lateral ganglia and mouth. Panel image taken from (Perillo *et al.,* 2018). C) Distribution of SoxC expression in scattered ciliary band cells and mouth cells, with Hnf6 marking the whole of the ciliary band. Panel image taken from (Garner *et al.,* 2016) D) *Sp-SoxB1* expression in neuronal precursor cells and Sp-SynB expression in differentiated neurons; in D' – D''' note the absence of *Sp-SoxB1* expression in Sp-SynB positive differentiated neurons. Panel image taken from (Wei *et al.,* 2011).

1.4.2.3 Neuropeptides

The expression of some neuropeptides has been investigated in the sea urchin and other echinoderm larvae. The first neuropeptides to be identified in an echinoderm were the SALMFamides S1 and S2, which were isolated from the starfish *Asterias rubens* (Elphick *et al.,* 1991a, 1991b). Using antibodies to S1 and S2, Beer and collaborators produced the first description of a neuropeptidergic component of the sea urchin larval nervous system (Beer *et al.,* 2001). However, the molecular identity

of the immunoreactive molecules was unknown. The sequencing of the sea urchin genome has enabled the identification of genes encoding candidate secreted peptides in *S. purpuratus* (Burke *et al.,* 2006a), including genes encoding two types of SALMFamide: 1) F-type SALMFamides, which have a C-terminal motif Phe-X-Phe-NH_2, and 2) L-type SALMFamides, which like S1 and S2 have a C-terminal motif (Leu/lle)-X-Phe-NH_2 and which are presumably the neuropeptides that are recognised by antibodies to S1 and S2 (Rowe and Elphick, 2010). Other neuropeptide precursor (NP) genes identified in the genome of *S. purpuratus* include genes encoding paralogous precursors of vasopression/oxytocin-type neuropeptide echinotocin and the neuropeptide NGFFFamide (Burke *et al.,* 2006a; Elphick and Rowe, 2009; Semmens *et al.,* 2015).

Furthermore, a detailed analysis of cDNAs derived from a radial nerve cDNA library enabled the identification of 20 putative neuropeptide precursors in *S. purpuratus,* including: seven that share sequence similarity with known neuropeptides and 13 with no sequence similarity to known neuropeptides (Rowe and Elphick, 2010, 2012). Six additional putative NP genes were identified in *S. purpuratus*, in parallel with the discovery of homologs in other echinoderms (starfish *Asterias rubens*, brittle stars *Ophionotus victoriae*, *Amphiura filiformis* and *Ophiopsila aranea*) and also through phylogenomic studies (Jékely, 2013; Mirabeau and Joly, 2013; Semmens *et al.,* 2016; Zandawala *et al.,* 2017a). Mass spectrometry has also been used to determine the structures of some of the neuropeptides encoded by NP genes (Menschaert *et al.,* 2010; Monroe *et al.,* 2018; Rowe and Elphick, 2012; Semmens *et al.,* 2015). Characterisation of neuropeptides and neuropeptide receptors in *S. purpuratus* and other echinoderms has provided important insights into the evolution of neuropeptide signalling. For example, discovery of the receptor for NGFFFamide in *S. purpuratus* facilitated the reconstruction of the common evolutionary history of neuropeptide-S-type signalling in vertebrates and crustacean cardio active peptide (CCAP)-type signalling in protostomes (Figure 1.1) (Semmens et al., 2015).

Secreted peptide signalling molecules have also been identified in association with secretory cells in the larval sea urchin gut (Annunziata et al., 2019; Perillo et al., 2016). Perillo and Arnone reported specific cells in the anterior region of the gut that express

the *Sp-Insulin-like peptide 1* (*Sp-ILP1*) gene, together with other molecular markers typical of pancreatic endocrine-like cell types (Perillo and Arnone, 2014). In addition, expression of the neuropeptide *Sp-AN* has been revealed in two different populations of neurons in the apical organ and lateral ganglia (Perillo *et al.,* 2018).

1.4.2.4 G-protein coupled receptors (GPCRs)

The sequencing of the sea urchin genome enabled the identification of 979 rhodopsin-type and 161 secretin-type receptors (Burke *et al.,* 2006a; Raible *et al.,* 2006; Sodergren *et al.,* 2006). Raible and colleagues identified 55 best reciprocal blast hits against the human genome and the remaining were identified as surreal GPCRs (Raible *et al.,* 2006). Surreal GPCRs are defined as 'sea urchin specific rapidly expanded lineage' of GPCRs. These surreal GPCRs were divided into four groups: group A weakly associated to acetylcholine and serotonin receptors; group B very weakly associated to adrenergic, opsin, dopaminergic and melatonin receptors; group C similar to opioid receptors and group D similar to glycoprotein hormone receptors. Additional studies have identified GPCRs belonging to particular neuropeptide families. Burke and colleagues identified 37 orthologues of human rhodopsin-type GPCRs (Burke *et al.,* 2006a). Rowe and Elphick identified three gonadotropin releasing hormone GPCRs and a secretin-type GPCR, *Sp-Calcitonin Receptor* (Rowe and Elphick, 2012).

Raible and colleagues also performed spatial-temporal characterisation of a few surreal GPCRs (Raible *et al.,* 2006). Quantitative PCR was performed on six surreal GPCRs and they found four were expressed in larvae. Chromogenic ISH revealed one surreal GPCR is localised in single cells in the ectoderm, with cells located at the top of the post oral arms (Raible *et al.,* 2006). In summary, much is known about larval sea urchin nervous system in terms of neuronal transcriptions factor, signalling molecules and neurotransmitters. However, only a few NP genes and GPCRs have been characterised in the sea urchin larval nervous systems.

1.5 Aims of this thesis

The above introduction has provided a description of NP signalling systems, nervous systems and neuronal cell type evolution. Larval nervous systems, with relatively

small number of cells, are ideal systems to investigate neuronal cell type and nervous system evolution and function. Further, the phylum Echinodermata are both deuterostomes and invertebrates and so their unique phylogenetic position gives an opportunity to provide important insights into the evolution of neuronal cell types and nervous systems. Within the phylum Echinodermata, *S. purpuratus* is the best organism for developmental biology studies being well-studied and a range of experimental tools/approaches available. The sea urchin larval nervous system has been characterised in terms of neurotransmitters, transcription factors and developmental signalling molecules. However, little is known about the characterisation of a much larger group of signalling molecules - the neuropeptides.

My investigations are therefore governed by two main objectives: a) characterising the neuropeptide systems in *S. purpuratus,* and b) investigating the roles of neuropeptides in the sea urchin embryo and larva. By fulfilling these two objectives the diversity of neuronal cell types present in larval *S. purpuratus* as well as the functions of neuropeptides in the sea urchin larva can be determined. Furthermore, insights into NP signalling evolution, neuronal cell type evolution and nervous system evolution can be obtained by comparing *S. purpuratus* larvae with other indirect developing larvae and other bilaterians.

I address the first of these objectives in chapters 3 and 4. For simplicity, I have split these investigations in two parts. In chapter 3, a late embryonic and larval characterisation was performed from the late gastrula stage (48 hpf), when the first differentiated neurons are detected, to the early pluteus larval stage (72 hpf) when several populations of neurons exist in different tissue types. NPs were characterised during this period to provide a basis for the functional understanding of the neurochemical complexity of the larval nervous system. In chapter 4, early embryonic characterisation was performed from fertilisation (0 hpf) to an early gastrula stage (45 hpf), before the first differentiated neurons are detected. NPs were characterised at this early embryonic stage to address the question: Do NP genes have a role in non-neuronal cells? Can they have a generic role as signalling molecules?

In the first part of chapter 3 I discuss the complement of NP signalling systems in the sea urchin. In the second part of chapter 3 I present the temporal expression of NP genes by quantitative PCR (QPCR) during late embryonic and larval development. In the first part of chapter 4 I present the temporal expression of NP genes by QPCR during early embryonic development. In the last sections of chapter 3 and 4 I present the spatial expression of many neuropeptides by chromogenic ISH. In chapter 3, I also present double fluorescent ISH data and create a single-cell resolution map of different combinations of NP genes in neuronal precursor cells and neuronal cells at the late gastrula (48 hpf) and pluteus larval (72 hpf) stage, respectively.

In chapter 5, I present work done to optimize a CRISPR/Cas9 gene-editing methodology to induce knockout mutations in sea urchin embryos. This chapter provides a prerequisite for my second objective, where I investigate the roles of NP genes in the sea urchin embryo and larva (Chapter 6). I provide a history of gene perturbation and describe the benefits of the CRISPR/Cas9 system. I then present how we tested and optimised the efficiency and specificity of the *in vivo* CRISPR/Cas9 system in the sea urchin. Finally, I present the optimisation of an *in vitro* Cas9 digestion assay and provide a comparison between *in vivo* and *in vitro* studies.

The second objective of my research is addressed in Chapter 6. Here I focus on the role of a Thyrotropin-releasing hormone (TRH) signalling system in the sea urchin embryo and larva. In the first part of this chapter I highlight the presence/absence of TRH signalling and the thyroid hormone (TH) synthesis pathway across Bilateria. I then reveal the presence of a TRH signalling system in *S. purpuratus*. In the second part, I present the spatial and temporal expression of *Sp-TRH*, *Sp-TRH-Receptor* and TH synthesis genes. In the final part, I investigate the role of *Sp-TRH* and *Sp-TRHR* by CRISPR/Cas9 knockouts and MO knockdowns. I then identify downstream genes of TRH NP signalling and I elucidate the molecular mechanism for TRH NP signalling in larval skeleton growth by using a combination of inhibitors, chromogenic ISH, immunohistochemistry and QPCR.

In chapter 7, I present a discussion of the work in this thesis with three main themes that are centred around NP signalling systems: 1) the identity of neuronal cell types,

2) the evolution and functions of TRH-type signalling, and 3) the evolution of neuronal cell types and nervous systems. Finally, I will provide some future directions and concluding remarks.

Chapter 2 Materials and Methods

Here I present the general materials and methods that were used in this thesis. They consist of bioinformatics tool (section 2.1), molecular cloning (2.2), CRISPR/Cas9 (section 2.3), embryological techniques (section 2.4), RNA quantification (section 2.5) and ligand assays (section 2.6).

To ease reading primers sequences (sections 8.1) and recipes (section 8.2) can be found in the appendix, while reaction mixtures are included in tables in this chapter.

2.1 Bioinformatics

2.1.1 Identification of homologues

To identify sea urchin and other bilaterian homologues of NP genes, GPCR genes and thyroid hormone (TH) control pathway genes, BLAST (Basic Local Alignment Search Tool) (Altschup *et al.,* 1990) search was performed against the sea urchin protein database (URL:http://www.echinobase.org/Echinobase/Blast/SpBlast/blast.php) and NCBI protein database. A reciprocal best hit with BLAST was always performed using the putative homolog as a query to confirm orthologue to the original query. (All genes identified in this thesis can be found in the appendix Table 8.14)

NP genes were validated by the identification of a signal peptide (URL :http://www.cbs.dtu.dk/services/SignalP-3.0/) and predicted cleavage sites and repetitive peptide sequences.

2.1.2 Phylogenetic Analysis

To validate the relationship of the echinoderm TRH receptors with TRH-type receptors from other taxa, a phylogenetic tree was generated using the maximum-likelihood method (see appendix Table 8.15 for the list of sequences). Receptor sequences were aligned using the MUSCLE plugin in MEGA 7 (iterative, 10 iterations, UPGMB as clustering method) (Edgar, 2004; Kumar *et al.,* 2016). The maximum-likelihood tree was generated using W-IQ-tree online version 1.0 (1000 bootstrap replicates, LG+G+I+F substitution model) (Trifinopoulos *et al.,* 2016) The phylogenetic tree was generated by Luis Alfonso Yañez Guerra.

2.2 Molecular cloning

2.2.1 Primer design

To clone specific fragments corresponding to the desired genes cloning primers were designed using Primer3 software (URL:http:// frodo.wi.mit.edu/primer3/) (Rozen and Skaletsky, 1999). Default parameters were used with a few exceptions max poly-x was changed to 3.00 and max 3' stability was changed to 8.00. The minimum product length for WMISH probes was set at 600 nucleotides, but we saw that the larger fragments gave better signal, thus primers were then designed to amplify the largest possible fragment based on the template sequence (Table 8.3). Suggested primers were searched in the sea urchin genome using BlastN to check for any off-target binding. Designed primers were then ordered from Eurofins Genomics (https://www.eurofinsgenomics.eu) and 100 mM stock solutions were prepared from the lyophilised product. For a complete list of cloning primers used and gene information, see appendix Table 8.2.

2.2.2 PCR amplification

Polymerase Chain Reaction (PCR) was used to amplify a specific fragment of a desired gene to clone into a plasmid vector for different purposes. The gene was amplified using the C100 Thermal Cycler PCR machine and Q5 High-Fidelity DNA Polymerase obtained from New England Biolabs according to manufacturer's instructions (see Table 2.1 and Table 2.2 below). The NEB Tm Calculator (URL:http://tmcalculator.neb.com/#!/) was used to determine the optimal annealing temperature for a given set of primers. In cases where we struggled to clone a specific fragment, a gradient PCR was performed where we used a range of annealing temperature ±5°C of the optimal NEB temperature. A positive control of a set of primers, known to work reliably, were used as well as a negative control where water was used in instead of cDNA.

PCR using Q5 High-Fidelity DNA Polymerase	
5X Reaction Buffer	5 µL
10mM dNTPs	0.5 µL
10uM Forward primer	1.25 µL
10uM Reverse primer	1.25 µL
Template DNA	variable
Q5 High-Fidelity DNA Polymerase	0.25 µL
Nuclease-free water	up to 25 µL

Table 2.1 Q5 High-Fidelity PCR

Thermocycler conditions for Q5 High-Fidelity PCR		
Step	Temperature	Time
Initial Denaturation	98°C	2 minutes
25-35 amplification Cycles	98°C	10 seconds
	50-72°C	30 seconds
	72°C	30 seconds/kb
Final extension	72°C	2 minutes
Hold	4°C	

Table 2.2 Thermocycling conditions for Q5 High-Fidelity PCR

2.2.3 PCR clean up and gel extraction

To determine the outcome of the PCR reaction, 3 µL of the reaction were analysed on a 1% TBE gel electrophoresis for the correct product size (base pairs) by comparing to a 1 kb plus molecular weight marker (Invitrogen). If a single band of the desired product size was detected, the remaining PCR product was purified to remove primer dimers, polymerase and unincorporated nucleotides using the Macherey-Nagel PCR clean-up and gel extraction kit. In cases where multiple PCR products were amplified,

the band corresponding to the predicted product size was excised from the gel, extracted using a dialysis membrane and purified with the kit used above. Manufacturer's instructions were followed, with the exception of the elution step. Samples were eluted in a total of 30 µl of 10 mM TRIS pH 8.5, in two series of 15 µl and heated to 70°C to increase the amount of DNA recovered. The DNA product quantity and quality were determined on a NanoDrop spectrophotometer and the DNA product was then re-analysed on a gel electrophoresis. Recipes for solutions in methods 2.2 can be found in appendix section 8.2.1.

2.2.4 A-tailing

The blunt end purified PCR products were then A-tailed to enable the PCR fragment to be ligated into the pGEM-T Easy vector (Promega) with a T-protruding overhang. The A-tailing reaction was incubated at 72°C for 20 to 30 minutes before progressing to the ligation step, see **Table 2.3** for reaction mixture details.

A-tailing	
DNA fragment	16 µL
10X buffer (without $MgCl_2$)	2 µL
dATP (100 µM)	0.5 µL
$MgCl_2$ (50 mM)	0.5 µL
Taq polymerasw (Invitrogen)	0.5 µL
Nuclease-free water	up to 25 µL

Table 2.3 A-tailing reaction

2.2.5 Ligation

In order to have a stable clone of the desired gene, A-tailed PCR products were ligated into the pGEM-T Easy Vector (Promega) according to manufacturer's instructions (see Table 2.4 below). An ideal ratio of vector to fragment of 1:3 or 1:6 was used. The ligation was either incubated at room temperature for 2 hour or 14°C overnight (or over weekend). A positive control of a control DNA insert, provided by Promega was

used, as well as a negative control where no DNA was inserted was used to count the percentage of background non-recombinant colonies after transformation.

Ligation	
Vector (50ng)	1 µL
2 x Ligation Buffer	5 µL
Insert (1:3 to 1:6 ratio)	X µL
T4 ligase	1 µL
DEPC-H_20	up to 10 µL

Table 2.4 Ligation reaction

2.2.6 Transformation into competent bacterial cells

The vector containing the desired PCR fragment was then transformed into bacterial cells, whereby chemically competent *E. coli* cells have foreign DNA inserted into them. 5 µL vector was transformed with 50 µL DH5α *E. coli* competent cells (Invitrogen) and incubated on ice for 30 minutes. The cells where then heat shocked at 42°C for 45-50 seconds and immediately cooled on ice for 2 minutes. 950 µL SOC medium (Invitrogen) was added to the tube and incubated at 37°C for 1 hour. 100 µL and 900 µL of transformed bacteria were plated onto separate Luria Broth (LB) plates containing 100 µl/mL of ampicillin and 50 µg/mL X-gal and were incubated overnight at 37°C. X-gal was added to each plate to select transformants using blue/white screening. Recombinant clones can be identified as white because they interrupt the coding sequence of the lacZ gene, so the ß- galactosidase enzyme is not produced and cannot break down X-gal to give blue pigmentation. If there was a low transformation efficiencies then highly efficient One Shot® TOP10 chemically competent *E. coli* cells were used, according to manufacturer's instructions.

2.2.7 Screening of recombinant colonies (Colony PCR)

To do large-scale screening of recombinant colonies with the desired length a colony PCR was used to amplify the fragment from T7 and SP6 primers at each side of the cloning site. Single white colonies were inoculated into 20 µL of LB broth containing

100 µl/mL of ampicillin and incubated at 37°C for 1 hour. A colony PCR reaction was set up using Invitrogen Taq Polymerase components in a final volume of 20 µl with 2 µl of LB containing the selected colony with the transformed plasmid (see Table 2.5 for reaction details). PCR thermo cycling conditions were as follows: denaturation at 95°C for 5 minutes, 30 amplification cycles as follows: denaturation at 95°C for 30 seconds, annealing at 55°C for 30 seconds, elongation at 72°C for 1 minute/kb of fragment size, and a final extension step of 72°C for 8 minutes. To determine the outcome, 10 µL of the reaction was analysed on a gel electrophoresis and recombinant colonies were selected.

Colony PCR	
10X Reaction Buffer (without $MgCl_{2)}$	2 µL
$MgCl_2$ (10mM)	0.6 µL
dNTPs (10mM)	0.4 µL
T7 primer (10µM)	0.8 µL
Sp6 primer (10µM)	0.8 µL
Template DNA	2 µL
Invitrogen Taq Polymerase	0.5 µL
Nuclease-free water	up to 20 µL

Table 2.5 Colony Invitrogen PCR

2.2.8 Plasmid DNA preparation (Miniprep)

To make large yields of cDNA, 5 µL of selected bacterial recombinant colonies were separately inoculated into 4 ml of LB broth as described above and grown overnight at 37°C in an agitating incubator at 225 RPM. The following day, a glycerol stock of the bacterial colony was made for long-term storage. 750 µL of 50% glycerol was mixed with 750 µL of the bacterial colony and stored at -80°C. A Nucleospin Plasmid Kit (Macherey-Nagel) was used to extract and purify the plasmid DNA contained within the remaining *E.coli*, following manufacturer's instructions. The concentration of plasmid DNA/miniprep was then tested on a NanoDrop spectrophotometer.

2.2.9 DNA digestion

Two methods were used to ensure we had the correct colony, firstly a restriction enzyme digestion and then secondly, sequencing. First, a restriction enzyme digestion was performed to check if we had the correct product size incorporated into the plasmid. For this the two EcoRI (12U/ µL; Promega) digestion sites at each side of the pGEM-T Easy Vector cloning site were used. A digestion reaction was performed in a final volume of 20 µL with 2 µL of the purified miniprep. The reaction was incubated 37°C for at least 1 hour and the digested product size was visualised by a gel electrophoresis.

Plasmid digestion	
10x H Buffer	2 µL
Miniprep	2 µL
EcoRI	0.2 µL
Nuclease-free H_20	15.8 µL

Table 2.6 Diagnostic digestion reaction

2.2.10 DNA sequencing

The correct insert sequence of a miniprep was determined by sequencing at Source Bioscience (URL:https://www.sourcebioscience.com). 1µg of the miniprep was sent and Sp6 or T7 primer was used (provided by the company) to amplify one strand of DNA and check the orientation of the insertion in the vector. The returned sequences were then blasted against the *S. purpuratus* genome (URL:http://www.echinobase.org/Echinobase/Blast/SpBlast/blast.php) to check they matched to the genes initially selected.

2.3 CRISPR/Cas9 system

2.3.1 sgRNA design

sgRNA were designed by comparing the predictions of several online CRISPR targets, ZiFIT (http://zifit.partners.org/ZiFiT/), CHOPCHOP (http://chopchop.cbu.uib.no), CRISPR direct (https://crispr.dbcls.jp), and gRNA Scorer 1.0 (https://crispr.med.harvard.edu/gRNAScorerV1/) and were shortlisted using criteria discussed in section 5.2.

2.3.2 sgRNA synthesis

2.3.2.1 Template oligos preparation

sgRNA were synthesised by making sgRNA DNA templates using a "cloning-free short-guide oligo" method adapted from Talbot and Amacher V3.2 protocol (Talbot and Amacher, 2014). The guide oligo is a synthetic DNA strand, which is used to generate a template for guide RNA synthesis. It consists of a short clamp, a T7 promoter, a variable targeting sequence and a Cas9 binding scaffold. To synthesise the guide oligo, three constant primers and one variable primer were used for each sgRNA and fused together by PCR (Table 2.7; Table 8.10; Table 8.11). See Table 2.7 below for PCR reaction. PCR thermocycling conditions were as follows: denaturation at 95°C for 1 minute, 35 amplification cycles as follows: denaturation at 95°C for 15 seconds, annealing at 57°C for 30 seconds, elongation at 72°C for 20 seconds, and a final extension step of 72°C for 5 minutes. This was adapted from the Talbot and Amacher protocol by reducing the number of PCR cycles and increasing the concentration of the longer primers (C and D) in order to reduce the occurrence of non-specific amplification (Talbot and Amacher, 2014). The PCR fusion product was then analysed on a gel electrophoresis with 3% high-resolution agarose (Sigma-Aldrich) and a 100 bp molecular weight ladder to confirm a single band at 120 bp. The PCR product was purified using the Macherey-Nagel PCR clean- up and gel extraction kit as described above.

PCR fusion	
10x Reaction Buffer	5 µL
$MgCl_2$	3 µL
gRNA Forward oligo (Primer C) (10µM)	1.25 µL
gRNA Reverse oligo (Primer D) (10µM)	1.25 µL
Specific-guide oligo (Primer A) (1µM)	2 µL
Guide-constant oligo (Primer B) (1µM)	2 µL
dNTPs (10µM)	1 µL
Invitrogen Taq Polymerase	0.75 µL
Nuclease-free H_20	33.75 µL

Table 2.7 PCR fusion reaction mixture

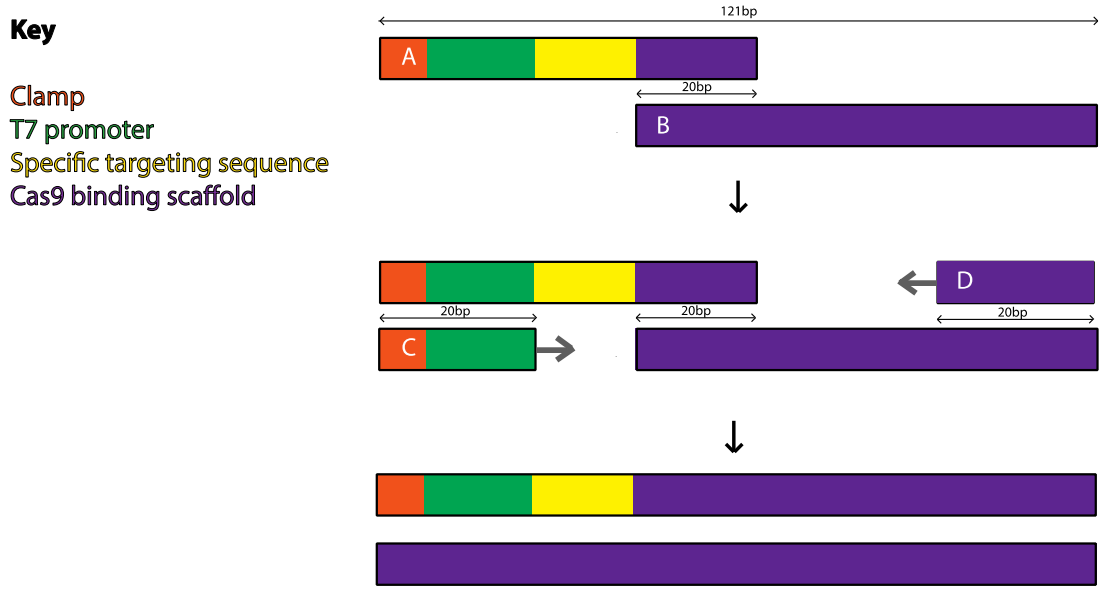

Figure 2.1 An illustration of sgRNA guide oligo synthesis via PCR fusion

The two longer primers, the specific -guide oligo and the guide-constant oligo (A and B) anneal in a 20-base pair region of the Cas9 binding scaffold. Two constant 21-base pair nucleotide primers (C and D) bind at the 5' end of each larger primer and extend the nucleotide sequence to make an sgRNA DNA template.

2.3.2.2 Guide-oligo transcription

The double-stranded guide fragment was then transcribed to mRNA using the MEGAshortscript T7 Transcription kit (Thermo Fisher), according to manufacturer's instructions with the following exceptions, a maximum of 500ng of sgRNA DNA template was transcribed. The transcription reaction was incubated for 4 hours at 37°C and then 1 µL of DNase was added and incubated at 37°C for 15 minutes to degrade the DNA. We had issues with the RNA containing free nucleotides after precipitating with 3M NaAc and therefore, the true concentration of sgRNA RNA was disguised. The following changes were introduced thereafter. Prior to precipitation, the transcribed product was purified using Mini Quick Spin RNA Columns G-50 Sephadex (Sigma-Aldrich) to remove any free nucleotides. The purified RNA was then precipitated following manufacturer's instructions using 3M NaAc. The RNA was eluted in DEPC-treated pyrogen-free water and working stock aliquots made at 100 ng/µL and stored at -80°C.

2.3.3 Cas9 synthesis

2.3.3.1 Template Cas9 preparation by plasmid digestion

pT3TS-ncas9n plasmid (Addgene #46757) was gifted from Ina Arnone. The pT3TS-ncas9n variant was chosen because it features a nuclear localisation sequence to promote transport to the nucleus after translation. The Cas9 template was linearised for transcription by digesting 5 µg of the plasmid with the restriction enzyme Xbal, located at the 3' end of the Cas9 insert fragment. 1 µL of the linearised plasmid DNA was analysed on a gel electrophoresis, next to the undigested plasmid to confirm the plasmid was fully digested. The linearised plasmid DNA was then purified using the Phase lock gel (PLG) phenol chloroform extraction kit (5 Prime), following manufacturer's instructions. The Cas9 linearised plasmid was precipitated using 3M NaAc and 100% ethanol at least overnight at -20°C. The linearised plasmid was eluted in 20 µL DEPC-treated pyrogen-free water. The quality and concentration of the purified linearised plasmid was analysed by gel electrophoresis and a Nanodrop.

2.3.3.2 Cas9 mRNA synthesis

The purified linearised plasmid was transcribed to give the sense strand using the T3 mMESSAGE mMACHINE Transcription Kit (Ambion CAT AM1348), following manufacturer's instructions with the exceptions discussed in section 2.3.2.2 above. The RNA was eluted in DEPC-treated pyrogen-free water and aliquots were stored at -80°C.

2.3.4 Genotyping

To validate a successful injection, individual larvae were genotyped using gel electrophoresis and DNA sequencing. Gel electrophoresis was suitable for large scale deletions induced by injecting multiple sgRNAs, while DNA sequencing could monitor smaller indels as well as larger deletions.

DNA was extracted from single larvae using the QIAamp DNA Micro Kit (Qiagen, #56304), following manufacturer's instruction with the following exceptions. Samples were lysed at 56°C for a minimum of 40-75 minutes and maximum overnight. DNA was eluted in 10 µL of Buffer AE incubated at room temperature for 5 minutes, centrifuged and repeated.

2.3.4.1 Gel electrophoresis visualisation

The genomic DNA of uninjected and injected larvae were PCR amplified for specific target gene regions (*Sp-Jun*, *Sp-PPLN1*, *Sp-PKS1* and *Sp-TPH*) (see appendix Table 8.13 for genotyping primers). 5 µL of the PCR product was analysed on a gel electrophoresis with the aim of visualising a larger wild type gene fragment in uninjected larvae and a smaller deleted gene fragment in the injected larvae.

2.3.4.2 DNA Sequencing

The PCR amplified specific target regions of *Sp-Jun* were purified using the Macherey-Nagel PCR clean-up and gel extraction kit and were sequenced using Sanger Sequencing, using a ABI3730xI DNA Analyzer (UCL, GEE). The sequenced reads of uninjected and injected larvae were compared on a chromatogram trace viewer (4 peaks).

2.3.5 *in vitro* assay

In vitro assays were performed with the aim of testing sgRNA efficiency. This protocol was adapted from the NEB *in vitro* digestion of DNA with Cas9 Nuclease V1 (URL: https://international.neb.com/protocols/2014/05/01/in-vitro-digestion-of-dna-with-cas9-nuclease-s-pyogenes-m0386). *In vitro* assay experiments were performed by David Axford.

The optimisation of the assay is described in section 5.4. The final optimised protocol is as follows, all reagents except the substrate DNA (see Table 2.8 below) were incubated at RT for 10 minutes in order for sgRNA to form complexes with the Cas9 protein (NEB M0386). The substrate DNA was then added in a molar ratio of 10 times more than the sgRNA and the digestion reaction was incubated at 37°C for 1 hour. 0.5 µL of 0.5M EDTA was added and the digestion was incubated at 65°C for 30 minutes to inactivate the Cas9 enzyme. Alternatively, 1 µL of Proteinase K (25 mg/mL) was added and the digestion was incubated at 37°C for 40 minutes to inactivate the Cas9 enzyme. DNA fragments were then analysed by gel electrophoresis.

***In vitro* digestion reaction**	
10X Cas9 nuclease reaction buffer	3 µL
sgRNA (100 ng/µL)	1 µL
Cas9 nuclease *S. pyogenes* (159 ng/µL)	2.5 µL
Nuclease-free water	up to 28µL including substrate DNA
Pre-incubation for 10 minutes at RT	
Substrate DNA (100nM)	2.0 µL

Table 2.8 *in vitro* digestion reaction

2.3.6 Gel Image Analysis

Gel images were analysed using the in-built gel analysis tool in FiJi software. The intensity of individual peaks was normalised against the intensity of the entire line. Efficiency scores were calculated as the proportion of DNA that has been digested compared with negative undigested control.

2.4 Embryological techniques

2.4.1 Animal Husbandry and embryonic and larval cultures

Adult purple sea urchin *Strongylocentrotus purpuratus* were obtained from Patrick Leahy (Kerchoff Marine Laboratory, California Institute of Technology, Pasadena, CA, USA) and housed in closed seawater aquaria at University College London at 14^{o}C. Gametes and embryos were obtained from *S. purpuratus* and cultured as previously described (Leahy, 1986). Spawning was induced by vigourous shaking of animals or by intracoelomic injection of approximately 1 mL of 0.5M KCL. Eggs were collected in 34.6 ppt salinity filtered artificial seawater (FASW) and kept at 15°C for up to 24 hours. In contrast, sperm were collected dry into a 1.5 mL e76ppendorf tubes and kept at 4°C for up to 2 weeks. Once sperm are added to FASW they remain active for approximately 30 minutes, therefore they were kept dry until needed. Eggs were passed through a 200 µM nitex filter to remove any large debris and washed twice with fresh FASW. Sperm were freshly diluted in FASW (1:1000) and added to a desired amount of unfertilised eggs, at a final 1:10 ratio of egg:sperm. Fertilization was monitored by observing the elevation of the fertilisation membrane through a dissecting microscope. The efficiency of fertilisation gives an indication of the quality of the eggs/sperm and generally cultures were only processed further when fertilisation efficiency was higher than 75%. Excess sperm was removed by washing fertilised eggs twice with FASW. Embryos are cultured at 15°C in FASW containing antibiotics streptomycin (50µg/mL) and penicillin (20U/mL) to stop bacterial growth. If the culture was needed before hatching (15 hpf) then 2mM 4-Aminobenzoic acid (PABA) was added to FASW to soften the fertilization membrane. Embryos were then passed through a 63 µM filter and their fertilization membrane could be easily removed. No ethical approval was needed as *S. purpuratus* is not subject to any animal care regulations. Recipes for solutions in methods 2.4 can be found in appendix section 8.2.

2.4.2 Inhibitor experiments

Both SU5402 (Calbiochem) and Axitibin (Sigma) were prepared as a 5 mM stock in DMSO, and were stored at -20°C. Embryos were cultured in 3 mL flat-bottom 12-well

plates (Falcon) with 2mL of culture (500 embryos/mL). SU5402 and Axitibin were added to the embryos at the late gastrula stage (48 hpf) at concentrations of 10 µM/20 µM and 50 nM, respectively. Additional embryos were also cultured in FASW and DMSO in parallel and were used as controls. Pluteus larvae were fixed for ISH experiments as described below.

2.4.3 EdU cell proliferation assay

The cell proliferation assay was carried using the Click-iT® EdU HCS Assay (Invitrogen). Embryos were fertilised and cultured in 3 mL flat-bottom 12-well plates (Falcon) with 2mL of culture (500 embryos/mL). Larvae at four days of development were incubated with a 10mM stock solution of ethynyl deoxyuridine (EdU) for two hours at room temperature. Larvae were fixed in 4% paraformaldehyde (PFA) (Electro Microscopy Sciences Cat. No.15710) in PEM buffer and washed as follows: 1) three times in PBST (0.1% Tween), 2) one time in PBSTx (0.01% Triton x-100) for 45 minutes, 3) two washes in PBST, 4) one wash in 100% methanol for two minutes on ice, 5) twice with PBS and 6) twice with PBST. The Click-iT reaction mixture (Click-iT™ EdU Alexa Fluor™ 555 Imaging Kit, Thermo Fisher) was added to the larvae and incubated for 30 minutes at RT. The larvae were then washed with the Click-iT reaction rinse buffer for 30 minutes and the washed twice with PBST.

2.4.4 Fixing embryos and larvae

Sea urchin embryos develop synchronously up to pluteus larval stage and thus, they reach a desired developmental stage at the same time if they are cultured at the same temperature. To fix embryos and larvae for whole mount *in situ* hybridisation (ISH), specimens were collected at the desired developmental stage and left to settle on ice in a falcon tube. A few µL's of 16% PFA were added to the falcon tube to help them 'settle'. Once specimens had settled FASW was removed and the samples were washed twice in fresh fixative solution. Embryos and early plutei larvae (up to 72 hpf) were fixed in Fixative 2, while later developing larvae were fixed in Fixative 1 at least overnight at 4°C with a 1:10 ratio of sample pellet to fixative solution. The specimens were then washed five times in cold MOPs buffer and gradually dehydrated on ice

with cold ethanol (30%, 50% and two 70% washes). Fixed specimens were stored indefinitely in 70% ethanol at -20°C.

To fix specimens for immunohistochemistry, they were collected as described above and fixed in 4% PFA in either phosphate-buffered saline (PBS), PEM or FASW at room temperature for 5-15 minutes. The specimens were then washed three times in PBS or PBST (PBS with 0.1% Tween) and stored temporarily at 4°C. For long term storage they were washed with 0.01% sodium azide (NaN_3) in PBS/PBST to stop bacterial growth and stored at 4°C.

2.4.5 Probe template preparation

In order to amplify the desired fragment from a miniprep, a PCR was performed using primers that sit outside of *both* RNA polymerase promoter sites. PCR was performed using the Invitrogen Taq Polymerase kit, M13F and M13R primers and 1 ng/µL of a miniprep. The product size of template PCR product was analysed on a gel electrophoresis, purified and concentration was measured on a NanoDrop spectrophotometer. The template DNA was stored at -20°C.

2.4.6 Orientation PCR

To rapidly prepare the probe template (before the sequencing results received) an orientation PCR was sometimes performed. This was done to quickly check the orientation of the insertion in the vector, relative to T7 and Sp6 polymerase promoters for subsequent *in vitro* probe transcription. Using Invitrogen Taq polymerase kit, the M13F or M13R primers in two separate reactions were paired with a gene specific forward primer and the one reaction that amplified a single band with the correct product size was purified and directly used for *in vitro* transcription of an anti-sense probe.

2.4.7 Antisense probe synthesis for *in situ* hybridization

In order to hybridise with target mRNA, a single strand anti-sense probe had to be transcribed using either Digoxigenin (DIG) or Dinitrophenol (DNP). The orientation of the insert fragment in the vector was determined from sequencing (and an orientation PCR) and the correct polymerase to synthesise the antisense strand was

chosen. Transcription reactions were carried out in a total volume of 20 µL using either Sp6 or T7 RNA Polymerase (Roche) depending on the miniprep, see Table 2.9 below. To prevent RNA degradation, RNase inhibitor (Roche) was used in all reactions. The transcription reactions with T7 polymerase were incubated at 37°C for 2-3 hours. The Sp6 enzyme seemed to be less efficient and so incubations with Sp6 were increased to 5 hours.

Transcription reaction	
10X transcription buffer	2 µL
10X DIG mix	2 µL
DNA (100-500ng)	X µL
RNA Polymerase (Sp6 or T7)	1.6 µL
RNase inhibitor	0.4 µL
Nuclease-free H_20	Up to 20 µL

Table 2.9 Transcription reaction

15-30 minutes before the end of the incubation, 1 µL of the transcription reaction was analysed on a gel electrophoresis to check for presence of RNA. After RNA was visualised, 1 µL of RNase-free DNase (10U/µL; Roche) and 2 µL of 10x incubation buffer were added and incubated for 15 minutes at 37°C to stop the reaction and remove the DNA template. To remove free nucleotides the RNA transcripts were precipitated with 30 µL DEPC-treated water and 25 µL 7.5M LiCl, the reaction was incubated at -20°C at least overnight. The following day the sample was centrifuged for 10 minutes at the maximum speed (Vmax) in a microcentrifuge (Eppendorf model 5424). The pellet was washed twice in 200 µL 80% ethanol. The supernatant was removed, and the pellet was left to dry underneath a heat lamp until all the residual ethanol had evaporated (for a maximum of 10 minutes). The RNA probe was dissolved in 50 µL DEPC-treated water and then the concentration was measured on a NanoDrop. RNA probes were analysed on a gel electrophoresis to check for absence of probe degradation.

To make a DNP labelled RNA probe, we followed the same protocol as above with the exception of adding the DIG labelling reagent. The cold RNA probe was subsequently labelled with Label It DNP labelling kit (Mirus corporation) in a total volume of 50 µL using the reagents in Table 2.10 see below.

DNP labelling reaction	
RNA (100-500 ng)	X µL
10X Mirus Labelling Buffer A	5 µL
Label it DNP reagent	5 µL
Nuclease-free H_20	Up to 50 µL

Table 2.10 DNP labelling reaction

The DNP labelling reaction was incubated for 2 hours at 37°C. To remove unincorporated DNP, the RNA probes were purified using the Mini Quick Spin RNA Columns G-50 Sephadex (Sigma-Aldrich) following manufacturer's instructions. Aliquots of DIG and DNP probes were made at a concentration of 50 ng/µL and stored at -80°C.

2.4.8 *In situ* hybridisation

To detect spatial gene expression, *in situ* hybridisation (ISH**)** techniques were used on wild-type, gene perturbed, or inhibitor-treated whole embryos at different developmental stages. The protocols for chromogenic and fluorescent ISH described in this section and the next have been adapted from (Andrikou *et al.,* 2013; Cole *et al.,* 2009; Croce and McClay, 2010; Minokawa *et al.,* 2004). ISH experiments were performed in 1.5 mL eppendorf tubes (Eppendorf) or 200 µL wells of 96-well plates (Costar). 1 mL washes were performed in tubes, while 100 µL washes were performed in the wells, with the exception of FISH detection step when as little as 50 µL was used. To ensure sufficient exchange of solutions additional washes were introduced for most steps when ISH experiments were performed in the 200 µL wells.

2.4.8.1 Fluorescent *in situ* hybridisation

The embryos/larvae were first rehydrated with graded ethanol washes (70%, 50% and 30%), washed four times in Tris-buffered saline and 0.1% Tween-20 (TBST) at RT, incubated for 1 hour in hybridisation buffer at 60-65°C and finally they were incubated overnight at 60-65°C in hybridisation buffer with 0.03-0.05 ng/µL of antisense DIG and DNP labelled probes. To remove excess probe the hybridized samples were washed in a 1:1 ratio of TBST:hybridisation buffer at 60 - 65°C, then washed four times in TBST at 60-65°C. This was followed by two washes in 1X Saline Sodium Citrate (SSC) and a single wash in 0.1X SSC at the same temperature. The samples were then re-equilibrated in TBST at RT (2X washes) and probe detection was carried out with the Tyramide Signal Amplification (TSA) Systems (Perkin Elmer) using antibodies conjugated with horse-radish peroxidase (HRP/POD). ISH probes were detected singularly and sequentially. Samples were incubated with 1:2000 dilution of Anti-DIG-POD Fab fragments (Roche) or Anti-FLUO-POD, Fab fragments (Roche) or Anti-DNP-HRP (Perkin Elmer) in Perkin Elmer blocking buffer (PERB-0.5M in TBST according to the manufacturer's instructions) for 1 hour at RT for anti-DIG antibodies, and overnight at RT for anti-DNP antibody. Samples were washed several times at RT with TBST, and then incubated in amplification wash diluent for 30 minutes at room temperature. Samples were then stained with 1X amplification diluent containing 1:400 dilution of Cy3 for 45 min or with 1X amplification diluent containing 1:400 dilution of Cy5, for 90 min. After washing with TBST to remove background staining, the horseradish peroxidase activity had to be completely eliminated to allow the second staining. For this purpose, the samples were washed once in 1% H_2O_2, once in TBST, then once in glycine solution and then washed three times with TBST. Samples were then blocked in PERB and incubated overnight, with the second antibody as described above.

FISH for *Sp-TRH* (DNP probe) and *Sp-TRHR* (DIG probe) was performed as described above, with the exception that MABT was used instead of TBST and SSC.

2.4.8.2 Chromogenic *in situ* hybridization

Chromogenic ISH was conducted as described above with the following modifications. All washes were done in MABT instead of TBST and SSC. Samples were

incubated in hybridization buffer with DIG-antisense labelled probes at 55-65°C for a minimum of three days to a maximum of a week. Post hybridization washes were done at the hybridization temperature, one wash with half fresh hybridization buffer and half MABT, two washes in 1X MABT for 10 minutes, two washes in 1X MABT for 30 minutes and one wash in 0.1X MABT for 30 minutes. Two washes in 1X MABT for 10 minutes were done at RT. The samples were then incubated in blocking buffer (1X MABT with 5% goat serum) for 30 minutes at RT. Anti-DIG- alkaline phosphatase (AP) Fab fragments (Roche) were added at the dilution of 1:2000 in blocking buffer. The excess of antibody was removed by washing the samples four times with 1X MABT at RT for 10 minutes. Samples were then washed twice with AP buffer for 30 minutes at RT. At this point embryos were transferred to staining buffer containing 10 µL of NBT/BCIP ready mix solution (Roche). Staining was developed in the dark, at RT and monitored under a dissecting microscope. When a suitable level of staining had developed, the staining reaction was stopped by washing few times in 1X MABT containing 0.05M EDTA and transferred gradually into 50% glycerol and stored at 4°C indefinitely.

2.4.9 Immunohistochemistry

Embryo and larvae at the desired stage were fixed as described above. For anti-serotonin, anti-acetylated tubulin and anti-Hnf6, samples were washed once in PBSTx (0.01% Triton x-100 in PBST) for 20 minutes, then twice in PBST. For anti-synaptotagminB (1E11) the samples had an extra step with 100% methanol for two minutes on ice, followed by two washed in PBS and two in PBST. anti-TRH samples were washed in PBS only and were not permeabilised with triton or methanol.

Before incubation with primary antibody, samples were incubated in blocking buffer (4% goat serum in PBST) for 30 minutes at RT. Primary antibodies were diluted in blocking buffer (see Table 2.11 below for dilutions) and incubated overnight at 4°C. The excess antibody was removed by washing the samples four times in PBST at RT. Secondary antibodies Alexa 488 goat anti-rabbit, Alexa 633 donkey anti-mouse and Alexa 488 goat anti-mouse (Thermo Scientifics) were used at a dilution of 1:250 in blocking buffer. The excess antibody was washed out with three PBST washes and

then samples were washed once with DAPI (5 mg/mL) for nuclei labelling at 1:5000 in PBST. The excess DAPI was washed out with two PBST washes.

Primary Antibody	Host species	Dilution	Source
anti-serotonin	rabbit	1:500	Sigma
anti-synaptotagmin (1E11)	mouse	1:5	Robert Burke (Nakajima *et al.,* 2004b)
anti-TRH	rabbit	1:200	Ina Arnone
anti-acetylated tubulin	mouse	1:500	Sigma
anti-Hnf6	rat	1:600	Robert Burke (Yaguchi et al., 2010)
anti-Cas9-nuclease[7A9-3A3]	mouse	1:400	AbCam #191468

Table 2.11 Primary antibody information

2.4.9.1 anti-TPH and anti-SynB immunohistochemistry

An alternative immunohistochemistry (IHC) protocol was used for anti-serotonin and anti- synaptotagminB on the *Sp-TPH* CRISPR/Cas9 experiment (Figure 5.7). This protocol was obtained from the Arnone Laboratory (Periklis Paganos).

Samples were washed once in PBST and once in methanol, followed by four-five washes with PBST. Samples were washed in blocking buffer (4% sheep serum, 1% BSA in PBST) overnight at 4^{o}C. Primary antibodies were diluted in blocking buffer (see Table 2.11 for dilutions) and incubated at 37^{o}C for 1.5 hours. Excess antibody was removed by the samples four-five times with PBST. Secondary antibodies Alexa 488 goat anti-rabbit and Alexa 488 goat anti-mouse (Thermo Scientifics) were used at a dilution of 1:1000 in blocking buffer and incubate at RT for 1 hour. Excess antibody was washed out four-five times with PBST.

2.4.10 Morpholino antisense oligonucleotides

Translational blocking morpholino antisense oligonucleotides (MOs) were designed and ordered from Gene Tools LLC (URL:http://www.gene-tools.com) for *Sp-TRH* and

Sp-TRHR, MO sequences are in the appendix, (Table 8.12). The 5' UTR sequence and the first 25 nucleotides of the coding region of target genes were submitted to the company. On arrival the lyophilised oligos were resuspended in distilled water and a stock solution of 1mM was made. The stock solution was divided into aliquots and stored at - 20°C.

2.4.11 Microinjection

2.4.11.1 Protamine plates

To microinject sea urchin eggs, unfertilised eggs were immobilised on protamine coated plates. Lids of 60 mm plastic petri dishes (Falcon) were filled for one minute with 1% Protamine Sulphate (Sigma CAT P4380) solution in distilled water. After coating, lids were washed thoroughly with distilled water to remove excess of solution and air dried over night at RT.

2.4.11.2 Glass pipettes

Glass Pasteur pipettes were pulled in a Bunsen flame and broken off at the end to obtain a desired size to collect eggs and embryos. The internal diameter of a rowing pipette should be roughly the same as the egg diameter (approximately 70 µM) to warrant optimal rowing of eggs.

2.4.11.3 Needle preparation

Needles for microinjection were prepared using borosilicate glass capillaries with a filament (1mm outside diameter and 0.75mm inside diameter, Sutter Instrument). These glass capillaries were pulled on a Sutter P-97 micropipette puller with the following parameters: P=500, H=496, Pu=160, V=60 and T=210. They were pulled on the same day they were used to avoid RNase contamination.

2.4.11.4 Injection solutions

MO and CRISPR/Cas9 injection solutions at a final volume of 5 µL were prepared the same day as injection experiments. See Table 2.12 and Table 2.13 below for solution details. CRISPR/Cas9 injection solutions were prepared on ice, while MO injection solutions were prepared at RT. Before this MOs were incubated at 55°C for 10

minutes. Injection solutions were vortexed and centrifuged on a microcentrifuge at maximum speed for 10 minutes.

To ensure the specifity of gene specific MOs, a CONT MO at the same concentration was used in parallel as negative control. For CRISPR/Cas9, *Sp-PKS1* sgRNA2 was used in parallel as a positive control (Oulhen and Wessel, 2016). Injection solutions were vortexed and centrifuged on a microcentrifuge at maximum speed.

MO injection solution (f.c.)	
MO (200 µM)	X µL
1M KCL (120 mM)	0.6 µL
5mg/mL Rhodamine Dextran (0.5mg/mL) (Optional)	1 µL
Nuclease-free water	Up to 5µL

Table 2.12 Morpholino injection solution

CRISPR injection solution (f.c)	
sgRNA (200ng)	X µL
Cas9 mRNA (450ng)	X µL
1M KCL (120mM)	0.6µL
Nuclease-free water	Up to 5µL

Table 2.13 CRISPR/Cas9 injection solution

2.4.11.5 Injection

Eggs and sperm were obtained as previously described. A small fertilisation test was carried out to make sure the gametes were healthy. The eggs were rowed using a pulled glass Pasteur pipette onto protamine plates and kept covered at 15°C in 2 mM PABA-FASW until they were ready to be injected. For each experiment, some rowed eggs remained uninjected as a negative control. Microinjection needles were loaded with the injection solution. The rowed eggs were then fertilised and injected with a specific injection solution using a Picospitzer III. When Rhodamine Dextrane was

added, the percentage of injected embryos (fluorescence of Rhoadmine Dextrane) was noted. After injection, embryos were incubated in protamine plates in 50 µg/mL Streptomycin and 20 U/mL penicillin PABA-FASW at 15°C until hatching. Embryos were then transferred to fresh 35 mm plastic petri dishes (Falcon) and incubated at 15°C. Embryos were observed for phenotypic change and imaged at various time points. At pluteus larval stage, embryos were collected for RNA extraction, ISH or IHC.

For RNA extraction, 50-100 larvae were collected using a mouthpiece and transferred to a 1.5 mL tube (Eppendorf), they were centrifuged at medium speed (2000-3000 RPM) for 10 seconds, then the supernatant was removed and embryos prepared for RNA (as described in the following section). For ISH and IHC, a desired number of larvae were collected using a mouthpiece, transferred to a 200 µL well plate (Costar) and fixed as described in a previous section. Injected larvae were always compared alongside uninjected and MO or *Sp-PKS1* CRISPR/Cas9 injected larvae.

For skeleton measurements, we measured in pixels the skeleton length of live larvae, using the length measurement option in ImageJ software (NIH). The four distinct parts of the larval skeleton were separately measured body rod (BR), post oral (PO), oral transvers (OT) and oral distal (OD). All skeleton measurements were averaged across 3-4 independent experiments with a total of 42-257 larvae counted.

2.4.12 Microscopy techniques

2.4.12.1 Differential Interference Contrast (DIC) and epi-fluorescent microscopy

40-50 µL of embryos/larvae were mounted under a 22 by 22 mm coverslip with plasticine on each corner to raise the cover slip on the glass slide. ISH samples were mounted in glycerol, while IHC samples were mounted in PBST. Brightfield and DIC images were taken with a Zeiss AxioImager M1 and a Zeiss AxioCam HRc using a 20X and 40X magnification. Images were usually taken at different focal planes and the larvae were often rolled to take images from different orientations. Photoshop CS5 (Adobe) was used to adjust brightness and contrast and to crop the image. For fluorescent stained larvae, each sample was imaged multiple time (at the same focal

plane) using the different channels and DIC. Photoshop was then used to merge the multiple channels into the same image using the linear dodge tool.

2.4.12.2 Confocal microscopy

Larvae were mounted as described above and then sealed with nail vanish, or alternatively samples were placed on a 35 mm glass bottom petri dish (Wilco) when imaged using an inverted microscope. Images were collected with a Leica TCS SPE2 (upright or inverted) or a Zeiss LSM 800. Z-stacks were collected for all channels required and optical sections were stacked and analysed using ImageJ software. The final merged images were produced using Photoshop CS5 and CC 2019 (Adobe).

2.5 RNA quantification techniques

RNA extraction was performed on large batches of embryos, larvae and juveniles for high resolution QPCR quantification for NP genes, GPCR genes and *Sp-SecV*. In addition, we also processed small batches of injected larvae (50-100) for analysis of putative downstream genes.

2.5.1 Extraction of total RNA

To eliminate RNase contamination, all the procedures were carried out in a dust free environment, using gloves and RNase free plastic instruments. Embryos/larvae at the correct developmental stage were collected in a 1.5mL tube, centrifuged at 2000-3000 RPM for 10 seconds and the supernatant was removed. At this point the ciliated embryos/larvae are still swimming, so we repeated this process until we had removed all except a few µL's of FASW without removing any samples.

The pellet of embryos/larvae were then processed for RNA extraction. The RNA was extracted using the RNAeasy Micro Kit (Qiagen) according to manufacturer's instructions with the following modifications. The pellet was resuspended in 300 µL of RLT buffer (Ambion). The solution was either stored at -80°C or processed immediately. An additional 50 µL of RLT buffer, 3.5 µL β-mercaptoethanol and 1 µL of carrier RNA was added to the tube. After the samples had been loaded to columns, a DNAsel step was added as suggested by manufacturer to ensure no contamination of genomic DNA. The wash with 500 µL of 80% ethanol was done twice to increase the quality of the RNA. The sample was eluted using 14 µL or 20 µL RNase-free water, depending on the inital starting materal. The total RNA samples were then generally processed directly for cDNA synthesis.

2.5.2 First strand cDNA synthesis

First-strand cDNA was synthesised in a 20 µL reaction using a maximum of 1 µg of total RNA using the iScript™ cDNA synthesis kit (Bio-Rad) as described by the manufacturer's instructions. The kit uses a mixture of both oligo(dT) and random primers in order to guarantee an unbiased copy of different target sequences. The reagents (except 5X reaction mix) were kept on ice and the reaction was set up at RT

(Table 2.14). Thermocycling conditions were as follows: primer annealing at 25°C for 5 minutes, reverse transcription at 42°C for 30 minutes and enzyme deactivation at 85°C for 5 minutes. cDNA was diluted to the correspondent of 1 embryo / µL using DEPC-water and stored at -20°C.

cDNA synthesis reaction mixture	
5X iScript Reaction Mix	4 µL
Template total RNA	14 or 15 µL
iScript Reverse Transcriptase	1 µL
Nuclease-free water	Up to 20 µL

Table 2.14 cDNA synthesis reaction

2.5.3 Quantitative Polymerase Chain Reaction (QPCR)

QPCR was used to monitor the abundance of PCR products intercalated with a fluorescent dye, SYBR green (Applied Biosystems) as previously described (Rast *et al.,* 2000). All QPCR reactions were carried out in quadruplicates on a 384-well plate (Applied Biosystems) on a QuantStudio™ 6 Flex Real-Time PCR System (ThermoFisher Scientific). In each reaction mix, a 9 µL reaction was set up as seen in Table 2.15. QPCR primers were designed as described above for cloning primers but with a product size of 120-200 base pairs (see appendix section Table 8.2 for QPCR primer sequences). The PCR was done in two steps: after an inital denaturing step at 95°C for 10 minutes, 40 cycles of 1 minute at 60°C and 15 seconds of 95°C were used. A final dissociation step was added to ensure a single fragment was amplified.

QPCR reaction mix (f.c)	
2.8 ng/µL cDNA	0.5 µL
2X Power SYBR green PCR Master Mix	4.5 µL
100mM Forward primer (2.5 µM)	0.55 µL
100mM Reverse primer (2.5 µM)	0.55 µL
Nuclease-free water	Up to 9 µL

Table 2.15 QPCR reaction mix

2.5.4 QPCR analysis

To ensure accuracy of quantification across different biological samples, mRNA for embryonic stage (0-70 hpf) was normalised against an internal, invariant standard. *Sp-ubiquitin* (*Sp-ubq*) has been previously shown to be expressed at a constant level in early sea urchin development (Nemer *et al.,* 1991). For larval stages 18S (Ransick *et al.,* 2002) was used, which are known to remain relatively constant during development. No cDNA samples (water) were used as a negative control to assess potential contamination. To calculate the level of expression of each gene at each embryonic stage we used the strategy describe in (Oliveri and Davidson, 2004). The cycle number (Ct) at which the fluorescence crosses a chosen threshold during the exponential phase of the amplification is proportional to the amount of starting material. The Ct for each combination of cDNA and primers (quadruplicate reactions) was averaged and standard deviation calculated. To quantify the expression level of each gene at each stage, each average replica value was normalised to the *Sp-ubq* average value for the given developmental stage: the Ct of the internal standard (*Sp*-ubq) is subtracted from the Ct of the gene of interest. To calculate the fold of difference relative to *Sp-ubq* expression we used a factor of the average of amplification efficiency (Oliveri and Davidson, 2004). The relative expression is calculated by identifying the maximum level of expression for the entire developmental series of each gene. Absolute numbers of transcripts per embryo were calculated based on the publicly available quantitative transcriptome data (Echinobase; URL: http://www.echinobase.org/Echinobase/) for various genes (Figure 3.3) and identifying an average conversion factor. The conversion factor was determined by comparing transcriptome and QPCR values for several genes of interest. Absolute quantification values should be considered a guide to the exact level of mRNA expression, given that there may still be some margin for error. Furthermore, readers should bear in mind that QPCR was typically performed as an initial step prior to high-resolution spatial expression analysis.

To quantify the effect gene perturbation has on a given gene, the QPCR data were treated as described in Oliveri and Davidson (2004). Each average replica was processed as described above. After normalisation to *Sp-ubq,* the different

experimental conditions are compared (the Ct value of the perturbed sample is subtracted from the Ct of the control). The cycles of difference between the two samples after normalisation to the internal standard is indicative of the change of level of transcripts caused by the perturbation. The cycles difference is converted into fold changes by using a factor of the average of amplification efficiency (Materna and Oliveri, 2008; Oliveri and Davidson, 2004).

2.6 Ligand assay

2.6.1 Pharmacological characterisation

Sp-TRH synthetic peptide was assessed as a ligand for the Sp-TRHR. Receptor DNA was cloned into a mammalian expression vector pcDNA3.1+ (5.4kb, Addgene, CAT V790-20). The recombinant pcDNA3.1+ vector was then transfected into Chinese Hamster Ovary (CHO-K1) cells that stably express the calcium-sensitive bioluminescent reportor GFP-aequorin fusion protein (Baubet *et al.,* 2000) and an *in vitro* calcium (Ca^{2+}) mobilization assay was performed. I performed the assay under the supervision of Luis Alfonso Yañez Guerra.

2.6.1.1 Linearisation of pcDNA3.1+

pcDNA3.1+ plasmid (Figure 8.1) was transformed, clones were selected and a miniprep performed, as described above. The pcDNA3.1+ was sequential digested with restriction enzymes Xbal and then EcoRV. Sequential digestion was necessary as restriction enzymes sites were only 30bp apart and both enzymes could not bind at once. 5 µg pcDNA3.1+ was digested with 20U Xbal (10UU/ µL; Promega) and 1X Multicore buffer (Promega) in a final volume of 50 µL. The digestion was incubated at 37°C for 1 hour and then 2 µL of the digestion was analysed on an electrophoresis gel to confirm the plasmid had completely linearised. Once plasmid linearization was confirmed, 40U EcoRV-HF (20U/ul; NEB) was added to remaining digestion and incubated at 25°C for few hours. The sequentially digested plasmid was analysed on a gel electrophoresis, cut out of the gel, electroeluted and purified as described above.

2.6.1.2 Cloning full-length *Sp-TRHR*

Full-length *Sp-TRHR* (XM_011684235_1) was amplified by PCR using total cDNA from 72 hpf *S. purpuratus* larvae and cloning primers with restriction enzymes sites (EcoRV and Xbal) added to the 5' end of the forward and reverse cloning primers, respectively. See appendix section 8.7 for the sequence. We had trouble directly cloning the full length *Sp-TrhR* directly into a mammalian expression vector pcDNA3.1+, so we first cloned it into a pGEM-T-Easy Vector as described above.

2.6.1.3 Digestion of Sp-TRHR pGEM-T-Easy Vector

3 µg of Sp-TRHR pGEM-T-Easy Vector was digested with 20U Xbal (10UU/ul; Promega), 20U EcoRV-HF (20U/ul; NEB) and 1X multicore buffer in a final volume of 100ul. The digestion was incubated for 2-3 hours at 37°C and analysed on a gel electrophoresis for a complete linearisation. Sp-TrhR insert was cut out of the gel and electroeluted and purified as described above. The linearised receptor DNA was sent for sequencing to confirm the complete ORF was included and a kozak sequence was part of the ORF, to improve expression once in the mammalian vector.

2.6.1.4 Directional sub-cloning into pcDNA3.1+

79 ng of purified linearised Sp-TRHR was ligated with 50 ng of purified linearised pcDNA3.1+ overnight at 15°C at a ratio of 6:1. The vector containing our Sp-TRHR was then transformed into Top 10 One Shot cells and large-scale colony screening was performed as described earlier.

2.6.1.5 Sp-TRHR pcDNA3.1+ Maxiprep

To make very large yields of DNA, 4 mL of selected bacterial recombinant colonies were separately inoculated with 200 mL of LB broth as describe above and grown overnight at 37°C in an agitating incubator at 225 RPM. A Macherey-Nagel NucleoBond Xtra BAC kit was used to extract and purify the plasmid DNA with isopropanol, following manufacturer's instructions. The plasmid DNA was eluted in Tris-EDTA buffer to get a concentration of 1 µg/µL. A diagnostic digestion was performed with EcoRV and Xbal, and the digestion was analysed on a gel electrophoresis to check for the presence of the correct size insert. Finally, the *Sp-TRHR* pcDNA3.1+ plasmid was sent for sequencing to confirm that: a) the receptor

was cloned in a forward position with respect to the CMV promoter, and b) the cloning procedure had not introduced a new start codon between the CMV promoter and the first start codon of the receptor.

2.6.1.6 CHO-k1 cell culturing

Cells were cultivated at 37˚C in either T25 or T75 culture flasks (USA Scienfic; Cat. No. CC7682-4325 and CC7682-4175) containing 6mL or 18mL of DMEM/F12 Nutrient Mixture culture medium (Thermo Fisher Scientific; Cat. No. 11039047) supplemented with 10% fetal bovine serum (Thermo Fisher Scientific; Cat. No. 10082147). Antibiotic-Antimycotic (Thermo Fisher Scientific, Cat. No. 15240062) to prevent bacterial growth and 200 μg/ml of Geneticin G418 sulfate (Thermo Fisher Scientific, Cat. No. 10131035) were added to select for apoaequorin expressing CHO cells.

2.6.1.7 Transfection

Once the cells reached a confluency of 80-90%, they were transfected with pcDNA3.1+ recombinant plasmid containing Sp-TRHR cDNA and pcDNA3.1+ recombinant plasmid containing Gα-16 cDNA. Gα-16 is a promiscuous protein that can couple a wide range of GPCRs to the phospholipase C pathway (Zhu and Birnbaumer, 1996). 5 μg and 15 μg of each plasmid was used for T25 and T75 culture flasks, respectively. The transfection was achieved by Lipofectamine 3000 following manufacturer instructions (Thermo Fisher Scientific; Cat. No. L3000008). Lipofectamine increases transfection efficiency of the plasmid DNA into the CHO cells by liposomes that can pass through the cell membrane. The transfected cells were cultured in medium as described above, without the addition of fetal bovine serum and geneticin.

2.6.1.8 Luminescence assay

The transfected cells were cultivated for approximately 48 hours. The culture medium was then removed, and the cells were detached by adding Ultrapore EDTA 0.5M pH 8.0 (Thermo Fisher Scientific; Cat. No. 15575020) diluted in 1X PBS buffer pH 7.4 (Thermo Fisher Scientific; Cat. No. 10010023), to a final concentration of 5mM. The transfected cells were collected by microcentrifuge at 4000 RPM in an Eppendorf 5702 centrifuge (Eppendorf; Cat No. 022626001), washed with DMEM/F12 Nutrient

Mixture culture medium to remove any remnants of EDTA. The cells were then resuspended in basal culture medium (DMEM/F12 Nutrient Mixture) supplemented with 0.1% Bovine Serum Albumim, Antibiotic-Antimyotic and 1mM coelenterazine-H (Thermo Fisher Scientific; Cat. No. C6780).

After a 2.5-3 hours of incubation on a magnetic stirrer, cells were exposed to synthetic Sp-TRH peptide (pQYP-NH_2; Cambridge Research Biochemicals) diluted in basal culture medium in concentrations ranging from 10^{-4} M to 10^{-14} M in clear flat-bottom 96-well plates (Sigma-Aldrich; Cat. No. CLS3603-48EA). Luminescence levels were recorded over a 35-second period using a FLUOstar Omega Plate Reader (BMG LABTECH; FLUOstar Omega Series multi-mode microplate reader). Data were integrated over a 35-second measurement period. Triplicate measurements were made for each concentration, and the average of each was used. Luminescence responses were normalised to the maximum response obtained in each experiment (100% activation) and to the response obtained with the basal culture medium (0% activation; negative control). Prism 6 (GraphPad, La Jolle, USA) was used to analyse data. Dose-response curves were fitted with a four-parameter logistic regression curve and EC_{50} values were calculated based on three measurements (with the exception of one experiment, where duplicate measurements were used after removing outliers) from three-four independent transfections.

2.6.2 ELISA

The affinity of anti-Sp-TRH to different peptides (Sp-TRH, pQYPG-NH_2; Sp-TRH, CQYPG-NH_2; Sp-GNRH pQ VHHRFSGWRPG- NH_2) was tested using Enzyme-Linked ImmunoSorbent Assays (ELISA). A positive control where the known binding of anti-Ar-Calcitonin (Ar-CT) (1:500) was shown to Ar-CT peptide was used (1uM) (Cai *et al.,* 2018). All washes were done in 200 µL volumes unless otherwise stated.

A fixed amount of peptides (100 µL at 1µM) in triplicate were added to clear flat-bottom 96-well plates and incubated at 4˚C overnight. The following day, the contents were removed, and the wells were washed three times with 1X PBS, incubated with 5% goat serum (in PBS) for at least 2 hours at 37˚C, washed three times with 1X PBS and incubated overnight with 100 µL anti-Sp-TRH (diluted in 5%

GS/PBST in concentrations ranging from 1:4000000 to 1:40). The day after, the contents were removed and the wells were washed three times with 1X PBS, incubated with 100 µL secondary antibody (anti-AP-conjugated goat anti-rabbit diluted 1:3000 in 5% GS/PBST; Vector Laboratories) for 3 hours at 37˚C. The wells were then washed four times with PBST, and then 100 µL p-Nitrophenylphosphate Alkaline Phosphatase Substrate (pNPP, Vector Laboratories) prepared in bicarbonate buffer was added to each well and incubated for 20 minutes at RT. The absorbance at 415 nm was measured using a FLUOstar Omega Plate Reader. Absorbance values were averaged from the three replicates.

Chapter 3 The complexity of the neuropeptidome in the sea urchin larvae, *Strongylocentrotus purpuratus*

The ultimate aim of this study was to determine the roles of neuropeptides in sea urchin embryos and larvae. To achieve this, it was necessary first to identify the entire complement of neuropeptide precursor (NP) genes in *S. purpuratus*. Then the spatial-temporal expression of NP genes and some G-protein coupled receptors (GPCRs) genes were molecularly characterised, from fertilisation to the pluteus larval stage. For simplicity, the investigation is split into two parts. Firstly, a late embryonic and larval NP expression was characterised, from the late gastrula stage (48 hpf), when the first differentiated neurons are detected, to the early pluteus larval stage (72 hpf) when several populations of neurons exist in different parts of the larval body (Chapter 3). NPs genes and neuropeptide receptor (GPCR) genes were investigated during this period to provide a basis for the functional understanding of the neurochemical complexity of the larval nervous system. Secondly, NP expression in early embryos was characterised, from fertilisation (0 hpf) to the early gastrula stage (45 hpf), before the first differentiated neurons are detected (Chapter 4). Gene expression was characterised at this early embryonic stage to provide a basis for functional understanding of peptidergic signalling in a non-neuronal context.

In this chapter I first present QPCR and transcriptome data for 32 NP genes and 26 GPCR genes during late embryonic and larval development. The temporal expression patterns of several NP genes in two postembryonic stages was also examined. Chromogenic ISH was used to characterise spatial expression and fluorescence ISH was used to investigate NP co-expression with known neuronal markers. Finally, the neurochemical complexity of the sea urchin larva was revealed by mapping expression of different combinations of NP genes onto larval neuronal cell types.

Some of the data presented in this chapter was obtained by Masters student Teresa Mattiello and undergraduate students Lizzy Ward and Caroline Citarella (working under my supervision).

This chapter is based on a paper published in *Frontiers in Endocrinology* (Wood *et al.,* 2018). See appendix section 8.9.

3.1 The complexity of the neuropeptidome in the developing sea urchin larvae

To obtain a detailed overview of neuropeptide precursor (NP) gene expression in the developing nervous system of the sea urchin embryo and larva, I first analysed *S. purpuratus* genome sequence data to characterise the complexity of the neuropeptidome in this species. Previous studies (Rowe & Elphick 2012; Menschaert *et al.,* 2010; Jékely 2013; Mirabeau & Joly 2013) have identified 34 NP genes belonging to over 20 different families (Figure 1.1). Of these genes, 14 NPs were found not to share sequence similarity with known NPs from other species (Rowe & Elphick 2012). The availability of genome (Hall *et al.,* 2017) and transcriptome (Semmens *et al.,* 2016; Tian *et al.,* 2017; Zandawala *et al.,* 2017a) sequence data from other echinoderms enabled the identification of a total of 38 NP genes, including the previously identified genes (Table 8.2). The latest version of the *S. purpuratus* genome (Echinobase, v 4.2; http://www.echinobase.org/Echinobase/) was analysed using newly identified echinoderm NP sequences as queries for BlastP searches and SignalP (http://www.cbs.dtu.dk/services/SignalP-3.0/; Bendtsen *et al.,* 2004) was used to determine the presence of a signal peptide, which is a characteristic feature of neuropeptides and other secreted proteins. This analysis enabled identification of *S. purpuratus* NP genes that have been reported previously as well as the *Sp-Kisspeptin* (*Sp-Kp*) *NP* gene. These findings were confirmed independently (Semmens *et al.,* 2016; Zandawala *et al.,* 2017).

Once the complement of NP genes present in the sea urchin genome was established, I studied their temporal expression during the development of the sea urchin nervous system: from the appearance of the first neuronal precursor cells at mesenchyme blastula (24 hpf), through embryonic development to the early larval stage (72 hpf) when several types of neurons are differentiated (Bisgrove and Burke, 1986, 1987; Burke, 1978; Mellott *et al.,* 2017). For this I used the available data from a *S. purpuratus* quantitative developmental transcriptome (http://www.echinobase.org/Echinobase/; Tu *et al.,* 2014) and I also carried out high-resolution (every 3 hours post fertilisation) quantitative real-time PCR (QPCR) measurements for most NP genes. To be directly comparable to the transcriptome data, QPCR time points were chosen only up to end of development (70 hpf).

Generally, NP transcripts are present at very low levels throughout mesenchyme blastula and early gastrula stages (Figure 3.1; Figure 3.2 Table 8.5; Figure 3.3B; Table 8.6), with the total number of transcripts ranging between 50 and 300 transcripts per embryo. Transcript levels then steadily increase throughout the prism and pluteus stages (48-70 hpf), with the total number of transcripts ranging between 300 and 42,000 transcripts per embryo (Figure 3.1; Table 8.5). There are eight NP genes that are exceptions to this pattern, *Sp-Orexin 1* (*Sp-Ox1)*, *Sp-Orexin 2* (*Sp-Ox2)*, *Sp-Insulin-like peptide 2* (*Sp-ILP2*), *Sp-Thyrotropin-releasing hormone* (*Sp-Trh*), *Sp-Somatostatin 1* (*Sp-SS1*) *Sp-Nesfatin* (*Sp-Nesf*), *Sp-Neuropeptide precursor 20* (*Sp-Np20*) and *Sp-Pedal peptide-like neuropeptide 1 (Sp-PPLN1)* (see Figure 3.1 and Figure 3.2). The QPCR data were largely in agreement with transcriptome data available from Echinobase (Tu *et al.,* 2014) (Figure 3.3; Table 8.6). Furthermore, these two techniques quantified gene expression in different batches of embryos, thus validating the overall expression trends and the absolute number of transcripts per embryo. The increase in expression at 48 hpf, seen with most NP genes (27 out of 38), is coincident with the onset of neural differentiation (Garner *et al.,* 2016; Nakajima *et al.,* 2004b) (Figure 1.11). Increase in expression at subsequent stages might reflect the increased number of neuronal precursors/neurons expressing NP genes (Figure 1.12B-C).

27 out the 38 NP genes were next analysed for their expression at two postembryonic stages: i) a late larval stage at five weeks (advanced rudiment stage) when both the larval and juvenile nervous systems are present and ii) the juvenile stage, when only the adult nervous system is present. A very early larval stage (70 hpf) when only the larval nervous system is present was used as a positive control. The temporal patterns of NP gene expression during post-embryonic stages are quite diverse (Figure 3.4; Table 8.7). The majority of NP genes, including *Sp-TRH* and *Sp-L-SALMFa*, among others (Figure 3.4A; Table 8.7), exhibit an increase in relative expression as larval development proceeds, with maximum expression at the juvenile stage. This trend correlates with an increase in the number of neuronal cells during the larval and juvenile stages. One group of NP genes, including *Sp-AN*, (containing an N-terminal alanine (A)/asparagine (N) (AN) motif) (Figure 3.4B; Table 8.7) also show a maximum

expression at the juvenile stage, but have higher expression at the end of embryogenesis (70 hpf, pluteus stage) than in the five week old larvae. Six NP genes, including *Sp-Echinotocin* and *Sp-SS1* show little or no expression in larval stages and have a sharp increase in expression in the juvenile stage (Figure 3.4C; Table 8.7). In contrast, *Sp-Glycoprotein hormone 3* (*Sp- GPH3)* and *Sp-Eclosion hormone 2 (Sp-EH2)* (Figure 3.4D; Table 8.7) have higher expression at the end of embryogenesis (70 hpf, pluteus stage) and then their expression steadily decreases in later larval and juvenile stages. Collectively, these data show that NP gene expression largely correlates with the development of the sea urchin larval nervous system and the increased complexity in post-embryonic stages, suggesting that these genes are expressed in neurons.

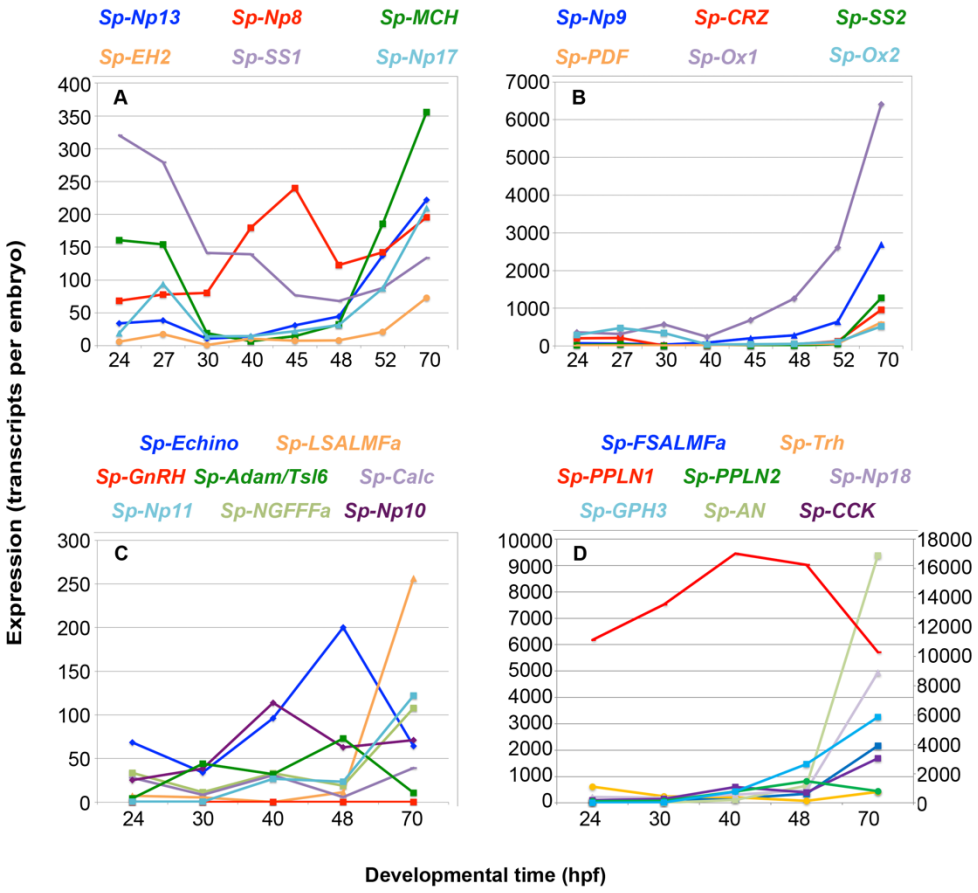

Figure 3.1 Quantitative PCR (QPCR) reveals that NP gene expression correlates with an increase in the complexity of the larval nervous system

NP gene expression (transcript per embryo) is shown from the appearance of the first neuronal precursor cells at mesenchyme blastula stage (24 hpf), through embryonic development to the early larval stage (70 hpf) when several types of neurons are differentiated. The line graphs depict different levels of gene expression for 27 NP genes, with lower expression in graphs (A and C) and higher expression in graphs (B and D). Graph D has two axes, the right axis reveals the number of *Sp-PPLN1* transcripts per embryo, while the left axis reveals the number of transcript per embryo for the other NP genes. An increase in expression is seen for most NP genes from 48 to 70 hpf, when the first serotonergic neurons differentiate. There are five exceptions to this pattern: i) *Sp-SS1* gene has a peak in expression at the mesenchyme blastula stage (>300 transcripts per embryo) followed by a gradual decrease in transcript levels for the remaining embryonic stages (Graph A). ii) *Sp-Ox1* and *Sp-Ox2* genes have a high number of transcripts (>300 transcripts per embryo) during mesenchyme blastula or early gastrula stages (Graph B). iii) *Sp-TRH* gene has a high number of transcripts (>300 transcripts per embryo) during mesenchyme blastula and then there is a reduction in expression during gastrula and prism stages, before the number of transcripts increase to around 400 transcripts per individual in the pluteus larva (Graph D). iv) *Sp-PPLN1* gene has a very high number of transcripts throughout all stages investigated here. The colour of the NP gene name above each

graph reflects the line colour in the corresponding graph. Part of this experiment was carried out by Teresa Mattiello.

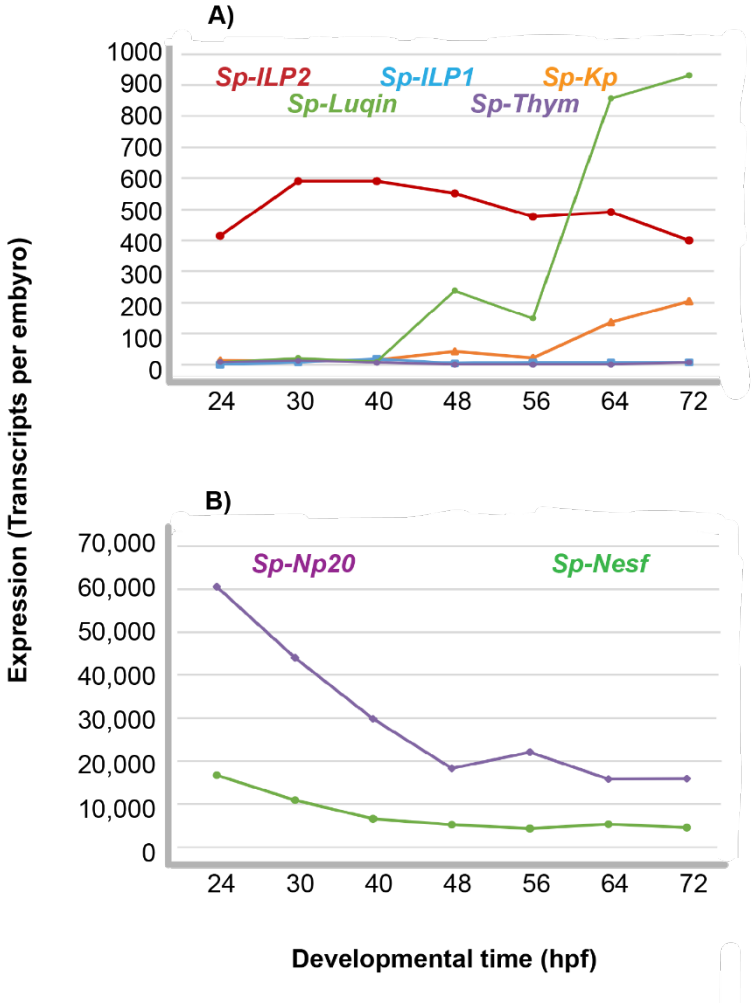

Figure 3.2 The expression of seven NP genes using a publically available transcriptome data set (Echinobase: http://www.echinobase.org/Echinobase/)

The expression (transcripts per embryo) of seven NP genes using a publicly available transcriptome data set (Echinobase: http://www.echinobase.org/Echinobase/). (Graph A-B) Four of these genes (*Sp-ILP1, Sp-Kp Sp-Luqin and Sp-Thymosin*) have an increase in expression, which correlates with the appearance of differentiated neurons. In constract three of these genes have different expression patterns. (Graph A) *Sp-ILP2* gene has a high number of transcripts (>300 transcripts per embryo) during mesenchyme blastula or early gastrula stages. (Graph B) *Sp-Nesfatin* (*Sp-Nesf*) and *Sp-Neuropeptide precursor 20* (*Sp-Np20*) have an increase in expression in the mesenchyme blastula (>15,000 transcripts per embryo) and are highly expressed (>4000 transcripts per embryo) throughout late embryonic and larval development.

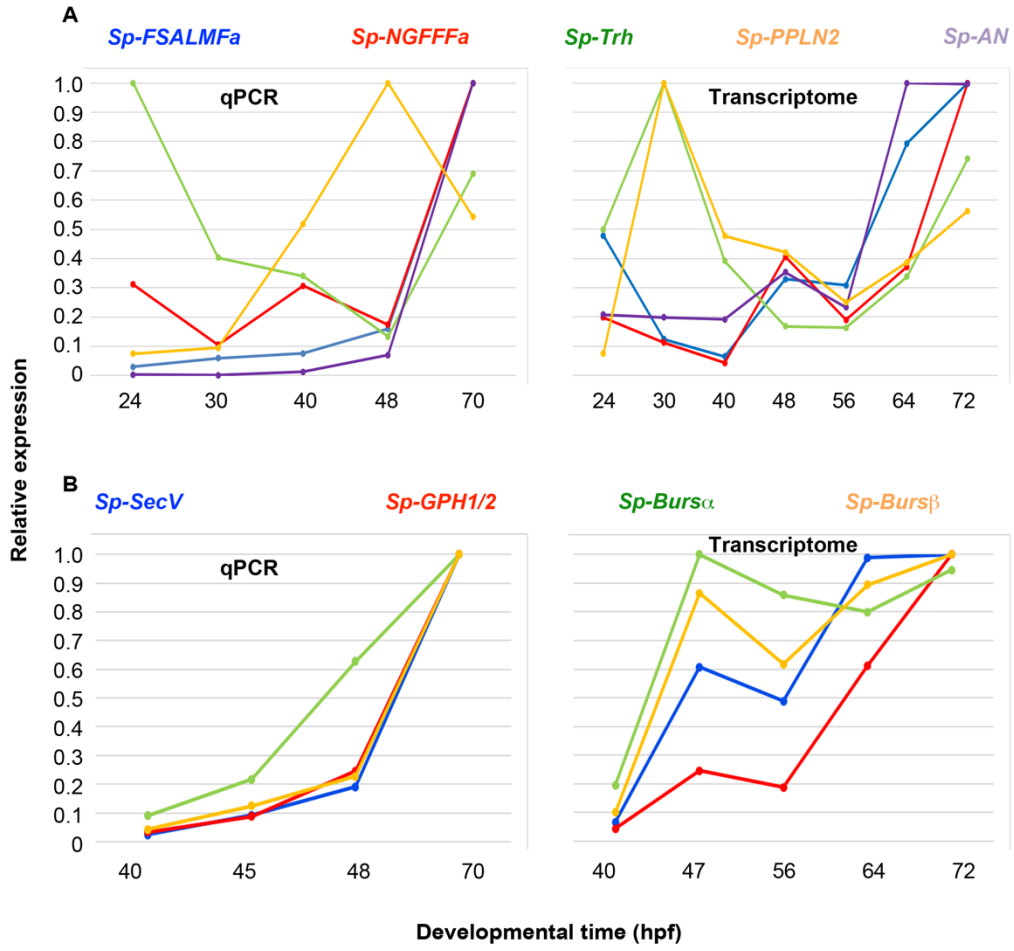

Figure 3.3 A comparison of the relative expression of nine NP genes determined by QPCR and by transcriptome sequencing

(A) The relative expression (individual maximum expression) of five NP genes, for which we show fluorescent *in situ* hybridisation (FISH) data, *Sp-FSALMFa*, *Sp-NGFFFa*, *Sp-TRH*, *Sp-PPLN2* and *Sp-AN* are mostly comparable in QPCR and transcriptome data. (B) The relative expression (individual maximum expression) of three NP genes, *Sp-GPH1/2, Sp-Bursα*, *Sp-Bursβ* and *Sp-SecV* are mostly comparable in QPCR and transcriptome data and show a general increase in relative expression in both QPCR and transcriptome data between 48 hpf and 72 hpf.

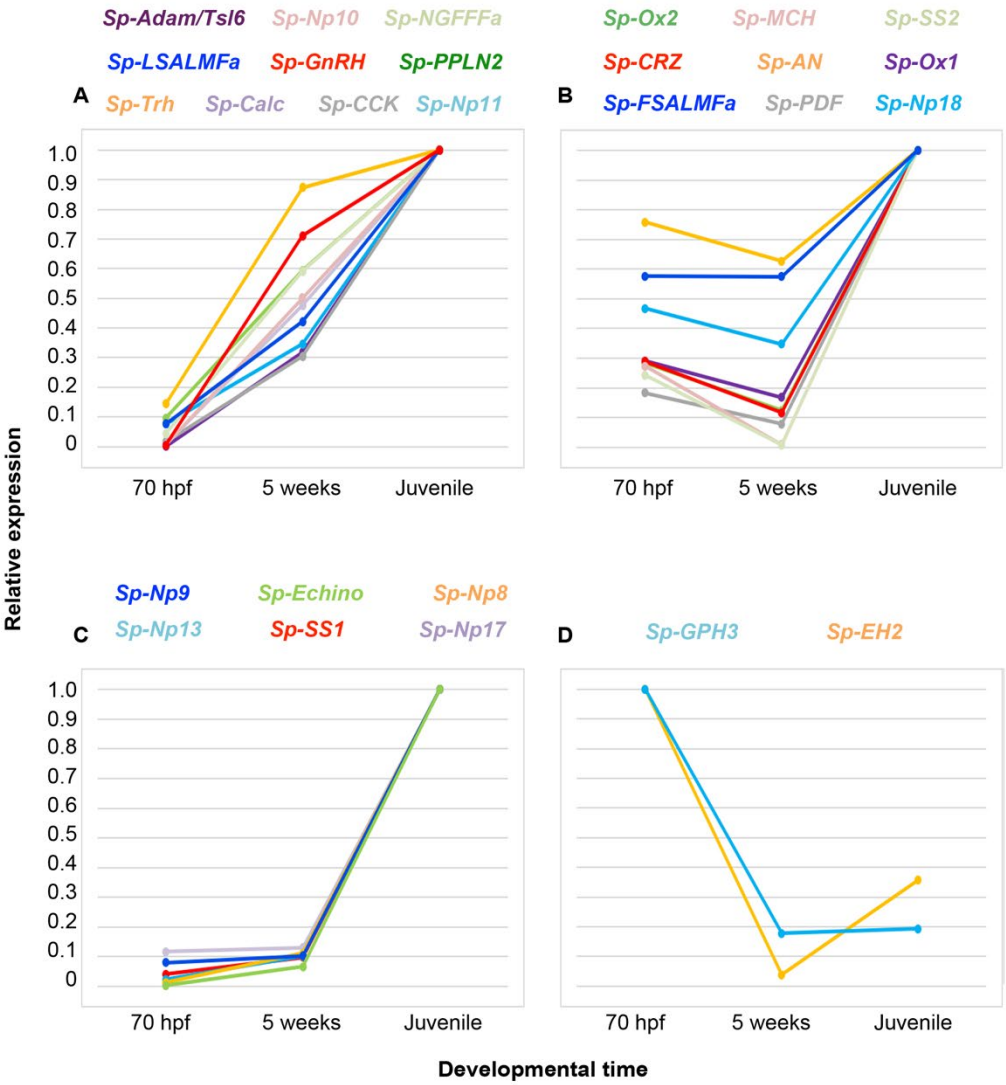

Figure 3.4 Relative expression of 27 NP genes during larval and juvenile development

The relative expression (individual maximum expression) of these NP genes are divided into line graphs A-D based on their expression profile. (A) Ten NP genes have a peak in expression at the juvenile stage. (B) Nine NP genes have a peak in expression at the juvenile stage, but preceded by a decrease in expression at 5 weeks of larval development. (C) Six NP genes have no or little expression in larval stages and a considerable increase in juveniles. (D) Two NP genes are expressed in the early larva (70 hpf) but then exhibit reduced expression in late larvae and juveniles. Experiment carried out by Teresa Mattiello.

3.1.1 Temporal characterisation of G-protein coupled receptors

Neuropeptides typically exert effects on target cells by binding and activating specific rhodopsin-type and secretin-type G-protein-coupled receptors (GPCRs) (Fredriksson *et al.,* 2003). Activation of GPCRs leads to changes in intracellular signalling, which induces a variety of physiological and behavioural responses at the level of the organ system and/or the whole animal. The characterisation of neuropeptide receptors, as well as their complementary ligand, will therefore help to provide insights on the functions of NP signalling systems.

To obtain a detailed overview of GPCR expression in the developing larval nervous system of the sea urchin I first analysed *S. purpuratus* genome sequence data. Previous studies have identified 979 rhodopsin-type and 161 secretin-type GPCRs (Burke *et al.,* 2006a; Raible *et al.,* 2006; Rowe and Elphick, 2012; Sodergren *et al.,* 2006). The identity of 41 rhodopsin-type and four secretin-type GPCRs that are homologs of vertebrate and/or invertebrate neuropeptide receptors have been identified (Burke *et al.,* 2006a; Rowe and Elphick, 2012; Yañez-Guerra *et al.,* 2018). I studied the temporal expression of 25 of these GPCRs during the development of the sea urchin nervous system: from the appearance of the first neuronal precursor cells at mesenchyme blastula (24 hpf), through embryonic development to the early larval stage (72 hpf) when several types of neurons are differentiated. For this available data from a *S. purpuratus* quantitative developmental transcriptome [URL:http://www.echinobase.org/Echinobase/] was used and quantitative real-time PCR (QPCR) measurement for five GPCRs was carried out. Orphan GPCR gene expression was divided into four categories; one high-expressing gene that reaches expression above 950 transcripts per embryo (Figure 3.5A); two mid-expressing genes that have expression between 320 and 949 transcripts per embryo (Figure 3.5B); seven low-expressing genes that have expression between 100 and 319 transcripts per embryo (Figure 3.5C); and ten very low-expressing genes that have expression below 100 transcripts per embryo (Figure 3.5D).

Sp-Leucine-rich repeat GPCR (*Sp-LG-Receptor*) is highly expressed during development (Figure 3.5A; Table 8.6), while the two mid-expressing GPCR genes are

Sp-Corticotropin-releasing hormone receptor (*Sp-CRH Receptor*) and *Sp-Prolactin-releasing hormone receptor* (*Sp-PRH-Receptor*) (Figure 3.5B; Table 8.6). There are 17 other GPCRs that are expressed during late embryonic and early larval development but have low expression, below 300 transcripts per embryo (Figure 3.5C-D; Table 8.6). They belong to a variety of additional NP receptor families, including receptors for RFamide, Neuromedin U/Neurotensin/Growth hormone secretagogue/Ghrelin, Gastrin-releasing peptides/Neuromedin B, vasopressin/oxytocin, orexin and gonadotropin-releasing hormone-type peptides. In summary, I identified three orphan *S. purpuratus* receptors that are highly expressed in the pluteus larva, of which two are also expressed in the early-late gastrula embryo, suggesting that they are likely functional at these stages. The majority of these orphan receptors are expressed at lower levels throughout development, revealing that they do not correlate with the development of the sea urchin larval nervous system. There are also hundreds of other genes encoding GPCRs in *S. purpuratus,* some of which may be neuropeptide receptors (Burke *et al.,* 2006a; Consortium, 2006). Therefore, it would be interesting to identify and couple these GPCRs to NP ligands and compare their expression in the sea urchin embryo and larva.

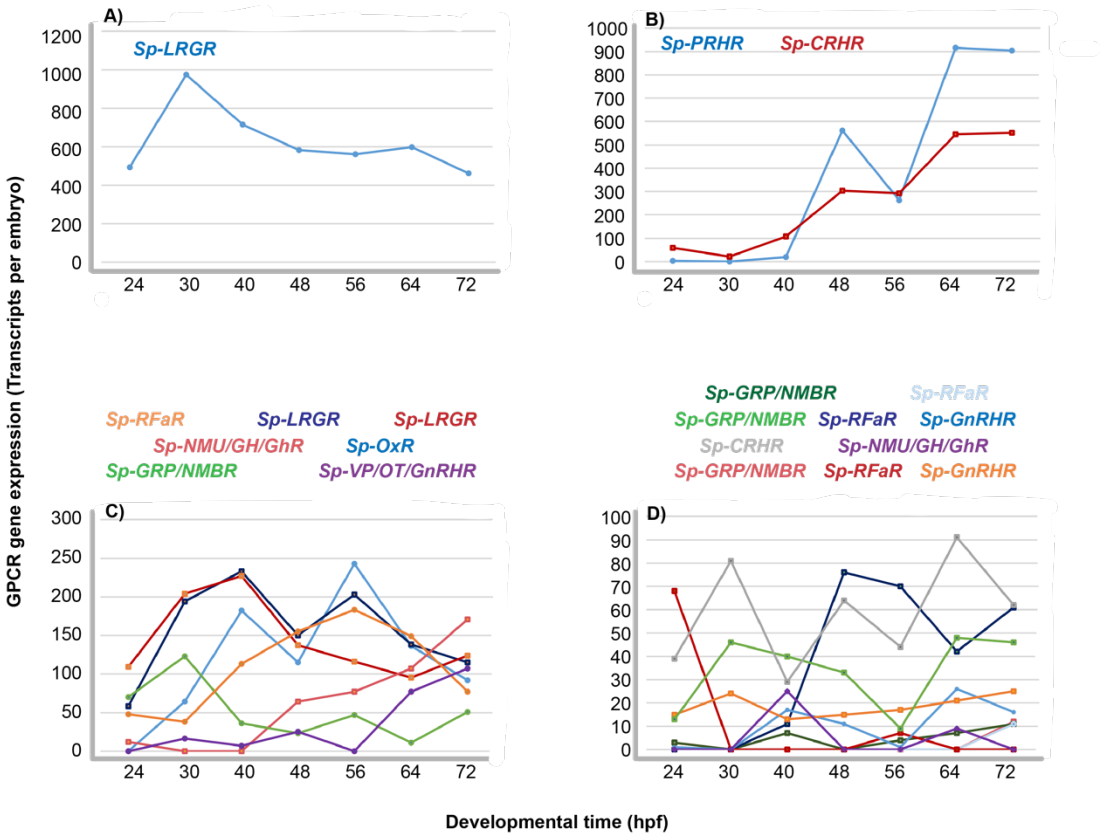

Figure 3.5 Some of the 20 orphan rhodopsin-type and secretin-type GPCRs are expressed during late embryonic development

Graphs representing the levels of expression of 20 GPCR genes that encode potential NP receptors (Burke *et al.,* 2006a). The data are taken from the developmental transcriptome available in Echinobase and are represented in transcripts per embryo at seven developmental stages: mesenchyme blastula (24 hpf), very early gastrula (30 hpf), early gastrula (40 hpf), mid gastrula (48 hpf), late gastrula (56 hpf), prism (60 hpf) and pluteus larva (70 hpf). A) One high-expressing gene *Sp-LGR* has an increase in expression at the beginning of gastrulation (30 hpf) to approximately 1000 transcripts per embryo, which is followed by a gradually decrease in expression as development progresses to the pluteus larval stage (72 hpf). B) Two mid-expressing genes, *Sp-CRHR and Sp-PRHR. Sp-CRHR* expression gradually increases as development progresses, with its highest expression at approximately 500 transcripts per embryo at pluteus larval stage (72 hpf). *Sp-PRHR* also increases in expression as development progresses, reaching almost 1000 transcripts per embryo at the pluteus larval stage. C) Seven low-expressing genes (more than 100 but less than 320 transcripts per embryo). D) Ten very low or not expressing genes (less than 100 transcripts per embryo). Of the 20 genes three corticotropin-releasing hormones (CRH)-type receptors are secretin-type GPCRs, while all the others are rhodopsin-type GPCRs.

To see if ligand receptor pairs were expressed at the same time and thus potentially functional, I compared the expression of five GPCRs with their putative/proven NP ligand. One NP signalling pair, TRH-type NP signalling system has both the ligand and receptor expressed at the pluteus larval stage (Figure 3.6A; Table 8.5), while two other NP signalling pairs, Echinotocin and NGFFFamide (NGFFFa) NP signalling system are also expressed at the same developmental stage, but expression is at a lower level (Figure 3.6 D and E; Table 8.5). Moreover, the ligand and receptor of the Calcitonin (Calc)- and Cholecystokinin (CCK)-type NP signalling systems are not expressed at the same developmental stage as their respective ligand receptor pair (Figure 3.6 B and C; Table 8.5).

Taken together, we have identified two proven ligand-receptor pairs (TRH and NGFFFa signalling systems) and one predicted pair (Echinotocin signalling system) that are expressed and could be functional in sea urchin late developing embryo and pluteus larva. The lack of a ligand or receptor expression suggests that Calc and CCK NP signalling systems might not function in the stages here considered. Although we cannot rule out that these are not ligand-receptor pairs and the true ligand or receptor is expressed.

Collectively, these data show that the GPCRs are mostly expressed at low levels in the development of the sea urchin larval nervous system. However, most NP genes are more highly expressed. Furthermore, the majority of GPCRs don't have a rapid increase in expression between the late gastrula (48 hpf) and pluteus larva (72 hpf), which is seen in the majority of NP genes (compare Figure 3.1 to Figure 3.5). The low level of expression of the potential receptors suggests either a) the analysed NP signalling systems are not functional at the considered stages, or b) that genes encoding other receptors are present in the sea urchin genome. Furthermore, the only two proven *S. purpuratus* ligand-receptor pairs (TRH and NGFFFa) do show expression at the same developmental stage, supporting the idea that NP ligand-receptor pairs should be identified and deorphanized and then we can accurately determine how many NP signalling systems are expressed and functional. Unfortunately, large scale deorphanization is a time-consuming process. From here on I focus only on neuropeptides that are highly expressed in development. I also

spatially characterise the only two deorphanized NP signalling systems in *S. purpuratus*.

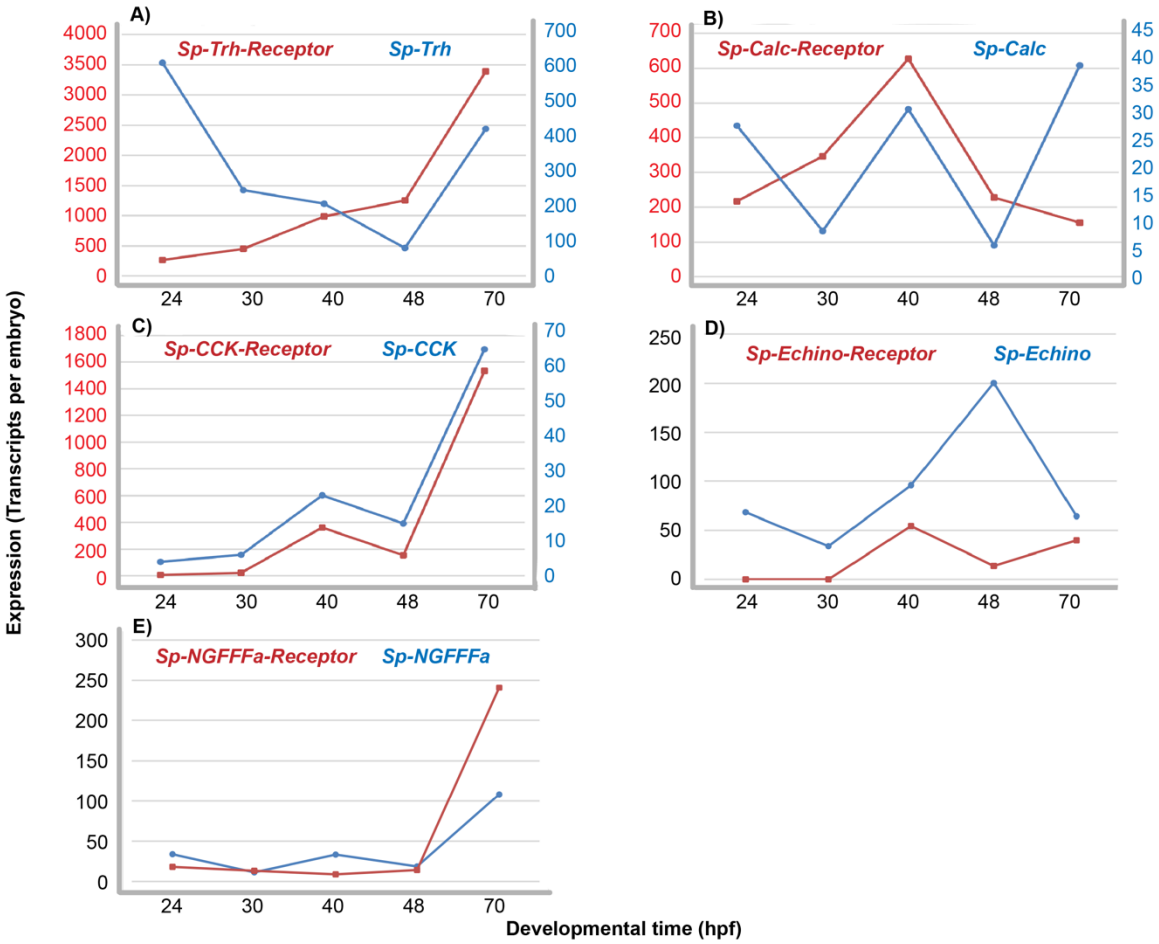

Figure 3.6 Expression of five NP genes and their putative/proven receptor during late embryonic development

Expression (transcripts per embryo) of five NP genes and their putative/proven receptor between mesenchyme blastula (24 hpf) and pluteus larval stage (72 hpf). These data are obtained from QPCR experiments. Each line graph shows a ligand (blue) and receptor (red) putative/proven pair. Both proven ligand-receptor pairs are expressed at the pluteus larval stage suggesting they are functional. Graphs A-C have different axes, the left (shows receptor expression) and right (shows precursor peptide expression). A) *Sp-Thyrotropin-releasing hormone* (*Sp-TRH*) and its proven receptor both increase in expression as development progresses, from late gastrula (48 hpf) to the pluteus larval stage (72 hpf), suggesting that TRH NP signalling becomes functional at late developmental stages and in the larval nervous system.

B) *Sp-Calcit*onin (*Sp-Calc*) and its predicted receptor have different expression patterns, *Sp-Calc-Receptor* has a peak in expression at early gastrula (40 hpf) but drops in expression as development progresses, while *Sp-Calc* NP gene ligand is not detected by QPCR throughout development. C) *Sp-Cholecystokinin* (*Sp-CCK*) and its predicted receptor also have different expression patterns, *Sp-CCK* NP gene ligand has a peak in expression at early gastrula (40 hpf), which further increases by the pluteus larval stage (70 hpf) to over 1600 transcripts per embryo. *Sp-CCK-Receptor* is barely detected by QPCR throughout development. D) *Sp-Echinotocin* and its predicted receptor have both very low expression throughout development, less than 200 transcripts per embryo. The *Sp-Echinotocin* NP gene has a peak in expression in the late gastrula and a smaller increase in *Sp-Echinotocin-Receptor* expression in the early gastrula embryo (40 hpf) and pluteus larva (72 hpf), suggesting that this NP ligand-receptor pair could function in a limited number of cells during sea urchin development.. E) *Sp-NGFFFa* and its proven receptor, (Semmens *et al.,* 2015) are both not expressed until the pluteus larval stage when ligand and receptor expression increases over 100 transcripts per embryo. This suggests, therefore, that this signalling system could be functional in the larva. QPCR experiment carried out by Teresa Mattiello.

3.2 Spatial analysis of neuropeptide precursor expression in the late gastrula embryo

To obtain a detailed insight into the expression of NP genes in the developing larval nervous system, I first used chromogenic ISH to examine the spatial expression patterns at the late gastrula stage (48 hpf), when the first differentiated neurons are detected. Two populations of neural precursors are present at this stage: the differentiating serotonergic neurons in the apical plate and post-oral neuronal precursors in the oral ectoderm (Garner *et al.,* 2016; Mellott *et al.,* 2017).

Single chromogenic ISH analysis was first undertaken to determine the expression pattern of gene encoding five NP genes and one GPCRs. Out of the six probes tested, five showed clear staining at the gastrula stage, consistent with QPCR and transcriptome data at 48 hpf (Figure 3.1; Figure 3.2; Figure 3.6; Figure 3.7; Table 8.5). Indeed, only genes with expression levels above 100 transcripts per embryo are detected by ISH at this stage (Table 8.5), while *Sp-Kp*, which has <100 transcript/embryo at 48 hpf, is not detected by this technique (Figure 3.7). These five genes show expression patterns in the endoderm and ectoderm. *Sp-Insulin-like peptide 2* (*Sp-ILP2*) and *Sp-Neuropeptide precursor 20* (*Sp-Np20*) are expressed in the archenteron (developing gut) at the gastrula (48 hpf) and prism (64 hpf) stages, respectively (Figure 3.7A and G-H). *Sp-ILP2* is one of two insulin-like peptides in the *S. purpuratus* genome, but only *Sp-ILP2* is expressed during late embryonic development (from gastrula to pluteus stages). Chromogenic ISH analysis reveals that *Sp-ILP2* is expressed in a ring of endodermal cells in the foregut at the late gastrula stage (Figure 3.7A). Endodermal derived neurons are not present in the foregut (esophagus) until the pluteus larval stage (Wei *et al.,* 2011), suggesting that *Sp-ILP2* is not expressed in neurons at the late gastrula stage. *Sp-Np20* is an uncharacterised neuropeptide precursor and is one of the most highly expressed NP genes. Expression analysis revealed that *Sp-Np20* is detected throughout the archenteron at the prism stage (64 hpf). Staining is stronger in the midgut and hindgut and weaker in the foregut (Figure 3.7G-H). Pancreatic-like secretory cells have been identified in the upper midgut (stomach) suggesting that *Sp-Np20* could be expressed in these

secretory cells. However, *Sp-Np20* probe has a wider staining in the midgut and hindgut, revealing that it is likely expressed in non-secretory endodermal cells as well.

Sp-Pedal peptide-like neuropeptide 1 (*Sp-PPLN1*), *Sp-TRH* and *Sp-Thyrotropin releasing hormone Receptor* (*Sp-TRHR*) are expressed in different ectodermal cell types. *Sp-PPLN1* is one of two pedal peptide-type neuropeptide precursors identified in *S. purpuratus*, but *Sp-PPLN2* has a low-level of expression during development. In contrast, *Sp-PPLN1* is highly expressed throughout the majority of development and has over 16,000 transcripts per embryo present in a gastrula stage embryo. Expression analysis revealed that *Sp-PPLN1* probe is strictly detected in the aboral ectoderm in the late gastrula embryo (Figure 3.7B-C). Neurons are not present in the aboral ectoderm, but there are axonal tracts, leading from the cell bodies in the ciliary band, to aboral ectodermal cells. *Sp-TRHR* is the receptor of *Sp-TRH* ligand. *Sp-TRHR* is highly expressed (1256 transcripts per embryo) in the late gastrula embryo, whereas *Sp-TRH* has approximately 100 transcript per embryo (Figure 3.6A). Expression analysis of *Sp-TRH* revealed that is was detected in one cell in the anterior ectoderm, adjacent to the apical plate and *Sp-TRHR* is detected in the ciliary band in two patches of cells next to the apical plate (Figure 3.7E-F). Differentiated neurons are present in the apical plate in the late gastrula embryo. In summary, chromogenic spatial expression data has revealed four NP genes and one GPCR gene expressed in non-neuronal cells at the late gastrula stage. Furthermore, only two genes (*Sp-ILP2* and *Sp-Np20*) are likely co-expressed.

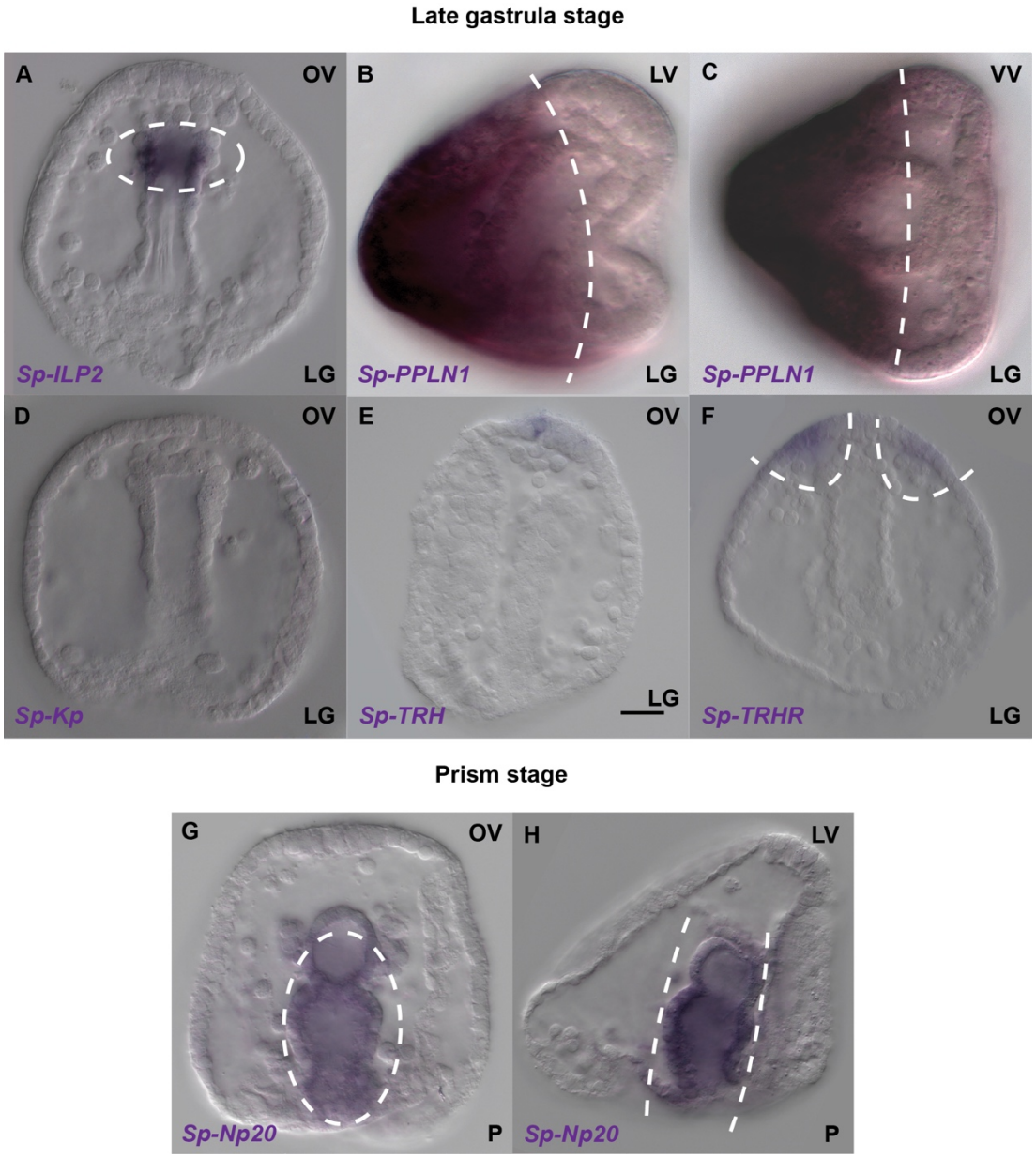

Figure 3.7 Expression of NP genes in ectodermal and endodermal cells at the late gastrula and prism stages

Spatial expression of NP genes and a rhodopsin-type GPCR revealed by chromogenic ISH in ectodermal and endodermal cells of the late gastrula (48 hpf) and prism stage (55 hpf) embryo. A) Expression of *Sp-ILP2* is detected in a ring of cells at the tip of the archenteron, which will form the foregut. B-C) Strong expression of *Sp-PPLN1* is revealed in cells of the aboral ectoderm. D) *Sp-Kp* is not detected by this technique even after several days of staining. E) The *Sp-TRH* probe labelled one cell in the anterior ectoderm, adjacent to the apical plate. F) The *Sp-TRHR* probe labelled cells on two sides of ciliary bands. G-H) Expression of *Sp-Np20* is detected in the developing archenteron at the prism stage. Top-right corner indicates the orientation of the embryo. For embryonic axes of developmental stages use Figure 8.2 as a reference for all images in this thesis. Bottom-right corner indicates the embryonic stage. Abbreviated labels refer to the following: OV (oral view), LV (lateral view), VV

(ventral view), LG (late gastrula) and P (prism stage). Dotted white lines highlight gene expression. PPLN1 experiment carried out by Paola Oliveri.

3.3 Spatial analysis of neuropeptide precursor expression in the pluteus larvae

During post gastrula development the number of neurons and neuronal precursor cells increases dramatically, consistent with the high level of proliferation detected by EdU staining, mainly in neurogenic tissues of the pluteus stage, such as the apical organ, ciliary band and oral ectoderm (Garner *et al.,* 2016). At the end of development, the simple nervous system of the pluteus larva (72 hpf) is composed of 40 to 50 neurons, which have differentiated in the apical organ (containing eight to nine serotonergic neurons (Byrne *et al.,* 2007)), ciliary band, lateral ganglia, post oral, around the mouth (lip) and gut regions (Bisgrove and Burke, 1986, 1987; Burke, 1978; Burke *et al.,* 2006a; Garner *et al.,* 2016; Mellott *et al.,* 2017; Wei *et al.,* 2011).

To obtain a detailed insight into the expression of NP genes in a larval nervous system comprising 40-50 neuron, I used chromogenic ISH to examine the spatial expression patterns of six NP genes and two GPCRs in *S. purpuratus* larvae (72 hpf). Out of the eight probes tested, seven showed a clear signal, consistent with the high level of expression determined by QPCR and transcriptome analysis (Figure 3.1; Figure 3.2; Figure 3.6; Table 8.5).

Six genes show expression patterns in the endoderm and ectoderm. *Sp-ILP2*, *Sp-Np20* and *Sp-Kp* are expressed in overlapping territories in the fully developed gut at pluteus larval stage (Figure 3.8A-B and I-J). Expression analysis of *Sp-ILP2* and *Sp-Np20* is revealed in the foregut and the whole gut, respectively, in the pluteus larva (Figure 3.8A-B, J), which is consistent with expression at an earlier stage. *Sp-ILP2* expression is consistent with published data (Perillo and Arnone, 2014). Perillo and Arnone also revealed that *Sp-ILP1* is expressed in the lower foregut and upper midgut, in more advanced larvae, at 10 days post fertilization (dpf) (Perillo and Arnone, 2014). Expression analysis revealed that *Sp-Kp* is weakly detected in the foregut and midgut (Figure 3.8I). Endodermal derived neurons are now present in the foregut, suggesting that *Sp-Kp*, *Sp-ILP2* and *Sp-Np20* are expressed in these neurons

and *Sp-Kp* and *Sp-Np20* are also expressed in the pancreatic secretory cells in the midgut, as well as other endodermal cells.

Sp-TRH, *Sp-TRHR* and *Sp-PPLN1* are detected in different cells in the ectoderm. Expression analysis reveals that *Sp-PPLN1* remains in the aboral ectoderm through gastrula to pluteus larval stage (Figure 3.7B-C; Figure 3.8F). *Sp-TRHR* expression expands in the number of ciliary band positive cells. *Sp-TRHR* is detected in two symmetrical strips running between the post oral and oral distal arms and is absent from the apical organ (between the oral distal arms) and from the region between the two post oral arms (Figure 3.8D-E). Expression analysis revealed that the gene encoding the ligand, *Sp-TRH* is expressed in two cells in the ciliary band, located on either side of the apical organ (Figure 3.8C). Comprehensive chromogenic ISH analysis revealed variability in the number of *Sp-TRH*-positive cells. The expression pattern of *Sp-TRH* was counted across 116 larvae (Table 8.8) revealing: 9% of larvae had one *Sp-TRH*-positive cell on each side of the apical organ, while 38% had only one *Sp-TRH* positive cell on one side of the apical organ. 7% had two or more cells on one side of the apical organ and 6% had two or more cells on each side of the apical organ. Furthermore, 40% of larvae had no *Sp-TRH* positive cells (Table 8.8). Overall, the majority of larvae had no *Sp-TRH* staining or only one *Sp-TRH* positive cell. Unlike embryonic development, larval development is not synchronous and, therefore variability in expression could be a result of larvae developing at different rates. *Sp-TRHR* is co-expressed with *Sp-TRH* (Figure 6.11) and *Sp-Opsin3.2* (Petrone, 2015) (Figure 1.12B) in these oral distal cells. Valero-gracia and colleagues revealed that the sea urchin larva has non-directional photoreceptor cells (*Sp-Opsin3.2* positive) next to the apical organ (Valencia *et al.,* 2019; Valero-gracia *et al.,* 2016). Taken together, these data indicate that TRH ligand-receptor positive cells are probably neurosecretory non-directional photoreceptors.

ISH analysis revealed that *Sp-NGFFFa* is strongly expressed in a single mouth/lip cell and weakly expressed in the gut. Neurons are found in the mouth and foregut at the pluteus larval stage (Figure 3.8G), and therefore NGFFFa could have a role linked to nutrient uptake. There are 142 *Sp-NGFFFaR* transcripts per embryo by transcriptome quantification and 241 transcripts per embryo by QPCR analysis (Figure 3.6; Table

8.5) and chromogenic ISH reveals weak ubiquitous staining (Figure 3.8H and K). The concomitant presence of the ligand and receptor pair at this stage suggests that the NGFFFa NP signalling system could be functional. The neurophysin-containing *Sp-NGFFFa* belongs to the NG family of neuropeptides. The divergent NG, NPS and CCAP-type peptides likely arose from the duplication of a neurophysin-containing vasopressin/oxytocin (VP/OT)-type precursor in a common ancestor of the bilateria (Semmens *et al.,* 2015).

Taken together, chromogenic spatial expression data has revealed six NP genes and two GPCR genes are expressed in neuronal/secretory cells in the gut and ciliary band, and non-neuronal cells in the aboral ectoderm and gut. These results show that 50% of the NP genes tested (12 NP genes tested, out of the total 38 NP genes identified in the *S. purpuratus* genome so far) and 100% of GPCR genes tested are specifically expressed in the developing *S. purpuratus* larvae. *Sp-PPLN1* maintains its restricted expression pattern, whereas the endoderm expressing NP genes are likely co-expressed in many cells. The wide expression pattern of *Sp-TRHR* in the ciliary band makes it likely that it is co-expressed with additional NP genes. However, chromogenic ISH does not confirm if these NP genes are expressed in neurons or co-expressed with each other.

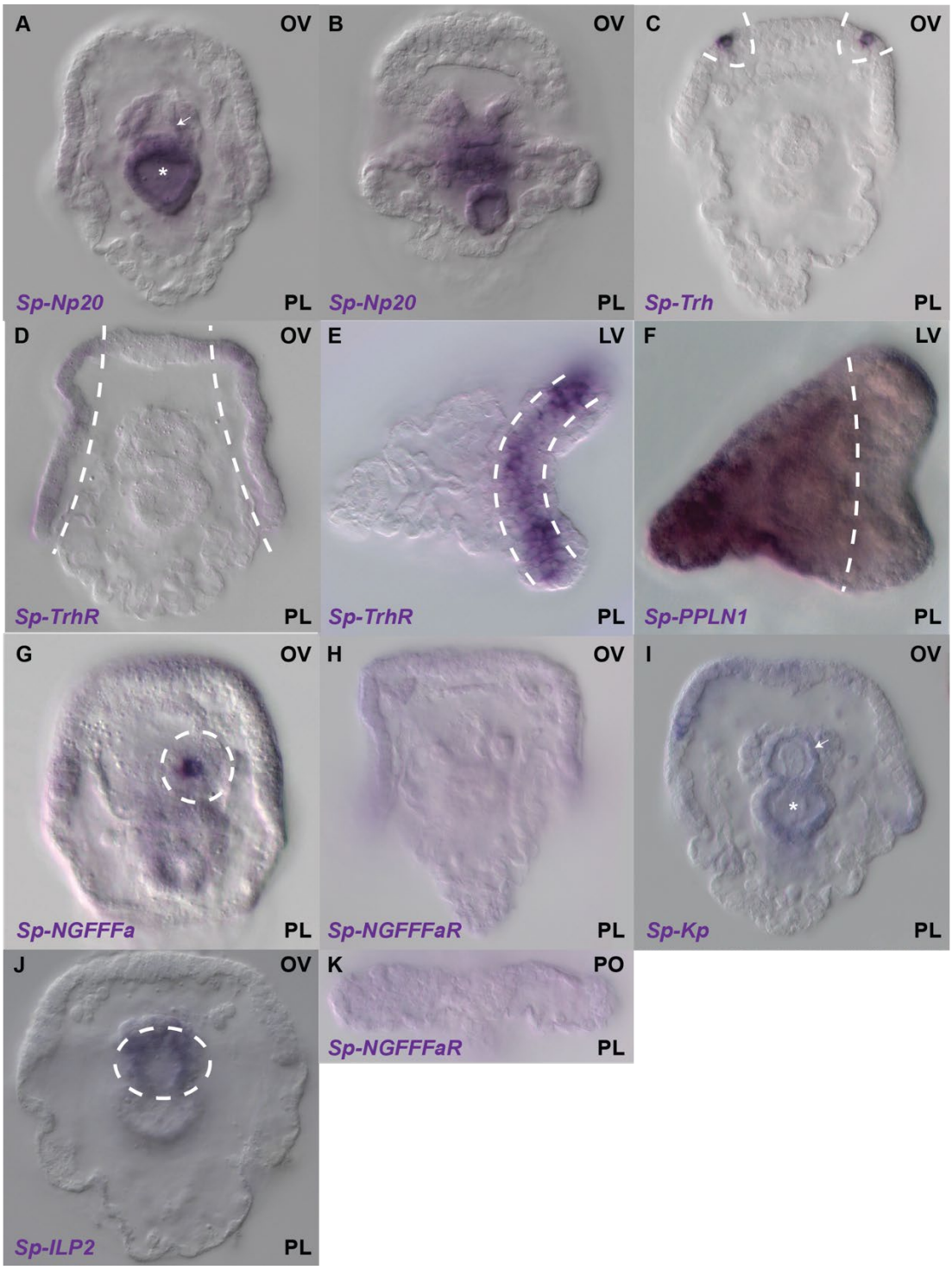

Figure 3.8 Expression of NP genes in ectodermal and endodermal cells at the pluteus larval stage

Spatial expression of NP genes and a rhodopsin-type GPCRs revealed by chromogenic ISH in ectodermal and endodermal cells of the pluteus larva (72 hpf). A-B) *Sp-Np20* expression marks the foregut (arrow) and midgut (asterisk). C) Expression of *Sp-TRH* is seen in two photoreceptor neurons. D-E) Expression of *Sp-TRHR* identifies two large symmetrical sections of the ciliary band. F) Strong expression of *Sp-PPLN1* highlights the aboral ectoderm. G) Expression of *Sp-NGFFFa* detected in one mouth cell. H and

K) *Sp-NGFFFa-Receptor* shows low ubiquitous expression at different larval focal planes. I) Expression of *Sp-Kp* throughout the foregut (arrow) and midgut (asterisk). J) Expression of *Sp-ILP2* highlights a ring of cells in the foregut. Top-right corner indicates the orientation of the embryo. Bottom-right corner indicates the embryonic stage. Abbreviated labels refer to the following: OV (oral view), LV (lateral view), PO (post oral arms) and PL (pluteus larva).. Dotted white lines show the gene expression domain. The PPLN1 and NGFFFa experiments were carried out by Paola Oliveri.

3.4 Most low-expressing genes do not have specific expression in the late gastrula and pluteus larval stages

The spatial patterns of expression of six NP genes that are highly expressed in late development have been determined (Figure 3.1; Figure 3.2). One NP gene (*Sp-NGFFFa*) has a lower expression level, but showed specific expression in a single cell around the mouth (Figure 3.8; Figure 3.1C). There are many other NP genes that had similar or lower levels of expression in the late gastrula (48 hpf) and pluteus (72 hpf) (Figure 3.1A-C). To check if this low-level NP gene expression was detectable using ISH. I attempted to clone cDNA encoding 12 NPs (that have the lowest expression levels out of the 32 NPs I had temporal expression data for) and used chromogenic ISH to analyse their expression patterns in late gastrula embryos and pluteus larvae. I performed two independent ISH experiments, using different batches of embryos. The probe detection step was carried out for seven days with constant changes of fresh staining solution every day to avoid non-specific background staining.

Out of the 12 NP genes, I successfully cloned seven NP cDNAs and used these as templates to generate probes for six NPs. I was unable to clone cDNAs encoding 4 NPs, which probably reflects a low-level of transcripts in the embryonic/larval cDNA (Table 3.1).

NP gene	Stage of cloning and probe synthesis	Highest expression level (t/e)	Amplified by PCR	cDNA length (nucleotides)
Sp-Np8	Probe synthesised	240	Yes	1124
Sp-Np9	Probe synthesised	2690	Yes	940
Sp-CRZ	Probe synthesised	957	Yes	3546
Sp-Np13	Probe synthesised	222	Yes	1387
Sp-MCH	Probe synthesised	823	Yes	677
Sp-SS2	Ligation step	1272	Yes	2460
Sp-Np17	Cloning PCR step	209	No	1666
Sp-SS1	Cloning PCR step	321	No	860
Sp-Ox1	Cloning PCR step	6405	No	1703
Sp-Ox2	Cloning PCR step	517	No	1760
Sp-Echinotocin	cDNA cloned	200	Yes	675
Sp-PDF	Probe synthesised	623	Yes	1124

Table 3.1 Details of cloning and probe synthesis for low-level expressing NPs

The stage of cloning and probe synthesis stage reached for 12 low-expressing NPs and details about genes including the highest expression level (transcripts per embryo) and clone length. Genes that had the lowest expression levels were generally difficult to clone.

All six probes tested produced low-level ubiquitous staining (Figure 3.9A-D). Note, however, that staining was done for at least a few days in an attempt to reveal more specific expression. It cannot be determined whether the low-level ubiquitous staining is specific, reflecting gene expression in all cell types, or if it is non-specific staining. A positive control (*Sp-FoxA*) was run simultaneously on the same batch of embryos and for this probe specific staining was observed within a few hours (Figure 3.9E). Tu and colleagues used a cut-off value of 300 transcripts per embryo as "the lower limit for a functional meaningful level of transcript representation" (Tu *et al.,* 2014a). This is equivalent to less than one transcript per cell for a ubiquitously expressed gene in a mesenchyme blastula embryo (24 hpf). However, this cut-off value is dependent on the expression pattern. For example, the *Sp-NGFFFa* NP gene and *Sp-TRH* NP gene have only approximately 100 transcripts per embryo by transcriptome quantification and quantitative PCR, but chromogenic ISH reveals specific detection of both probes in single cells. Thus, our data indicates that 100 transcripts per cell seems to be the limit of detection by ISH.

The six low-level expressing NP genes analysed here do seem to have ubiquitous expression, resulting in much less than one transcript per cell. However, we cannot rule out that we have reached the limit of detection of the chromogenic ISH. Furthermore, the length of the a given probe may also affect the limit of detection. Longer probes show reduced non-specific staining. An example is seen for *Sp-NGFFFa* and *Sp-TRH* with approximately 100 and 400 transcripts per embryo, respectively in the pluteus larva and both are expressed in a few isolated cells at this stage (Figure 3.8; Table 8.5). *Sp-NGFFFa* has a probe length of 1650 nucleotides and *Sp-TRH* has a probe length of 3900 nucleotides. Unfortunately, five out of six probes made for low-level expressing NP genes had a probe length between 677 and 1387 nucleotides (Table 3.1).

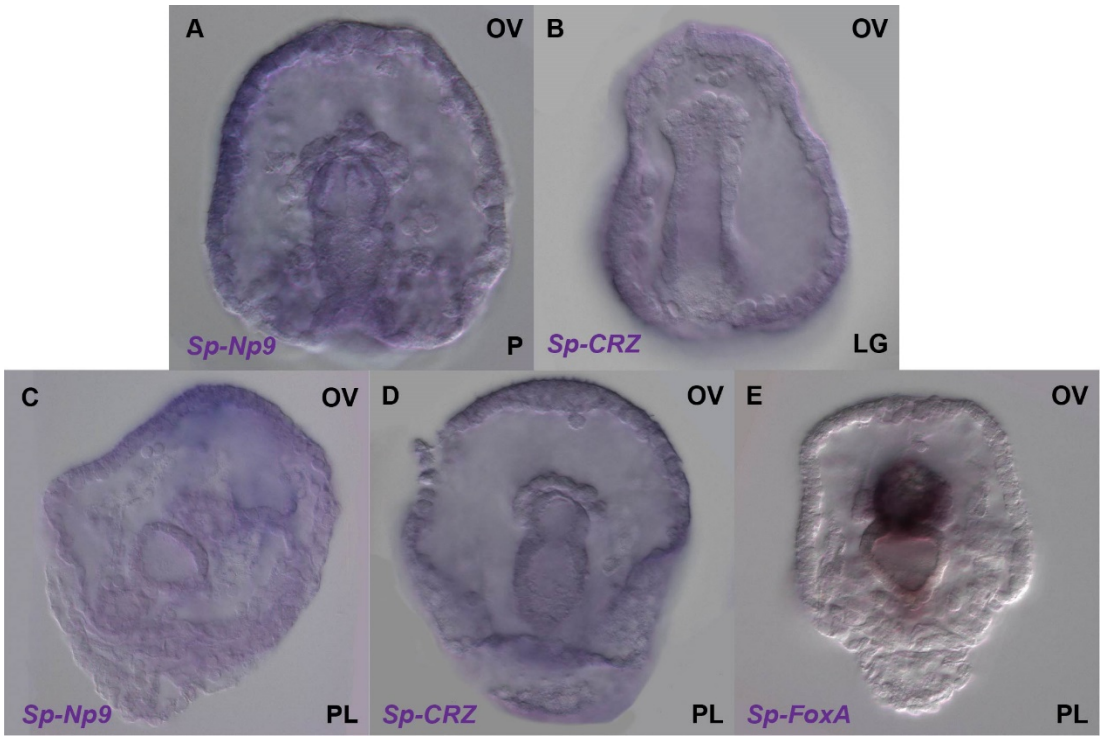

Figure 3.9 Examples of low-level expression of NP genes in sea urchin embryos and larvae

Spatial expression of two low abundance NP transcripts and *Sp-FoxA* (positive control) revealed by chromogenic ISH in the late gastrula/prism embryo and pluteus larva. A and C) *Sp-Np9* expression in a prism embryo (approximately 64 hpf) and a pluteus larva (72 hpf). B and D) Detection of *Sp-Corazonin* (*Sp-CRZ)* expression in a late gastrula (48 hpf) embryo and a pluteus larvae (72 hpf). Staining for both probes was performed for at least five days. E) Chromogenic ISH analysis of *Sp-FoxA* expression, used here as a positive control (Oliveri *et al.,* 2006). Top-right corner indicates the orientation of the embryo. Bottom-right corner indicates the embryonic stage. Abbreviated labels refer to the following: OV (oral view), LG (late gastrula), P (prism), PL (pluteus larva). ISH experiment and cloning of some cDNA used for probe synthesis was done by Caroline Citarella.

3.5 Summary of NP gene expression analysis using chromogenic ISH

In this chapter I have so far characterised the temporal expression pattern of 32 NP genes, 25 GPCRs and the spatial expression pattern of six NP genes and two receptors during late embryonic development, from the late gastrula to pluteus larval stage. QPCR and transcriptome data reveal that almost all NP genes analysed here (84% of the total NP genes and 58% of the total GPCR genes so far identified in the *S. purpuratus* genome) are detected in the developing sea urchin and larval stages. Furthermore, the two proven ligand-receptor pairs are expressed in the pluteus larva.

Chromogenic ISH has revealed that all eight genes tested (16% total NP genes and 4% of the total GPCR genes) have diverse expression patterns (disregarding the low-level expressing genes in section 3.4). Four genes, *Sp-PPLN1, Sp-TRH*, *Sp-TRHR and Sp-NGFFFa* are expressed in different ectodermal territories. Three genes, *Sp-ILP2*, *Sp-Kp* and *Sp-Np20* are expressed in overlapping endodermal territories. *Sp-TRH* and *Sp-NGFFFa* are both only expressed in one to two cells, while *Sp-NGFFFaR* has the widest expression pattern, present in all cell types (Figure 3.10). The expression of these NP genes in diverse cell types, suggests that they have different functions in the embryo.

To better characterise the larval nervous system, from here on I focus on investigations of NP genes that are expressed in cells with a neuronal phenotype.

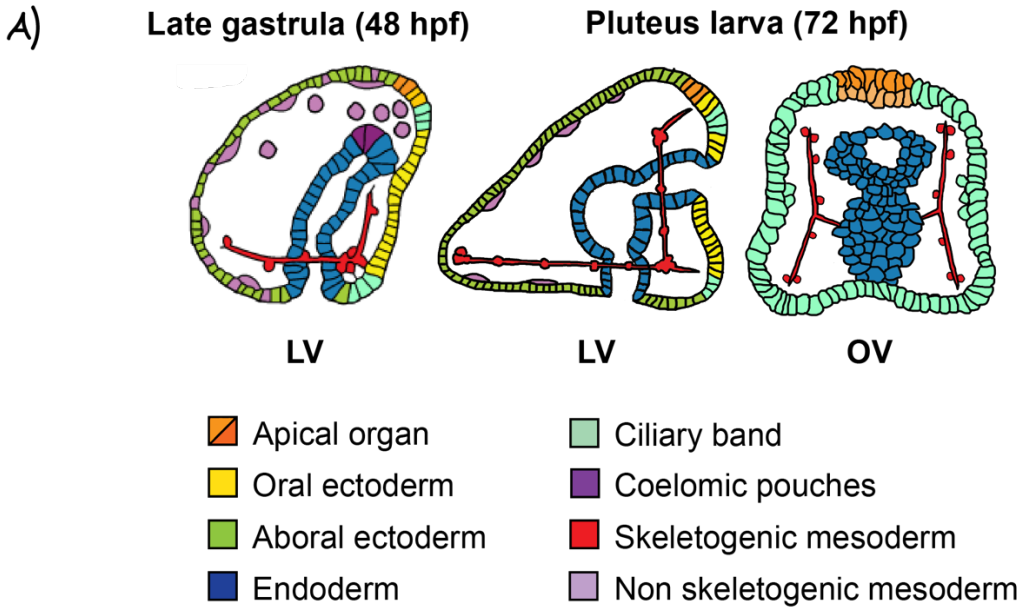
A)
Late gastrula (48 hpf)
Pluteus larva (72 hpf)
LV
LV
OV
Apical organ
Oral ectoderm
Aboral ectoderm
Endoderm
Ciliary band
Coelomic pouches
Skeletogenic mesoderm
Non skeletogenic mesoderm

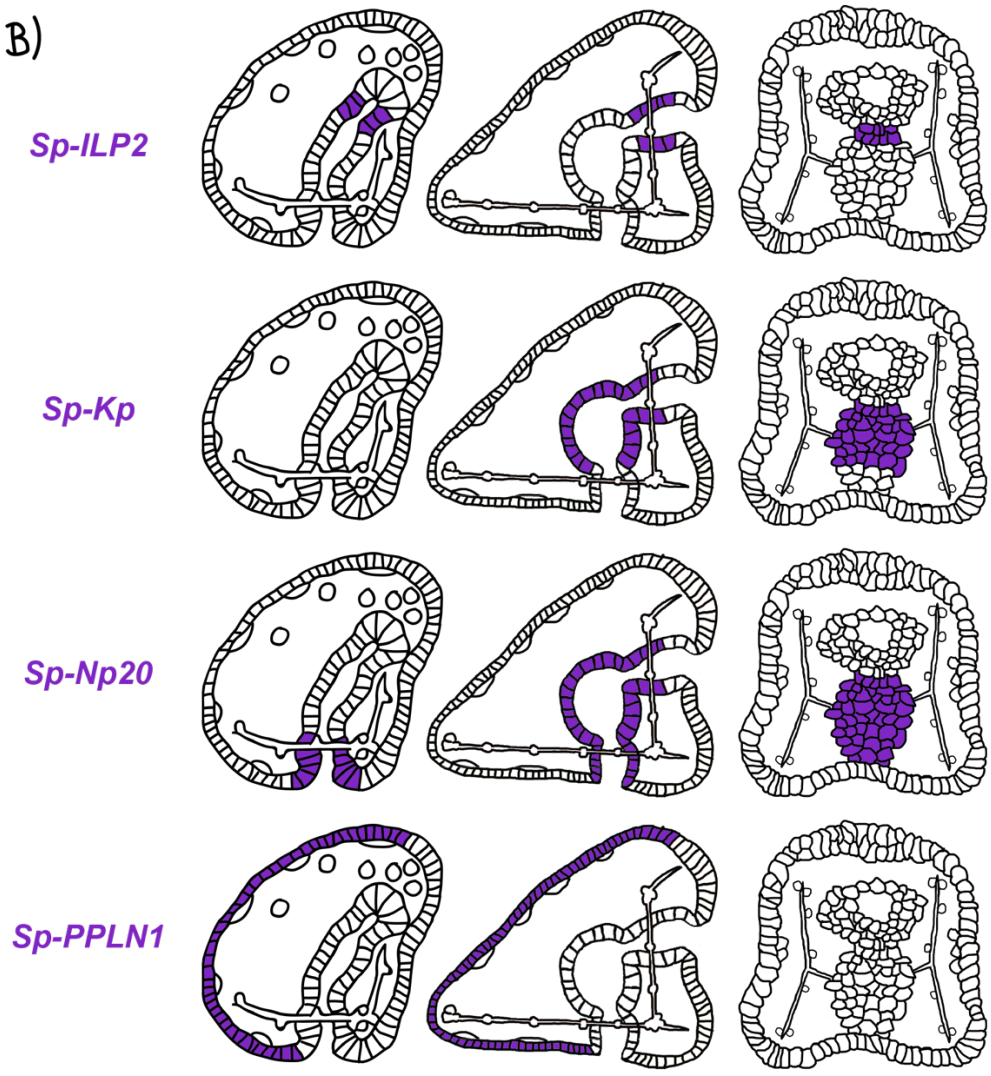
B)
Sp-ILP2
Sp-Kp
Sp-Np20
Sp-PPLN1

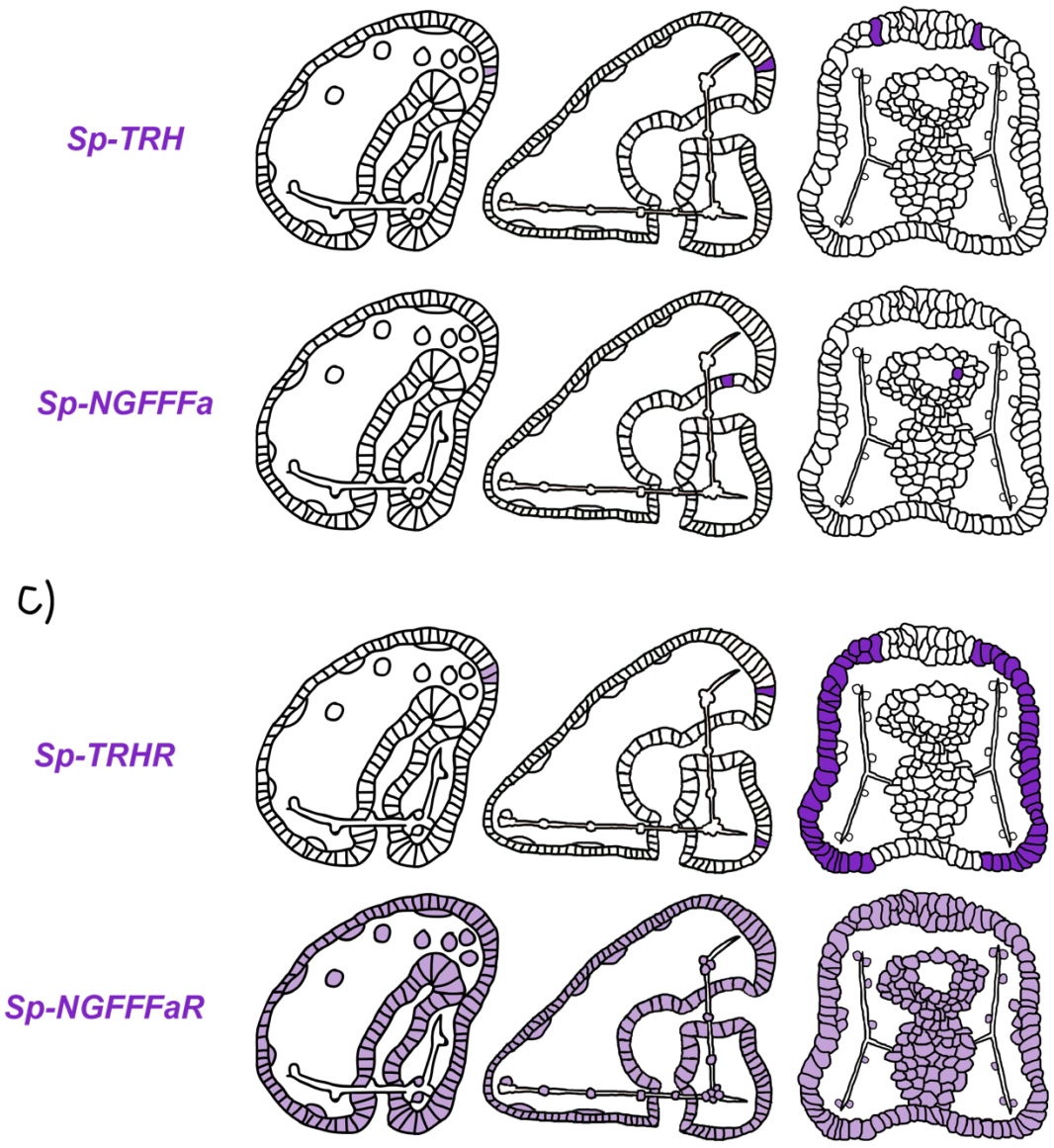

Figure 3.10 Summary map of NP and GPCR gene expression in the late gastrula and pluteus larva stages

A) Cartoon schematic of a late gastrula embryo and pluteus larva. Different colours depict the known cell-type territories at each developmental stage. Oral ectoderm (yellow), aboral ectoderm (green), apical plate/organ (orange), endoderm (archenteron/gut) (blue), non-skeletogenic mesoderm (light purple), skeletogenic mesoderm (PMCs/skeleton) (red), coelomic pouches (dark purple), ciliary band (light blue). B) Gene expression (purple) of *Sp-ILP2, Sp-Kp, Sp-Np20, Sp-PPLN1, Sp-TRH, Sp-NGFFFa* NP genes. C) Expression (purple) of GPCR genes: *Sp-TRHR* and *Sp-NGFFFaR*. The shade of purple represents the level of expression. The darker the colour the higher the staining. Abbreviated labels refer to the following: OV (oral view) and LV (lateral view).

3.6 Combinatorial neuropeptide precursor gene expression studies in neural precursor cells

To obtain a more detailed comparison of NP gene expression in the developing nervous system of sea urchin larvae, I next examined the co-expression patterns at gastrula stage (48 hpf) when the first differentiated neurons are detected and an overall increase in NP gene expression is evident (Figure 3.1) (Garner *et al.,* 2016; Mellott *et al.,* 2017).

Double fluorescent ISH analysis was undertaken to determine the expression pattern of eight NP genes in the larval nervous system, relative to serotonin, a marker for apical plate neurons, and synaptotagmin, a pan-neuronal marker. NP genes were chosen that were highly expressed (Figure 3.1) and previous chromogenic data had shown isolated cell(s) expression, consistent with neuronal cells. In this work, for simplicity, I will refer to **neurons** if the co-expression of a NP gene with one or both of these two neuronal markers is reported, while we will refer to **neuron-like** cells, when the position and the shape of the NP-positive cell(s) is consistent with previously described neurons, but no expression with a neuronal differentiation marker is reported.

Out of the eight probes tested, five show clear staining at this stage, consistent with QPCR and transcriptome data at 48 hpf (Figure 3.1C-D; Table 8.5; Figure 3.11). Co-expression of three NP genes, *Sp-AN*, *Sp-Np18* and *Sp-Pedal peptide-like neuropeptide 2* (*Sp-PPLN2),* is detected in two cells in the apical region, which are also positive for serotonin and *Sp-SynB* (Figure 3.11 A-D), whereas expression of the *Sp-FSALMFamide* (*Sp-FSALMFa*), *Sp-NGFFFa* and *Sp-PPLN2* NP genes is detected in one or two bilaterally arrayed cells in the oral ectoderm, in a position consistent with post oral neuronal precursors (Figure 3-8A ; D-E ; Mellott *et al.,* 2017; Garner *et al.,* 2016).

In summary, spatial expression data revealed that various NP genes are expressed before the neurons are fully differentiated. Furthermore, distinct combinations of NP genes are co-expressed in specific populations of neuronal precursors at the gastrula stage.

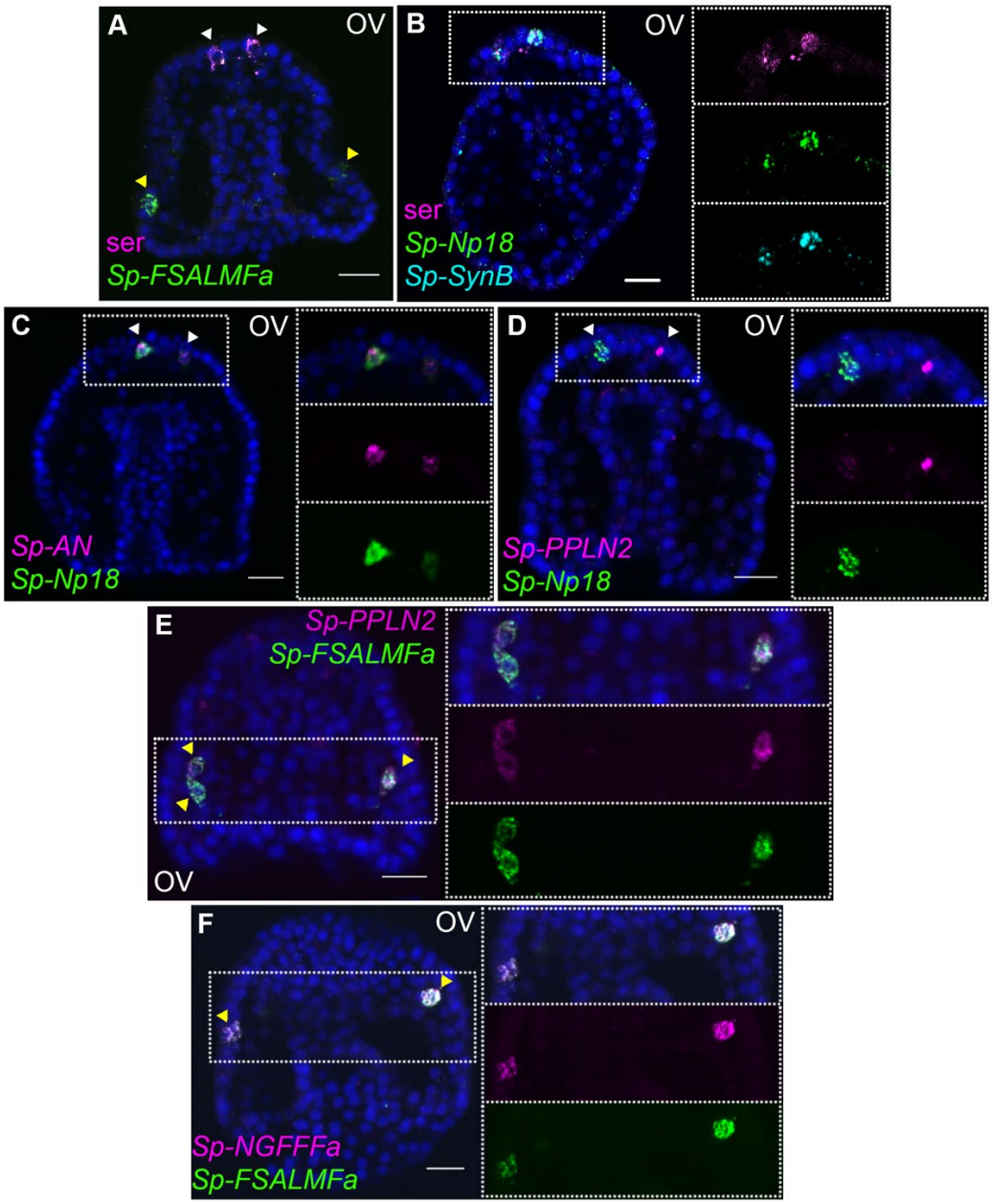

Figure 3.11 Co-expression of NP genes in the apical plate and post-oral neuron-like precursor cells of the gastrula embryo

Expression of NP genes in the apical plate and post oral neuron-like precursor cells of the gastrula embryo. Merged and single channel confocal images of 48 hpf embryos labelled using double fluorescent ISH and immunohistochemistry are shown. (A) Expression of serotonin and *Sp-FSALMFa* identifies two populations present at 48 hpf, the serotonergic (white arrowheads) and post oral (yellow arrowheads) neuron-like precursor cells, respectively. B) *Sp-Np18* NP gene and *Sp-SynB* probe co-expressed in serotonergic sensory neuronal precursor cells in gastrula embryo. (C-D) Co-expression of three NP genes in the apical plate sensory precursor cells. (E-F) Co-expression of three NP genes in two-three post oral neuron-like precursor cells. Bottom-left/Top-right corner indicates the probe or antibody used and oral view (OV) orientation. Dotted white boxes highlight the magnified region shown to the right. Scale bars: 20 µm. Experiment carried out by Teresa Mattiello and Lizzy Ward.

3.7 Combinatorial analysis of neuropeptide precursor gene expression in the larval nervous system

At the end of development, the simple nervous system of the pluteus larva (72 hpf) is composed of several dozens of neurons located in different parts of the larvae and likely having different functions. The number of neurons and the complexity of the nervous system continues to increase during postembryonic larval development (Bisgrove & Burke 1987). To gain more detailed insights into the expression of NP genes relative to the known neuronal structures and the complexity of the larval nervous system, I used double fluorescent ISH to study the co-expression of genes that have high levels of expression (Figure 3.1) and where previous chromogenic data had shown expression in isolated cell(s), consistent with neuronal cells. Furthermore, I also analysed the expression of an ortholog of the human *SecretograninV (7B2L)* gene, *Sp-SecV*, a marker of neuroendocrine cells (Bartolomucci *et al.,* 2011).

3.7.1 Apical organ and ciliary band

At the pluteus stage (72 hpf), the number of serotonergic neurons in the apical organ has increased from 1-3 (at the gastrula stage) to 8-11 and this continues to increase during larval development, consistent with findings from EdU labelling, which illustrate a high rate of cell proliferation almost exclusively in neurogenic tissues including the apical plate, ciliary band, lip and foregut tissues (Garner *et al.,* , 2016) (Figure 3.12A). Furthermore, EdU labelling coupled with immunohistochemistry with the neuronal marker SynB (1E11; Nakajima *et al.,* 2004) reveals that neurons in the ciliary band are both mitotic ($SynB^+/Edu^+$) or post-mitotic ($SynB^+/EdU^-$) (Figure 3.12A). This is important to explain the different numbers of NP gene expressing cells identified in pluteus larvae.

The apical organ, considered the central nervous system of the sea urchin larva, consists of two types of serotonergic neurons: bottle shaped primary sensory neurons associated with long cilia of the apical tuft (Figure 3.12B) and small interconnected serotonergic neurons that form a ganglion (Figure 3.12), along with support cells (Hinman and Burke, 2018). Fluorescent ISH (FISH) analysis of the expression of the neuroendocrine marker *Sp-SecV* only labelled the primary sensory

serotonergic neurons in the apical organ (Figure 3.12C), indicating a neuroendocrine role for these cells. Furthermore, various probe combinations in FISH experiments revealed that the *Sp-Np18*, *Sp-AN* and *Sp-PPLN2* NP genes continue to be co-expressed in 2-5 cells with a morphology typical of sensory neurons that also express *Sp-SecV* and serotonin (Figure 3.12C-G; Figure 3.13C). On either side, next to the serotonergic central neuronal system, two neuron-like cells at the base of the oral distal arms (Figure 3.12H-J) were identified by the expression of the *Sp-TRH* and *Sp-FSALMFa* NP genes (Figure 3.12H-J). These cells are associated with the ciliary band and send projections towards the apical ganglion and their fibres intermingle with the fibres of the serotonergic interneurons, which is most clearly seen in one-week old larvae (Figure 3.13A). The cells do not express serotonin or *Sp-SecV*, suggesting they are a different population of neurons that communicate with the serotonergic central ganglion.

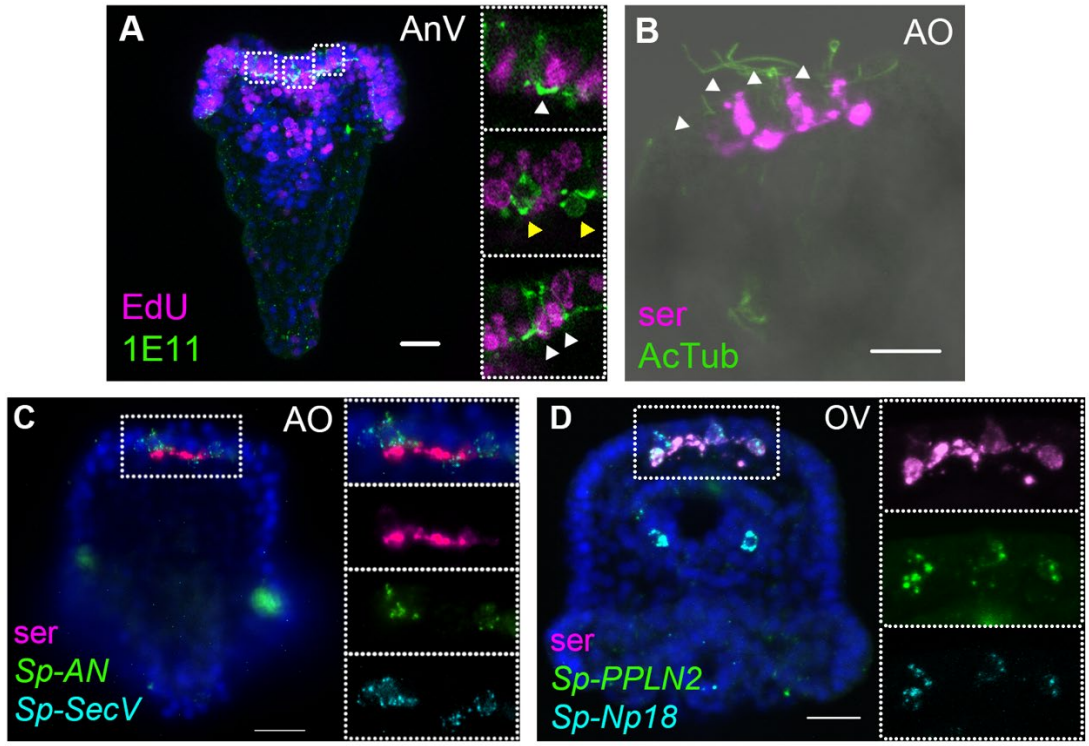

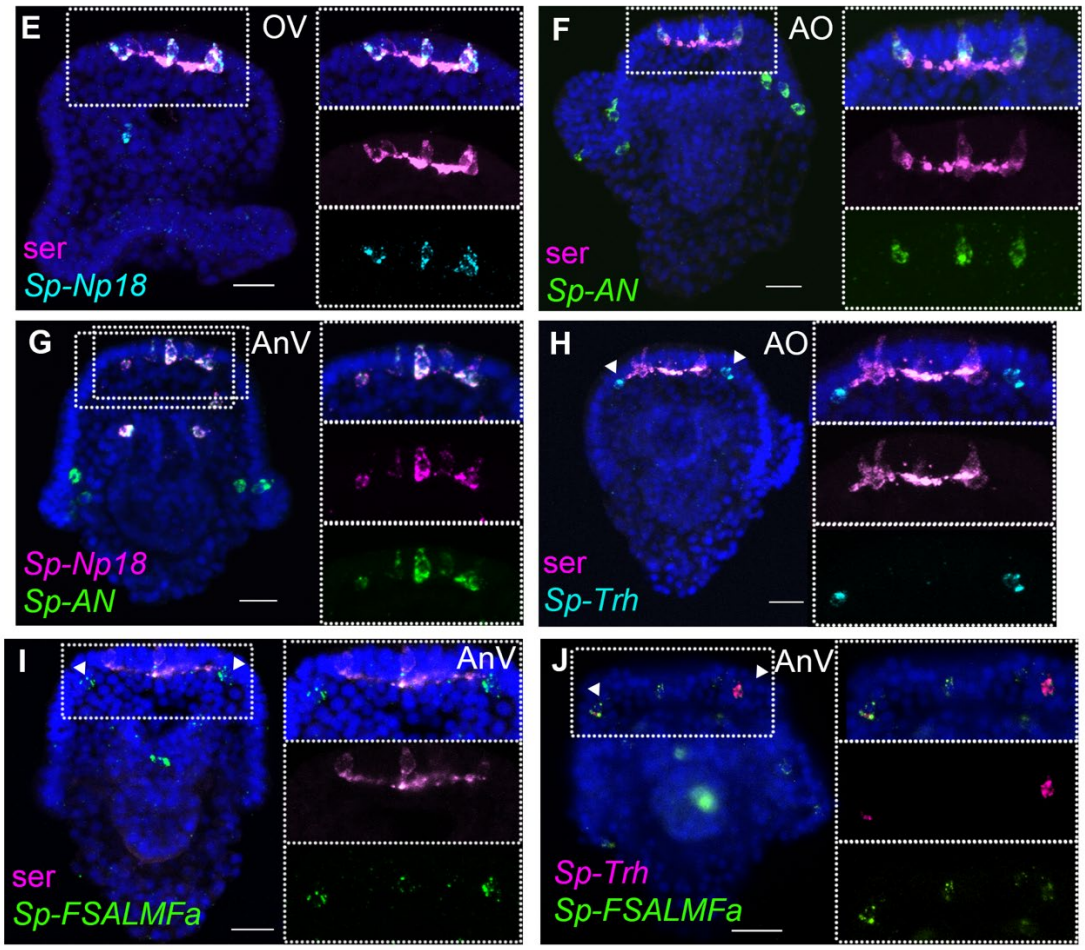

Figure 3.12 Expression of NP genes in the apical organ serotonergic neurons and ciliary band neuron-like cells

Expression of NP genes in the apical organ serotonergic neurons and ciliary band neuron-like cells. Merged and single channel confocal images of pluteus larvae (72 or 96 hpf) labelled using double fluorescent ISH and immunohistochemistry are shown. (A) EdU-and SynB (1E11) (Nakajima *et al.,* 2004) labelling experiment showing a high rate of cell proliferation in the neurogenic territories (apical organ and ciliary band, lip and foregut). Generally the SynB+ neurons are not dividing (yellow arrowhead), although some EdU+ cells are also SynB+ when analysed in single confocal z-slices (white arrowhead). Larvae at four days of development were incubated with a 10mM stock solution of EdU for two hours at room temperature and then immediately fixed as described in methods section 2.4.3. (B-C) Labelling of the larval nervous system using antibodies to serotonin and to acetylated tubulin (AcTub) and using *Sp-SecV* ISH. (B-G) NP gene expression in the apical organ serotonergic neurons. (H-J) *Sp-TRH* and *Sp-FSALMFa* co-expressed in the ciliary band, at the base of the oral distal arms, adjacent to the apical organ. Bottom-left corner indicates the probe or antibody used. Top-right corner indicates the orientation of the larva, Anal view (AnV), apical organ (AO) and oral view (OV). Dotted white boxes highlight the magnified region shown to the right. Scale bars: 20 µm. Images in panels C-J were carried out by Teresa Mattiello and Lizzy Ward.

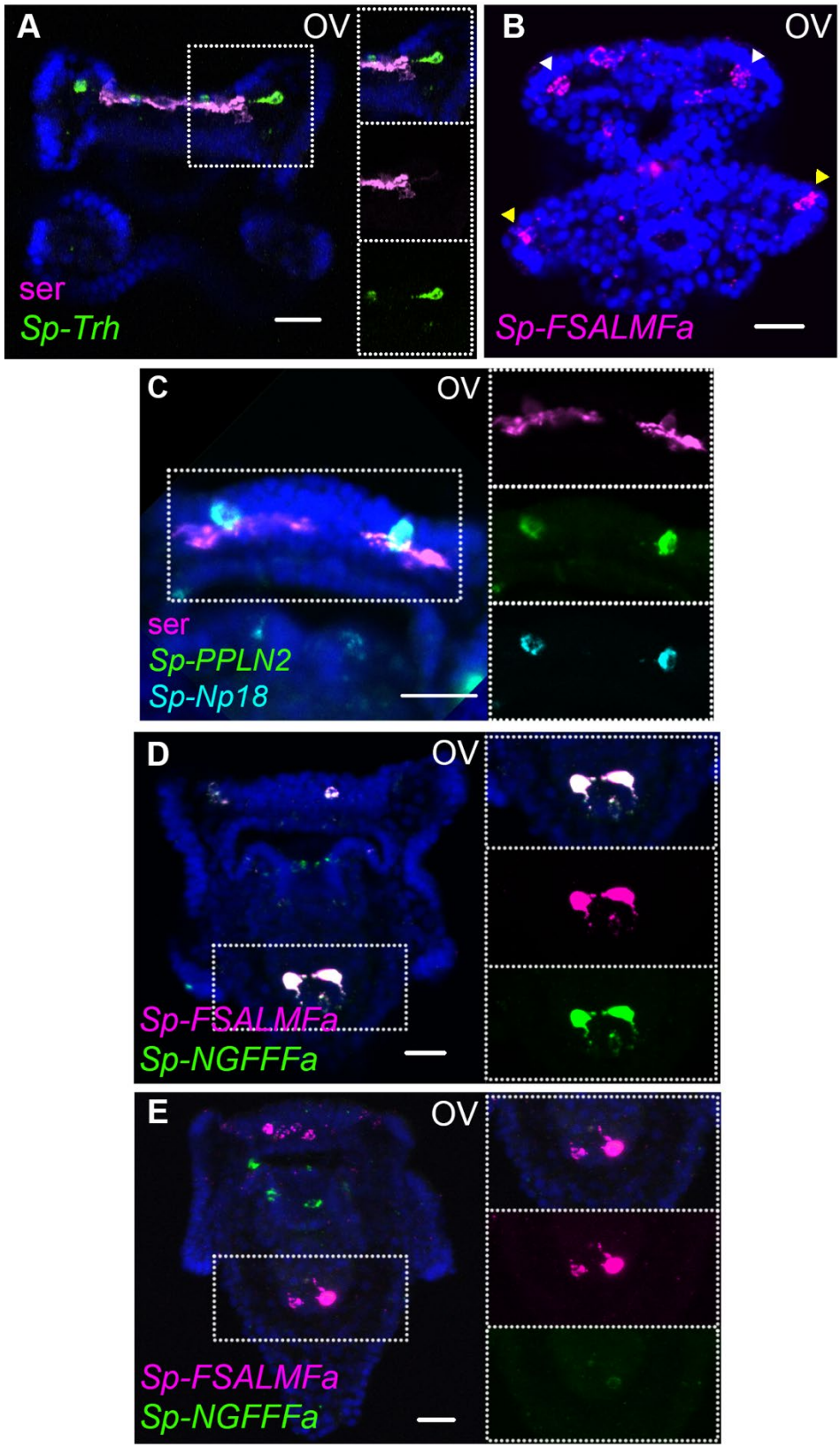

Figure 3.13 Expression of NP genes in the ciliary band, gut and apical plate

Expression of NP genes in the ciliary band, gut and apical plate in one-week old larvae. Maximum projection of merged confocal images of single and double FISH, and

immunohistochemistry. (A) *Sp-TRH* NP expressed in cells at the base of oral distal arms, connected to serotonergic ganglion by long projection in a pluteus larvae. (B) *Sp-FSALMFa* NP gene expressed in presumed oral distal and post oral neurons of a pluteus larva. White arrows indicate presumed oral distal neurons and yellow arrows indicate presumed post oral neurons. (C) *Sp-PPLN2* and *Sp-Np18* co-expressed in sensory serotoninergic neurons in the apical plate. (D and E) *Sp-FSALMFa* and *Sp-NGFFFa* NP genes both co-expressed and differentially expressed in the mid-gut of a pluteus larva. Bottom-left corner indicates the probe or antibody used. Top-right corner indicates the orientation of the larva, oral view (OV). Dotted white boxes highlight the magnified region shown to the right. Scale bars: 20µM. Images in panels A, C-H was carried out by Teresa Mattiello and Lizzy Ward.

The peripheral nervous system of the sea urchin larva is composed of neurons in the ciliary band, post oral neurons and lateral ganglion. Sp-FSALMFa is expressed in two single cells in the ciliary band at the base of the post oral arms (Figure 3.13B). The location is consistent with the expression of the Sp-FSALMFa NP gene in the presumptive dopaminergic post oral neurons (Burke et al., 2014; Bisgrove & Burke 1987), and with the expression of this gene at the gastrula stage (Figure 3.11A; E-F). Interestingly, the expression of no other NP gene analysed in this study was detected in these cells at the pluteus stage (Figure 3.12; Figure 3.13A-B). The lateral ganglion neurons consist of two clusters of two-three neurons on the left and right side of the larva (Burke *et al.,* 2006) and are associated with the ciliary band. This population of neurons has been described as dopaminergic (Bisgrove & Burke 1987). At 72 hpf the hybridization signal associated with *Sp-SecV* and *Sp-AN* NP expression is specifically revealed in two groups of cells bilaterally arranged in a manner that resembles the lateral ganglia neurons (Figure 3.14A-B). The expression of the *Sp-SecV* and *Sp-AN* NP genes suggests a neurosecretory role of these cells.

Taken together these data revealed that several NP genes are expressed in single or groups of cells and identifies several neuronal and neuronal-like sub-types in the nervous system of sea urchin larvae. Each subtype of cells is characterized by a specific combination of expressed NP genes.

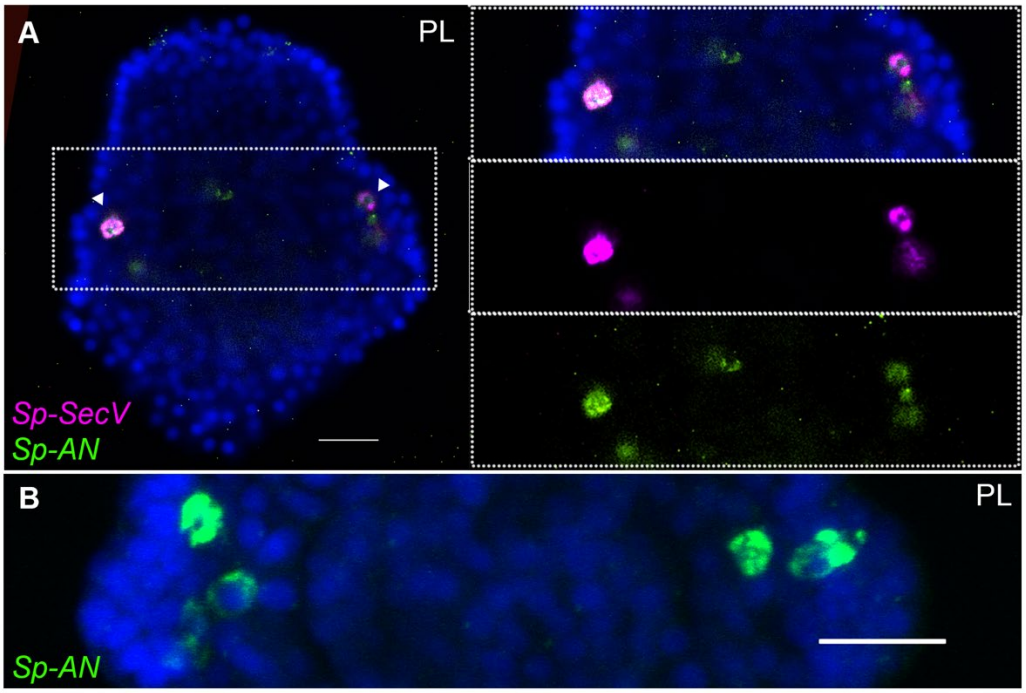

Figure 3.14 Expression of an NP gene in two clusters of two-three lateral ganglia neuron-like cells

Maximum projection of confocal image of *Sp-AN* NP gene and *Sp-SecV* in a pluteus larva (Anal View). Merged and single channel images are revealed by single and double FISH. (A) *Sp-SecV* and *Sp-AN* NP gene expression in lateral ganglia neuron-like cells. (B) Magnification of *Sp-AN* NP gene expression in the lateral ganglia neuron-like cells. Bottom-left corner indicates the probe used. Top-right corner indicates the pluteus larval stage (72 hpf). Dotted white boxes highlight the magnified region shown to the right. Scale bars: 20 µm. Experiment carried out by Teresa Mattiello and Lizzy Ward.

3.7.2 Mouth and gut cell systems

Several neurons expressing GABA or dopamine have been described around the mouth and in the oesophagus (foregut) of the sea urchin larva (Bisgrove & Burke 1987). At the early pluteus stage (72 hpf), approximately four to six neurons appear around the mouth (lip) and these have been described as dopaminergic neurons (Bisgrove & Burke 1987), while a few neurons of endodermal origin differentiate in the oesophagus (Wei *et al.,* 2011). Single and double whole-mount ISH experiments show that *Sp-FSALMFa*, *Sp-NGFFFa, Sp-Np18*, *Sp-PPLN2* and *Sp-AN* NP genes are all expressed in two to four isolated and bilaterally arranged cells around the mouth (Figure 3.15A-F) in the 72 hpf larvae. Although there is variation in the number of

cells and the degree of co-expression of NP genes around the mouth, signals associated with *Sp-PPLN2, Sp-AN* and *Sp-Np18* expression are largely co-localized in two to four cells in the larval lip, as they are co-localized in the apical domain (Figure 3.15A-B; Figure 3.12D and G). The *Sp-FSALMFa* and *Sp-NGFFFa* NP genes are mostly co-expressed in another population of cells around the mouth of the larva (Figure 3.15D), which rarely coincide with the cells expressing *Sp-PPLN2* (Figure 3.15C). Even the cells expressing the *Sp-FSALMFa* and *Sp-NGFFFa* NP genes around the mouth show a high degree of variability of co-expression (compare Figure 3.15D with Figure 3.15E and Table 3.2). The number and type of neurons around the mouth increase in the larva, as well as the number of NP gene-expressing cells, as shown by the expression of *Sp-FSALMFa* (Figure 3.15F) in one week old larvae, which is consistent with large cell-proliferation occurring in this domain of the larvae as shown by EdU staining (Figure 3.12A). To better understand the variation in NP genes expressed in various cells we counted single and double gene expressing cells in several larvae in each experiment (N>7, with exception of *Sp-FSALMFa* and *Sp-Np18* NP genes where N>2). Table 3.2 summarizes the results and shows that the single cells surrounding the mouth never express *Sp-TRH* or *Sp-SecV* (Figure 3.12C and H). Four double fluorescent ISH experiments are analysed in the 72 hpf and one week old larval mouth. The co-expression of *Sp-Np18* with either *Sp-AN* or *Sp-PPLN2* shows a high degree of variability when several embryos are analysed. In contrast, *Sp-FSALMFa* with *Sp-NGFFFa* fluorescent ISH experiments generally show a more consistent co-expression in the cells around the mouth (Table 3.2).

Two to three GABAnergic neurons have been identified in the early pluteus foregut (Bisgrove & Burke 1987). Chromogenic ISH hybridization reveals the expression of three NP genes, *Sp-Np20, Sp-ILP2* and *Sp-Kp*, with a diffuse pattern in the foregut and not only in individual neurons (Figure 3.8A, B, I and J). Later in larval development, at one week-old, *Sp-FSALMFa*, *Sp-NGFFFa* (Figure 3.13D and E) and *Sp-PPLN2* are co-expressed in two to three isolated cells in the mid-gut (Figure 3.15F and G). There is also variability in the expression of *Sp-FSALMFa* and *Sp-NGFFFa* - compare Figure 3.13D with Figure 3.13E. None of the other NP genes analysed in this study were detected in these cells, not even in one-week old larvae (Figure 3.15G; Figure 3.13A).

Neuronal cell types have so far not been described to be in association with the midgut, however other cell types with endocrine/digestive function are known to be present in the midgut (Perillo *et al.,* 2016). Our results in the gut/mouth reveal a similar situation as described for the apical organ and ciliary band neuronal cells: several cell populations are identified by specific NP gene expression signatures. Furthermore, our fluorescent ISH analysis has revealed a variable pattern of NP gene expression in the neuron-like cells around the mouth and the presence of a specific population of cells in the midgut.

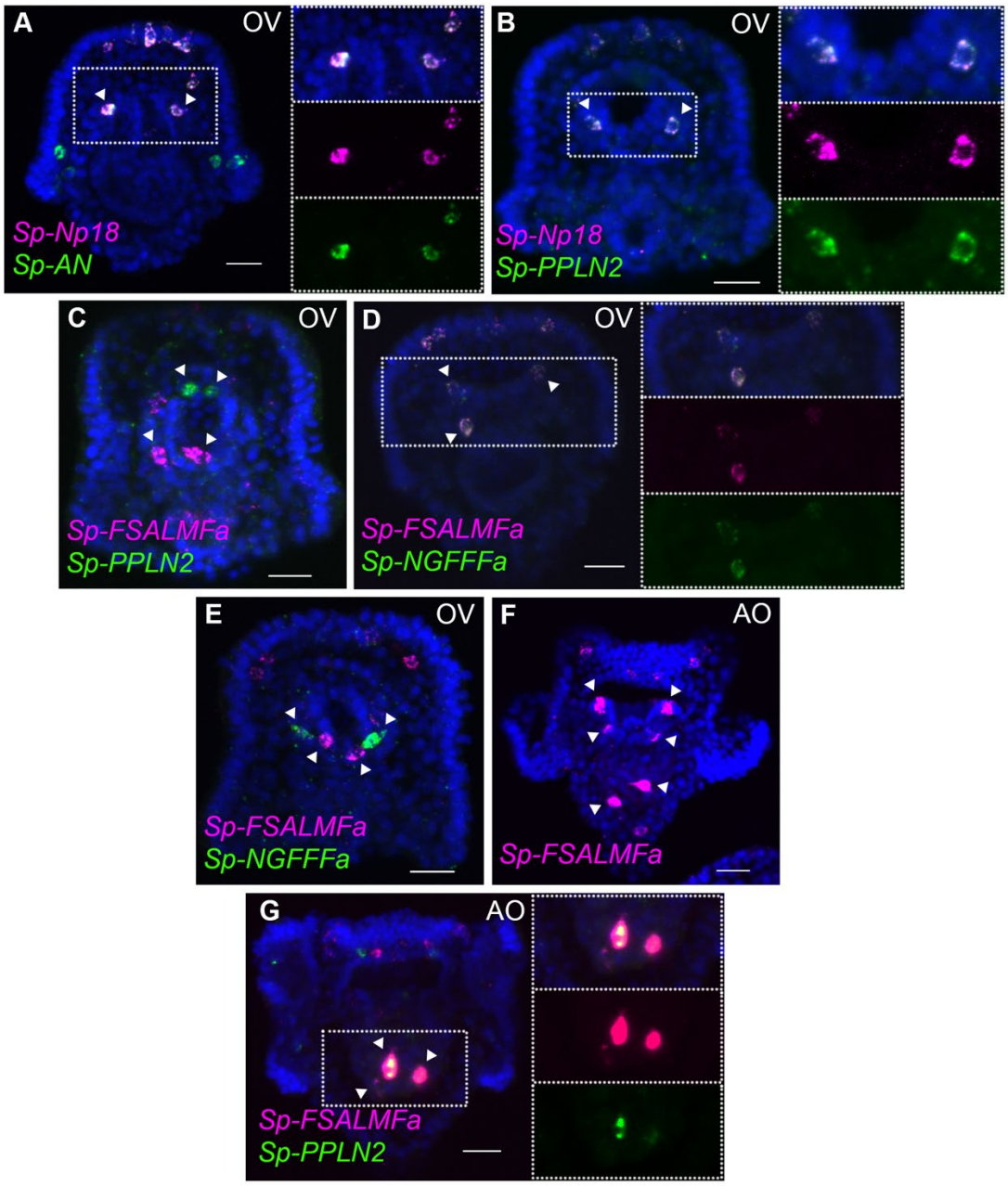

Figure 3.15 Expression of NP genes in the mouth and gut cells

Maximum projection confocal images for FISH analysis of NP gene expression in the pluteus larva (72 hpf (A-E) and 1 week (F-G)). Merged and single channel images labelled using single and double fluorescent ISH. A-E) NP gene expression in mouth neurons (white arrows). F) *Sp-FSALMFa* NP gene expression in mouth neurons and midgut cells (yellow arrows) in a later larval stage. G) *Sp-FSALMFa* and *Sp-PPLN1* positive cells in the midgut. Bottom-left corner indicates the probe used. Top-right corner indicates the orientation of the larva, oral view (OV) or Apical Organ (AO) view. Dotted white boxes highlight the magnified region shown to the right. Asterisk indicates the midgut. Scale bars: 20 µm. Images in panels A-F and I was carried out by Teresa Mattiello and Lizzy Ward.

A)

Mouth expression							
Sp-FSALMFa* and *Sp-NGFFFa	*Sp-NGFFFa* only	*Sp-FSALMFa* only	No expression	Co-expression	No co-expression	Both co-expression and no co-expression	**Total individuals counted**
72 hpf				6	1	1	8
1 wpf	2				3	2	7

B)

Mouth expression							
Sp-AN* and *Sp-Np18	*Sp-AN* only	*Sp-Np18* only	No expression	Co-expression	No co-expression	Both co-expression and no co-expression	**Total individuals counted**
72 hpf		4		3			7
1 wpf		2		4		1	7

C)

Mouth expression							
Sp-PPLN2* and *Sp-Np18	*Sp-PPLN2* only	*Sp-Np18* only	No expression	Co-expression	No co-expression	Both co-expression and no co-expression	**Total individuals counted**
72 hpf	1		4	4		2	11
1 wpf	3			3	2	1	9

D)

Mouth expression							
Sp-FSALMFa* and *Sp-PPLN2	*Sp-PPLN2* only	*Sp-FSALMFa* only	No expression	Co-expression	No co-expression	Both co-expression and no co-expression	**Total individuals counted**
72 hpf		2			1		3
1 wpf					1	1	2

Table 3.2 Four pairs of NP genes exhibit variable gene expression in cells in the mouth at larval stage

Four pairs of NP genes exhibit variable gene expression in cells around the mouth at larval stages (72 hpf and 1 wpf). The number of embryos with a particular gene expression pattern around the mouth with respect to the total number of embryos imaged by double fluorescent WMISH is shown. Generally, these four pairs of NP genes have variable expression patterns between individual embryos imaged. *Sp-AN* and *Sp-NP18*, and *Sp-PPLN2* and *Sp-Np18 NP* gene pairs have a more variable expression pattern. *Sp-FALMFa* and *Sp-PPLN2* NP genes are never co-expressed, and *Sp-FSALMFa* and *Sp-NGFFFa* NP genes are mostly co-expressed in the mouth neurons at 72 hpf. Furthermore, these expression patterns vary in later larval development (1 wpf).

3.8 Discussion

The early sea urchin larval nervous system is composed of 40-50 neurons, characterised by the expression of specific neurotransmitters (Bisgrove & Burke 1987; Angerer *et al.,* 2011). Understanding the diversity and distribution of NP gene and GPCR genes expression is essential for identification of the diverse neuronal subtypes in echinoderm larval nervous systems. Here I report the first multi-gene analysis of NP gene and GPCR gene expression in larvae of a sea urchin species (Figure 3.16). *S. purpuratus* has at least 38 NP genes and expression of almost all NP genes analysed here was detected in the developing sea urchin or larval stages (Figure 3.1). The identity of 41 rhodopsin-type and four secretin-type GPCRs that are homologs of vertebrate and/or invertebrate neuropeptide receptors have been identified in *S. purpuratus* (Burke *et al.,* 2006a; Rowe and Elphick, 2012; Yañez-Guerra *et al.,* 2018). The expression of 26 GPCR genes analysed here were mostly not detected at high levels (Figure 3.5; Figure 3.6). Spatial expression patterns of nine NP genes and two GPCR genes were revealed in the early pluteus larvae and the expression of eight NP genes and one GPCR gene was detected already in the gastrula. The existence of diverse neuronal subtypes in the echinoderm larval nervous system has been revealed by immunocytochemical analysis of the neurotransmitters serotonin, dopamine and GABA (Bisgrove & Burke 1987). Localisation of NP gene expression, as reported here, has revealed distinct subpopulations of neuropeptidergic cells, demonstrating that the sea urchin larval nervous system is far more complex than previously thought (Figure 3.16). Furthermore, QPCR analysis and chromogenic ISH detected the expression of a few NP genes and GPCR genes prior to the gastrula stage and in undifferentiated and non-neuronal/non-secretory cells, suggesting that these signalling molecules also have a role during the early development of the sea urchin embryos (Chapter 4).

Neuronal co-expression of multiple neuropeptide precursor genes and/or neuropeptides derived from different precursor proteins has been reported in a variety of taxa including, for example, cnidarians (Hansen *et al.,* 2002), molluscs (De Lange *et al.,* 1997), annelids (Williams *et al.,* 2017) and vertebrates (Herget and Ryu, 2015). Here I report this property of neuropeptide signalling systems for the first time

in the larval nervous system of an echinoderm. Thus, the results show that consistent co-expression signatures were found for two different combinations of NP genes: i) *Sp-FSALMFa* and *Sp-NGFFFa* and *ii) Sp-AN*, *Sp-PPLN2* and *Sp-Np18*. The former two genes are initially co-expressed in cells that resemble the precursor of post oral neurons in the gastrula and then in neuron-like cells around the mouth, while the latter three genes are expressed in the primary sensory neurons located in the apical organ. Their co-expression starts as soon as the precursor sensory cells express the serotonin marker at the gastrula stage (48 hpf) and then remains in these cells in all subsequent stages analysed here. The same three genes are also co-expressed in neuron-like cells around the mouth at the pluteus stage (Table 3.2). These co-expression signatures suggest similar regulation of these genes, possibly by a combination of transcription factors, which may work as terminal selector genes to control the differentiated state of post-mitotic neurons (Hobert, 2016a). Recent studies have shown the role of several transcription factors and signalling molecules in determining the identity of large subpopulations of neurons (for review see Hinman and Burke 2018), including, for example, *ac-sc* regulation of the development of serotonergic neurons (Slota and McClay 2018). However, none of the data so far published can explain the highly restricted expression pattern of NP genes that we have identified in this study. This suggests that more studies need to be done to investigate the regulation of neuronal subtypes. Accordingly, a paper by Perillo and colleagues (Perillo *et al.,* 2018), identifies for the first time a precise combination of transcription factors (*lox, brn1/2/4* and *islet-1*) that is consistent with the restricted expression of the *Sp-AN* NP gene in the lateral ganglia neurons.

A few distinct sub-populations of neurons or neuron-like cells have been identified in this study, which have not been described before. For instance, the isolated cells associated with the ciliary bands, at the base of the arms, the oral distal and post oral arms, all express *Sp-FSALMFa.* Perillo and colleagues (2018) also identified *Sp-AN* NP gene expression in the post oral neurons. Two types of neurons have been recently described in the ciliary bands of sea urchin larvae: cholinergic neurons are widely distributed throughout this structure and dopaminergic neurons are concentrated in a post oral location (Slota and Mcclay, 2018). Adams and collaborators identified the

post oral dopaminergic neurons to be involved in controlling arm length in response to food (Adams *et al.,* 2011). *Sp-FSALMFa* is expressed in four cells, one at the base of each arm and so neuropeptides encoded by the *Sp-FSALMFa* gene may likewise have a role in controlling arm length or arm growth, possibly in response to an environmental signal. In comparison, the *Sp-TRH* NP gene is expressed only in two cells and these are at the base of the oral distal arms, likely co-expressed with *Sp-TRHR*. Interestingly, TRH is known to have a role in growth in vertebrates and in the nematode *C. elegans* (Duncan Bassett and Williams, 2016; Galas *et al.,* 2009; Sinay *et al.,* 2017b) and therefore it is plausible to hypothesize that TRH-type peptides may also affect arm growth in *S. purpuratus* larvae, perhaps asymmetrically. Furthermore, *Sp-Opsin3.2* has been detected in two cells, adjacent to the apical plate (Petrone, 2015; Valencia *et al.,* 2019; Valero-gracia *et al.,* 2016), in a similar position to the *Sp-TRH* positive cells. Double fluorescent ISH has revealed that these two genes are co-expressed (Petrone, 2015) (Figure 1.12) and are probably neurosecretory non-directional photoreceptors. Taken together, these observations suggest that neuropeptides expressed in the cells at the base of the arms may be involved in controlling arm length in response to food and/or light.

Neuropeptides derived from precursor proteins are packed in dense core vesicles (DCV). The maturation and release of functional neuropeptides is regulated by several factors, among them the family of chromogranin/secretogranin proteins, which play a key role in the regulated secretory pathway (Taupenot *et al.,* 2003). This chapter has shown the expression of *Sp-SecV,* previously identified in proteomic studies (Monroe *et al.,* , 2018), specifically in the primary sensory neurons of the apical organ and in the pancreatic-like neurons of the lateral ganglia (Perillo *et al.,* 2018). Interestingly, human Secretogranin V (SGC5, Gene ID 6447) is specifically expressed in the brain, pancreas, adrenal and stomach, highlighting the conservation in deuterostomes of an ancient neuroendocrine molecular pathway.

The three GPCRs that were identified as mid- or high-expressing genes, *Sp-LGR*, *Sp-CRHR* and *Sp-PRHR*, are orphan receptors with no proven ligand binding. Leucine-rich repeat-containing GPCRs (LGRs) have been identified as glycoprotein hormone receptors. Glycoprotein hormone receptors include luteinizing hormone (LH), follicle-

stimulating hormone (FSH) and thyroid-stimulating hormone (TSH) receptors and are often bound by insulin-type, glycoprotein-type and buriscon-type hormones (Elphick *et al.,* 2018; Shea Yu Hsu *et al.,* 2000). There are three subtypes of LGRs, which differ in the following features: the number of LRR motifs, the absence or presence of an LDLa motif (low density lipoprotein receptor-like cysteine-rich motif) and the type-specific hinge region (Van Hiel *et al.,* 2012). Echinoderms have all three types of LGRs. *Sp-LG-Receptor* with high expression during embryonic development is a type C LGR (Van Hiel *et al.,* 2012). It has been suggested that the insulin superfamily of peptides, including insulins, relaxins, insulin-like peptides and insulin-like growth factors are the ligands of type C LGRs (Hopkins *et al.,* 2007; Scott *et al.,* 2003; Van Hiel *et al.,* 2012). Interestingly, *Sp-ILP2* NP gene has a peak in expression at the same embryonic stages (Figure 3.2*;* Figure 3.5*;* Table 8.6) and therefore it is plausible to hypothesise that Sp-LGR may be a receptor for Sp-ILP2.

CRH-receptors are secretin-type receptors, and there is a huge expansion of 161 secretin-type receptors in *S. purpuratus,* compared with *H. sapiens* that only has 15 secretin-type receptors (Burke *et al.,* 2006a; Consortium, 2006). Deuterostomian CRH NP signalling system is orthologous to the protostomian diuretic hormone 44 (DH44) and likely evolved from an ancestral bilaterian peptidergic system (Mirabeau and Joly, 2013). First identified as a stress hormone in mammals, CRH is also involved in metabolism by interacting with TRH and has many other diverse physiological roles (Lovejoy et al., 2014; Lovejoy and Balment, 1999). A CRH peptide has not yet been identified in *S. purpuratus*, but has been identified in the echinoderm *Asterias rubens* (Semmens *et al.,* 2016). *Sp-Prolactin-releasing hormone receptor* (*Sp-PRH-Receptor)* has a similar, but higher expression pattern to *Sp-CRH-Receptor* (Figure 3.5B; Table 8.6). PRH is one of many families of neuropeptides that have a C-terminal RFamide motif (Elphick and Mirabeau, 2014). Prolactin-releasing peptides and their receptors originated from the neuropeptide Y/F (NPY/F) NP signalling systems (Elphick and Mirabeau, 2014; Lagerström *et al.,* 2005). NPY peptides have not yet been identified in echinoderms (Yañez-Guerra *et al.,* 2019). Prolactin is best known for its role in enabling mammals to produce milk but has many other physiological functions. In mammals, TRH stimulates the release of thyroid-stimulating hormone and prolactin

from the pituitary gland. Interestingly, TRH NP signalling is present at the pluteus larval stage and later I show that it has a conserved role in growth (Chapter 6). We know that *Sp-CRH-Receptor* and *Sp-PRH-Receptor* are present at the pluteus larval stage. The discovery of a CRH and PRH peptide in *S. purpuratus*, and the characterisation of CRH and PRH ligand-receptor pairs will provide further insights into the evolution of physiological roles of the CRH and PRH NP signalling system and could highlight a possible involvement with the TRH NP signalling system.

The quantitative analysis of the whole-mount ISH results (Table 3.2; Figure 3.17) reveals variability of the NP gene combinations expressed during embryonic development and larval stages, suggesting a constant modulation of the expression of NP genes, in response to both developmental and possibly environmental cues. For instance, the post oral neuron precursors seem to exhibit a transient expression of NP genes between 48 hpf and 72 hpf: at 48 hpf, they specifically express *Sp-FSALMFa*, *Sp-NGFFFa* and *Sp-PPLN2,* whereas only the *Sp-FSALMFa* precursor gene is expressed at 72 hpf. A similar combination of NP genes is expressed in the lip and midgut cells at 72 hpf, suggesting that these newly formed neuronal or secretory cells might acquire a similar NP gene signature. Therefore, the two initial post oral neuron-like cells (Figure 3.16) either turn off *Sp-NGFFFa* and *Sp-PPLN2* NP genes, or the cells at 72 hpf are actually newly differentiated, consistent with the constant production of neurons identified by EdU labelling (Figure 3.12) (Garner *et al.,* 2016). Cell-tracing experiments have not been performed on those cells, and so despite previous literature referring to both sets of neurons as 'post oral' we cannot be sure these are the same cells. In both situations, our analysis identifies a highly dynamic regulation of NP genes in the larvae, as already discussed for neuron-like cells associated with the mouth (Table 3.2).

Figure 3.16 summarises the expression of NP genes at the gastrula (48 hpf) and pluteus (72 hpf) stages. At the gastrula stage the first NPs genes are expressed in a pattern consistent with the appearance of post mitotic precursors of serotonergic neurons and post oral neurons (Garner *et al.,* 2016). Furthermore, two distinct combinations of NP genes are expressed in each population of cells consistent with these neuronal precursors, overlapping only by the expression of *Sp-PPLN2,*

suggesting they have diverse functions. In the early pluteus (72 hpf) the number of NP genes expressed (Figure 3.1) largely correlates with the increased complexity of the nervous and secretory systems in the apical plate, ciliary band, lateral ganglia, lip and foregut. At the early pluteus stage, the NP genes are expressed in a pattern suggesting the apical plate and lip each have at least two distinct subpopulations of neurons and neuron-like cells. The expression of *Sp-FSALMFa* in the post oral dopaminergic neuron-like cells and *Sp-FSALMFa* and *Sp-TRH* in the oral distal neuron-like cells identifies two distinct populations of cells, separate from rest of the ciliary band. Taken together, I propose the following populations of neuronal and/or secretory cells in the sea urchin pluteus (Figure 3.16): the apical plate is divided into: 1) primary sensory serotonergic neurons that express various NP genes and *Sp-SecV*; and 2) serotonergic interneurons that do not express any of the NP genes investigated; 3) the oral distal neuron-like cells in the ciliary band, adjacent to the apical plate, characterized by the expression of *Sp-TRH* and *Sp-FSALMFa* NP genes; 4) two post oral neuron-like cells associated with the ciliary band, at the bases of the post oral arms, identified by the expression of *Sp-FSALMFa*; 5) other ciliary band neurons generally identified by SynB neuronal markers (Angerer *et al.,* , 2011); 6) lateral ganglia neurons associated with the left and right ciliary bands and expressing *Sp-AN* (Perillo *et al.,* 2018) and *Sp-SecV* NP genes; 7) the larval neuron-like cells associated with the mouth, which are divided into at least two sub-types, each with a distinct combination of NP gene expression; 8) foregut GABAergic neurons described by Bisgrove and Burke (1987) not expressing any of the NP genes studied here; and 9) midgut cells expressing NP genes.

In conclusion, this chapter has revealed that the sea urchin larval nervous system is far more complex at a neurochemical level than was previously known.

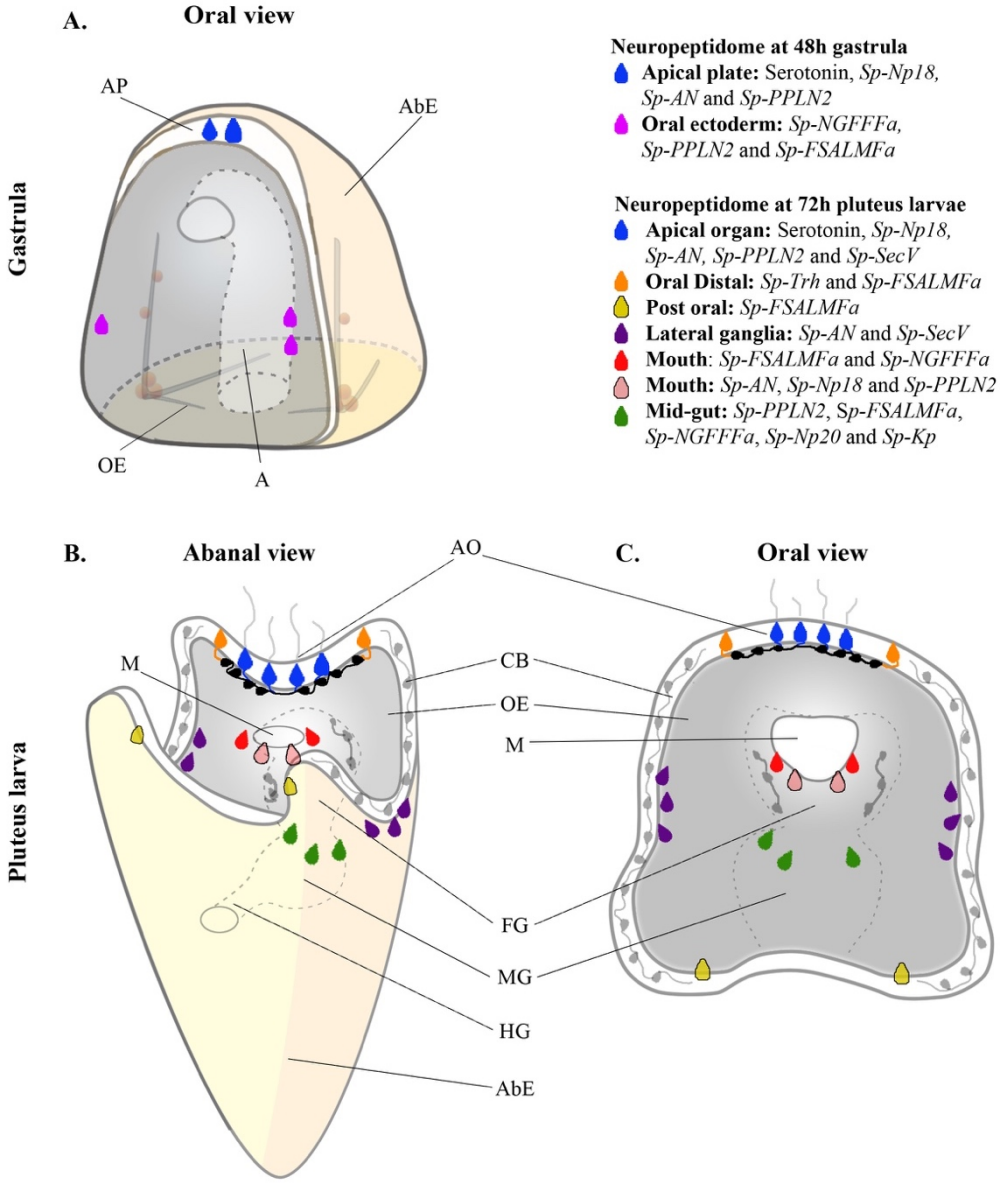

Figure 3.16 Single cell map of the developing sea urchin nervous system

Colour coded cartoon map showing various combinations of NP gene and *Sp-SecV* expression at single cell resolution in the sea urchin at the gastrula stage and in pluteus larvae. (A) NP gene expression in two populations of cells at the gastrula stage. Serotonergic neuronal precursor cells (blue) and post oral neuronal-like precursor cells in the oral ectoderm (magenta). (B-C) NP gene expression in eight different neuronal and presumed neuronal populations in the larval nervous system, shown from abanal and an oral view. Sensory serotonergic neurons (blue), lateral ganglion neurons (purple), presumed oral distal neurons (orange), presumed post oral neurons (yellow), presumed lip neurons (red and pink) and mid-gut exocrine-like cells (dark green). Black and grey neurons (in foregut, ciliary band and serotonergic interneurons) have been identified in previous studies but do not express any of the NP genes examined in this study. Abbreviated labels refers to the following, AP (Apical Plate), AbE (Aboral Ectoderm), OE (Oral Ectoderm), A (Archenteron), AO (Apical Organ), CB (Ciliary band), M (Mouth), FG (Foregut), MG (Midgut) and HG (Hindgut).

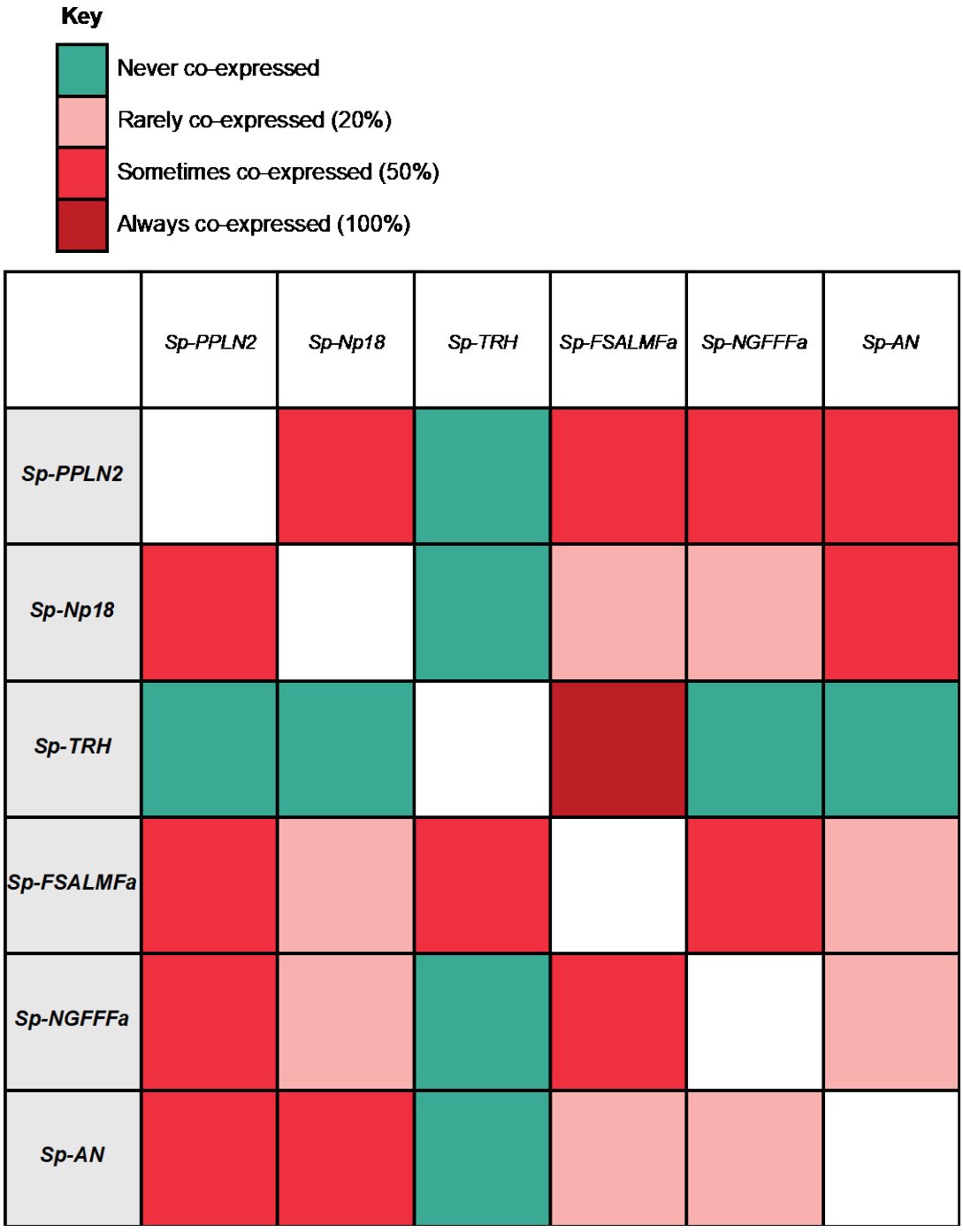

Figure 3.17 Summary of co-expression profiles of NP genes in the pluteus larvae

The occurrence of co-expression between six NP genes (*Sp-PPLN2*, *Sp-Np18*, *Sp-TRH*, *Sp-FSALMFa*, *Sp-NGFFFa*, *Sp-AN*) in the pluteus larvae. For the NP gene names (in bold in the first column) the occurrence of co-expression is categorised as the following: never expressed (green); rarely co-expressed (light pink, co-expression in 20% of cells); sometimes co-expressed (dark pink, co-expression seen in 50% of cells); and always co-expressed (red, co-expression in 100% of cells). For example, *Sp-TRH* is always co-expressed with *Sp-FSALMFa* and never expressed with one of the other 4 neuropeptides, while *Sp-FSALMFa* is sometimes co-expressed with *Sp-TRH* and sometimes co-expressed with *Sp-PPLN2* and *Sp-NGFFFa*.

Chapter 4 Embryonic expression of neuropeptide genes

In this chapter, I continue my spatial-temporal characterisation of neuropeptide expression in *S. purpuratus*, with the specific aim of investigating if NPs can play a role in early embryonic development in a non-neuronal context. Here I focus the investigation on the peptidergic complexity from a fertilised egg (0 hpf) through to an early gastrula stage (45 hpf), before the first neurons differentiate. I first present QPCR and transcriptome data to obtain quantitative temporal expression patterns for NP genes and some GPCR genes. I then use ISH to characterise the spatial expression for some NP genes and their receptors at blastula, mesenchyme blastula and early gastrula stage embryos. Finally, I summarise the chemical complexity found in the sea urchin embryo by mapping distinctive combinations of NP genes onto different cell types, both neurogenic and non-neurogenic.

Aspects of this experimental work reported in this chapter were carried out by Masters student Teresa Mattiello and undergraduate students Lizzy Ward and Jeremie Subrini (under my supervision).

4.1 Quantitative PCR (QPCR) reveals NP gene expression during embryonic development

38 NP genes have been identified in the *S. purpuratus* genome (see section 3.1). To obtain a detailed overview of NP gene expression in the early embryo, I analysed their temporal expression from a fertilised egg at 0 hpf, to the mid-gastrula stage at 45 hpf. For this I used available data from an *S. purpuratus* quantitative developmental transcriptome (Echinobase; http://www.echinobase.org/Echinobase/), and I also carried out high-resolution quantitative real-time PCR (QPCR) measurements. To obtain higher resolution data, I chose developmental times that were more frequent than the transcriptome data (every 3 hours). Furthermore, I analysed the expression of a potential ortholog of the human Secretogranin V (7B2L) gene, *Sp-SecV*. Chromogranin/secretogranin proteins play a key role in the regulated secretory pathway (Taupenot *et al.,* 2003).

Gene expression was split into three categories: high-expressing, mid-expressing and low-expressing genes. Four high-expressing genes reach or surpass 950 transcripts per embryo at an embryonic stage(s) (Figure 4.1). Some of those genes reach over 3500 transcripts per embryo, with the highest expressing gene, *Sp-Pedal peptide-like neuropeptide 1* (*Sp-PPLN1*) reaching approximately 17,000 transcripts per embryo at 40 hpf (Figure 4.1). Eight mid-expressing genes have more than 320 transcripts per embryo, but less than 950 transcripts per embryo at an embryonic stage(s) (Figure 4.2). 20 low-expressing genes have less than 320 transcripts per embryo at an embryonic stage(s) (Figure 4.3).

High-, mid- and low- expressing genes generally are not detected in the unfertilised egg (0 hpf) or at cleavage stage and their expression increases as development proceeds. In the majority of cases, the onset of expression is after mesenchyme blastula (24 hpf), when none of the different embryonic cell types are differentiated; however, precursors of various cell lineages are specified and segregated (Figure 4.1 C-D; Figure 4.2 D-E; Figure 4.3 A-D; Table 8.5) (Cameron *et al*., 1987; Davidson, 1989; Davidson *et al*., 1998). An example is *Sp-SecV* which increases in expression in the mid-gastrula embryo (40 hpf) (Figure 4.1 B; Table 8.5). The exception to this pattern

is five high- and mid- expressing NP genes that have an onset of expression before mesenchyme blastula (24 hpf). *Sp-PPLN1* has very high expression before the mesenchyme blastula stage (24 hpf) (Figure 4.1 A). Mid-expressing genes *Sp-TRH*, *Sp-Ox1*, and *Sp-Ox2* begin increasing in transcript levels before the mesenchyme blastula stage (Figure 4.2B-C; Table 8.5) Lastly, *Sp-MCH* has its highest embryonic expression in unfertilized eggs (0 hpf), reflecting maternal expression (Figure 4.2A; Table 8.5).

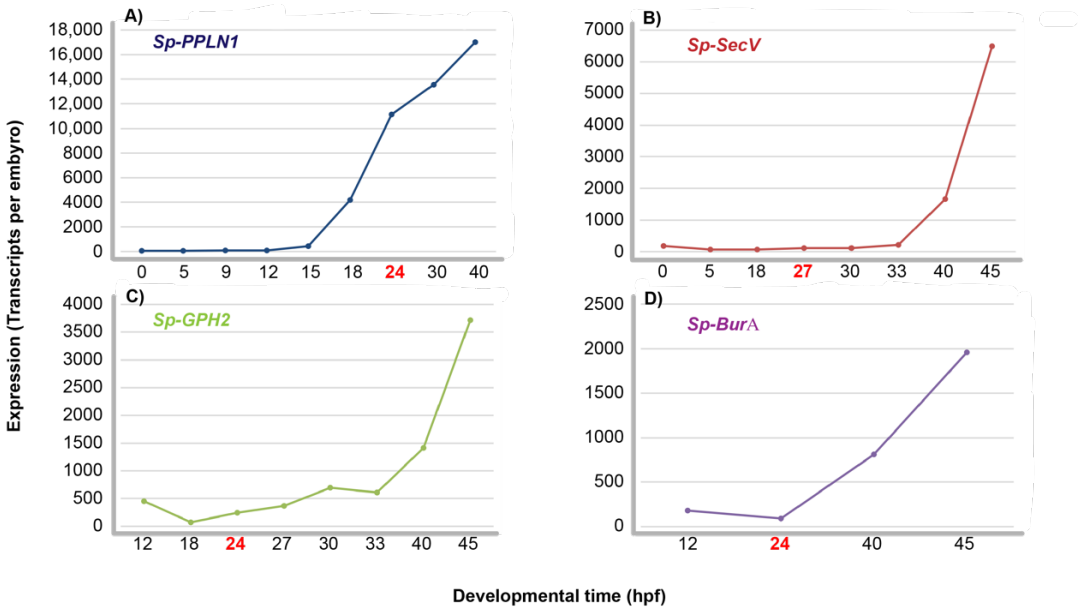

Figure 4.1. Temporal expression of highly expressed NP genes and *Sp-SecV* during early embryonic development

The line graphs depict the highest expressing NP genes (graph A, C-D) and *Sp-SecV*, a neuroendocrine marker (graph B) from unfertilized eggs (0 hpf) to the mid-gastrula stage (45 hpf), before any neurons differentiate in *S. purpuratus* development. Gene expression quantification (expressed in transcripts per embryo) has been carried out with QPCR and normalized against an internal standard (see methods section 2.5.4) and known expression levels of genes. An increase in expression is seen for most genes at the beginning of gastrulation. Graph A) *Sp-PPLN1* is an exception where the number of transcripts per embryo of *Sp-PPLN1* rises from approximately 400 transcripts per embryo at the hatched blastula stage (15 hpf) to over 4000 transcripts per embryo at the blastula stage (18 hpf), almost a ten-fold increase in 3 hours. *Sp-PPLN1* continues to increase, reaching over 17,000 transcripts per embryo at 40 hpf. The time of appearance of neuronal precursor cells is labelled in red. Highest expressing genes are defined as those reaching at least 950 transcripts per embryo. Genes are colour-coded, and their names are above each graph. Different line graphs have slightly different developmental times, which mostly reflect similar embryonic stages (for more details on sea urchin embryonic development see introduction section 1.4.1). QPCR data were collected by Teresa Mattiello.

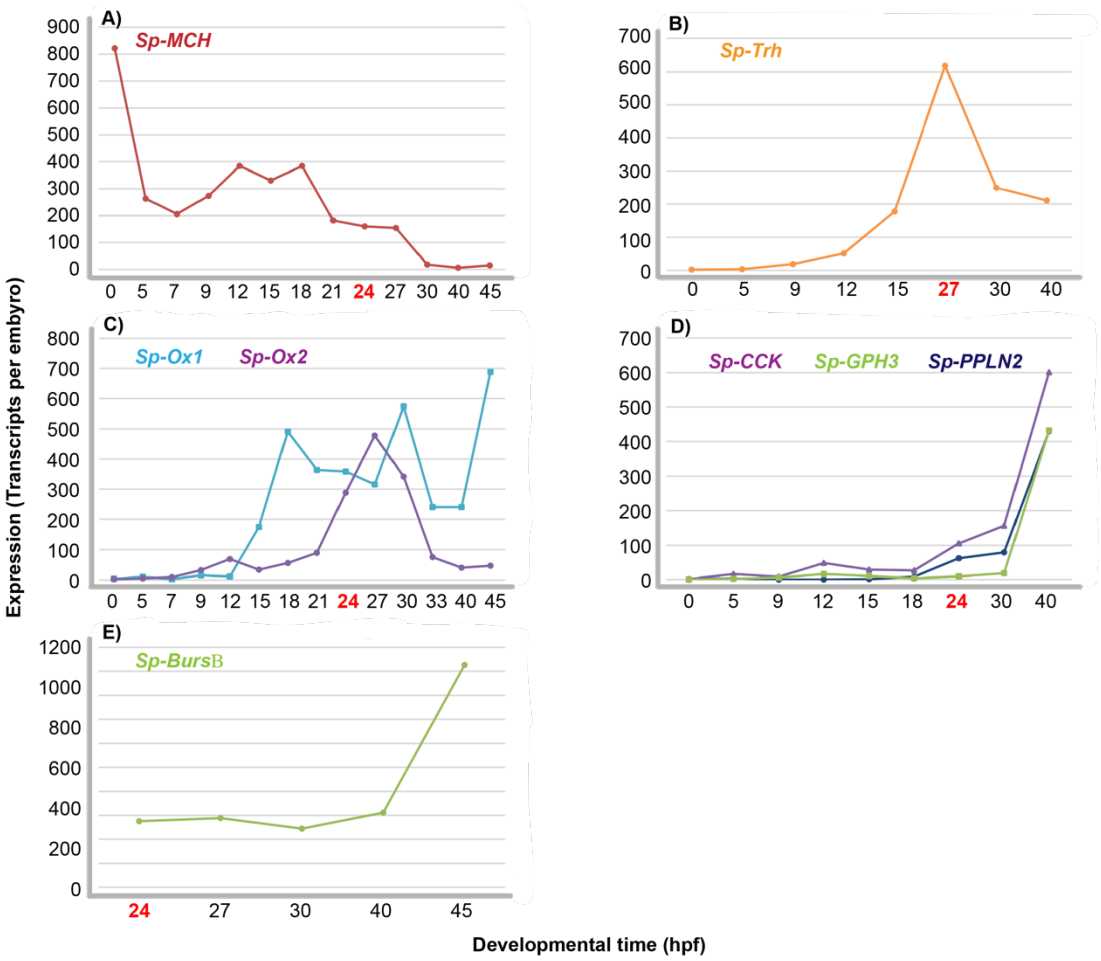

Figure 4.2 Temporal expression of mid-expressing NP genes during early embryonic development

See caption for Figure 4.1. The line graphs A-E depict mid-expressing NP genes. Mid-expressing genes are defined as those above 320 transcripts per embryo and less than 950 transcripts per embryo. Graph A) *Sp-MCH* has its highest embryonic expression (approximately 800 transcripts per embryo) in unfertilized eggs (0 hpf), reflecting maternal expression, followed by a rapid decrease to around 200 transcripts per embryo at 7 hpf. Zygotic expression then starts around 9 hpf and reaches levels higher than 300 transcripts per embryo between end of cleavage and late blastula stage (18 hpf), followed by a gradual decrease in transcript levels as embryonic development continues. Graph B-C) *Sp-TRH*, *Sp-Ox1*, and *Sp-Ox2* begin increasing in transcript levels before the mesenchyme blastula stage. Graph D-E) *Sp-CCK, Sp-GPH3, Sp-PPLN1* and *Sp-BursB* increase in expression at the beginning of gastrulation. QPCR data in graphs A, B, D and E were collected by Teresa Mattiello.

Most NP genes, 20 out of 31 fall into the low-expressing gene category revealed by QPCR analysis (Figure 4.3). Many of these genes also exhibit a highly fluctuating expression, which could reflect transcriptional pulsing (Chubb *et al.,* 2006) or the levels of expression may be so low that this amounts to 'background noise'. An example is provided by the uncharacterised neuropeptide, *Sp-Neuropeptide precursor 18* (*Sp-Np18*) gene, which has fluctuating expression, with each time point the transcript levels increase and decrease across a range of approximately 100 transcripts per embryo (Figure 4.3A). In addition to the fluctuation the overall trend of expression increases through embryonic development (Figure 4.3). Other NP genes show more constant levels of expression. *Sp-Corazonin* (*Sp-CRZ*) and *Sp-Somatostatin 1* (*Sp-SS1*) both have a peak in expression during blastula and mesenchyme blastula stages (Figure 4.3C and E; Table 8.5).

Transcriptome data available from Echinobase reveals five out of seven NP genes are expressed during embryonic development. Two insulin-like peptides have a high maternal expression (Figure 4.4A; Table 8.6), while *Sp-Neuropeptide precursor 20* (*Sp-Np20*) and *Sp-Nesfatin* (*Sp-Nesf)* have much higher expression levels throughout embryonic development (Figure 4.4B; Table 8.6). In contrast, *Sp-Kisspeptin* (*Sp-Kp*) has much lower expression throughout embryonic development, with an increase in expression only during the blastula stage (18 hpf) (Figure 4.4A; Table 8.6). *Sp-Luqin* and *Sp-Thymosin* are not detected above 22 transcripts per embryo (Figure 4.4A).

In summary, QPCR and transcriptome data reveal that 17 NP genes (out of at least 38 NP genes identified in the *S. purpuratus* genome) and *Sp-SecV* are expressed during at least one stage of embryonic development before neurons first differentiate at 48 hpf. Furthermore, many of these genes have peaks in expression before neuronal precursor cells are specified at mesenchyme blastula stage (24 hpf), suggesting that these genes are expressed in cells other than differentiated neurons and neuronal precursor cells.

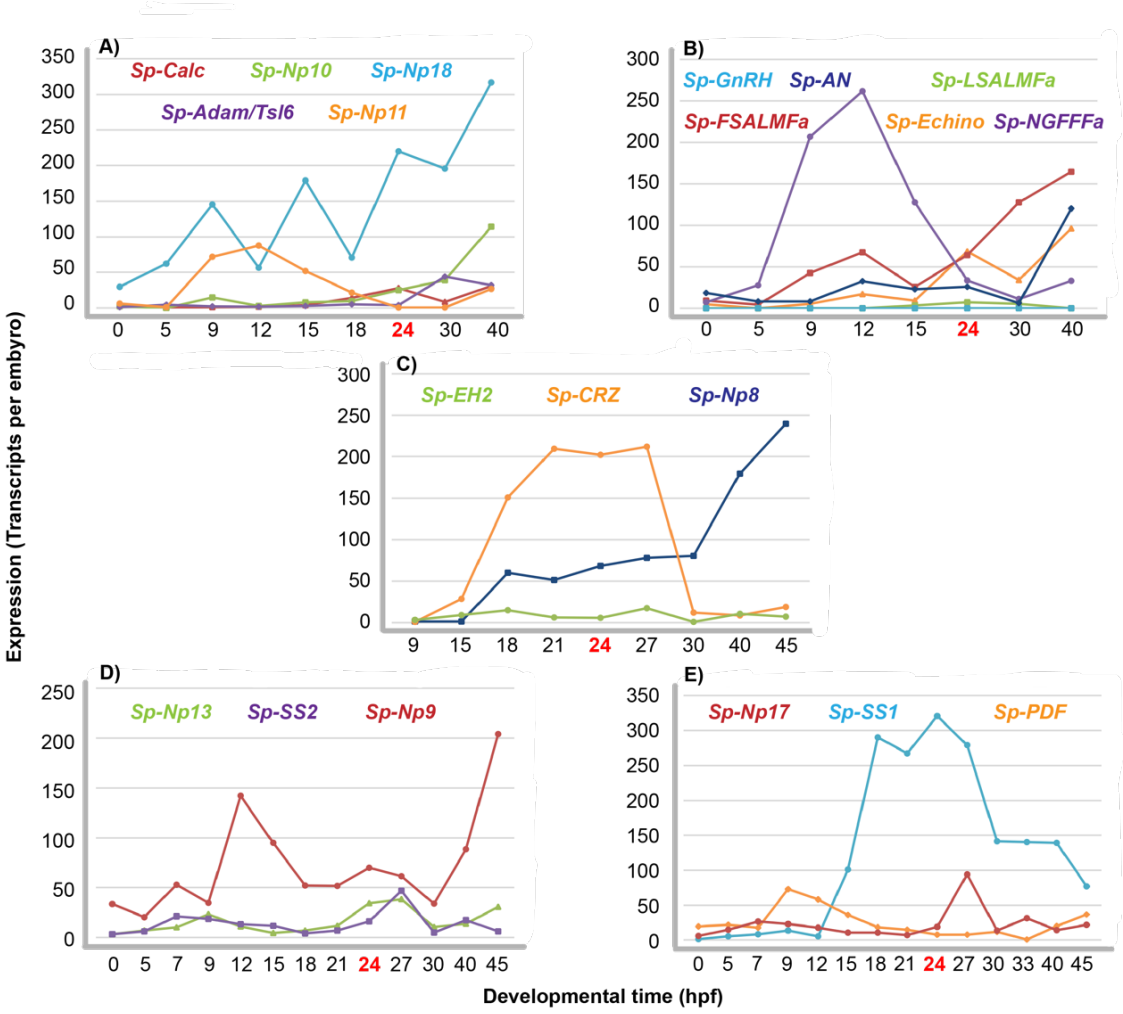

Figure 4.3 Temporal expression of low-expressing NP genes and GPCR genes during early embryonic development

See caption for Figure 4.1. The line graphs A-E depict low-expressing genes. Low-expressing genes are defined as those with less than 320 transcripts per embryo. Most genes increase in expression at the beginning of gastrulation or are not detectable above approximately 100 transcripts per embryo. Exceptions to this are: Graph C) *Sp-CRZ* NP gene has higher expression throughout blastula and mesenchyme blastula stages and Graph E) *Sp-SS1* NP gene has even higher expression throughout blastula and mesenchyme blastula stages. QPCR data in graphs A and B were collected out by Teresa Mattiello.

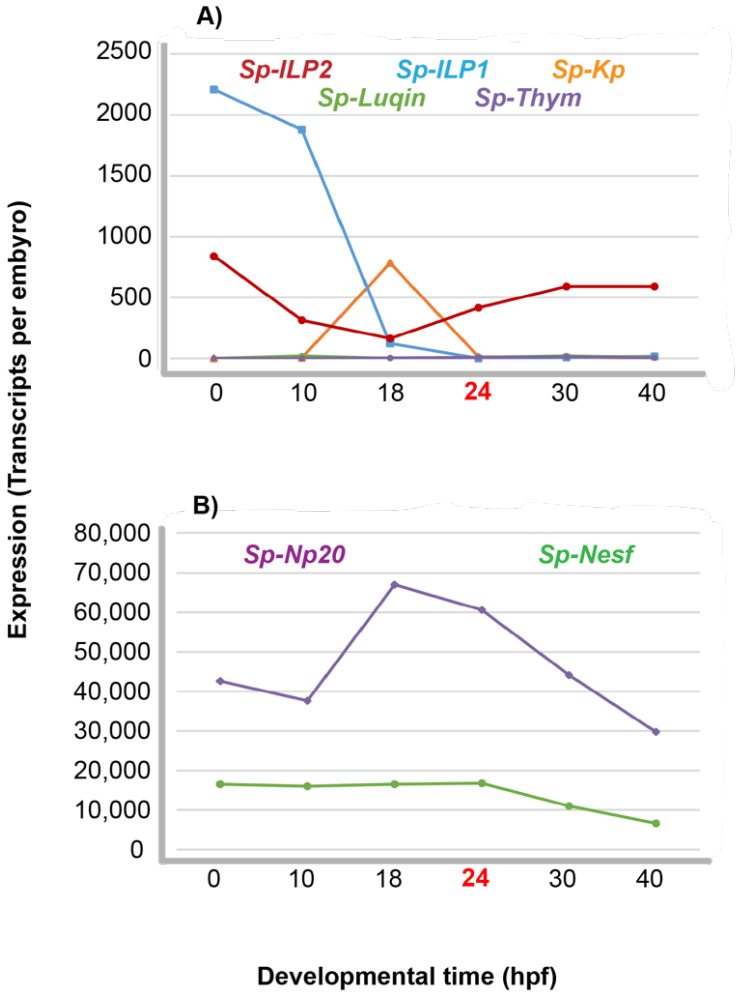

Figure 4.4 Embryonic expression of seven NP genes using a transcriptome data set

The transcriptome data set was obtained from Echinobase (http://www.echinobase.org/Echinobase/). Gene expression (transcripts per embryo) is shown from fertilisation (0 hpf) to the mid-gastrula stage (45 hpf), before the first neurons differentiate. The line graphs depict different levels of gene expression for seven NP genes, with lower expression in graph (A) and higher expression in graph (B). Graph A) *Sp-Insulin-like peptide 1* (*Sp-ILP1*) has over 2,000 transcripts per embryo at 0 hpf, while *Sp-Insulin-like peptide 2* (*Sp-ILP2*) has approximately half as many transcripts per embryo. There is a rapid decrease in *Sp-ILP1* expression by the blastula stage and it isn't expressed throughout embryonic development up to 40 hpf. *Sp-ILP2* has a slight decrease in expression to the blastula stage, followed by an increase in expression through the mesenchyme blastula and gastrula stages to similar levels as maternal expression at 0 hpf. In contrast, *Sp-Kisspeptin* (*Sp-Kp*) only has an increase in expression during the blastula stage (18 hpf) only to approximately 800 transcripts per embryo. *Sp-Luqin* and *Sp-Thym* are barely detected during this developmental time. Graph B) *Sp-Nesf* has a constantly high level of transcripts through 0 hpf to the mesenchyme blastula stage (24 hpf), followed by a small drop in transcript levels just before the onset of gastrulation (30 hpf). *Sp-Np20* gene has very high expression (> 28,000 transcripts per embryo) throughout embryonic development, up to 40 hpf. Genes are colour-coded, and their names are above each graph.

4.1.1 Temporal characterization of G-protein coupled receptors

As mentioned previously, neuropeptides act through GPCRs and therefore it is useful to assess the expression of GPCR genes to help provide insights on the functions of NP signalling systems. The temporal expression of 25 GPCR genes (previously mentioned in Chapter 3) during early development, from fertilization (0 hpf) through to mid-gastrula stage (45 hpf) was revealed by transcriptome data (Echinobase) and high-resolution QPCR.

Orphan GPCR gene expression was divided into four categories: 1) A single highly expressing gene that reaches expression above 950 transcripts per embryo (Figure 4.5A); 2) two mid-expressing genes that have expression between 320 and 940 transcripts per embryo (Figure 4.5B); 3) eight low-expressing genes that have expression between 100 and 319 transcripts per embryo (Figure 4.5C) and unlikely detectable with ISH; and 4) eight very low-expressing genes that have expression below 100 transcripts per embryo (Figure 4.5D). One *Sp-GnRH-type-Receptor* was barely detected throughout embryonic development and so was not included (Table 8.6).

Sp-LGR is highly expressed during early embryonic development and during later embryonic and larval development (compare Figure 4.5A with Figure 3.5A). As mentioned earlier in section 3.1.1, the insulin superfamily of peptides are ligands for type C LGRs. Maternal expression is seen for both *Sp-ILP1* and *Sp-ILP2* (Figure 4.4A), which correlates with an increase in *Sp-LGR*. There are two mid-expressing GPCR genes, *Sp-RFamide (GPR54/kisspeptin)-type-Receptor* (*Sp-RFaR*) and *Sp-Gonadotropin-releasing hormone-type Receptor* (*Sp-GnRHR*). These are different to the mid-expressing genes seen later in development (Figure 3.5B). Both receptor genes are maternally expressed, *Sp-GnRHR* transcripts then drop in expression while *Sp-RFaR* has an increase in zygotic expression at 40 hpf (Figure 4.5B; Table 8.6). One *Sp-GnRH* ligand is present in *S. purpuratus*, but is not detected by QPCR in embryonic development (Figure 4.3B and D; Table 8.5) (Roch *et al.,* 2011; Rowe and Elphick, 2012). There are 16 other GPCRs that are expressed during embryonic development but have low expression, below 300 transcripts per embryo (Figure 3.5C-D). They

belong to a variety of NP families, including CRH, Ox, GRP/NMB, NMU/GH/Gh-like and VP/OT-like.

To see if ligand-receptor pairs were expressed at the same time during early embryonic development, and thus potentially functional, we compared the expression of five GPCRs with their putative/proven NP ligands. No ligand-receptor pairs were expressed at the same embryonic stage above 100 transcripts per cell/embryo, the ISH detection limit we defined earlier (Figure 4.6; Table 8.5). Taken together, these data reveal only three orphan GPCR receptors are expressed at considerable levels that could be functional in the early sea urchin embryo.

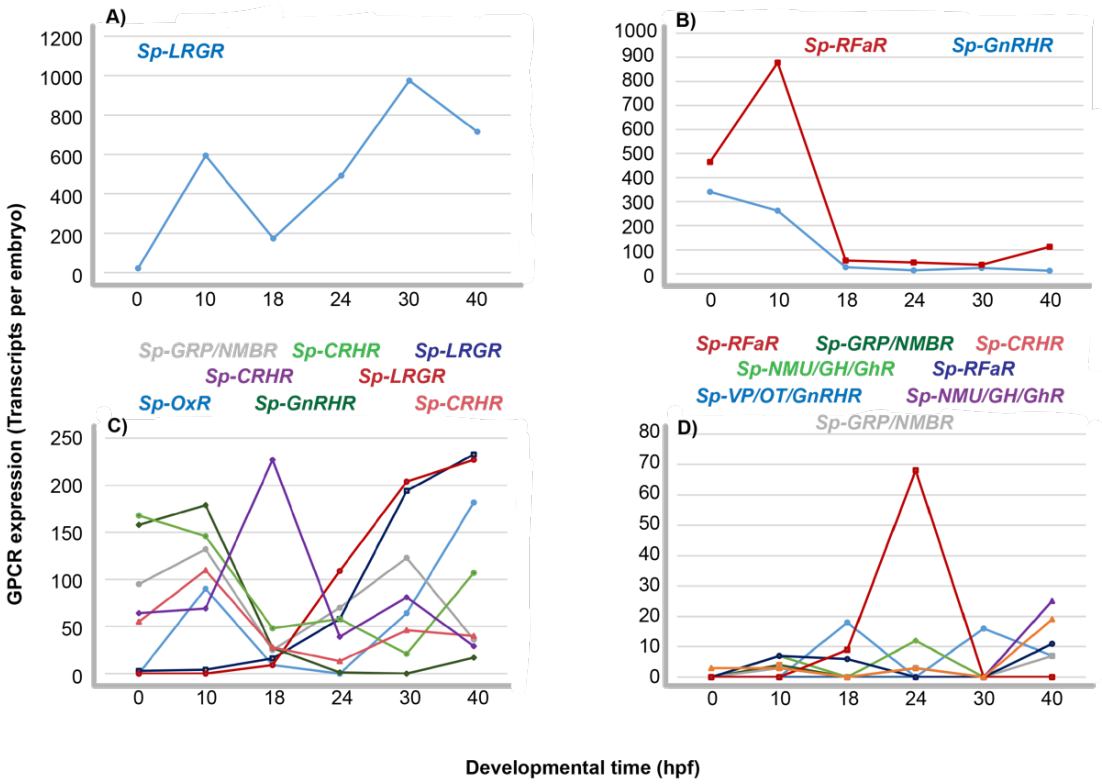

Figure 4.5 Expression of potential NP receptors, rhodopsin-type and secretin-type GPCRs during early embryonic development

Graphs representing the levels of expression of 19 GPCR genes that are potential NP receptors (Burke *et al.,* 2006a). The data are taken from a developmental transcriptome available in Echinobase and are represented in transcripts per embryo at six developmental stages: unfertilised egg (0 hpf), early blastula (10 hpf), hatched blastula (18 hpf), mesenchyme blastula (24 hpf), very early gastrula (30 hpf) and early gastrula (40 hpf). (A) A high-expressing gene , *Sp-LGR* has an increase in expression in a pre-hatched early blastula embryo (10 hpf), followed by a drop and subsequent increase in expression through gastrulation to almost 1000 transcripts per embryo at 30 hpf; (B) Two mid-expressing genes, *Sp-RFaR* and *Sp-GnRHR* are maternally expressed, with expression reaching above the ISH detection limit. *Sp-RFaR* then increases in zygotic expression at 10 hpf to over 800 transcripts per embryo, but drops drastically in expression for the remaining embryonic development, while *Sp-GnRHR* zygotic expression is barely detected . (C) Low-expressing genes (between 100 and approximately 320 transcripts per embryo); and (D) Very low-expressing genes (less than 100 transcripts per embryo) below the level of ISH detection. Of the 19 genes, three *Sp-CRHR* are secretin-type GPCRs, while all the others are rhodopsin-type GPCRs.

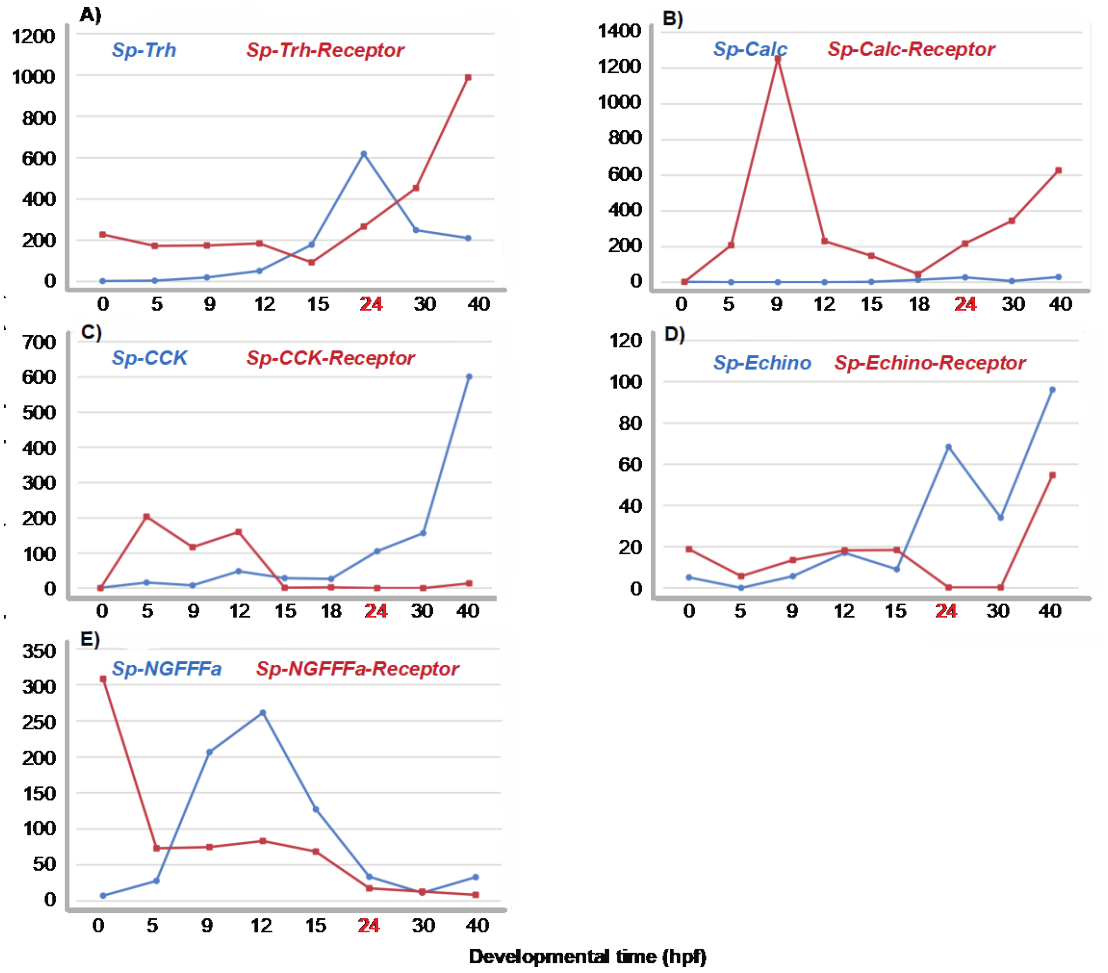

Figure 4.6 Expression of five NP ligand-receptor pairs during early embryonic development

High-resolution temporal expression of five NP ligand-receptor pairs revealed by QPCR. Data are represented in transcripts per embryo at eight developmental stages: unfertilised egg (0 hpf), very early blastula (5 hpf), early blastula (9 hpf), blastula (12 hpf), hatching blastula (15 hpf), mesenchyme blastula (24 hpf), very early gastrula (30 hpf) and early gastrula (40 hpf). Each line graph shows a ligand (blue) and receptor (red) NP pair. (A) *Sp-Thyrotropin-releasing hormone* (*Sp-TRH*) and its proven receptor are expressed at different embryonic stages. *Sp-TRH* NP gene has an increase in expression at mesenchyme blastula (24 hpf) to over 600 transcripts per embryo, the transcript level then drops to less than 300 transcripts per embryo at the early gastrula stage (40 hpf). *Sp-TRHR* has a lower level of expression at mesenchyme blastula and begins increasing in expression during gastrulation, reaching around 1000 transcripts per embryo at 40 hpf. (B) *Sp-Calc* and its predicted receptor show that only the receptor is expressed during development. *Sp-Calc* ligand is not detectable by QPCR through early development, while, *Sp-CalcR* has a peak in maternal expression to over 1000 transcripts per embryo at early blastula (9 hpf) and an increase in zygotic expression during gastrulation. (C) *Sp-CCK* and its predicted receptor are expressed at different embryonic stages, with *Sp-CCK* receptor gene maternally expressed (approximately 200 transcripts per embryo at 5 hpf) and *Sp-CCK* NP gene increasing in expression to around 600 transcripts per embryo at early

gastrula (40 hpf). D) *Sp-Echinotocin* and its predicted receptor are barely detected by QPCR during early embryonic development. (E) *Sp-NGFFFa* and its receptor are expressed at different embryonic stages. *Sp-NGFFFaR* gene is expressed maternally, with approximately 300 transcripts per embryo at 0 hpf, followed by a low zygotic expression below the ISH detection limit during blastula stages. The gene encoding its ligand *Sp-NGFFFa*, NP gene has a sharp increase in zygotic expression, with approximately 200 transcripts per embryo at cleavage (9 hpf) and the early blastula embryo (12 hpf).

4.2 Spatial analysis of neuropeptide precursor and receptor gene expression in the early embryo

To obtain a more detailed insights into the embryonic expression of NP signalling, I performed chromogenic ISH for six NP genes and two GPCR genes. I looked at three embryonic developmental stages, the blastula (12-18 hpf), the mesenchyme blastula (20-24 hpf) when cells are specified, and an early gastrula stage (33-36 hpf) before cells differentiate.

Seven out of eight genes tested showed clear expression at one or more embryonic stages. Many NP genes had ubiquitous expression at the blastula and/or the mesenchyme blastula stages, but some NP genes had a restricted expression pattern. The early gastrula stage had more restricted NP gene expression patterns, which varied between genes.

4.2.1 Sp-Insulin like peptide 2 expression

ISH analysis first revealed expression at the early gastrula stage (36 hpf), where *Sp-ILP2* is detected in a ring of cells near the tip of the archenteron (the developing gut) (Figure 4.7B). No expression was detected in blastula or mesenchyme blastula stages (Figure 4.7A). As development proceeds expression remained in the endoderm, specifically in the foregut (Figure 3.8J). Perillo and Arnone have reported the continuous expression of *Sp-ILP2* in the foregut in gastrula and pluteus larval stages (Perillo and Arnone, 2014). Neurons present in the foregut endoderm are fully differentiated by the pluteus larval stage (Wei *et al.,* 2011). The expression of *Sp-ILP2* in an entire ring of cells, rather than the salt and pepper fashion consistent with the appearance of neurons, tells us that *Sp-ILP2* is likely expressed in all of the foregut's undifferentiated cells, including neural progenitors.

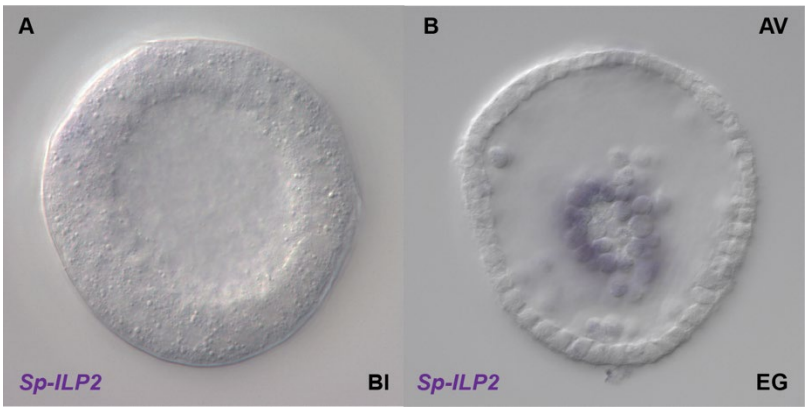

Figure 4.7. Expression of *Sp-Insulin like peptide 2* in the foregut of an early gastrula stage.

Spatial expression of *Sp-ILP2* at (A) blastula (18 hpf) and (B) early gastrula (36 hpf) stages revealed by chromogenic ISH. (A) Localisation is seen in the foregut of the developing archenteron at early gastrula stage. (B) No expression is detected in the blastula stage. Top-right corner indicates the orientation of the embryo or larva. Bottom-right corner indicates the embryo/larval stage. Abbreviated label AV refers to apical view.

4.2.2 *Sp-Pedal-peptide like neuropeptide 1* expression

ISH analysis of *Sp-PPLN1* from the blastula (18 hpf) to the mesenchyme blastula stage (24 hpf), revealed strong staining on one side of the ectoderm (Figure 4.8C and E). No staining was revealed in earlier blastula stages (Figure 4.8A-B). *Sp-PPLN1* expression later in development is confined to the morphologically distinct aboral ectoderm (Figure 3.8F; Figure 4.8G). Early embryonic expression is therefore presumed to be also aboral ectoderm. To determine the ectodermal localisation, double FISH analysis of *Sp-PPLN1* with a well-known oral ectodermal marker, *Sp-gsc* was performed at a mesenchyme blastula stage (Angerer *et al.,* 2001). FISH revealed that *Sp-PPLN1* NP gene is more strongly detected in the aboral ectoderm, albeit there is some weaker *Sp-PPLN1* staining in the oral ectoderm in the early mesenchyme blastula (Figure 4.8D and F). By 48 hpf, the boundary between *Sp-PPLN1* and *Sp-gsc* expression is well-defined and no *Sp-PPLN1* probe is seen in oral ectoderm (Figure 4.8H).

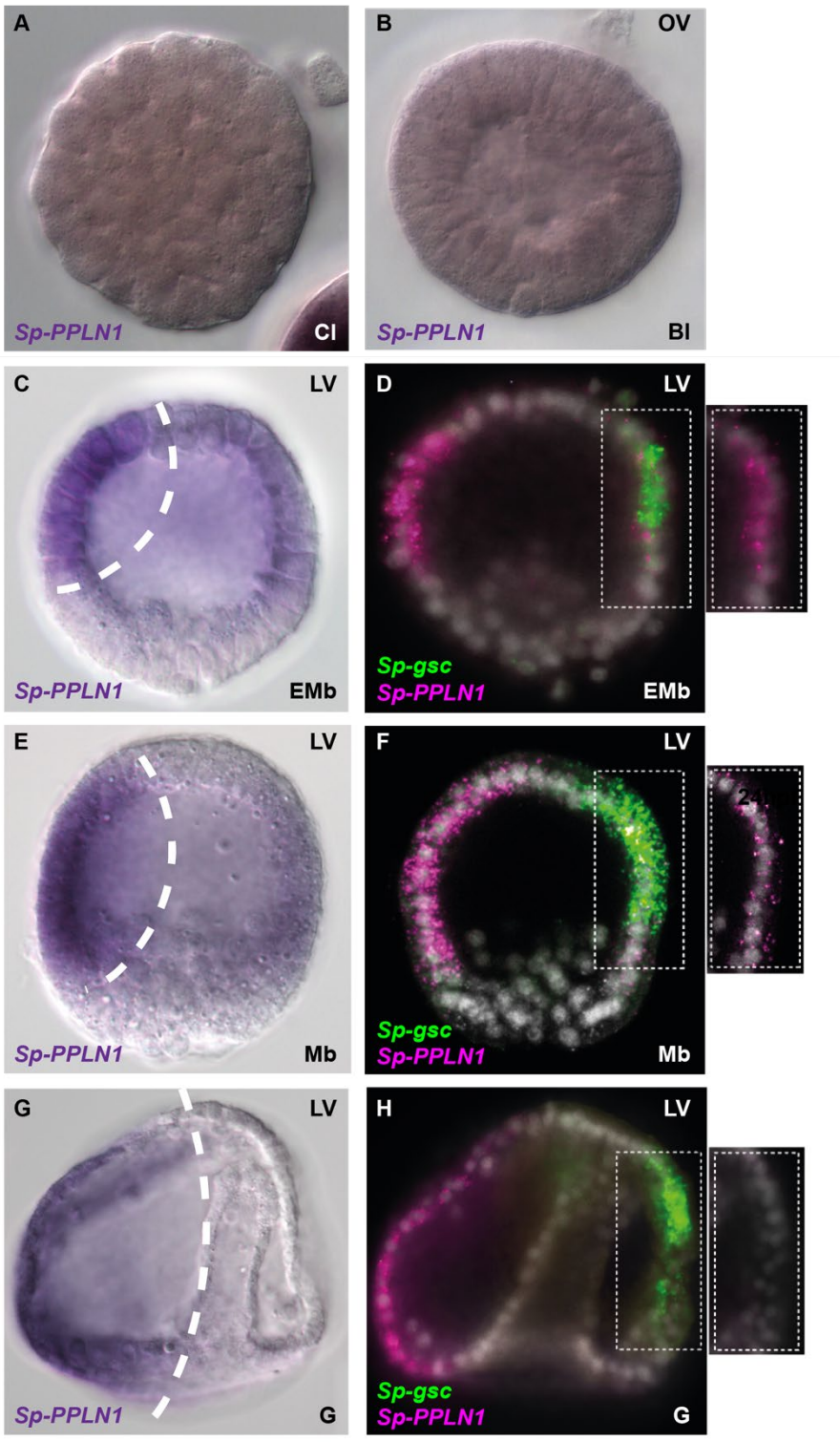

Figure 4.8 Expression of *Sp-Pedal peptide-like neuropeptide 1* in the aboral ectoderm through early embryonic development

Spatial expression of *Sp-PPLN1* and *Sp-gsc*, an oral ectodermal marker at (A) cleavage, (B) blastula, (C-D) early mesenchyme blastula, (E-F) mesenchyme blastula and (G-H) gastrula stage embryo revealed by chromogenic (A, B, C, E and G; purple) and fluorescent ISH (D, F and H). Double FISH shown as merged and single channel confocal images (of selected z-slices) with DAPI (grey) staining the nuclei. (A-B) No expression is seen in early cleavage (9 hpf) and early blastula stages (12 hpf). (C) *Sp-*

PPLN1 expression in the ectoderm and stronger in one side. (D) *Sp-gsc* (green) is shown in the oral ectoderm with weak co-expression of *Sp-PPLN1* (pink) and stronger *Sp-PPLN1* expression on the opposite aboral ectoderm. (E) *Sp-PPLN1* expression is even stronger on one side of the ectoderm and weaker on the other side. (F) *Sp-PPLN1* is very strongly expressed in the aboral ectoderm and to a lesser extent in the oral ectoderm co-expressed with *Sp-gsc*. (G-H) *Sp-PPLN1* is restricted to the aboral ectoderm, while *Sp-gsc* expression remains in the oral ectoderm. Top-right corner indicates the orientation of the embryo or larva. Bottom-right corner indicates the embryo/larval stage. Abbreviated labels refer to the following, OV (oral view), LV (lateral view), AbV (aboral view), Cl (cleavage), Bl (blastula), EMb (early mesenchyme blastula), Mb (mesenchyme blastula) and G (gastrula). (C, E, G) Dotted white line separates the aboral ectoderm from the rest of the embryo. (D, F, H) Dotted white boxes highlights the region shown to the right with a single channel. Images in panels A-B were carried out by Paola Oliveri and images in panels C-H were carried out by Jeremie Subrini.

4.2.3 *Sp-Neuropeptide precursor 20* expression

Chromogenic ISH expression analysis of *Sp-Np20,* an uncharacterised neuropeptide precursor shows staining in the ectoderm and endoderm through blastula and mesenchyme blastula stages. The probe is not detected in the mesodermal cells (Figure 4.9A-D). At blastula stages the gene is not detected in a domain at the vegetal pole (Figure 4.9B). Extension of the domain suggests that both NSM (non-skeletogenic mesoderm) and SM (skeletogenic mesoderm) cells are voided from the *Sp-Np20* expression. Interestingly, the embryonic expression of *Sp-Np20* changes at early gastrulation, when staining becomes restricted to endodermal cells (Figure 4.9E).

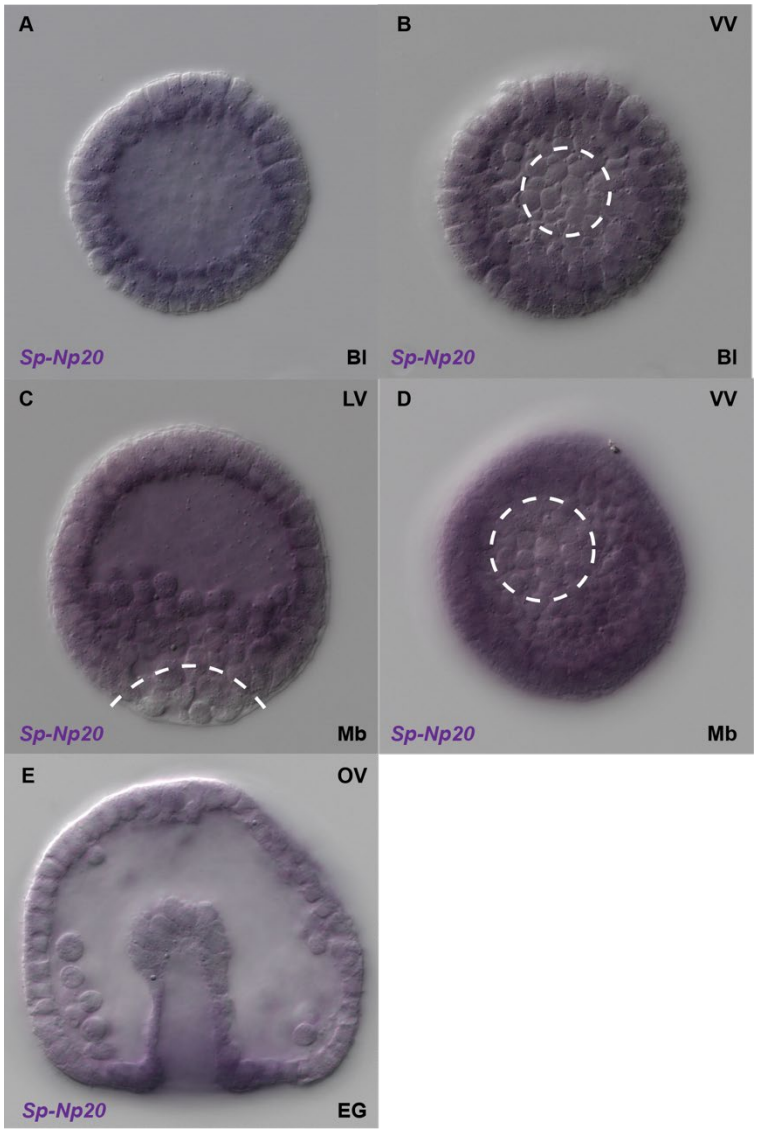

Figure 4.9 Expression of *Sp-Neuropeptide precursor 20*, precursor of an uncharacterised neuropeptide, in the ectoderm and endoderm of blastula, mesenchyme blastula and early gastrula stages

Spatial expression of *Sp-Np20* at (A-B) blastula stages, (C-D) mesenchyme blastula stages and (E) early gastrula stage revealed by chromogenic ISH. (A-D) Localisation in the ectoderm and endoderm, and absent from the NSM and SM cells. (E) The strongest staining is detected in the invaginating archenteron. Top-right corner indicates the orientation of the embryo or larva. Bottom-right corner indicates the embryo/larval stage. Abbreviated labels refer to the following: VV (ventral view), LV (lateral view), OV (oral view) Bl (blastula), Mb (mesenchyme blastula) and EG (early gastrula). Dotted white lines/circles separate staining from no staining.

4.2.4 *Sp-Kisspeptin* expression

ISH expression analysis of *Sp-Kp* reveals ubiquitous staining at blastula stage and no detection at the mesenchyme blastula stage (Figure 4.10), consistent with transcriptome data (Figure 4.4A). Ubiquitous staining suggests that *Sp-Kp* may have a role in all territories present in the blastula embryo.

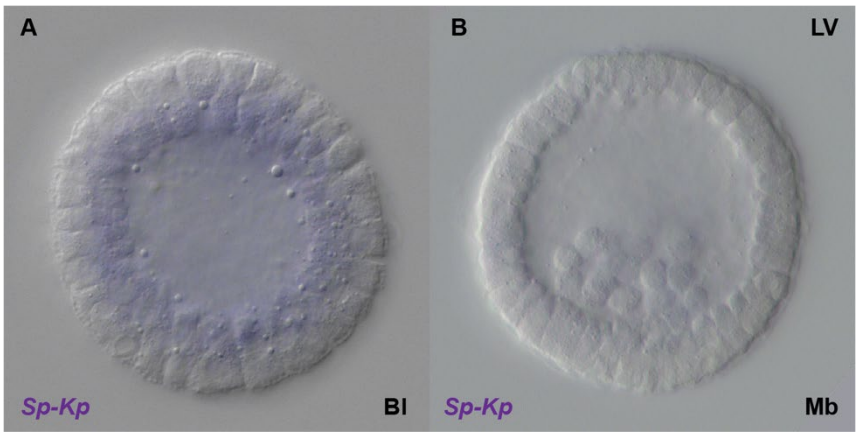

Figure 4.10 Ubiquitous expression of *Sp-Kisspeptin* at blastula stage

Spatial expression of *Sp-Kp* at (A) blastula and (B) mesenchyme blastula revealed by chromogenic ISH. (A) Ubiquitous expression is seen in the blastula embryo and (B) Expression is not detected in any cell type of the mesenchyme blastula. Top-right corner indicates the orientation of the embryo or larva. Bottom-right corner indicates the embryo/larval stage. Abbreviated labels refer to the following: LV (lateral view), Bl (blastula) and Mb (mesenchyme blastula).

4.2.5 *Sp-NGFFFamide* and *Sp-NGFFFamide-receptor* expression

Sp-NGFFFamide (*Sp-NGFFFa)* NP gene is one of a few *S. purpuratus* NP genes that has a proven receptor. The *Sp-NGFFFa-receptor* is an orthologue of the vertebrate neuropeptide-S (NPS) receptors and crustacean cardioactive peptide (CCAP) receptors (Semmens *et al.,* 2015). ISH analysis of *Sp-NGFFFa* reveals ubiquitous staining at early blastula stage (12 hpf) (Figure 4.11F). *Sp-NGFFFaR* is barely detectable in unfertilised egg, blastula and gastrula embryo (Figure 4.11A-B and E). At mesenchyme blastula stage, *Sp-NGFFFaR* Is either not detected, or if we push the staining, signal is detected ubiquitously (compare Figure 4.11C with Figure 4.11D) QPCR data is consistent with expression in the unfertilised egg. However, *Sp-NGFFFaR* only has less than 100 transcripts per embryo at blastula (18 hpf), mesenchyme blastula (24 hpf) and mid gastrula (40 hpf) stages (Figure 4.6) (below the ISH detection limit established earlier), while the probe give a clear ubiquitous staining (Figure 4.11B-E). This could be explained by: 1) the probe cross reacting with some other genes; or 2) an underestimation of the level of expression obtained by both QPCR and transcriptome analysis. In summary, both NP ligand and receptor are potentially co-expressed in every cell of the blastula embryo, indicating that the pair could be functional at this stage.

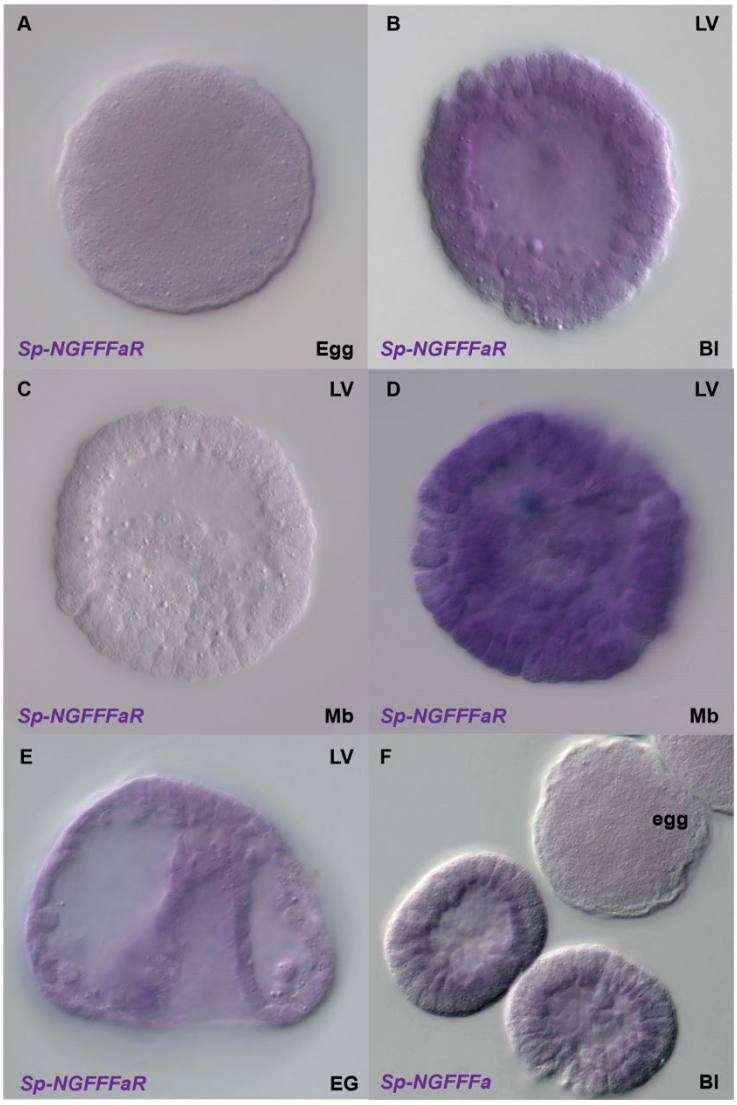

Figure 4.11 Ubiquitous expression of *Sp-NGFFFa* and its receptor at blastula stage

Spatial expression of *Sp-NGFFFa* and its receptor in the (A) unfertilised egg, (B and F) blastula stage, (C-D) mesenchyme blastula stage and (E) early gastrula embryo, revealed by chromogenic ISH. (A-B, D-E) *Sp-NGFFFaR* is ubiquitously expressed in the. (C) *Sp-NGFFFaR* is not detected in 9/9 mesenchyme blastula embryos stained for 2 days. (F) *Sp-NGFFFa* is ubiquitously expressed in 2/2 blastula stained for >3 days. No staining is detected in unfertilised eggs in the same well (negative control). Top-right corner indicates the orientation of the embryo or larva. Bottom-right corner indicates the embryo/larval stage. Abbreviated labels refer to the following: LV (lateral view), Bl (blastula), Mb (mesenchyme blastula) and EG (early gastrula). Images in panels F were carried out by Paola Oliveri.

4.2.6 *Sp-Thyrotropin-releasing hormone* and *Sp- Thyrotropin-releasing hormone –receptor* expression

Sp-Thyrotropin-releasing hormone (*Sp-TRH*) NP gene also has a deorphanised receptor (See Chapter 6). ISH expression analysis of *Sp-TRH* reveals no staining at an early blastula stage and ubiquitous staining at mesenchyme blastula stage (24 hpf) (Figure 4.12A-B). *Sp-TRHR* has no expression detected in the embryo (Figure 4.12C-D), until a late gastrula stage (48 hpf) when it is detected in the ciliary band (48 hpf) (Figure 3.8). In the mesenchyme blastula (24 hpf) ISH expression is detected for the gene encoding the ligand (over 600 transcripts per embryo) but barely detected for the receptor (less than 300 transcripts per embryo) (Figure 4.6; Table 8.5).

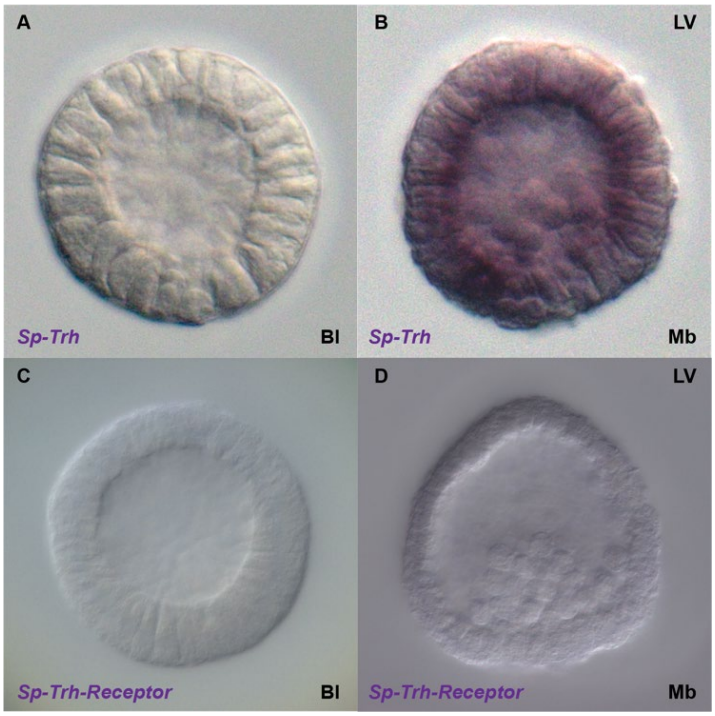

Figure 4.12 Ubiquitous expression of *Sp-Thyrotropin-releasing hormone* at mesenchyme blastula stage

Spatial expression of *Sp-TRH* and its receptor at (A and C) blastula stages and (B and D) mesenchyme blastula stage revealed by chromogenic ISH. (A) No expression is detected for *Sp-TRH* at the blastula stage. (B) Ubiquitous expression is shown for *Sp-TRH* NP gene at mesenchyme blastula stage. (C-D) No expression is detected for *Sp-TRHR* at blastula and mesenchyme blastula stages. Top-right corner indicates the orientation of the embryo or larva. Bottom-right corner indicates the embryo/larval stage. Abbreviated labels refer to the following: LV (lateral view), Bl (blastula) and Mb (mesenchyme blastula).

4.3 Discussion

Neuropeptides are well known as signalling molecules involved in neuronal communication. Here I report the first analysis of neuropeptides precursor and receptor genes in early embryonic development of the sea urchin, *S. purpuratus*. I investigated the expression of all 38 NP genes present in *S. purpuratus* at early embryonic stages and found that 17 NP genes are detected at one or more of these stages (Figure 4.1; Figure 4.2; Figure 4.4). I also investigated the expression of 25 GPCR genes and found that only three orphan GPCR genes are detected in the early embryonic development (Figure 4.5). Spatial expression patterns of six NP genes and one GPCR gene were revealed (out of six NP genes and two GPCR genes tested) in one or more early embryonic stages: blastula (18 hpf), mesenchyme blastula (24 hpf) and early gastrula (38 hpf) (Figure 4.13). Extensive work in the sea urchin *S. purpuratus* has revealed the embryonic cell types that will give rise to one or more cell types later in development (Cameron *et al.,* 1987; Davidson, 1989; Davidson *et al.,* 1998) (Figure 1.10). For example, the aboral ectoderm will give rise to the squamous epithelium that forms most of the wall of the late embryo and larvae, while the non-skeletogenic mesoderm will give rise to pigment cells, immunocytes and muscle cells. Therefore, we can map the early embryonic NP gene expression to one or more of these specified territories and draw hypotheses about their function(s).

Early expression of neuropeptides has been reported in few vertebrate taxa including chickens and zebrafish (Erhardt *et al.,* 2001; Sherwood and Wu, 2005). Expression of neuropeptide-like proteins has also been reported in the secretory cells of the Placozoan, *T. adhaerens* (Senatore *et al.,* 2017). Here I report this early expression of neuropeptide signalling systems for the first time in an invertebrate embryo. Three NP genes, *Sp-PPLN1*, *Sp-Np20* and *Sp-ILP2* showed a localised expression pattern. *Sp-PPLN1* is expressed in the aboral ectoderm in all three of developmental stages we investigated, the blastula, mesenchyme blastula and the early gastrula. It is expressed to a lesser extent in the oral ectoderm in the blastula and mesenchyme blastula stage, and is not expressed in the oral ectoderm by the early gastrula stage (Figure 4.13). Interestingly, *Sp-PPLN1* continues to be strongly expressed in the aboral ectoderm in the gastrula and pluteus larval stages (Figure 3.10). The constant expression in the

aboral ectoderm, and gradually weaker expression in the oral ectoderm (Figure 3.10) could suggest that *Sp-PPLN1* is involved in maintaining the oral aboral axis or perhaps in specifying or differentiating the aboral ectoderm. The oral aboral specification in the sea urchin embryo has been extensively studied. Nodal is a key gene, which triggers a signalling cascade to activate the expression of orally expressed genes, including *Sp-chordin* (which inhibits *Sp-Bmp2/4*) and *Sp-lefty* (which inhibits *nodal* from the ciliary band region. *Sp-Nodal* also triggers the expression of *Sp-Bmp2/4* which translocates to the aboral ectoderm to induce aboral expressing genes such as *Sp-Tbx2/3* (Duboc *et al.,* 2004; Lapraz *et al.,* 2009; Molina *et al.,* 2013). Interestingly, there are still unidentified signals that have been predicted to exist in the sea urchin oral aboral specification (Lapraz *et al.,* 2009; Su *et al.,* 2009) and therefore it may be worthwhile to investigate *Sp-PPLN1* as a potential candidate for this currently unidentified signal.

Sp-ILP2 is expressed in a ring of cells near the tip of the developing archenteron in the early gastrula embryo. The archenteron will divide into a functional tripartite gut containing a foregut (esophagus), midgut (stomach) and hindgut (intestine) in the pluteus larva. Differentiation markers are already active in mutually exclusive domains at the end of gastrulation (Annunziata *et al.,* 2014b) thus, the early expression could suggest that *Sp-ILP2* is acting as a foregut differentiation marker. Neurons appear in a salt and pepper manner in the foregut of the pluteus larva and so it is possible *Sp-ILP2* is expressed in both foregut neuronal precursor cells as well as endodermal precursor cells. The third NP gene that shows a localised expression pattern is the uncharacterised *Sp-Np20*. *Sp-Np20* is expressed throughout the ectoderm and endoderm in blastula and mesenchyme blastula stages and then in the early gastrula embryos expression becomes restricted to the endoderm. In the pluteus larval stage, expression is further localised to the hindgut and midgut. The expression pattern suggests a potential role of *Sp-Np20* is establishing the boundaries of the mesodermal territories and/or in the developing gut.

Two other NP genes, *Sp-Kp* and *Sp-TRH* are ubiquitously expressed which makes it difficult to predict their function. The absence of *Sp-TRH-receptor* expression when the ligand is present, suggests that *Sp-TRH* has no function in the mesenchyme

blastula. I cannot rule out that there is another receptor that the peptide can bind. In addition, it is unknown if the *Sp-TRH* gene is transcribed and processed into a functional mature peptide and this could be easily tested in future immunohistochemistry experiments using a specific antibody that recognises the Sp-TRH peptide. Finally, ISH analysis revealed that *Sp-NGFFFa* and its receptor seem to be ubiquitously expressed in early embryonic stages. However, this ubiquitous expression is inconsistent with the QPCR data, and the limit of detection by ISH that I defined as 100 transcripts per cell/embryo (section 3.4).

The quantitative analysis also revealed three orphan GPCR genes *Sp-LGR*, *Sp-RFaR* and a *Sp-GnRHR* expressed in early development. Interestingly, early NP gene expression may provide some reasonable hypotheses about the potential ligands of these GPCRs. *Sp-LGR* is a type C LGR (Van Hiel *et al.,* 2012) and the insulin superfamily of peptides are ligands for type C LGRs (Hopkins *et al.,* 2007; Scott *et al.,* 2003; Van Hiel *et al.,* 2012). Maternal expression is seen for both *Sp-ILP1* and *Sp-ILP2* (Figure 4.4A), which correlates with an increase in *Sp-LGR*; therefore it would be intriguing to test if either of these two peptides are the ligands for *Sp-LGR*. In addition, *Sp-RFaR* (GPR54) is one of five receptors identified as homologs of vertebrate and/or invertebrate neuropeptide kisspeptin-type receptors (Burke *et al.,* 2006a). This receptor is highly expressed several hours before *Sp-Kp* is ubiquitously expressed in the blastula stage embryo (Figure 4.13). Although this ligand gene and receptor gene are not expressed at the same embryonic stage, it would be interestingly to test if the encoded protein of the GPCR gene is detected in the blastula, in which case the *Sp-Kp* may be a good candidate for a deorphanisation assay. Furthermore, QPCR analysis, also revealed that *Sp-SecV* increases in expression in the mid-gastrula (40 hpf) and therefore modulated secretion starts after gastrulation begins (Figure 4.1B).

To conclude, this chapter has revealed a novel early embryonic expression of some NP genes and GPCR genes in the sea urchin pluteus larvae, suggesting that NP genes can play a role in early embryonic development in a non-neuronal context. This provides a basis for future work, aimed at understanding the additional non-neuronal functions of neuropeptides in the sea urchin embryo and larvae.

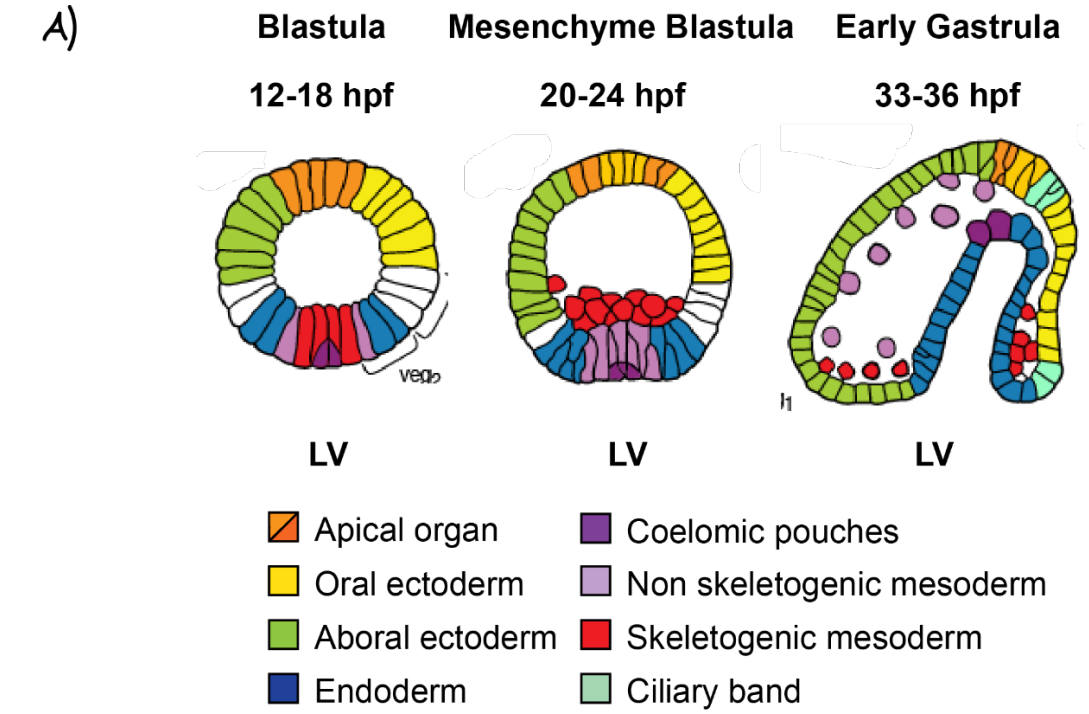
A)
Blastula
Mesenchyme Blastula
Early Gastrula
12-18 hpf
20-24 hpf
33-36 hpf
LV
LV
LV
Apical organ
Oral ectoderm
Aboral ectoderm
Endoderm
Coelomic pouches
Non skeletogenic mesoderm
Skeletogenic mesoderm
Ciliary band

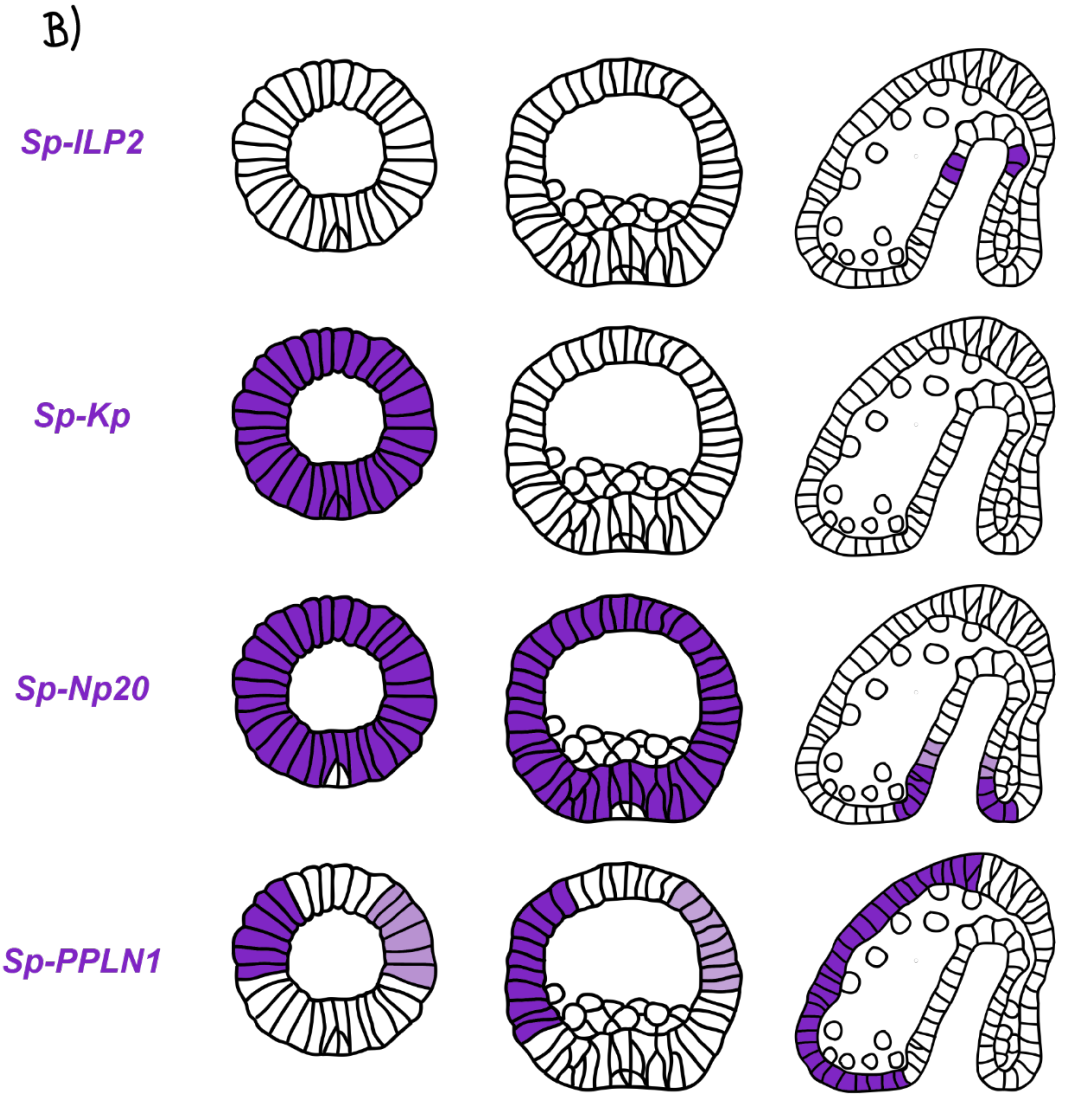
B)
Sp-ILP2
Sp-Kp
Sp-Np20
Sp-PPLN1

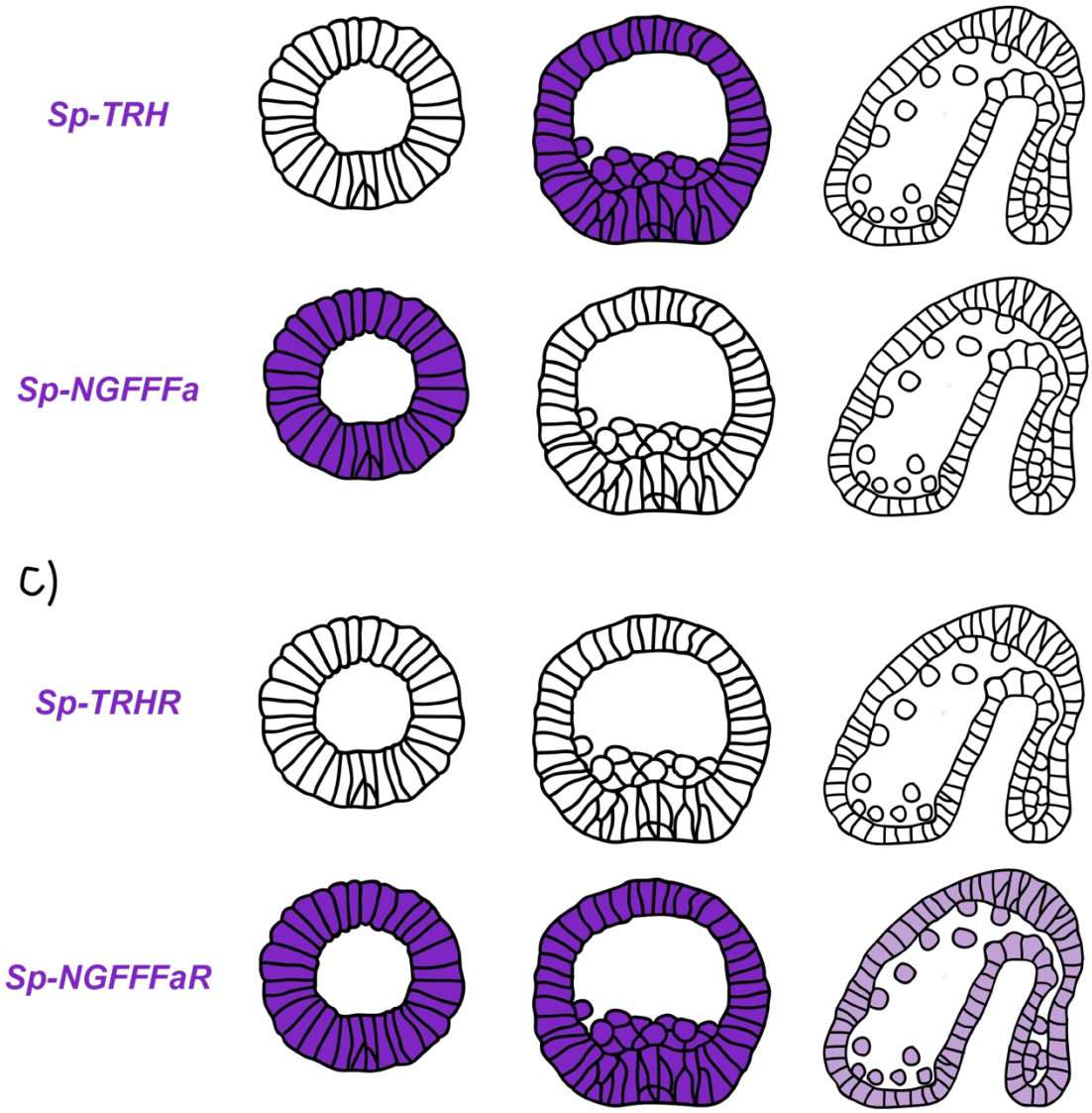

Figure 4.13 Summary map of NP gene and GPCR gene expression in early embryonic stages

A) Cartoon schematic of a blastula, mesenchyme blastula and early gastrula stage. Different colours depict different cell-type territories through development. Oral ectoderm (yellow), aboral ectoderm (green), apical plate/organ (orange), endoderm (archenteron/gut) (blue), non-skeletogenic mesoderm (light purple), skeletogenic mesoderm (PMCs/skeleton) (red), coelomic pouches (dark purple), ciliary band (light blue). B) Gene expression (purple) of NP genes: *Sp-ILP2, Sp-Kp, Sp-Np20, Sp-PPLN1, Sp-TRH* and *Sp-NGFFFa.* C) Gene expression (purple) of GPCR genes: *Sp-TRHR* and *Sp-NGFFFaR*. The shade of purple represents the level of expression. The darker the colour the higher the staining. Abbreviated labels refer to the following, B (blastula), Mb (mesenchyme blastula) and EG (early gastrula).

Chapter 5 Optimizing CRISPR/Cas9 genome editing in the sea urchin *S. purpuratus*

In this chapter, I present a CRISPR/Cas9 methodology to induce knockout mutations in the F0 generation of the sea urchin *S. purpuratus*. This chapter provides the prerequisite for my second objective where I investigate the roles of NP genes in the sea urchin embryo and larva (Chapter 6). Here I provide a brief history of gene perturbation and describe the benefits of the CRISPR/Cas9 system. I then present how I tested and optimised the efficiency and specificity of the *in vivo* CRISPR/Cas9 system. Finally, I present the optimisation of an *in vitro* Cas9 digestion assay and provide a comparison between the *in vivo* and *in vitro* studies to see if the *in vitro* assay can predict sgRNA *in vivo* efficiency.

Aspects of this experimental work reported in this chapter were carried out by undergraduate students David Axford and Anne Ritoux (under my supervision).

5.1 The history of gene perturbation techniques

The sequencing of genomes was an incredible challenge, but only a small step towards understanding how a genome encodes an entire organism. The challenge now is to decipher billions of base pairs of DNA. What functions do thousands of genes have and how do they interact to build an organism? Many genes encoding proteins involved in neuronal signalling, including genes encoding neurotransmitter-synthesizing enzymes and neuropeptides, have been identified in a variety of genomes. 38 NP genes have so far been found in the *S. purpuratus* genome (Chapter 3). This large complement of NP signalling systems provides a basic for comprehensive analysis of peptidergic signalling in the larval nervous systems and characterisation of different neuronal cell types. The first step was to spatially and temporally characterise expression of NPs, relative to other neuronal signalling molecules. In this thesis I have so far characterised the expression of seven NP genes in the larval nervous system and found at least ten sub-populations of neuronal and/or neuronal-like cells (Chapter 3). I have also found early expression of NP genes in non-neurogenic tissue, highlighting the possible role of NP genes in the embryonic development of *S. purpuratus* (Chapter 4). The next step is to understand their role in the larval nervous system and their non-neuronal developmental roles.

Analysis of gene function was originally determined by classical forward genetics, where genomic mutations were first generated, the phenotype was analysed and finally the affected gene(s) were identified. This type of mutagenesis is still common in some organisms, including mice, zebrafish and *Drosophila*, where thousands of mutant lines are readily available. The genomic revolution led to the reverse genetics approach, a targeted approach where a gene sequence of interest is first identified, then directly mutated and the phenotype is analysed. A variety of targeted gene knockdown methods have been developed over the past 30 years.

In 1998, Fire and Mello discovered that injection of double stranded RNA (dsRNA) into the worm *C. elegans* leads to the specific degradation of the corresponding mRNA. This process is termed RNA interference (RNAi) (Fire *et al.,* 1998). Fire and Mello won the 2006 Nobel Prize for Physiology or Medicine for their discovery of RNA

interference. Another gene knockdown agent are morpholino oligonucleotides (MOs). MOs are nucleotide analogs (about 25 nucleotides long) that block the translation of genes by binding to the transcription start site or splice sites. MOs are stable in biological systems, highly efficient, and have fewer off-targets than other methods making them a popular choice for gene knockdown studies (Summerton, 2007). Around 80% of morpholinos that are designed and produced by Gene Tools (a spin-off of ANTIVIRALS Inc, the pioneer antisense company founded by James Summerton; https://www.gene-tools.com) give successful knockdowns, typically achieving 70% to 98% knockdown of target gene expression (Summerton, 2007). Problems with these knockdown techniques have come to light. Morpholinos work optimally at 37°C and at this temperature they have few off-targets (Summerton, 2007). However, many embryos are cultured at far lower temperatures, such as sea urchin embryos, which are cultured at 15°C. At such low temperatures, off-target effects have been reported and it has been suggested that this is a result of a reduced minimum inhibitory length. The minimum inhibitory length is "the shortest length of a gene knockdown oligo that must bind to an RNA transcript in order to inhibit expression of that RNA" (Summerton, 2007). Therefore, a shorter minimum inhibitory length, increases the chances of finding inadvertent target sequences. Other issues, such as the length of developmental time should also be considered when thinking of MOs as the knockdown method of choice.

Additional gene perturbation techniques are genome editing endonucleases, such as zinc-finger nucleases (ZFNs), transcription activator-like effector nucleases (TALENs) and clustered regulatory interspaced short palindromic repeats/(CRISPR)-associated Cas system. The CRISPR system was discovered as a naturally occurring genome editing system in bacteria and it is part of their defense system against foreign DNA. In the type II CRISPR/Cas system, the DNA cutting Cas9 nuclease and an RNA molecule guides the Cas9 to cause a double strand break (DSB) at a specific location in the genome (Mali *et al.,* 2013). The error-prone cellular DNA repair mechanism, non-homologous end joining (NHEJ), frequently causes small nucleotide insertions and deletions at the DSB site. These heritable mutations in target DNA sometimes result in amino acid deletions, insertions and frameshifts leading to premature stop codons

and a non-functional protein. CRISPR/Cas9 is a flexible system with multiple gene-editing functions, it can induce multiple gene knockouts as well as gene knock-ins and single nucleotide editing. Furthermore, CRISPR is far simpler and less time consuming than other techniques, as it requires only a different 18-20 nucleotide target sequence in order to change the genomic target of the Cas9 protein. In contrast, ZFNs or TALENs require the design and generation of a new nuclease pair for each genomic target. The CRISPR/Cas9 genome-editing system has been successfully demonstrated in human cells, vertebrates and invertebrates (Kleinstiver *et al.,* 2016; Shen *et al.,* 2013; York *et al.,* 2017) as a result of the system being versatile and easy to use.

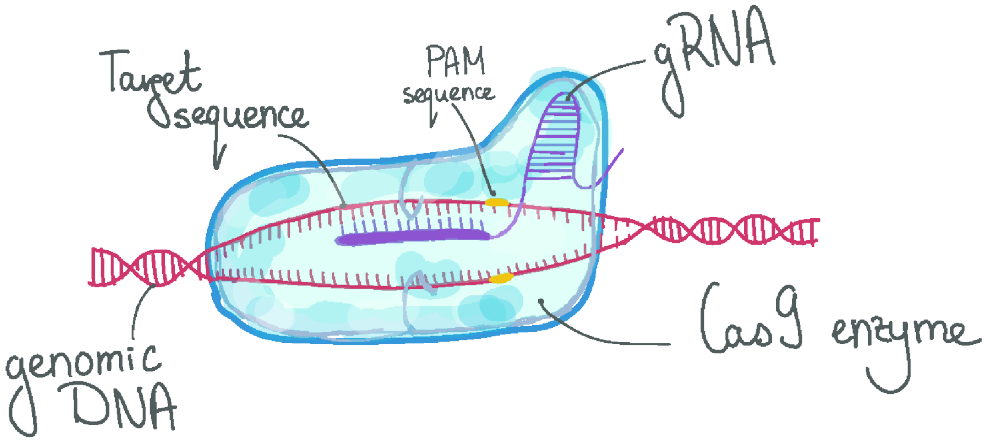

Figure 5.1 Illustration of the CRISPR/Cas9 gene-editing system

sgRNA (purple) is made up of two parts, a binding scaffold for the Cas9 nuclease and a variable 18-20 nucleotide sequence that is complementary to a DNA target. Thus, the sgRNA forms a complex with the Cas9 nuclease (blue) and guides the Cas9 nuclease to a specific DNA target where it makes a double stranded break immediately upstream of the PAM sequence (yellow). Illustration courtesy of Kalina Kyutchukova.

5.1.1 Gene perturbation in the sea urchin

The sea urchin *S. purpuratus* is a great model for studying developmental mechanisms. The availability of genomic and transcriptomic data, coupled with sea

urchin eggs being amenable to experimental manipulation, has resulted in a variety of perturbation methods being used to answer many developmental questions, including the experimental study of GRNs that underlie developmental processes. Perturbation in sea urchin embryos is mostly done by microinjection, at the one cell stage, of MOs, which are simple to design, and a non-time-consuming procedure.

Many studies have reported efficient MO knockdowns (Angerer *et al.,* 2001; Angerer and Angerer, 2004; Davidson *et al.,* 2002b; Oliveri *et al.,* 2006), however there are some specificity, efficiency and toxicity issues that should be taken into account. Coffman and colleagues tested morpholino effectiveness in the sea urchin (Coffman *et al.,* 2004), designing five morpholinos against *Sp-Runt,* three translational-blocking and two splice-blocking morpholinos. They then measured the efficiency of the knockdown by co-injecting the MO with exogenous *Sp-Runt* mRNA. They found that one was not effective at all, two partially blocked exogenous *Sp-Runt* mRNA, whilst two morpholinos completely blocked exogenous *Sp-Runt* mRNA. However, they also revealed that some morpholinos had off-target effects (Coffman *et al.,* 2004). Overall, the MO is a useful technique for investigating early developmental processes, however late-expressing genes are subject to less knockdown due to the dilution of the MO.

Endonuclease techniques, including ZFN and TALEN have been used in recent years. However, the efficiency of mutagenesis in the sea urchin is quite low using these techniques. Ochiai and colleagues reported that mutagenesis using ZFNs is feasible in the sea urchin *Hemicentrotus pulcherrimus*, but it is a laborious process, with a low efficiency and high toxicity rate. Only 9.5% of *Hp-HesC* ZFN mRNA injected embryos showed the *Hp-HesC* morpholino phenotype (Ochiai *et al.,* 2010). In 2014, Hosoi and colleagues reported that mutagenesis using TALENs was also feasible in the sea urchin *H. pulcherrimus.* However, they showed that the efficiency was also very low, with the expected phenotype seen in only 12.6% of injected embryos (Hosoi *et al.,* 2014). Further, they revealed that TALEN mutations were mainly introduced between the unhatched blastula stage and mesenchyme blastula stages (Hosoi *et al.,* 2014). In comparison, ZFN mutations were introduced between the eight-cell and hatched

blastula stage (Ochiai *et al.,* 2010). Taken together, when compared with ZFNs and TALENs, MOs are a far superior gene perturbation technique in the sea urchin.

5.1.2 CRISPR/Cas9 system in the sea urchin

The discovery of the CRISPR/Cas endonuclease system was appealing as a genome-editing tool for many scientific communities. This simple, user-friendly, low-cost and efficient tool was hugely attractive. In 2015, Lin & Su published the first CRISPR/Cas9 genome-editing study in the sea urchin They targeted *Sp-Nodal*, a gene central to the specification of the ectoderm along the dorsal ventral axis and showed that CRISPR/Cas9 can be an efficient gene-editing tool in the sea urchin (Lin and Su, 2015). This was a remarkable step, showing efficient mutations in the F0 generation. Since then several papers reporting use of CRISPR/Cas9 in the sea urchin have been published and these have further developed the gene editing system for use in the sea urchin. Oulhen and Wessel efficiently made a knockout of the enzyme, polyketide synthase 1, *Sp-PSK1*, which is essential for the final pigment product in pigmented immune cells. The CRISPR/Cas9 knockout gave the same albino phenotype as seen when using MOs (Oulhen and Wessel, 2016). This provided a good visualisation of a functional knockout system. Mellott and colleagues successfully made a knockout of *Sp-Delta*, resulting in additional neural progenitors and neurons (Mellott *et al.,* 2017). Additionally, they illustrated that the Cas9 protein was expressed and localised to the nuclei of two-cell stage embryos and therefore CRISPR/Cas9 is capable of inducing mutations earlier than other endonucleases (Hosoi *et al.,* 2014; Mellott *et al.,* 2017; Ochiai *et al.,* 2010). Shevidi and colleagues successfully modified the CRISPR/Cas9 system by fusing it to a cytosine deaminase and inducing a single nucleotide conversion in target genes, this perturbs gene function while also decreasing the risks of genomic abnormalities (Shevidi *et al.,* 2017). Significant advances in the sea urchin CRISPR methodology have been made, but there are still a few issues remaining. Firstly, there is no consenus on the best ingredients to inject into sea urchin eggs. The concentration and ratio of injected sgRNA, Cas9 mRNA and Cas9 protein seems to vary hugely between studies. Secondly, the efficiency of mutated embryos seems to be hugely variable, and sgRNAs seem to be part of the

cause for variability. Thirdly, further studies are needed to assess the specificity of the system (Lin and Su, 2015; Mellott *et al.,* 2017; Oulhen and Wessel, 2016).

5.1.3 Aims of this chapter

Here the efficiency of the CRISPR/Cas9 system under different conditions was tested. The amount of Cas9 components was optimised, using two easy visualisations of functional gene-editing. I targeted two genes *Sp-PKS1* and *Sp-TPH*. *Sp-PKS1* knockouts result in albino larvae (Oulhen and Wessel, 2016). *Sp-TPH* is an enzyme tryptophan hydroxylase, which is involved in the synthesis of serotonin. The distribution of serotonin in the nervous system of the pluteus larvae has been well characterised immunohistochemically using a commercially available antibody (Beer *et al.,* 2001; Bisgrove and Burke, 1986). Therefore, successful knockouts of both of these genes would be clear by live imaging or a simple two-day immunohistochemistry protocol. To test the efficiency of on-target mutations, DNA extraction of single larvae was optimised and visualisation of knockouts by PCR amplification and sequencing was attempted. An *in vitro* Cas9 digestion assay was also optimised and *in vitro* and *in vivo* studies were compared in an attempt to provide an easy and quick prediction of sgRNA *in vivo* efficiency.

5.2 Optimising the concentration of reagents used for CRISPR/Cas9

sgRNA were designed by comparing the predictions of several online CRISPR targets, ZiFIT (http://zifit.partners.org/ZiFiT/), CHOPCHOP (http://chopchop.cbu.uib.no), CRISPR direct (https://crispr.dbcls.jp), and gRNA Scorer 1.0 (https://crispr.med.harvard.edu/gRNAScorerV1/). To increase specificity shortlisted sgRNA were chosen based on the following criteria; 1) they were predicted by more than one algorithm; 2) they had greater than 50% GC content; 3) there were no off-targets hits when subject to BLAST analysis of the *S. purpuratus* genome; and 4) they had no similarity to the rest of gRNA template (Figure 5.6). sgRNA were synthesised by making sgRNA DNA templates (see methods section 2.3.2 for details; Table 8.10; Table 8.11), whereby the predicted variable targeting site (18-20 nucleotides) is surrounded by a 5' T7 promoter sequence and a 3' tail sequence recognised by the Cas9 enzyme. DNA templates are made via PCR fusion and then transcribed using T7 polymerase to produce sgRNA mRNA. This method of synthesising sgRNA was inexpensive and extremely rapid (I could produce the final sgRNA mRNA and be ready to microinject within a few days of the primers arriving). Cas9 mRNA was linearised from a pT3TS-nCas9n plasmid (Addgene; Plamid 46757) and transcribed using T3 polymerase. Both sgRNA and Cas9 mRNA were purified using G50 columns (Sigma Aldrich) to remove any free nucleotides and ensure the accurate concentration is injected. The microinjection solution injected into fertilised sea urchin eggs contained sgRNA mRNA, Cas9 mRNA along with a final concentration of 120mM KCL. A total of 32 sgRNA across seven different genes have so far been tested, illustrating the simplicity of using the CRISPR/Cas9 system.

To obtain an efficient CRISPR/Cas9 system, two different sgRNAs with varying concentrations of Cas9 mRNA were tested. Previous sea urchin CRISPR/Cas9 papers have used a large range of sgRNA and Cas9 mRNA concentrations (Figure 5.2A). sgRNA concentrations ranged from 6 ng/µl to 150 ng/µl, a 25-fold difference, while concentrations of Cas9 mRNA ranged from 150 ng/µl to 1000 ng/µl, a six-fold difference. Papers reporting use of CRISPR/Cas9 in other species, including zebrafish and Cnidaria, also use a range of concentrations. Talbot and Amacher inject 40 ng/µl sgRNA and 90 ng/µl Cas9 mRNA into zebrafish eggs (Talbot and Amacher, 2014).

Nakanishi and colleagues inject 500 ng/µl sgRNA and 1000 ng/µl cas9 mRNA into *Nematostella vectenis* fertilised eggs (Nakanishi *et al.,* 2018). It is important to establish the correct concentration of mRNA to produce sufficient Cas9 protein, but not too much foreign mRNA as to cause developmental defects.

Using as a positive control the sgRNA2 targeting *Sp-PKS1,* described previously by Oulhen and Wessel (2016), two concentrations of Cas9 mRNA, 90 ng/µl and 500 ng/µl were tested, giving a ratio of 1:2.5 and 1:12.5 of sgRNA to Cas9 mRNA. The lower concentration was used in the zebrafish protocol and the higher concentration has been used in sea urchin protocols (Lin and Su, 2015; Mellott *et al.,* 2017). Larvae injected with 500 ng/µl Cas9 mRNA had a higher percentage of abnormal development, when compared with uninjected larvae and larvae injected with less Cas9 mRNA (Figure 5.2B), indicating that there is a general toxic effect of high concentrations of Cas9 mRNA. In addition, the percentage of albino larvae was much higher in those larvae injected with a lower concentration of Cas9 mRNA. 30% of larvae were albino in the higher concentration, compared with 75% albino larvae in the lower concentration (Figure 5.2C-D). These results were obtained from 2-20 independent experiments, counting between 40 and 843 individuals, per treatment (Figure 5.2E). To conclude, CRISPR/Cas9 is a feasible gene-editing system in the sea urchin and a lower ratio and concentration of Cas9 mRNA seems to be more efficient and less toxic to the larvae.

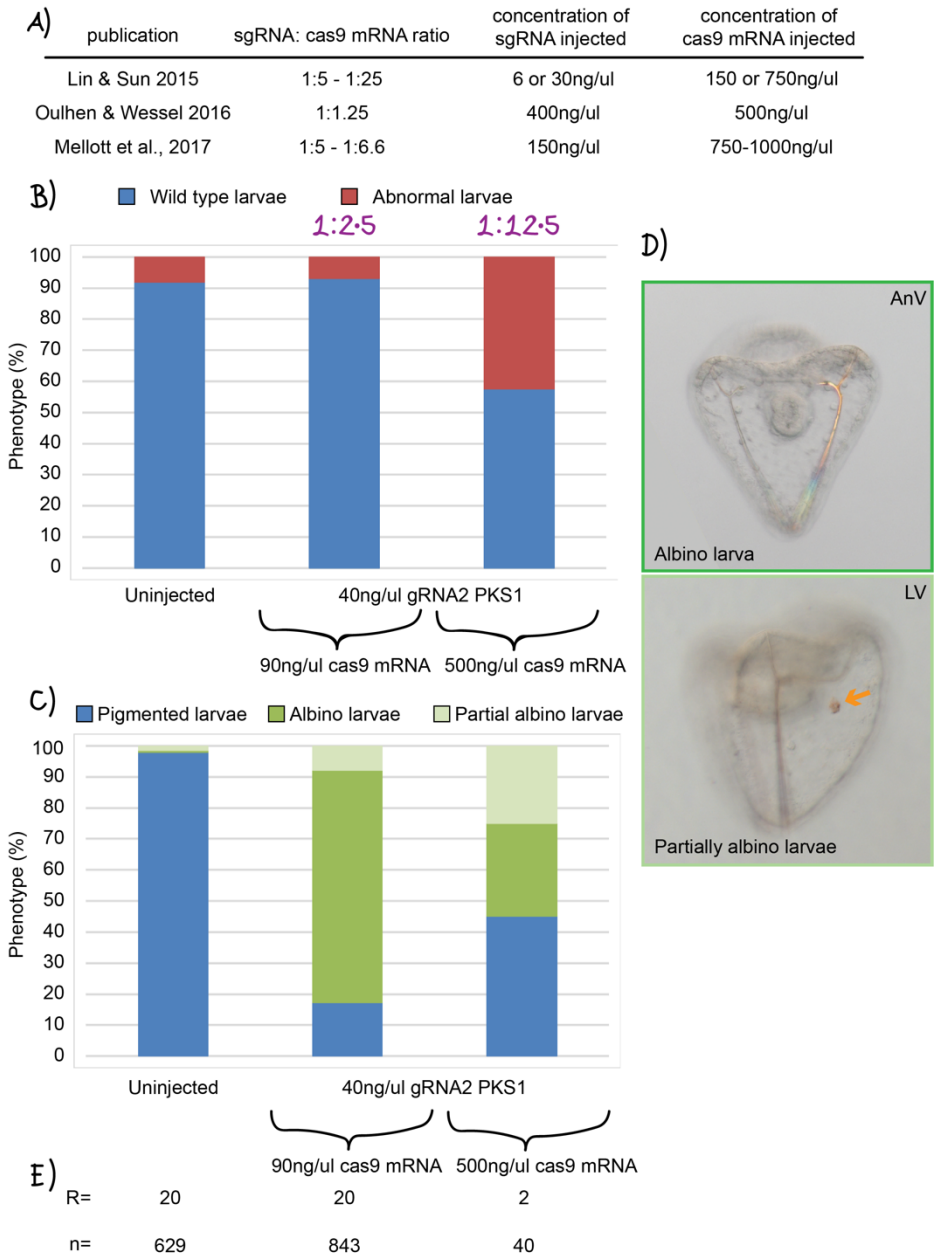

Figure 5.2 Optimisation of gRNA/Cas9 ratio and concentration

A) The different ratios and concentrations used by three sea urchin CRISPR/Cas9 publications are shown (Lin and Su, 2015; Mellott *et al.,* 2017; Oulhen and Wessel, 2016). B) A bar graph plotting the percentage of wild type and abnormal larvae for three treatments; uninjected larvae, 40 ng/µl gRNA2 *Sp-PKS1* with 90 ng/µl Cas9 mRNA injected larvae and 40 ng/µl gRNA2 *Sp-PKS1* with 500 ng/µl Cas9 mRNA injected larvae. C) A bar graph plotting the percentage of pigmented, albino and partially albino larvae in the three different treatments. Albino larvae develop normally but do not have any pigment cells. Partially albino larvae also develop normally and have less pigment cells. Orange arrow points to one of the pigmented cells that is still present. Top right corner indicates the orientation of the pluteus larva, anal view (AnV) or lateral view (LV). D) Representative images of a completely albino larva and a partially albino larva. E) The number of individuals (n) counted across a number of independent experiments (R).

To further optimise the CRISPR/Cas9 system, the efficiency of two sgRNAs targeting the *Sp-PKS1* gene, sgRNA2 and sgRNA3 were compared. Oulhen & Wessel predicted sgRNA2 and sgRNA3 using CRISPRscan, and they are both 19bp long and have a GC content of 55% (Figure 5.3B). sgRNA2 and sgRNA3 targets *Sp-PKS1* in exon 3 (Figure 5.3A). Larvae were injected with 90 ng/µl Cas9 mRNA and either 40 ng/µl *Sp-PKS1* sgRNA2 or sgRNA3. Individuals injected with either sgRNA had approximately the same percentage of poorly developed larvae (8-12%), when compared with uninjected controls, confirming that neither are toxic at that concentration (Figure 5.3C). Larvae injected with sgRNA3 *Sp-PKS1* exhibited albinism with 48% of larvae were partially albino and 7% were completely albino (Figure 5.3D). However, this is much lower than the 75% completely albino larvae and the 8% partially albino larvae seen in those injected with sgRNA2 *Sp-PKS1* (Figure 5.3D). Interestingly, sgRNA3 had more off-targets than sgRNA2 (Figure 5.3B) when both were used as queries in a blastn against the *S. purpuratus* genome 3.1. Results were obtained from 6 to 20 independent experiments, counting between 265 and 843 individuals per condition (Figure 5.3E). To conclude, there is much variation in the efficiency of knockout mutations depending on the sgRNA and the concentration of Cas9 mRNA.

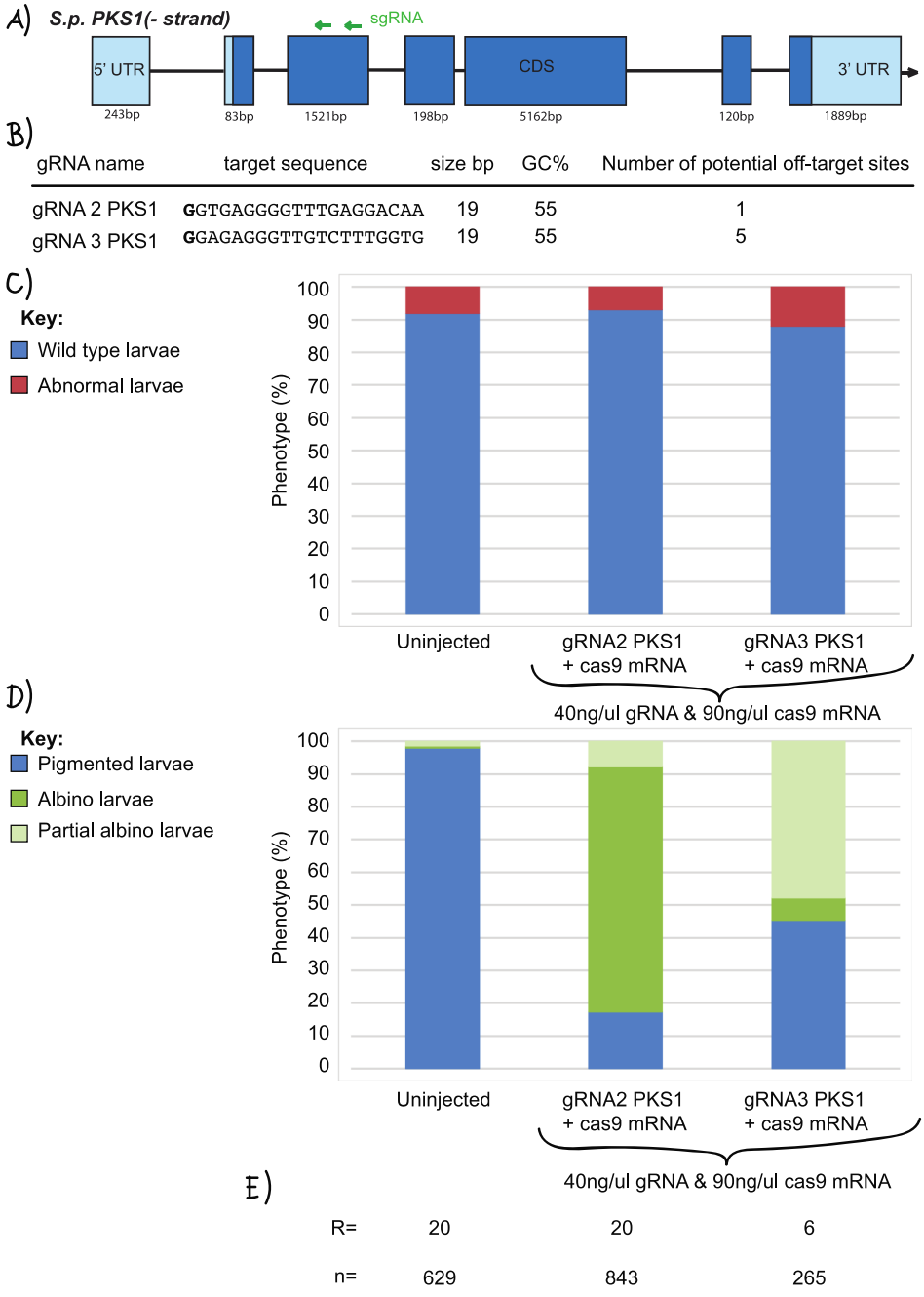

Figure 5.3 sgRNA2 targeting *Sp-polyketide synthase 1* is more efficient than sgRNA3

A) *Sp-PKS1* (SPU_002895; WHL22.202707.0) gene structure including introns, exons and the target location of sgRNA sequences on exon 3. Not drawn to scale. B) *Sp-PKS1* sgRNA target sequences and details including the length of target sequence, GC content and the number of potential off-target sites. C) A bar graph plotting the percentage of wild type and abnormal larvae for three treatments: uninjected larvae, 40 ng/µl gRNA2 *Sp-PKS1* with 90 ng/µl Cas9 mRNA injected larvae and 40 ng/µl gRNA3 *Sp-PKS1* with 90 ng/µl Cas9 mRNA injected larvae. D) A bar graph plotting the percentage of pigmented, albino and partially albino larvae in the three different

treatments. E) The number of individuals (n) counted across a number of independent experiments (R).

As an alternative to the injection of Cas9 mRNA, which first needs to be translated before it can be translocated to the nuclei, a Cas9 protein can be directly injected into the fertilised egg (York *et al.,* 2017). Theoretically better efficiencies would be expected with protein injection due to the fact that the complex gRNA/Cas9 protein can be preloaded *in vitro* and can be readily translocated to the nucleus of the one cell stage embryo and induce a DNA double strand cut. To understand if the Cas9 protein could be a better alternative in the sea urchin, the efficiency of a Cas9 protein (NEB) was compared to the Cas9 mRNA. The percentage of albino larvae in those injected with 40 ng/µl of the less efficient sgRNA3 *Sp-PKS1* and 90 ng/µl Cas9 mRNA was compared, to those injected with varying concentrations of the less efficient sgRNA3 *Sp-PKS1* with 10 ng/µl Cas9 protein. Larvae injected with 40 ng/µl gRNA3 *Sp-PKS1* and 10 ng/µl Cas9 protein had only 40% partially albino larvae, while larvae injected with Cas9 mRNA, which had 55% albino or partially albino larvae (Figure 5.4B). Larvae injected with the protein and only 4 ng/µl gRNA3 *Sp-PKS1* had the lowest albino efficiency, with only 12% partially albino larvae (Figure 5.4B). Thus, the NEB Cas9 protein method is not as efficient as the mRNA method. Importantly, those larvae injected with the Cas9 protein have a higher percentage of abnormal larvae (Figure 5.4A). There are only 10 to 12% larvae abnormal in uninjected and Cas9 mRNA injected larvae (Figure 5.4B). In comparison, 22 to 34% of the Cas9 protein injected larvae are abnormal, illustrating that the NEB protein is toxic to sea urchin embryos (Figure 5.4A).

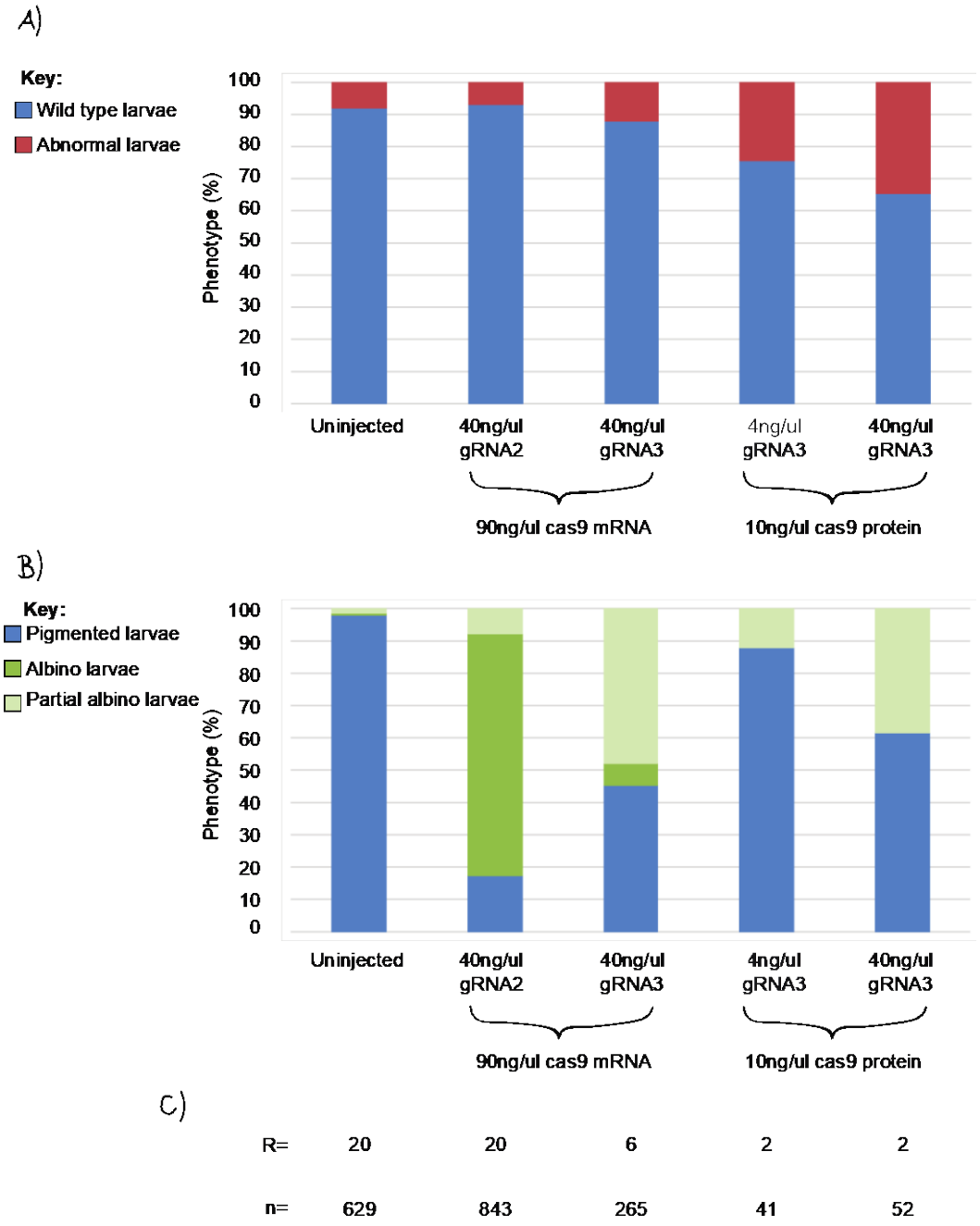

Figure 5.4 Comparison of Cas9 mRNA and NEB protein efficiency in the sea urchin embryos

A) A bar graph plotting the percentage of wild type and abnormal larvae for five treatments; uninjected, 40 ng/µl gRNA2 Sp-PKS1 with 90 ng/µl Cas9 mRNA (positive control), 40 ng/µl gRNA3 Sp-PKS1 with 90 ng/µl Cas9 mRNA, 4 ng/µl gRNA3 Sp-PKS1 with 10 ng/µl Cas9 protein and 40 ng/µl gRNA3 Sp-PKS1 with 10 ng/µl Cas9 protein. B) A bar graph plotting the percentage of pigmented, albino and partially albino larvae in the five treatments. C) The number of individuals (n) counted across a number of independent experiments (R). NEB protein experiment carried out by David Axford.

So far, the data has revealed that the Cas9 mRNA is more efficient and less toxic than the NEB Cas9 protein. The Cas9 mRNA needs to be translated and then translocated to the nuclei before it can work as an endonuclease on the target gene. The first cell division in *S. purpuratus* embryo happens after 90 minutes. If the DNA cut happens before the first cleavage then all cells in the embryo will inherit the mutation. On the contrary, if the DNA cut happens after the first cleavage then only some of the cells in the embryo will inherit the mutation, generating a mosaic embryo. In the case of *Sp-PKS1,* a DNA cut after the first cleavage results in a partially albino larvae (Figure 5.2C). Therefore, I wanted to visualise how long it takes for the Cas9 mRNA to be translated and the protein localised in the nuclei of sea urchin embryos. Immunohistochemistry (IHC) using an anti-Cas9 nuclease (7A9-3A3) (AbCam #191468) was performed on embryos injected with Cas9 mRNA. Four developmental stages were looked at: a one-cell fertilised egg, two-cell embryo, eight-cell embryo and blastula embryo (Figure 5.5). Expression analysis revealed that the Cas9 protein is not present in the nucleus at the one-cell stage, but is present in a two-cell stage embryo (Figure 5.5A-B). Expression remained localised to the nuclei of most eight-cell stage embryos (Figure 5.5C). Furthermore, expression was still seen in the nuclei of blastula stage embryos (Figure 5.5D). In summary, it seems that when injected with Cas9 mRNA the Cas9 protein induces a DNA cut at the two-cell stage, likely resulting in mosaic embryos. If the endonuclease does work at the two-cell stage, four independent mutations in each allele would be needed for a complete knockout. Analysis done in other labs shows that CRISPR/Cas9 mutations are introduced far earlier than ZFN and TALENs (Hosoi *et al.,* 2014; Ochiai *et al.,* 2010), making this system still more efficient than the other endonuclease techniques.

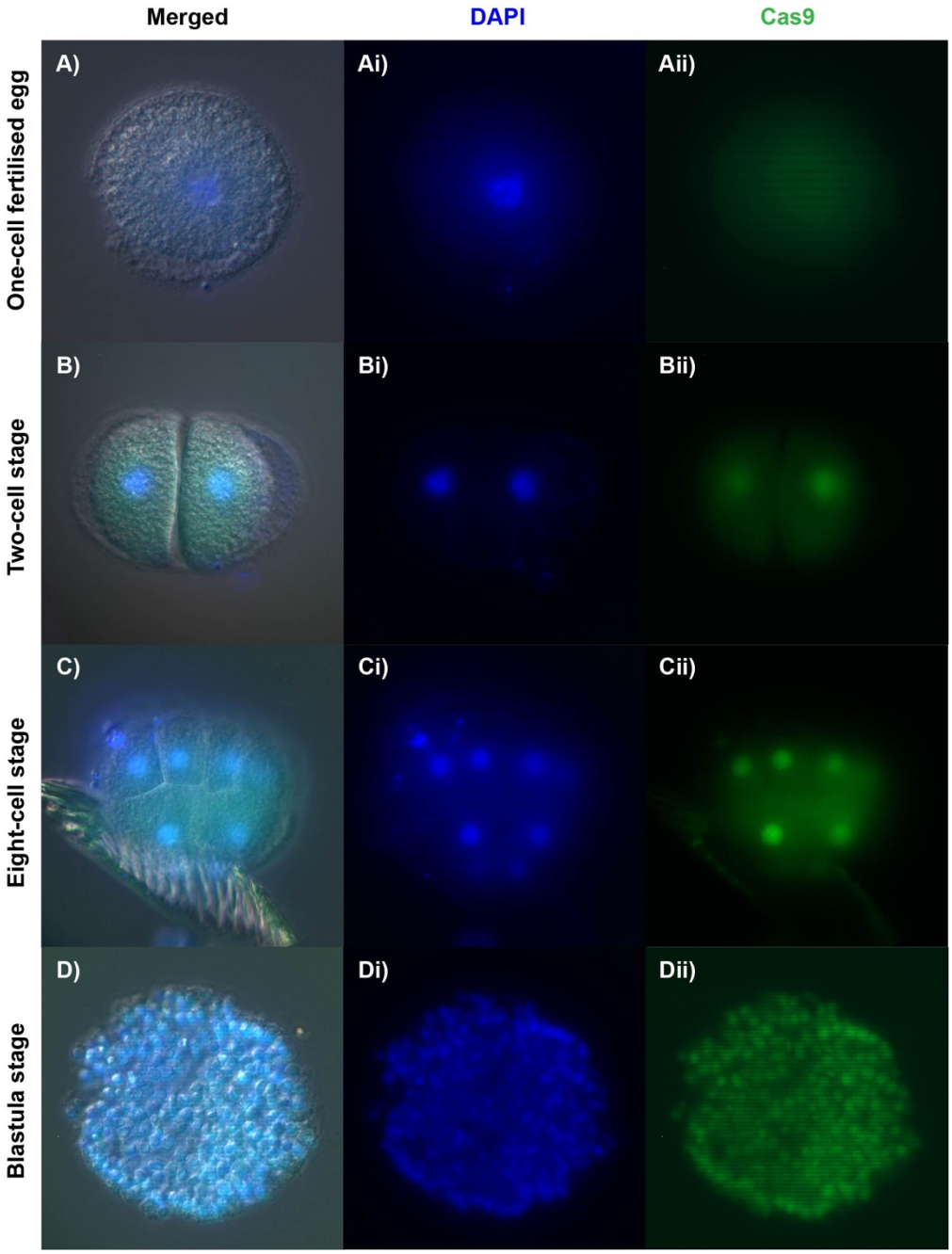

Figure 5.5 Localisation of Cas9 protein in early sea urchin embryos

To assess the first appearance and duration of Cas9 protein expression, eggs were injected with 90 ng/µl Cas9 mRNA and cultured at 15°C. Embryos were then fixed at the one-cell fertilised egg, two-cell embryo, eight-cell embryo and blastula stages, and prepared for IHC with anti-Cas9 nuclease (7A9-3A3) (AbCam #191468). Cas9 is localised in the nuclei of a two-cell embryo and remains in nuclei through the blastula stage. Cas9 is absent from the one-cell fertilised egg. Merged channels and separate DAPI and Cas9 channels are shown for each stage. A) one-cell fertilised egg. B) Two-cell embryo. C) Eight-cell embryo. D) Blastula stage (18 hpf) embryo. I) DAPI ii) Cas9. Immunohistochemistry carried out by David Axford.

5.3 Successfully detecting mutated individuals

To further optimise the CRISPR/Cas9 system in the sea urchin, another positive control better tailored to our work on neurons was designed, using sgRNA that target *Sp-Tryptophan hydroxylase* (*Sp-TPH*), an enzyme involved in the synthesis of serotonin. A two-day serotonin immunostaining protocol is frequently performed in our laboratory, enabling a quick assessment for a successful CRISPR/Cas9 functional gene disruption. A combination of six TPH sgRNA along with Cas9 mRNA were injected into fertilised sea urchin eggs (Figure 5.6). A different Cas9 protein (PNA BIO) was also tested that has successfully been used in lampreys to perturb *snail*, a key regulatory gene of neural crest EMT and migration (York *et al.,* 2017).

Interestingly, the majority of larvae injected with 40 ng/µl *Sp-TPH* sgRNAs and 500 ng/µl Cas9 protein (PNA BIO) developed normally (wild type development >85%); this percentage of wild type larvae is similar to uninjected larvae and larvae injected with Cas9 mRNA (Figure 5.7A). This reveals that PNA BIO Cas9 protein is not toxic to the sea urchin development, unlike the NEB Cas9. The number of serotonergic positive neurons is known to be variable and increase as the larva develops (Bisgrove and Burke, 1986). At the pluteus larval stage 3-4 days post fertilisation (dpf), samples were fixed and immunohistochemistry was performed using anti-serotonin (as described in methods 2.4.9). An average of six serotonergic neurons were observed in the apical organ of uninjected larvae (Figure 5.7C; Table 8.9), but with 7% of uninjected larvae having as many as 10-11 serotonergic neurons (Figure 5.7B; Table 8.9). Larvae injected with Cas9 mRNA, had an average of five serotonergic neurons with no embryos showing a complete absence of serotonergic neurons, whilst larvae injected with Cas9 protein had a lower average of four serotonergic neurons (Figure 5.7B-C; Table 8.9) and a small percentage of embryos showing no serotonin staining, revealing mostly mosaic mutants (Figure 5.7; Table 8.9).

To give the Cas9 protein more time to cause a DNA cut at the one cell stage, the temperature of developing embryos was lowered to 12°C. At this temperature the embryos still develop quite well, but they develop much slower. Larvae cultured at 12°C had an average of four serotonergic neurons (Figure 5.7C; Table 8.9), slightly

lower than the control of PNA BIO Cas9 protein injected embryos cultured at 15°C. Although this experiment needs to be repeated, interestingly, only PNA BIO Cas9 protein injected larvae had complete *Sp-TPH* knockouts. 15% of larvae injected with Cas9 protein and cultured at 12°C had no serotonergic neurons, compared with only 2% of larvae cultured at 15°C (Table 8.9), suggesting that Cas9 mutations were likely introduced earlier when cultured at 12°C.

A)

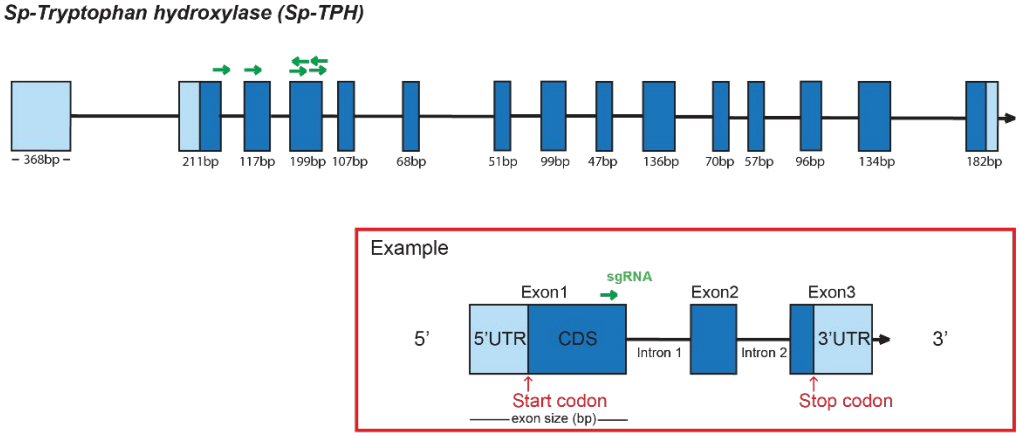

B)

gRNA name	target sequence	size bp	GC%	Number of potential off-target sites
gRNA 1 TPH	GGGGCCGAGGTGCTGGAAGA	19	70	0
gRNA 2 TPH	GGAAGACGGGGTCATAACCT	20	55	0
gRNA 3 TPH	GGCTCACATGAGCTCGGAGC	20	65	0
gRNA 4 TPH	GGCGTCGTGCCTTGTTAAGA	18	55	0
gRNA 5 TPH	GGCCCCGTCTTCCAGCACCT	20	70	0
gRNA 6 TPH	GGTGTTGGCGTGGTTCATGT	20	55	0

Figure 5.6 Gene structure and sgRNA for *Sp-Tryptophan hydroxylase*

A) Sp-TPH gene (SPU_003725; WHL22.635790) structure including introns, exons and location of target sgRNA sequences. Not drawn to scale. B) *Sp-TPH* sgRNA target sequences and details including the length of target sequence, GC content and the number of potential off-target sites.

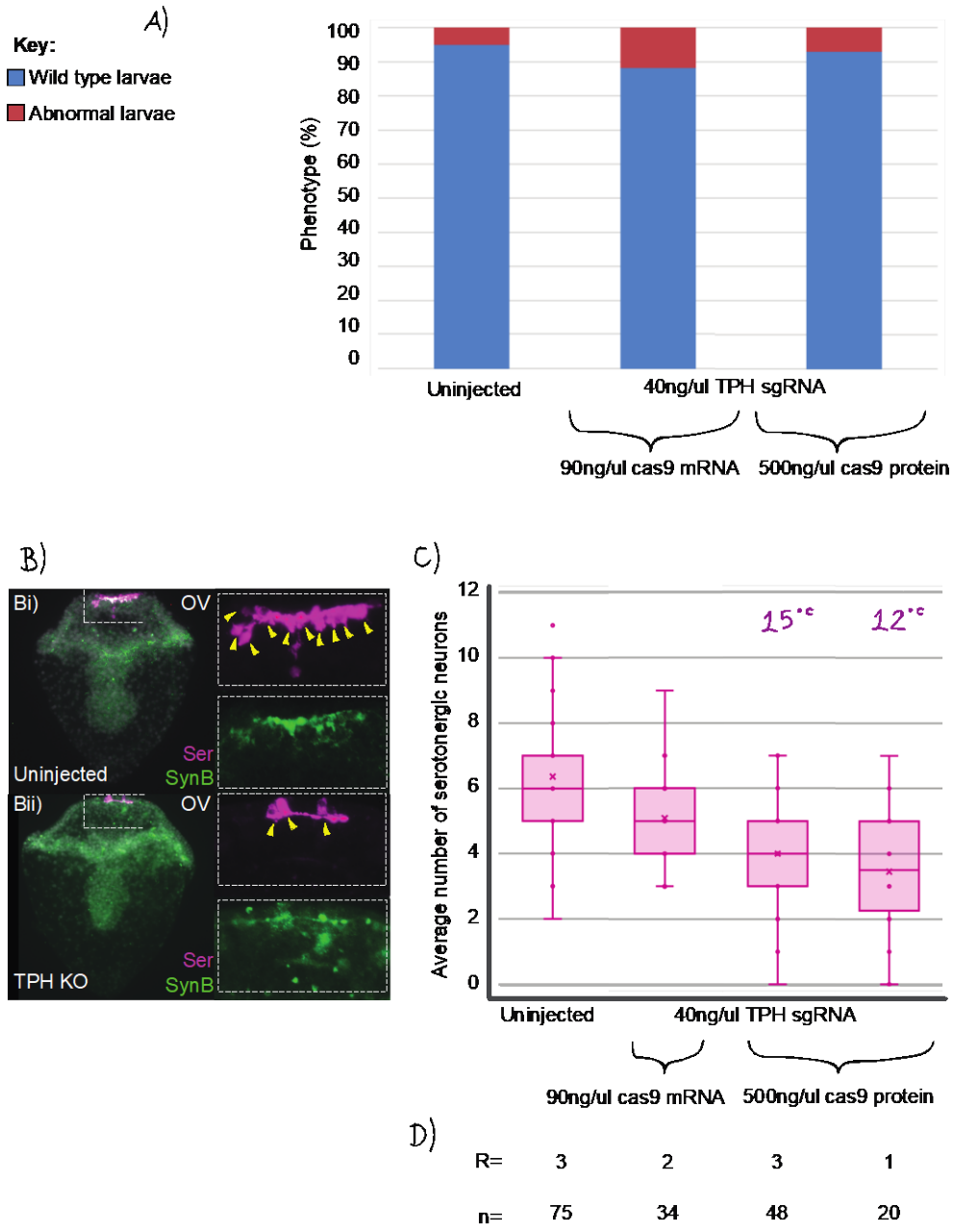

Figure 5.7 *Sp-Tryptophan hydroxylase* CRISPR/Cas9 knockout reduces the amount of serotonergic positive neurons

A) A bar graph plotting the percentage of wild type and abnormal developing larvae for three treatments: uninjected larvae, 40 ng/µl Sp-TPH sgRNAs with 90 ng/µl Cas9 mRNA injected larvae and 40 ng/µl Sp-TPH sgRNAs with 500 ng/µl Cas9 protein (PNA BIO) injected larvae. B) Labelling of the larval nervous system using antibodies against serotonin and synaptotagminB (SynB/1E11). Merged and single channels are shown with DAPI (grey), serotonin and synaptotagminB. Bi) An uninjected larva showing 10 serotonergic positive sensory neurons in the apical organ. Bii) A larva injected with 40 ng/µl TPH sgRNA and 500 ng/µl Cas9 protein showing three serotonergic positive sensory neurons. Yellow arrows point to the neurons. Top-right corner indicates the orientation of the larva. Bottom-right corner indicates the antibody used.

Abbreviated label OV refers to oral view. C) Box and whisker plot revealing the average number of serotonergic neurons in the three treatments. Cas9 protein injected larvae are incubated at 12°C and 16°C, all other treatments were incubated at 16°C. D) The number of individuals (n) counted across a number of independent experiments (R). Sp-TPH CRISPR/Cas9 and immunohistochemistry performed by Anne Ritoux.

Live imaging and immunostaining are appropriate methods for detecting successfully mutated larvae for the genes *Sp-PKS1* and *Sp-TPH,* respectively, where visualisation of an abnormal phenotype is easy. However, to successfully detect mutant larvae with other mutated genes a different standardized method was needed. I optimised a protocol to genotype injected embryos/larvae by performing DNA extraction on single individuals using the QIAamp DNA Micro Kit (Qiagen) (see methods section 2.3.4). The advantage of extracting DNA from single larvae, rather than pooling individuals, as done before in other studies on sea urchin embryos (Mellott *et al.,* 2017), is to detect different mutations that might be present in each embryo/larva and have a better understanding of the timing and mosaicism of mutations induced by the CRISPR/Cas9 system.

After single larva DNA extraction genes of interest were then PCR amplified. Amplified DNA was analysed on an agarose electrophoresis gel to visualise potential small deletion occurring after multiple cuts, given the fact that several sgRNA where pooled together. Larvae injected with multiple sgRNAs should cut out the piece of DNA in between the sgRNA. The absence of this piece of DNA can be visualised by a gel electrophoresis gel (Mellott *et al.,* 2017).

As a control for the DNA extraction and optimisation a fragment of a single exon gene, *Sp-FoxB* was first PCR amplified from varying amounts of DNA with 1, 3, or 10 larvae. *Sp-FoxB* was successfully amplified from all DNA extractions, except those where carrier RNA was added (Data not shown). The genomic DNA was individually extracted from five to eight single larvae per knock out condition, along with uninjected controls. In the case of *Sp-Jun,* which is a single exon gene expressed in skeletal cells. DNA extraction was separately performed on five larvae injected with *Sp-Jun* sgRNA and Cas9 mRNA and analysis on a gel electrophoresis showed that

three larvae has visible deletions (Figure 5.8A). However, amplification problems arose for most NP genes because they typically have a large first intron (>10 kb), which was too long to PCR amplify using a standard Taq polymerase.

The long-range amplified genomic target from individual larvae was then sent to sequence. Once again, the best results were obtained with the single exon gene *Sp-Jun*, 2 out of the 10 individually sequenced larvae showed a clear deletion in the gene (Figure 5.8, see B for an example). Both of these two larvae were mosaic for the deletion, in agreement with the detection of Cas9 protein in the nuclei after the first division. The results were more confusing for multi exon genes (such as *Sp-PPLN1* and *Sp-TPH*) likely due to long-range PCR problems, which need further optimisation. The observation of few mutant larvae in both genotyping strategies is in agreement with the low mutation efficiency observed in most of the genes (see *Sp-TPH* result in Figure 5.7). Furthermore, in many cases no obvious morphological phenotype is present to help isolate and sequence only mutated larvae. Taken together, single larval DNA extraction is feasible but requires more optimisation to consistently work on any targeted gene.

A)

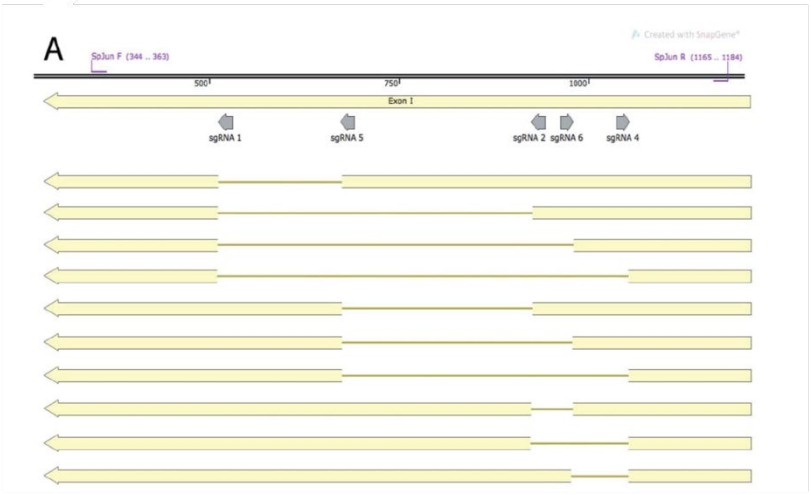

B)

Figure 5.8 DNA extraction from a single larva and sequencing results of a *Sp-Jun* CRISPR/Cas9 knockout

A) A schematic of the different mutations induced in the single exon *Sp-Jun* CRISPR/Cas9 knockouts inferred from gel electrophoresis. At the top is a wild type amplicon (841 bp) with sgRNA mapped to their targeting location. Underneath are predicted deletions in individual larvae based on smaller amplicons. For example, two larvae have a smaller amplicon of 450 bp, which seems to correspond to a deletion of DNA between sgRNA4 and sgRNA5. B) An illustration of a deletion in an *Sp-Jun* CRISPR/Cas9 larvae, with the sgRNA targeting sites highlighted. Data from panel B and C were performed by David Axford. Figures B and C courtesy of David Axford.

5.4 *In vitro* studies not comparable to *in vivo*

The efficiency of the CRIPSR/Cas9 system for seven genes in the sea urchin embryo has so far been tested and shown that it can work, but there is much variability. Consistent with the literature, genotype analysis and single sgRNA injection on *Sp-PKS1*, show a great variability of sgRNA efficiency not predicted by any of the computational tools used. I therefore decided to test the sgRNA efficiency in an *in vitro* assay and compare to the *in vivo* experiments with the aim to screen for the best acting sgRNA. An *in vitro* digestion assay was optimised by testing a range of variables and a few were found that were necessary for the *in vitro* assay to be functional. Five to six sgRNAs for five different genes were screened using this enhanced *in vitro* digestion assay. The percentage efficiency of Cas9 digestion was measured using Fiji image analysis software (see methods section 2.3.6 for details).

We began with an *in vitro* digestion assay protocol from NEB (see methods section 2.3.5), using a Cas9 nuclease (NEB; M0386). The *in vitro* assay was then optimised using sgRNA2 *Sp-PKS1* and sgRNA3 *Sp-PKS1* with the aim of consistently improving *in vitro* efficiency for both sgRNAs. The purification of sgRNA didn't consistently affect the efficiency of Cas9 digestion (Figure 5.9A). The degradation of the Cas9 nuclease by either a Proteinase K treatment or heat denaturation was found to be necessary to analyse *in vitro* Cas9 digestion, by allowing the digested DNA to be visualised on a agarose gel (Figure 5.9B). An increase in Proteinase K temperature from 20°C to 37°C increased the efficiency of the digestion by at least 13% (Figure 5.9C) and a longer Proteinase K treatment (from 30 to 45 minutes) also increased the efficiency of the digestion by 10% (Figure 5.9D). However, incubations that were longer than 45 minutes did not increase efficiency further (Figure 5.9D). The addition of EDTA in an attempt to prevent further Cas9 nuclease activity was found to reduce the efficiency of Cas9 digestion (Figure 5.9H). Two other variables also increased the efficiency of the assay, Cas9 concentration and duration of digestion. A Cas9 concentration of 83nM, lower than the recommended 100nM (1:10:10 molar ratio of DNA:sgRNA:Cas9), increased the digestion efficiency the most (Figure 5.9E). The Cas9 protein (NEB; M0386) is dissolved in glycerol, may inhibit the reaction and seems to be a more important factor than the optimal molar ratio (recommended by NEB

protocol, see methods section 2.3.5). Cas9 digestion duration also seems to be an important variable. An incubation time of 15 minutes was recommended by the NEB protocol. However, both sgRNAs had at least a 3-fold increase in efficiency with a Cas9 incubation of 60 minutes, rather than the recommended 15 minutes. Lastly, the temperature of the *in vitro* Cas9 digestion was tested. It is recommended that *in vitro* Cas9 digestion is done at 37°C, but *S. purpuratus* embryos are cultured at 16°C. To test if the Cas9 protein was more efficient at 37°C, the efficiency of the *in vitro* assay at both 16°C and 37°C was compared. Digestion of DNA by the Cas9 protein and sgRNA2 *Sp-PKS1* was more efficient at 37°C, with a decrease in efficiency when incubated at 16°C by 44% (Figure 5.9F). However, incubation of the Cas9 protein and sgRNA3 *Sp-PKS1* gave the same efficiency at both temperatures (Figure 5.9F), revealing that an *in vivo* temperature of 16°C should be effective for Cas9 to function. Taken together, we optimised the *in vitro* Cas9 assay conditions and showed that a Cas9 duration of 60 minutes and a degradation of Cas9 nuclease are necessary, a 83nM concentration of Cas9 and a Proteinase K treatment for 45 minutes at 37°C increase the efficiency and lastly, Cas9 temperature and purification of sgRNA does not consistently affect the efficiency.

A wide range of sgRNAs, across five different genes were then screened including; *Sp-PKS1* and *Sp-TPH* sgRNA our control genes; three neuropeptide precursor (NP) genes *Sp-Trh*, *Sp-PPLN1*, and *Sp-Np20;* and two skeletogenic genes, *Sp-pmar1* and *Sp-Jun.* The *in vitro* assay showed that all sgRNA for *Sp-TRH* and *Sp-Jun* were highly efficient (96% and above) (Figure 5.10). Most *Sp-TPH* sgRNAs were efficient (four out of five above 92%) and *Sp-Pmar1* and *Sp-PPLN1* sgRNAs have a variable efficiency (ranging from 11% to 100%) (Figure 5.10). Furthermore, sgRNA3 *Sp-PKS1* is consistently more efficient *in vitro*, than the sgRNA2 *Sp-PKS1* (Figure 5.9). This is contradictory to the well replicated *in vivo* results for sgRNA2 and sgRNA3 *Sp-PKS1*. sgRNA2 *Sp-PKS1* injected with Cas9 mRNA gives 80% completely albino larvae (across 20 independent experiments), whereas sgRNA3 *Sp-PKS1* gives only 7% completely albino larvae and 48% partial albino larvae (Figure 5.3C-D). Taken together, an *in vitro* assay to test Cas9 efficiency with different sgRNAs was successful set up and optimised. Unfortunately, *in vitro* efficiency does not seem to an accurate predictor

of *in vivo* efficiency. There are likely unknown factors in the *in vivo* system (e.g. chromatin structure), that haven't been incorporated into the *in vitro* assay that could explain this result and these are worthy of further exploration.

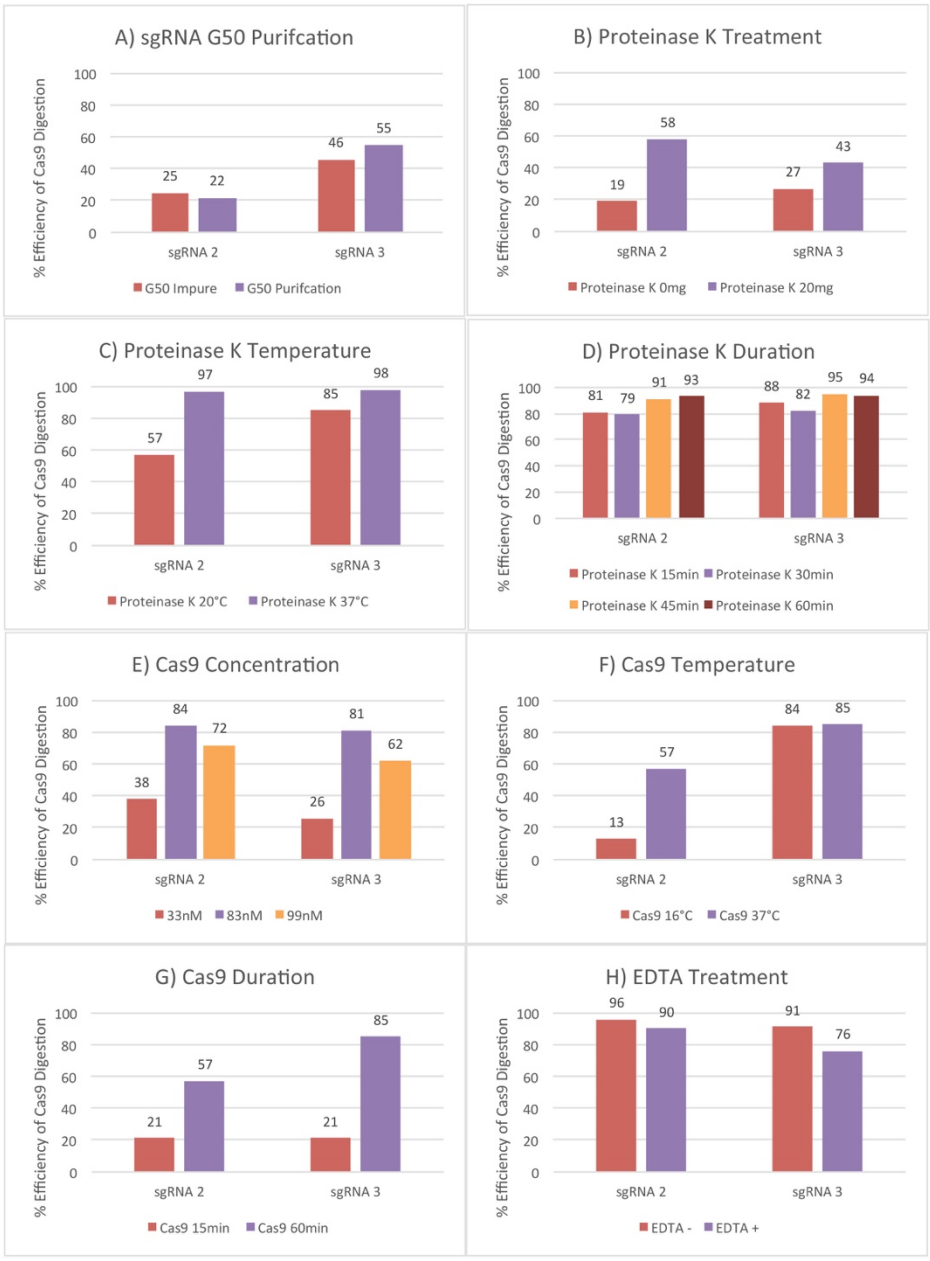

Figure 5.9 Optimisation of *in vitro* assay conditions

In vitro assay digestion with Cas9 protein (NEB) and sgRNA2 and sgRNA3 targeting *Sp-PKS1* was performed on *S. purpuratus* genomic DNA to test the *in vitro* efficiency of sgRNA. Percentage efficiency of Cas9 digestion was measured by Fiji image analysis software (see methods section 2.3.6 for further details). A number of conditions

including concentration, temperature, duration of Proteinase K, Cas9 digestion, sgRNA purification and EDTA treatment were tested on two sgRNAs targeting *Sp-PKS1*. A) G50 purified and impure sgRNA doesn't affect the efficiency of Cas9 digestion. B) 20mg Proteinase K treatment increases the efficiency of Cas9 digestion in both sgRNAs compared to no treatment. C) Proteinase K treatment at 37°C increases the efficiency of Cas9 digestion in both sgRNAs compared to a 20°C Proteinase K treatment. D) Proteinase K treatment for 15, 30, 45 and 60 minutes. Increasing the duration of Proteinase K treatment from 30 minutes to 45 minutes slightly increases the efficiency of Cas9 digestion in both sgRNAs. E) Three Cas9 concentrations 33nm, 83nm and 99nm are tested. A Cas9 concentration of 83nM (is most efficient at Cas9 digestion in both sgRNAs. F) Lowering Cas9 digestion incubating temperature from 37°C to 16°C lowers the efficiency of sgRNA2, but not sgRNA3. G) Increasing the duration of Cas9 incubation from 15 to 60 minutes, increases the efficiency of both sgRNAs. H) An EDTA treatment slightly lowers the efficiency of Cas9 digestion in both sgRNAs. *in vitro* assay experiment performed by David Axford. Figure courtesy of David Axford.

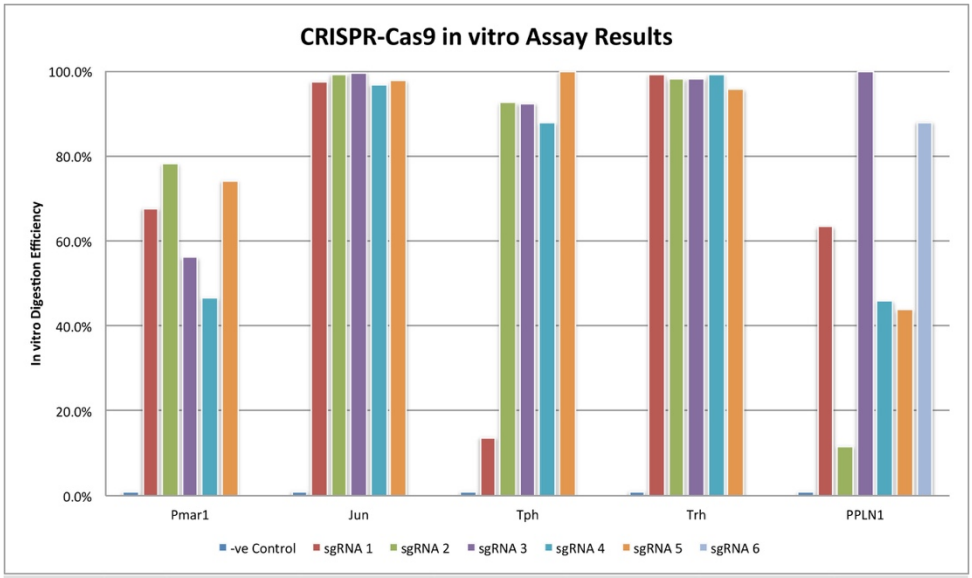

Gene	-ve	sgRNA 1	sgRNA 2	sgRNA 3	sgRNA 4	sgRNA 5	sgRNA 6
Pmar1	1%	68%	78%	56%	48%	74%	-
Jun	1%	98%	99.2%	99.7%	97%	98%	-
Tph	1%	14%	93%	92%	88%	100%	-
Trh	1%	99.2%	98%	98%	99.2%	96%	-
PPLN1	1%	63%	11.7%	100%	46%	44%	88%

Figure 5.10 *in vitro* assay efficiency is variable across different sgRNAs and genes

In vitro digestion assay for five-six sgRNAs of five genes. A) A bar graph showing the percentage of Cas9 digestion efficiency, measured by Fiji image analysis software. *Sp-Jun* and *Sp-TRH* sgRNAs were highly efficient. *Sp-TPH* sgRNAs were mostly efficient. *Sp-PPLN1* and *Sp-Jun* sgRNAs have the most variable efficiency. The colour of the box next to the sgRNA name, below the graph reflects the bar colour in the graph. A negative control, without a sgRNA shows no digestion B) The table below reflects the actual percentage values for each sgRNA. *in vitro* assay experiments performed by David Axford. Figure courtesy of David Axford.

5.5 Conclusions

To conclude, in agreement with previous publications, CRISPR/Cas9 has been shown to be a feasible gene-editing technology in the F0 generation of the sea urchin. Here I show that its can be an employed as a perturbation tool using both Cas9 mRNA and Cas9 protein (PNA BIO). In addition, several conditions (concentration of sgRNA and Cas9 mRNA) have been optimised, however it seems quite hard to predict sgRNA *in vivo* efficiency. Furthermore, mutations are likely introduced at the two-cell stage, but seems to be improved by injecting the PNA BIO protein and increasing the length of the first cleavage division. Additionally, a working *in vitro* digestion assay was established, however this cannot be used to accurately predict *in vivo* efficiency. One strategy has therefore been to inject all sgRNAs at once and hope one or more induce mutations. Lastly, the efficiency of on-target mutations was tested by genotyping. DNA was successfully extracted from a single larva permitting us to genotype individuals. However, more individuals need to be sequenced and further optimisation of large DNA amplification and detection on a gel electrophoresis is needed to determine on-target effects.

In Chapter 7, I discuss the work to be done to further improve the efficiency of the CRISPR/Cas9 system in sea urchin.

Chapter 6 Evolutionary conserved role of thyrotropin-releasing hormone-type signalling in regulation of growth revealed in sea urchin larvae

This final results chapter will focus on the second of my main objectives; investigating the roles of NP genes, specifically the role of TRH NP signalling in the sea urchin embryo and larva. I will highlight the conservation of TRH NP signalling across the Bilateria and the similarities found in the thyroid hormone (TH) signalling pathway in an invertebrate deuterostome, *S. purpuratus,* and a vertebrate, *H. sapiens*. I will show that the TRH-like peptide pQYPG-NH_2 acts as a ligand for an *S. purpuratus* receptor (Sp-TRHR), which is an ortholog of vertebrate TRH receptors. I will present the combinatorial expression analysis of *Sp-TRH* and its receptor. Additionally, I will present spatio-temporal expression analysis of other TH regulatory and synthesis genes. I will also investigate the role of *Sp-TRH* and *Sp-TRHR* by clustered regularly interspaced short palindromic repeats (CRISPR/Cas9) knockouts and morpholino oligonucleotides (MO) knockdowns. Finally, by using a combination of inhibitors, chromogenic ISH, immunohistochemistry and QPCR I attempt to identify downstream genes of *Sp-TRH* and *Sp-TRHR* and elucidate the molecular mechanisms of TRH NP signalling as a regulatory of larval skeleton growth.

This chapter is partially based on a paper in preparation (Wood et al., *Larval growth is regulated by thyrotropin-releasing hormone neuropeptide signalling 2020*) and experimental work reported in Figure 6.20 was carried out by undergraduate student Anne Ritoux (under by supervision).

6.1 Thyrotropin releasing hormone NP signalling systems are conserved across the Bilateria

TRH has been well characterised in vertebrates and the sequencing of the sea urchin *S. purpuratus* genome led to the discovery of the first invertebrate TRH-type peptide (see introduction 1.1 for more information). Phylogenetic analysis of the distribution of the TRH NP signalling system throughout the Bilateria has revealed the presence of genes encoding precursors of TRH-type peptides and TRH receptors in vertebrates, cephalochordates, ambulacraria (hemichordates and echinoderms), lophotrochozoa (annelids and molluscs) and ecdysozoa (arthropods and nematodes) (Bauknecht and Jékely, 2015; Conzelmann *et al.,* 2013; Jékely, 2013; Mirabeau and Joly, 2013; Rowe *et al.,* 2014; Rowe and Elphick, 2012; Semmens *et al.,* 2016; Sinay *et al.,* 2017b; Wilber *et al.,* 1992; Zandawala *et al.,* 2017b) (Figure 6.1A). In 2015, Bauknecht and colleagues discovered that the peptide "FSEFLGamide" is the ligand for a TRH-type receptor in the annelid *Playneresis dumerilii* (Bauknecht and Jékely, 2015). It has therefore been proposed that "EFLGamides" peptides in lophotrochozoans are orthologous to the deuterostomian TRH-type peptides (Bauknecht and Jékely, 2015; Conzelmann *et al.,* 2013). Sinay and colleagues then revealed the presence of TRH-type peptides with a EFLamide motif and their cognate TRH-type receptors in ecdysozoans (Figure 6.1A) and showed that an EFLGamide-type peptide is the ligand for a TRH-type receptor in the nematode *C. elegans* (Sinay *et al.,* 2017a).

BLAST analysis using the *H. sapiens* TRHR protein and insect TRH precursor protein sequences as queries enabled the identification of novel TRH-type precursor proteins in the insect *Bermisia tabaci* and crustaceans *Penaeus vannamei*, *Homarus americanus* and *Hyalella Azteca,* and novel TRH-type receptors in *B. tabaci, Limulus polyphemus*, *Daphnia pulex*, *P. vannamei*, *H. azteca* and *Armadillidium vulgare*. This data, together with data from Sinay and colleagues expands the repertoire of TRH NP signalling systems identified in arthropods (Sinay *et al.,* 2017b). TRH signalling is present in insect species but likely lost in diptera (true flies), an order containing the model species *Drosophila melanogaster*. This highlights the limitation of using only a single model species to define a genetic toolkit of a class/phylum.

In summary, *TRH* and *TRHR* genes are found in all major clades of Bilateria except for Urochordata (Figure 6.1A). Thus, the evolutionary origin of the TRH NP signalling system likely dates back to the common ancestor of the Bilateria, which existed over 550 MYA.

Here a more thorough BlastP analysis of sequence data from species belonging to the phylum Echinodermata was performed, searching for TRH-type neuropeptide precursors and TRH-type receptors in each extant class: the feather stars (Crinoidea), sea stars (Asteroidea), brittle stars (Ophiuroidea), sea cucumbers (Holothuroidea) and sea urchins (Echinoidea). I used publicly available data from NCBI (URL://https://blast.ncbi.nlm.nih.gov/Blast.cgi) and other echinoderm transcriptome sequence data (Dylus *et al.,* 2016; Elphick *et al.,* 2015). Previous studies have revealed the presence of a TRH-type precursors in all echinoderm classes except the feather star (Rowe *et al.,* 2014; Rowe and Elphick, 2012; Semmens *et al.,* 2016; Zandawala *et al.,* 2017b) and the presence of a TRH-type receptor gene in the sea urchin *S. purpuratus* (Burke *et al.,* 2006a) (Figure 6.1B). An *in silico* search using the *S. purpuratus* TRHR protein as a query, revealed the presence of TRH-type receptors in the brittle star *Amphuira filiformis*, sea cucumber *Apostichopus japonicus* and the feather star *Antedon mediterranea* (sequence IDs. can be found in the appendix Table 8.14 and Table 8.15) (Figure 6.1B). However, I could not find a TRH-type receptor in the genome or transcriptome of three sea star species analysed, *Asterias rubens*, *Patiria miniata* and the crown-of-thorns starfish *Acanthaster planci* (Figure 6.1B). I also didn't get any hits when searching for a TRH-type neuropeptide precursor protein in the transcriptome of the feather star, *A. mediterranea*. It would be worth searching in additional feather star transcriptomes/genomes when they become available in the future. To conclude, TRH NP signalling systems are present in at least three extant classes of echinoderms, the sea urchins, brittle stars and sea cucumbers (Figure 6.1B). Thus, given the Urbilaterian origin of TRH-type signalling, sea stars and feather stars either lost the system or it became so divergent that a simple BLAST search is not sufficient and more sophisticated analysis should be done.

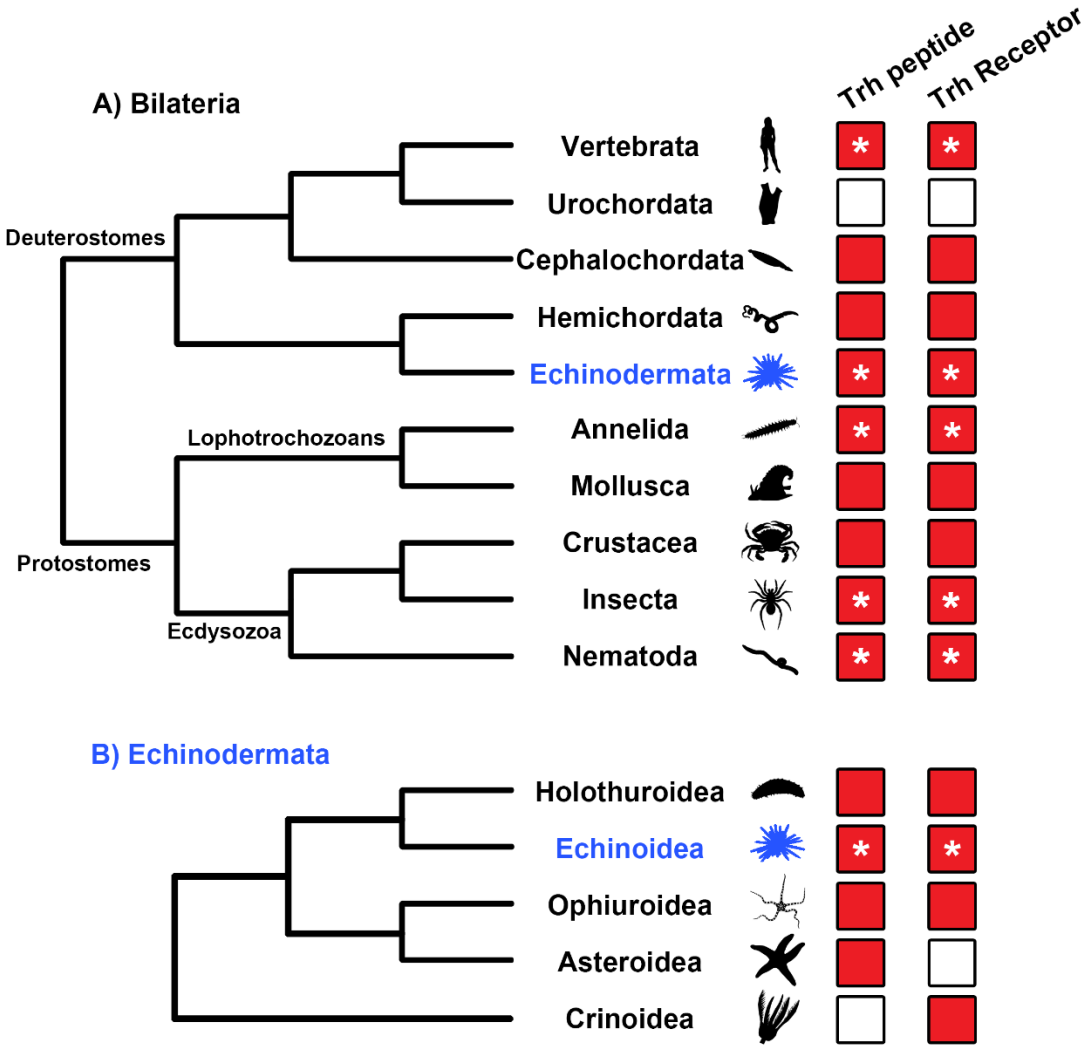

Figure 6.1 Evolution of TRH NP signalling system across Bilateria

Two phylogenetic trees showing the relationship of: A) selected bilaterian phyla/sub-phyla, and B) the five extant classes of Echinodermata, based on the well-supported Asterozoa clade (Reich *et al.,* 2015; Telford *et al.,* 2014). Each phylogenetic tree displays the distribution of TRH-type neuropeptide signalling system. A clade in which TRH-type neuropeptide precursors and TRH-type receptors have been identified in more than two species are labelled with a red-filled box. The loss of TRH neuropeptide precursors and/or receptors is illustrated with a white-filled box. An asterisk indicates that the peptide ligand and receptor been determined experimentally (Bauknecht and Jékely, 2015; Van Sinay et al., 2017; Veenstra and Šimo, 2020; Wilber et al., 1992). Note that the sea urchin *S. purpuratus* is the first and only invertebrate deuterostome in which the neuropeptide ligand for a TRH-type receptor has been experimentally demonstrated, as reported in this chapter. Animal silhouettes are from PhyloPic (http://phylopic.org).

Neuropeptide precursors can produce many mature peptides. To identify motifs common to particular clades I aligned the most frequent mature peptide for representative species of all major bilaterian phyla, including the novel TRH genes identified here (Figure 6.1; Figure 6.2). Most TRH peptides have short sequences (3-6 amino acids) and a C-terminal amide group (Figure 6.2). Deuterostomes have an N-terminal Glutamine (Gln) that is part of a tripeptide (chordates) or tetrapeptide (echinoderms) (Figure 6.2 (grey and blue coloured species boxes)) (Rowe and Elphick, 2012). Hemichordates have a longer sequence, but retain the C-terminal amide group and the Gln residue (Figure 6.2 (light blue)) (Mirabeau and Joly, 2013). The protostomian orthologs were not easily identified as the sequence differs. The protostomian TRH peptides have a Glutamic Acid (Glu; E) residue, instead of the Gln residue found in deuterostomes (Figure 6.2) (Bauknecht and Jékely, 2015). The E-[L/F]-[F/L/V]-[G/-]-NH_2 motif is common to all protostomian TRH-type peptides (Figure 6.2) and has no N-terminal modification. In contrast, the deuterostomian N-terminal Gln (Q) residue gives rise to a N-terminal pyroglutamate (pQ) residue. It has therefore been suggested that the post-translational modification at the N–terminus likely arose after the deuterostomes and protostomes diverged (Sinay *et al.,* 2017b). Furthermore, the total number of mature peptides varies considerably across Bilateria, ranging from two peptides in *C. elegans* to more than 20 peptides in *Branchiostoma floridae* and *Ophiuroidea victoriae*. Finally, demonstrating orthology across the Bilateria is difficult because TRH peptides, among some others (for example see Semmens *et al.,* 2015) are very short, therefore is it important to show that these peptides are ligands for orthologous TRH-type receptors. In contrast, peptides like VP/OT are so well conserved across the Bilateria that their orthology is clearly evident.

.

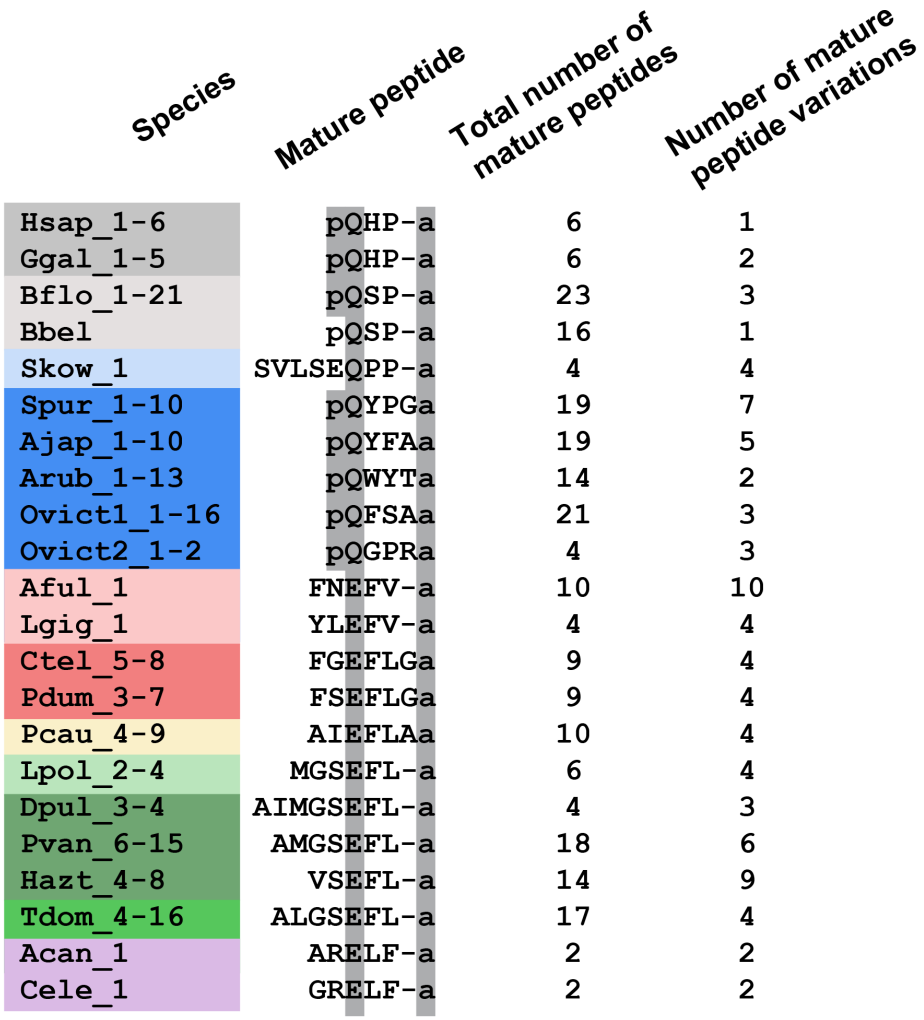

Species	Mature peptide	Total number of mature peptides	Number of mature peptide variations
Hsap_1-6	pQHP-a	6	1
Ggal_1-5	pQHP-a	6	2
Bflo_1-21	pQSP-a	23	3
Bbel	pQSP-a	16	1
Skow_1	SVLSEQPP-a	4	4
Spur_1-10	pQYPGa	19	7
Ajap_1-10	pQYFAa	19	5
Arub_1-13	pQWYTa	14	2
Ovict1_1-16	pQFSAa	21	3
Ovict2_1-2	pQGPRa	4	3
Aful_1	FNEFV-a	10	10
Lgig_1	YLEFV-a	4	4
Ctel_5-8	FGEFLGa	9	4
Pdum_3-7	FSEFLGa	9	4
Pcau_4-9	AIEFLAa	10	4
Lpol_2-4	MGSEFL-a	6	4
Dpul_3-4	AIMGSEFL-a	4	3
Pvan_6-15	AMGSEFL-a	18	6
Hazt_4-8	VSEFL-a	14	9
Tdom_4-16	ALGSEFL-a	17	4
Acan_1	ARELF-a	2	2
Cele_1	GRELF-a	2	2

Figure 6.2 Alignment of the sequences of mature TRH-type neuropeptides from Bilaterians

The most frequent predicted/proven mature peptide for TRH-type precursor proteins are aligned C-terminally in the second column. TRH-type peptides have a characteristic C-terminal amide group. Deuterostomes have an N-terminal pyroglutamate residue (pQ), whilst protostomes have a glutamic acid (E). Column three list the total number of mature peptides that are present in the precursor sequence and the fourth column lists the number of mature peptide variants. Species are listed in the first column, and are colour-coded based on their phylum. The number after the species name refers to most frequent mature peptides. Vertebrata (dark grey), Cephalochordata (light grey), Hemichordata (light blue), Echinodermata (dark blue), Mollusca (pink), Annelida (red), Prioplod (yellow), Chelicerate (light green), Crustacea (medium green) Insecta (dark green) and Nematoda (purple). Full species names can be found in the Appendix Table 8.15.

A gene encoding a TRH-type receptor is present in the sea urchin *S. purpuratus* and to confirm that *Sp-TRHR* encodes for a G-protein coupled receptor (GPCR), its amino acid sequence was analysed using the online software Protter (URL://http://wlab.ethz.ch/protter/start/), which identified the seven transmembrane domains that are a characteristic of GPCRs (Figure 6.3).

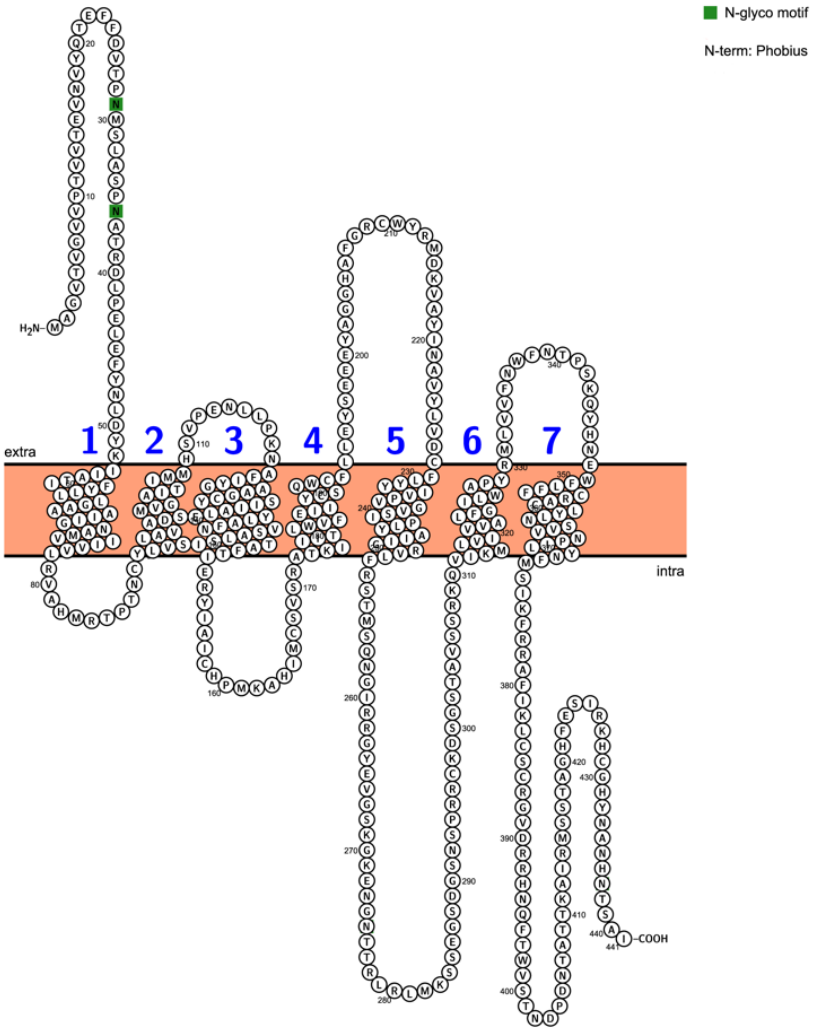

Figure 6.3 Sp-TRHR has seven transmembrane domains that are characteristic of G-protein coupled receptors

In silco analysis of the amino acid sequence of Sp-TRHR was performed using Protter (URL://http://wlab.ethz.ch/protter/start/) (Omasits *et al.,* 2014). The seven transmembrane domains are numbered successively in the blue and predicted N-glycosylation sites are show with green boxes.

In addition, to confirm the identification of the *S. purpuratus* receptor as a TRH-receptor ortholog, a phylogenetic analysis was performed which shows that the *S. purpuratus* TRHR is most closely related to other bilaterian TRHRs (Figure 6.4). The tree clearly shows that Sp-TRHR forms a monophyletic clade with all other bilaterian TRHRs (a bootstrap value of 100), and a different clade from the Neuromedin U (NMU) and Orexin GPCRs that form the outgroup (Figure 6.4). More specifically, Sp-TRHR forms a group with other ambulacrarian TRHR proteins (Figure 6.4). I also show that novel arthropod GPCRs (mentioned above) are orthologs to other known TRHRs (Figure 6.4).

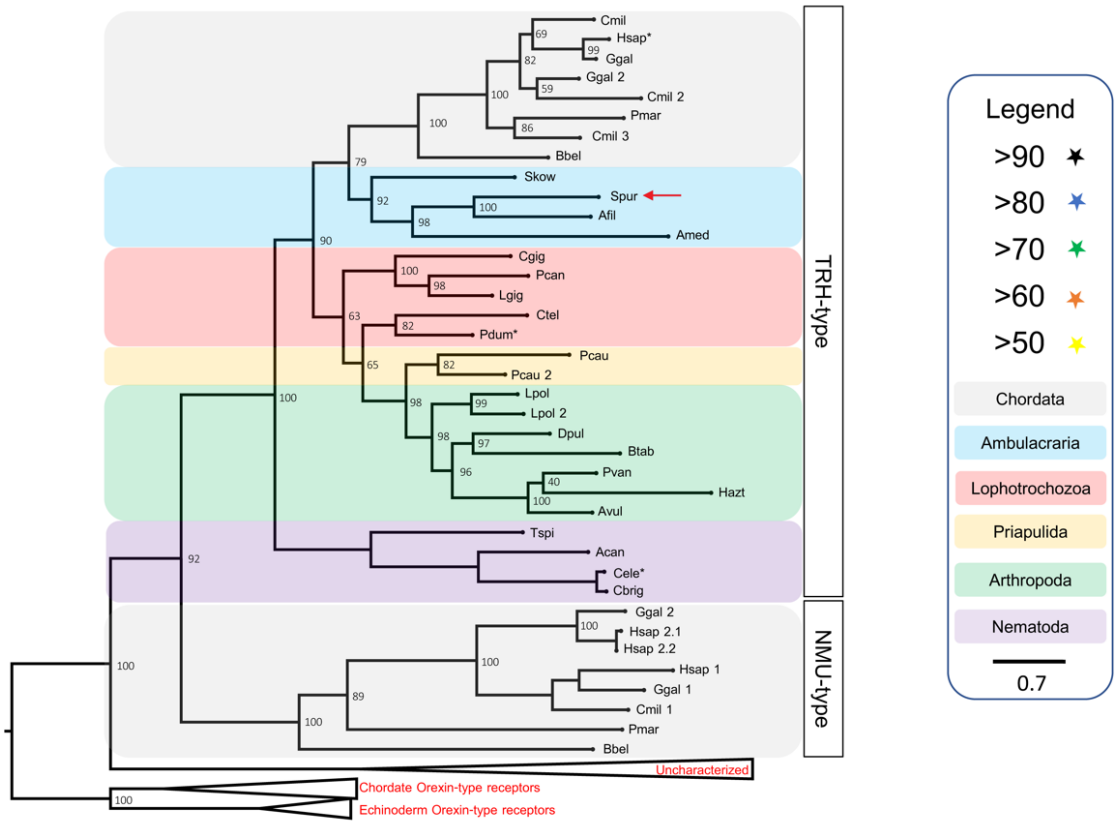

Figure 6.4 Phylogenetic tree showing TRH-type receptors from bilaterians, including the sea urchin *S. purpuratus* TRH-type neuropeptide receptor Sp-TRHR

The tree, which was generated using the Maximum likelihood method, shows the *S. purpuratus* candidate receptor (red arrow) as part of the TRH clade of receptors, together with other ambulacrarian orthologues. The numbers next to the branches represent bootstrap support (1000 replicates, see legend) and the coloured backgrounds represent different taxonomic groups, as shown in the key. The names with asterisks represent the receptors in which ligands have been experimentally confirmed. Full species names and GPCR sequences can be found in the Appendix

Table 8.15. NMU-type and orexin receptors were included as an outgroup. Phylogenetic tree produced by Luis Alfonso Yañez Guerra.

In summary, I have revealed that: a) the sea urchin *S. purpuratus* Sp-TRHR is orthologous to other bilaterian TRH-type receptors; B) the TRH NP signalling system was likely present in Urbilateria and has since undergone many divergences; and C) the TRH NP signalling system was likely lost/highly diverged in a few clades including Urochordata and Diptera. The presence of a putative TRH-type neuropeptide, but absence of a TRH-type receptor in seastars requires further investigation because it suggests that TRH-type peptides may be non-functional in seastars or exert their effects via a different receptor.

6.2 Demonstration that the peptide pQYPG-NH_2 (Sp-TRH) is a ligand for Sp-TRHR

Although phylogenetic and sequence analysis strongly supports the hypothesis that the TRH-like peptide pQYPG-NH_2 is a ligand for the *S. purpuratus* TRH-type receptor (Sp-TRHR) it is important that this proposed interaction is verified experimentally. To investigate if Sp-TRH peptide is indeed the ligand for Sp-TRHR, *in vitro* cell-based assays were performed.

To enable pharmacological characterisation of Sp-TRHR, a full-length cDNA encoding the receptor gene was amplified using total cDNA from 72 hpf *S. purpuratus* larvae and then subcloned into the eukaryotic expression vector pcDNA3.1+ (see methods section 2.6.1 and appendix section 8.7 for more details), which allows high expression in Chinese Hamster Ovary (CHO) cells. The assay used CHO cells that stably express aqaequorin and then these were transfected with the promiscuous G-protein Gα16 and Sp-TRHR. Control experiments on cells transfected with an empty vector were used as a negative control.

Synthetic Sp-TRH (pQYPG-NH_2) was tested as a candidate ligand for this receptor at concentrations ranging from 1 x 10^{-4} M to 1 x 10^{-14} M. Sp-TRH induced a dose-dependent bioluminescence signal in the Sp-TRHR transfected CHO-cells, with a half-maximal response concentrations (EC_{50}) of 2.4 x 10^{-8} M (Figure 6.5; Figure 6.6). Luminescence measurements were made for 35 seconds and Sp-TRHR transfected CHO-cells were exposed to varying peptide concentrations after 5 seconds and bioluminescence was observed within 5 seconds of exposure, with more concentrated peptides, cells responding more quickly and to a larger extent (Figure 6.6B). No response to Sp-TRH was observed in CHO-cells transfected with the pcDNA3.1+ vector alone, revealing that the response in Sp-TRHR-transfected cells can be attributed to the expression of Sp-TRHR in these cells (Figure 6.5A). The specificity of Sp-TRHR as a receptor for Sp-TRH was further assessed by testing two other neuropeptides on cells transfected with the Sp-TRHR: 1) Sp-GnRH, a sea urchin peptide that shares C-terminal sequence similarity with Sp-TRH; and 2) Ar-TRH, an ortholog of Sp-TRH from the seastar *A. rubens* (Semmens *et al.,* 2016). These peptides were tested at concentrations ranging from 1 x 10^{-4} M to 1 x 10^{-12} M. Neither

peptide induced bioluminescence in Sp-TRHR transfected CHO-cells (Figure 6.5B) and therefore it can be concluded that Sp-TRH is the specific ligand for Sp-TRHR.

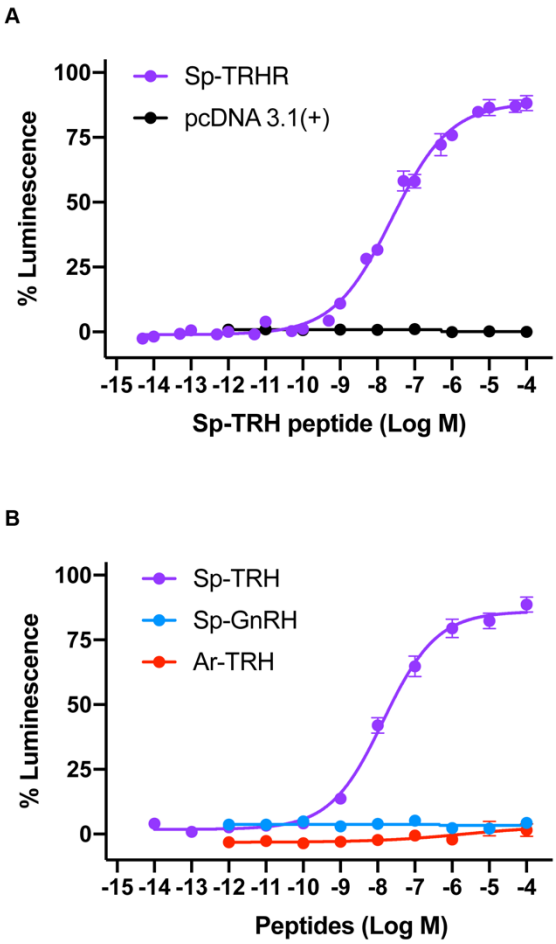

Figure 6.5 Sp-TRH causes dose-dependent activation of the Sp-TRH-Receptor

A) Sp-TRH peptide causes dose-dependent activation of luminescence in CHO cells expressing the Sp-TRH-Receptor, the promiscuous G-protein Gα16 and the calcium-sensitive luminescent GFP-apoaequorin fusion protein G5A, whereas no response is observed in cells transfected with an empty pcDNA3.1+ vector. B) Graph showing the luminescence emitted in the presence of different concentrations of Sp-TRH peptide, which specifically activates Sp-TRH receptor, Sp-GnRH and Ar-TRH do not activate the Sp-TRH-Receptor. Each point represents mean values (error bars are indicated by standard error of the mean, S.E.M) from at least four independent experiments, with each experiment performed in triplicate. Luminescence is expressed as a percentage of the maximal response observed in each experiment. The EC_{50} values for activation of Sp-TRHR with Sp-TRH are 2.4×10^{-8} M.

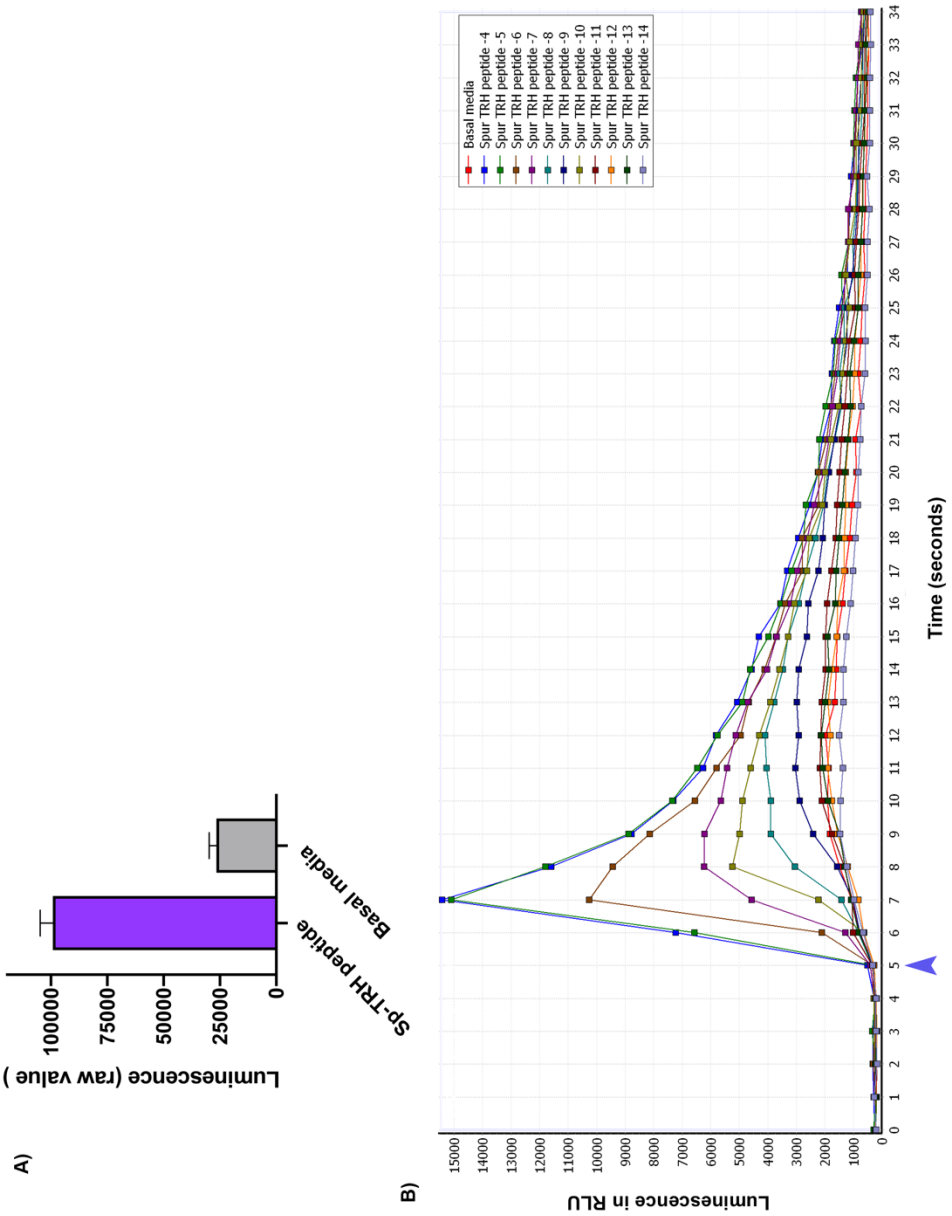

Figure 6.6 Raw data showing the level of bioluminescence induced by Sp-TRH in CHO cells transfected with Sp-TRHR

A) Bar graph showing mean luminescence values (+/- S.E.M) recorded in CHO cells expressing Sp-TRHR when exposed to Sp-TRH peptide (purple) or basal medium (grey; negative control). The graph shows that luminescence is at least 4 times more in presence of Sp-TRH peptide compared to basal medium. Relative luminescence unit (RLU) is the raw detection unit. B) Line graphs showing the dose-dependence and kinetics of Sp-TRH activation of luminescence in CHO cells expressed Sp-TRHR. Luminescence is measured for 35 seconds and an increase in luminescence is observed after 5 seconds. Each line indicates a different Sp-TRH peptide concentration (1 x 10-4 M to 1 x 10-14 M) and basal medium (negative control). Time in seconds is plotted on the x axis and RLU plotted on the y axis. The blue arrow marks when Sp-TRHR transfected CHO cells were exposed to the Sp-TRH peptide.

6.3 Discovery of other components of the Thyroid Hormone (TH) signalling pathway in *S. purpuratus*

As described in the introduction, activation of TRHR by TRH is the first step in the thyroid hormone (TH) signalling pathway in vertebrates, with the production of thyroxine (T4) and triiodothyronine (T3) being the final step. In vertebrates, T3 and T4 then travel through the body to exert their effects by binding to thyroid hormone receptors (THR) on targets cells (Figure 1.2). Most studies have focused on the TH pathway in vertebrates, and much less is known about the TH pathway in invertebrates. The presence of some components of the TH signalling pathway in invertebrates, including echinoderms, has been reported (Heyland, 2005; Miller and Heyland, 2013; Wu *et al.,* 2007). Interestingly, Heyland and colleagues showed that the addition of thyroid hormones can accelerate sea urchin larval skeletogenesis (Taylor and Heyland, 2018).

To establish whether other components of the TH signalling pathway are present in the sea urchin, human proteins associated with TH signalling were submitted as queries for BlastP searches of the *S. purpuratus* genome on NCBI non-redundant protein database (Figure 1.2). I searched for homologs of 10 genes encoding proteins involved in the regulation and synthesis of TH (excluding the already identified TRH and TRHR) and found 6 genes in the *S. purpuratus* genome: *Sp-Glycoprotein hormone Alpha 2* (*Sp-GPA2*) and *Sp-Glycoprotein hormone Beta 5* (*Sp-GPB5*) (Zandawala *et al.,* 2017b), *Sp-Thyroid-stimulating hormone-receptor* (*Sp-TSHR*), *Sp-Thyroid Peroxidase* (*Sp-Pxdn*), *Sp-Thyroid hormone receptor* (*Sp-THR*) and a *Sp-Iodothyronine deiodinase* (*Sp-DIO*) (Figure 6.7). Other genes that were not found include genes encoding three binding proteins, thyroxine binding globulin (TBG), Transthyretin (TTR) and serum albumin. Thyroid hormones are generally transported in the blood bound to serum proteins to ensure they are evenly distributed in larger animals (Power *et al.,* 2000).

Two other orthologous TH control genes that were not found were thyroid-stimulating hormone (TSH) and a solute carrier family member 5 (SLC5A5). SLC5A5 is a transmembrane protein that acts as a sodium iodide cotransporter. Thus, it is key for the uptake of iodide in the vertebrate thyroid gland (Eskandari *et al.,* 1997). TSH

binds to TSH-R and hence is a crucial part of the TH control pathway. Interestingly, the *S. purpuratus* genome does contain an ortholog of thyrostimulin, a glycoprotein hormone which has also been shown to activate TSH-R (Nakabayashi *et al.,* 2002). This glycoprotein hormone is made up of 2 subunits, alpha 2 (GPA2) and beta 5 (GPB5). The heterodimer A2/B5 was found to increase thyroxine levels in TSH suppressed rats *in vivo* and therefore named thyrostmulin, due its thyroid-stimulating activity, while not stimulating other glycoprotein hormones receptors (FSH, LH/CG receptors) (Nakabayashi *et al.,* 2002). Thyrostimulin has since been identified in other invertebrates (Sudo *et al.,* 2005; Zandawala *et al.,* 2017b). TSH was classically thought to be the main activator of TSH- receptor but has so far only been identified in vertebrate genomes (Hsu et al. 2002). It therefore seems likely that thyrostimulin was ancestrally the activator of TSH-R, and TSH was subsequently gained in vertebrates to stimulate TSH-R. Thus, as *S. purpuratus* is an invertebrate deuterostome it is unsurprising that TSH is absent in the *S. purpuratus* genome.

The three other TH control genes that were found in *S. purpuratus* are genes encoding a thyroid peroxidase, a iodothyronine deiodinase and a thyroid hormone receptor (Figure 6.7). Thyroid peroxidase (Pxdn) is extremely important for thyroid hormone synthesis. Iodide is primarily obtained from the environment and Pxdn is responsible for the oxidation of iodide to the unstable iodine, which then immediately reacts with tyrosine to make thyroxine (Lagorce *et al.,* 1991). Iodothyronine deiodinase (DIO) is a peroxidase enzyme that catalyses the activation and inactivation of thyroid hormones by removal of iodine (Bianco *et al.,* 2002). Three *DIO* genes are present in humans that are have different roles in activation and inactivation. DIO1 and DIO2 can convert the prohormone T4 to the bioactive form of T3 and can also inactivate T3 and T4, while DIO3 seems to only inactivate T3 and T4 (Bianco *et al.,* 2002). In the *S. purpuratus* genome I found one *Sp-DIO. Sp-THR* is a nuclear receptor which is bound by thyroid hormones. Howard-Ashby and colleagues have previously identified this nuclear receptor as belonging to the NR1 family (Howard-Ashby *et al.,* 2006a) of transcription factors. Wu and colleagues also reported the presence of *THR* in *S. purpuratus* and other invertebrates (Wu *et al.,* 2007).

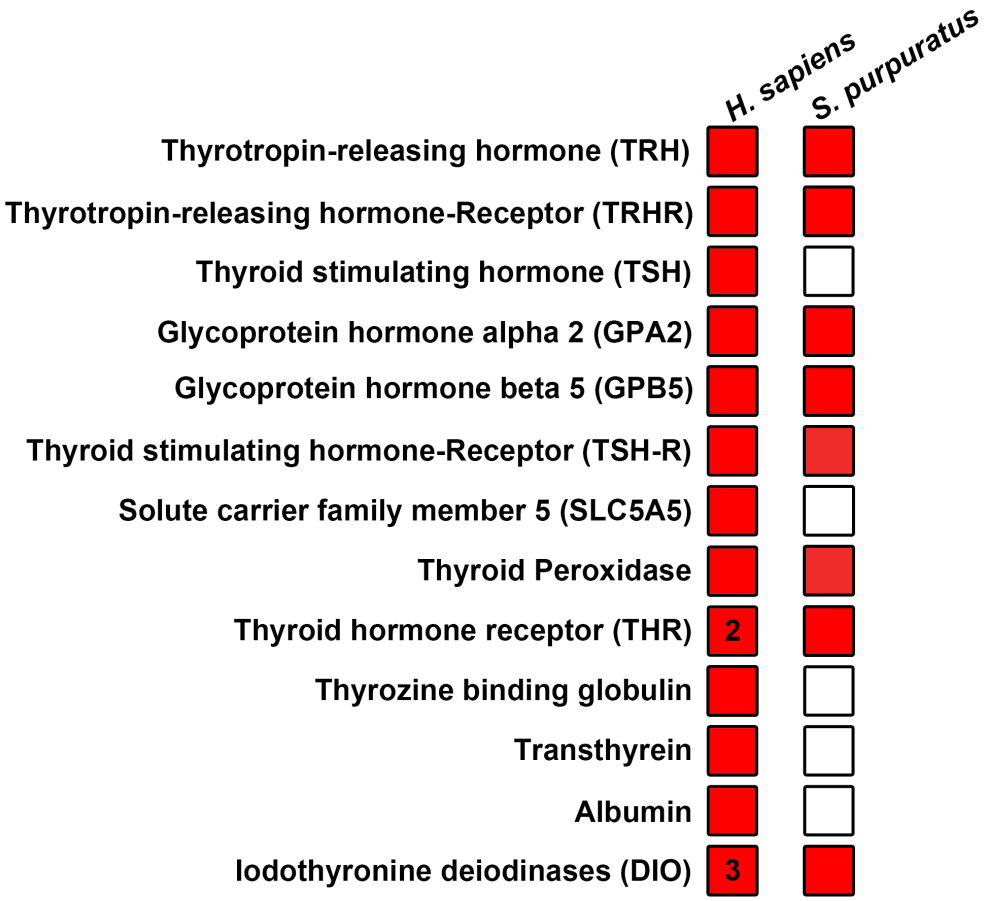

Figure 6.7 Presence and absence of gene encoding proteins associated with thyroid hormone signalling in *S. purpuratus* and *H. sapiens*

Genes that have been identified in the *H. sapiens* or *S. purpuratus* genome are labelled with a red-filled box. Genes not found are labelled with a white-filled box. Numbers inside a box indicate how many copies of that gene are present in a particular species.

To investigate if orthologs of genes associated with TH signalling are expressed at the same developmental stage as TRH NP signalling and hence could be regulated by TRH NP signalling, transcriptome data from Echinobase (URL://http://www.echinobase.org/Echinobase/Blast/SpBlast/blast-run.php) was analysed (Tu *et al.,* 2014b). Temporal data revealed that all six TH control genes are expressed during larval development (Figure 6.8). Interestingly, four out of six genes (*Sp-GPA2*, *Sp-GPB5*, *Sp-TSHR*, *Sp-THR*) increase in expression from the early gastrula (40 hpf) to pluteus larval (72 hpf) stage (Figure 6.8; Table 8.6), at a time when larval skeletal growth is occurring. Two enzymes *Sp-Pxdn* and *Sp-DIO* have different

temporal expression patterns. *Sp-Pxdn* maintains a high level of expression throughout embryonic development with maternal expression at 0 hpf over 9000 transcripts per embryo and zygotic expression (over 5000 transcripts per embryo) at the blastula stage (18 hpf). *Sp-DIO* has an increase in expression at the gastrula stage (48 hpf) with over 10000 transcripts per embryo, followed by a decrease in expression to less than 400 transcripts per embryo at the pluteus larval stage (72 hpf) (Figure 6.8).

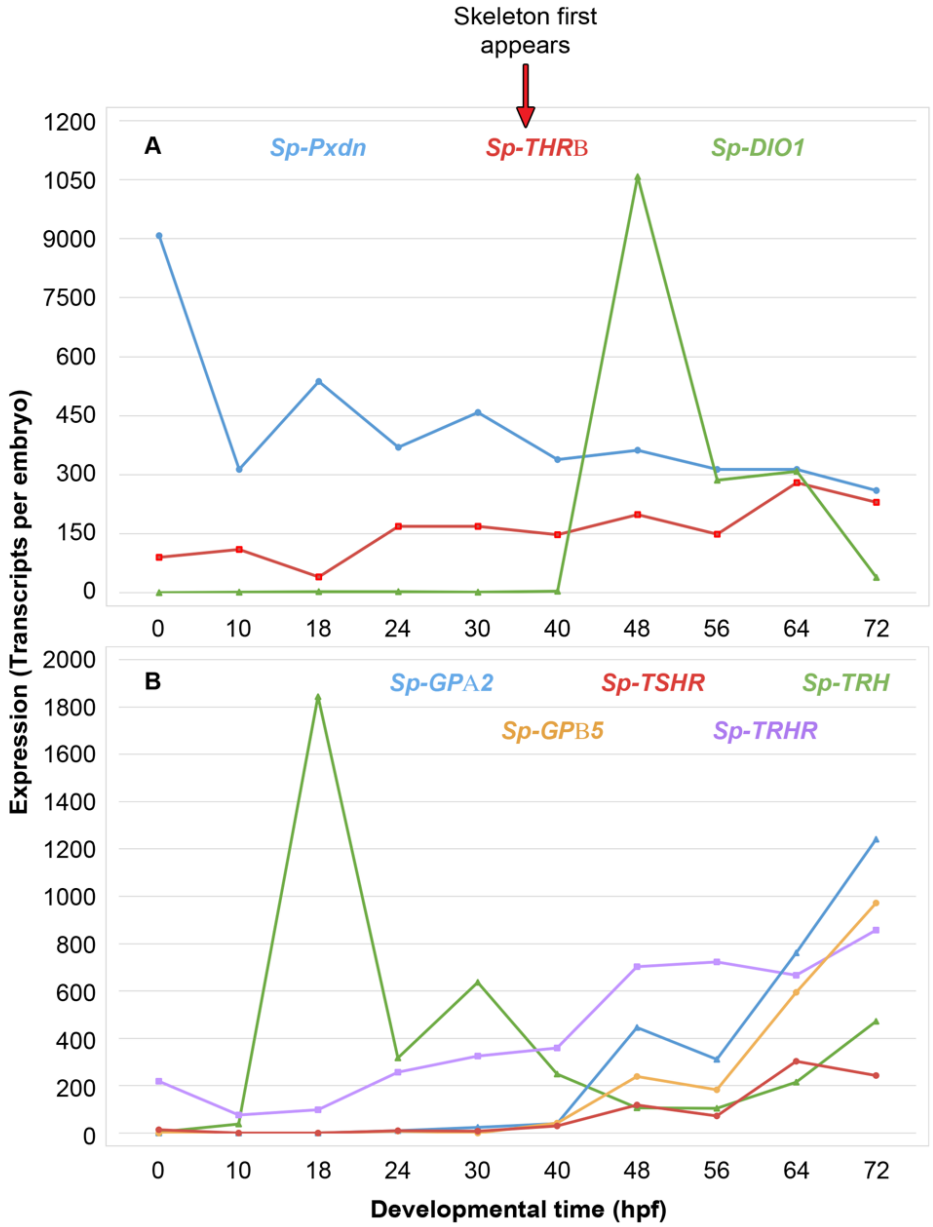

Figure 6.8 Transcriptome data reveals thyroid hormone signalling associated genes are expressed during embryonic development

Gene expression (transcripts per embryo) is shown at: the unfertilised egg stage (0 hpf), early blastula (10 hpf), hatched blastula (18 hpf), mesenchyme blastula (24 hpf), very early gastrula (30 hpf), mid gastrula (40 hpf), late gastrula (48 hpf), early prism (56 hpf), late prism (64 hpf), and pluteus larval stage (72 hpf). The line graph depicts different levels of gene expression for eight genes, with higher expression in graph A and lower expression in graph B. The colour of the gene name at the top of each graph reflects the line colour in the corresponding graph.

To summarise, I have revealed the presence of genes encoding orthologs of proteins associated with TH signalling in the late embryonic and pluteus larval stages of *S. purpuratus*. The TRH NP signalling system is also present in the pluteus larvae, providing a basis for the hypothesis that TRH may regulate endogenous TH production in *S. purpuratus,* similar to vertebrates.

6.4 Iodide accelerates larval skeleton growth

Analysis of *S. purpuratus* genome/transcriptome data reveals the presence and expression of genes encoding orthologs of various components of the TH signalling pathway in the sea urchin pluteus larvae. Iodine is also essential for thyroid hormone production. Trace amounts of iodide are normally present in sea water (Fuge and Johnson, 1986) and therefore marine animals are constantly able to obtain iodide either from the diet or directly from the sea water. Our embryonic cultures at UCL are grown in filtered artificial sea water (FASW) that does not contain iodide or iodine (see recipe in appendix section 8.2). While laboratories located at marine stations use filtered sea water directly from oceans and hence their water will likely contain iodide. While our embryonic cultures do develop properly, we have had issues with slow larval development and metamorphosis and perhaps the lack of iodine is a problem for our larvae to grow.

To test if iodine does accelerate skeleton growth, I grew *S. purpuratus* cultures in normal FASW (recipe in section 8.2) and FASW with sodium Iodide (NaI) (57ug/L) (Fuge and Johnson, 1986). At pluteus larval stage (4 days post fertilisation) I measured the length of the skeleton. The larval skeleton can be divided into the body rod, the post oral, oral transverse, and the oral distal skeletal parts (Figure 6.9B). Each part of the skeleton was measured. Data showed that sodium iodide significantly increased the rate of skeletal growth in all parts of the skeleton, but a larger increase was seen in the post oral, oral distal and oral transverse skeletal parts (Figure 6.9). Taken together, the acceleration of skeleton growth by the addition of iodide, a crucial element for TH synthesis, and the presence of TH control genes in the *S. purpuratus* genome, it would be plausible to reason that the TH pathway is functional and has a role in skeleton growth in *S. purpuratus* larvae.

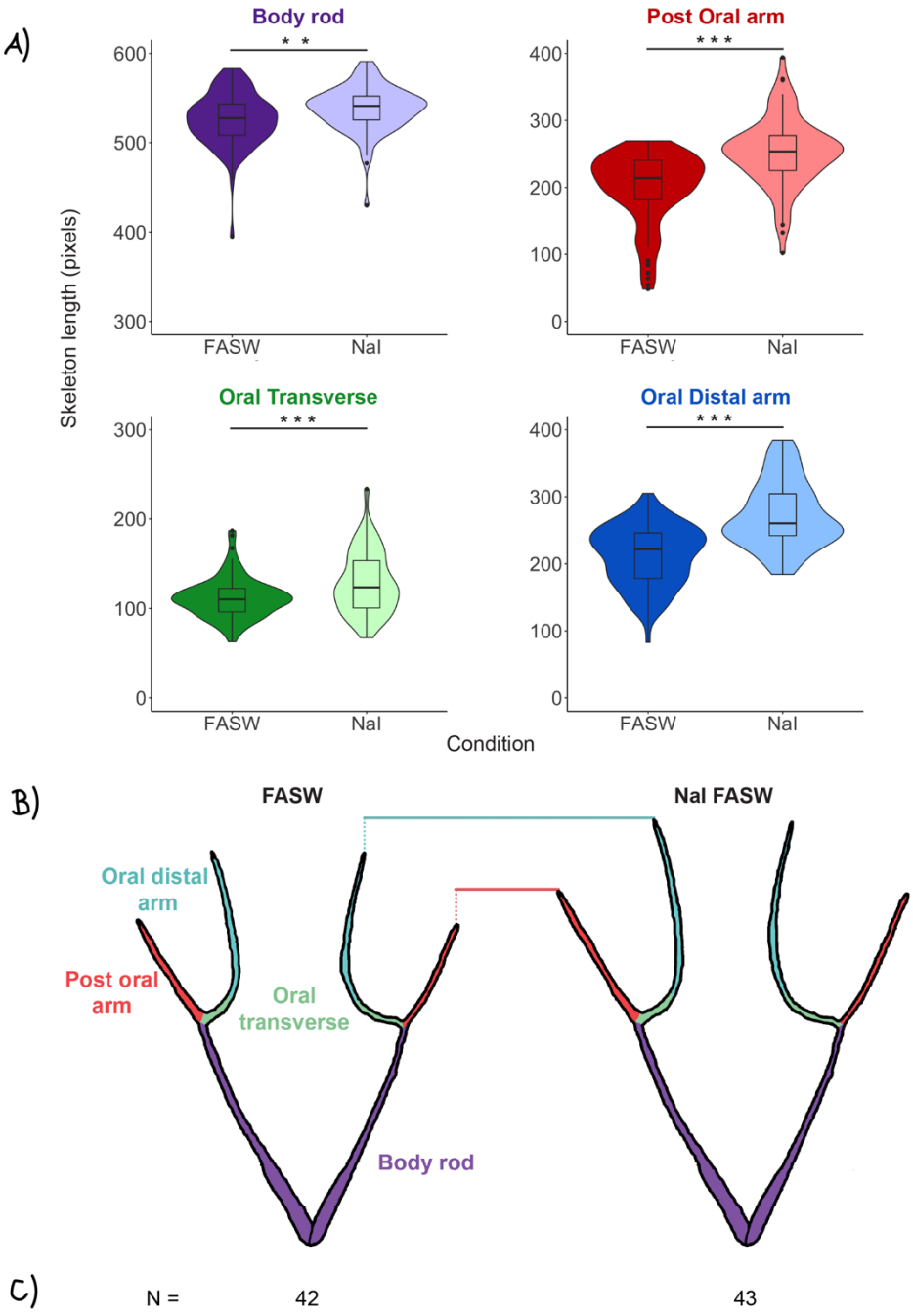

Figure 6.9 Iodide accelerates skeleton growth in sea urchin larvae

A) Four violin plots with box and whisker plots overlaid plotting the length of skeleton (pixels) for the different skeletal parts in filtered artificial sea water (FASW) (negative control) and sodium iodide (NaI) in FASW. Boxes show the median, lower and upper quartiles, while the whiskers extend to the minimum and maximum data points. A student's two-tailed t-test was performed, ** (P<0.01) and *** (P<0.001) and reveals that larval skeletal parts are significantly longer when cultured in NaI FASW, with the post oral, oral transverse and oral distal skeletal lengths the longest and body rod a little longer. B) Cartoon skeletons illustrating the longer skeletal lengths in the NaI FASW condition compared to normal FASW. C) The total number of individual larvae counted per treatment and data collected from three independent experiments.

6.5 Spatial expression analysis of genes associated with thyroid hormone signalling in *S. purpuratus* larvae

To investigate if genes associated with thyroid hormone signalling are expressed in a similar region to *Sp-TRH* and its receptor, I performed chromogenic ISH for *Sp-Pxdn*, *Sp-DIO* and *Sp-THR* at the pluteus larval stage and other key developmental stages. I was unable to clone *Sp-TSHR,* most likely a result of its low expression in embryonic and larval development (less than 300 transcripts per embryo) (Figure 6.8B). The cloning of *Sp-GPA2* and *Sp-GPB5* is in progress.

Expression of *Sp-THR* is first detected during late gastrulation (48 hpf) when staining is stronger in the endoderm, oral ectoderm and apical plate and weaker staining is present in the aboral ectoderm (Figure 6.10A-C). At the late prism stage (66 hpf) *Sp-THR* probe staining is stronger in the apical plate and endoderm, and in the late pluteus larvae (96 hpf) *Sp-THR* is strongly localised to the ciliary band and gut (Figure 6.10D-E). Expression of *Sp-Pxdn* is ubiquitously detected in the mid gastrula stage (42 hpf), with stronger staining seen in apical plate and gut (Figure 6.10G). In the late prism stage (66 hpf), *Sp-Pxdn* expression is stronger in the ciliary band and endoderm (Figure 6.10H) and in the pluteus larvae (72 hpf) expression is detected in all cell types (Figure 6.10I-J). Expression of *Sp-DIO* is not detected in the late gastrula (48 hpf) (Figure 6.10L). In the pluteus larvae (72 hpf) *Sp-DIO* is detected in all cell types, with stronger staining in the ciliary band and gut and the strongest expression seen in a few cells at the boundary of ciliary band and aboral ectoderm (see white arrows) (Figure 6.10M-N). In a later pluteus larval stage (96 hpf) staining remains strong in the ciliary band and gut (Figure 6.10O). Staining was not detected in the unfertilised egg for any probe (Figure 6.10A, F and K). These chromogenic ISH data are consistent with pluteus larval stage single cell sequencing data produced by the Arnone Laboratory (P. Paganos, personal communication).

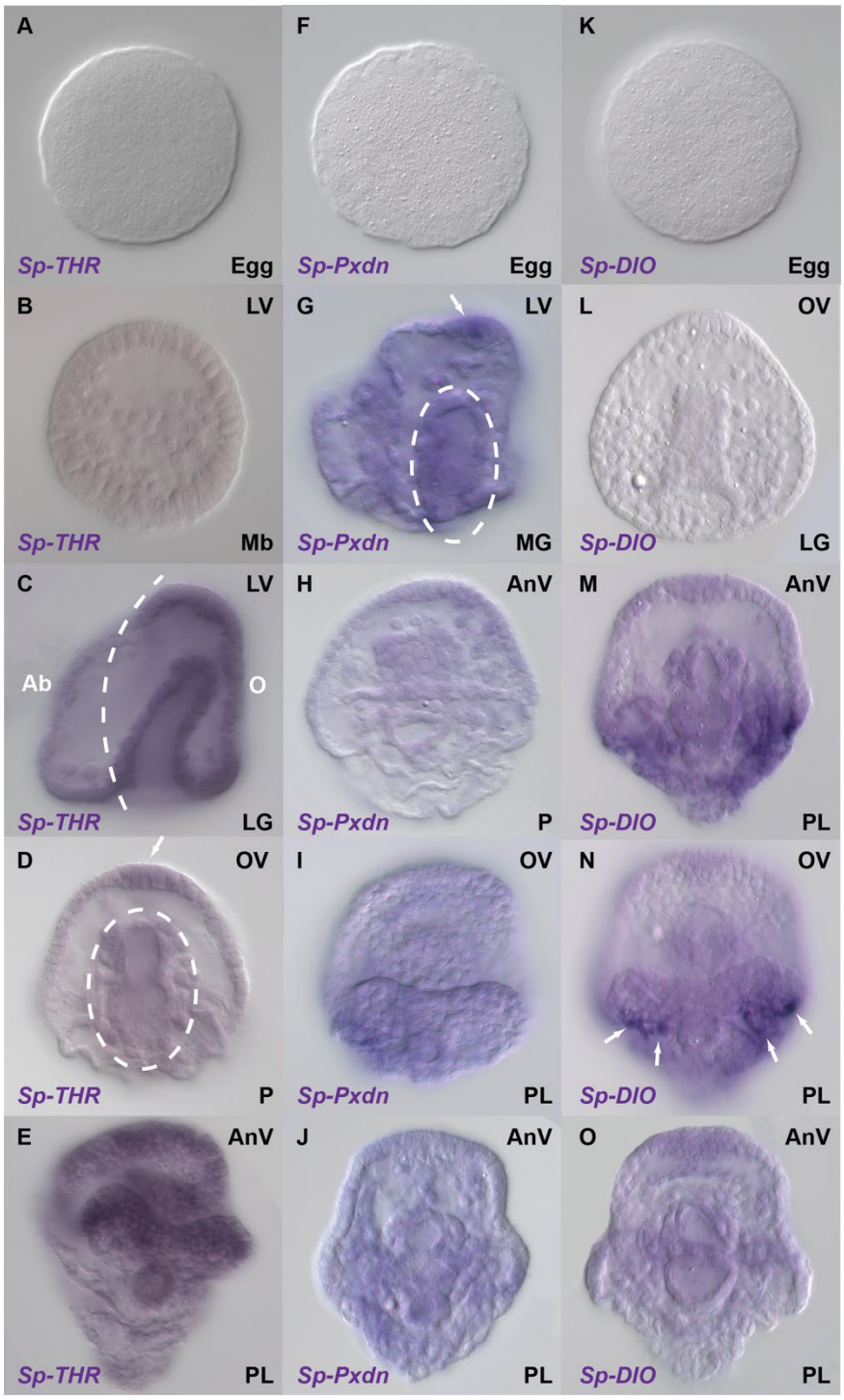

Figure 6.10 Thyroid hormone (TH) signalling associated genes are expressed in many cell types during embryonic and larval development

Spatial expression of genes associated with TH signalling (*Sp-THR*, *Sp-Pxdn* and *Sp-DIO*) in the (A, F and K) unfertilised egg, (B) mesenchyme blastula, (G) mid-gastrula, (C and L) late gastrula, (D and H) late prism, (I-J and M-N) pluteus larval and (E and O) late pluteus larval stages, as revealed by chromogenic ISH. (A, F and K) Staining was not detected in the unfertilised egg for any probe. (B) *Sp-THR* is not detected in the mesenchyme blastula stage (24 hpf). (C-E) *Sp-THR* is strongly detected in the

endoderm and ciliary band and apical plate/apical organ, and also in the oral ectoderm in the late gastrula (48 hpf). (G and I-J) *Sp-Pxdn* is detected in all cell types at the mid gastrula (42 hpf) and pluteus larval (72 hpf) stages. Stronger staining is detected in the endoderm and apical plate in the mid gastrula (H) *Sp-Pxdn* expression in the late prism (66 hpf) is stronger in the ciliary band and endoderm. (L) *Sp-DIO* is not detected in the late gastrula embryo (48 hpf). (M-N) *Sp-DIO* expression in the ciliary band and gut with stronger staining in few cells at the aboral ectoderm/ciliary band boundary in the post oral arms (white arrows). One embryo is shown at the pluteus larval stage (72 hpf) from two different focal planes. (O) *Sp-DIO* is strongly detected in the ciliary band and gut in a later larval stage (96 hpf). Dotted white lines isolate cells that have a stronger staining. Top-right corner indicates the orientation of the embryo or larva. Bottom-right corner indicates the embryo/larval stage in hours post fertilisation. Abbreviated labels refer to the following: LV (lateral view), OV (oral view) and AnV (anal view).

6.5.1 Combinatorial analysis studies of *Sp-TRH* and *Sp-TRHR* expression in sea urchin larvae

In Chapter 3 (see section 3.3) I used chromogenic ISH to reveal the expression of *Sp-TRH* and *Sp-TRHR* in the ciliary band. *Sp-TRH* is detected in one-two cells on either side of the apical organ, while *Sp-TRHR* probe staining is distributed throughout the ciliary band and seems to overlap with the location of *Sp-TRH* expression in the two oral distal neuronal cells (Figure 3.8). To determine if *Sp-TRH* and *Sp-TRHR genes* are truly co-expressed I performed double fluorescent ISH (FISH) in the pluteus larvae (72 hpf) and a later larval stage (6 dpf). FISH expression analysis shows that *Sp-TRH* and *Sp-TRHR* are both detected in two cells, located on either side of the apical organ (Figure 6.11). The co-expression of this ligand-receptor pair suggests that they are acting on these OD neuronal cells in an autocrine manner. The receptor's wider expression pattern in the ciliary band indicates that Sp-TRH could also act in a paracrine, or endocrine manner.

Taken together, single chromogenic ISH of TH signalling genes and double FISH of Sp-TRH and Sp-TRHR suggest that all are likely expressed in the two oral-distal Sp-TRH positive neuronal cells. Furthermore, *Sp-DIO*, *Sp-THR* and *Sp-Pxdn* are likely widely co-expressed with *Sp-TRHR* in many ciliary band cells (Figure 6.10 E, I-J, M-O and Figure 6.11C).

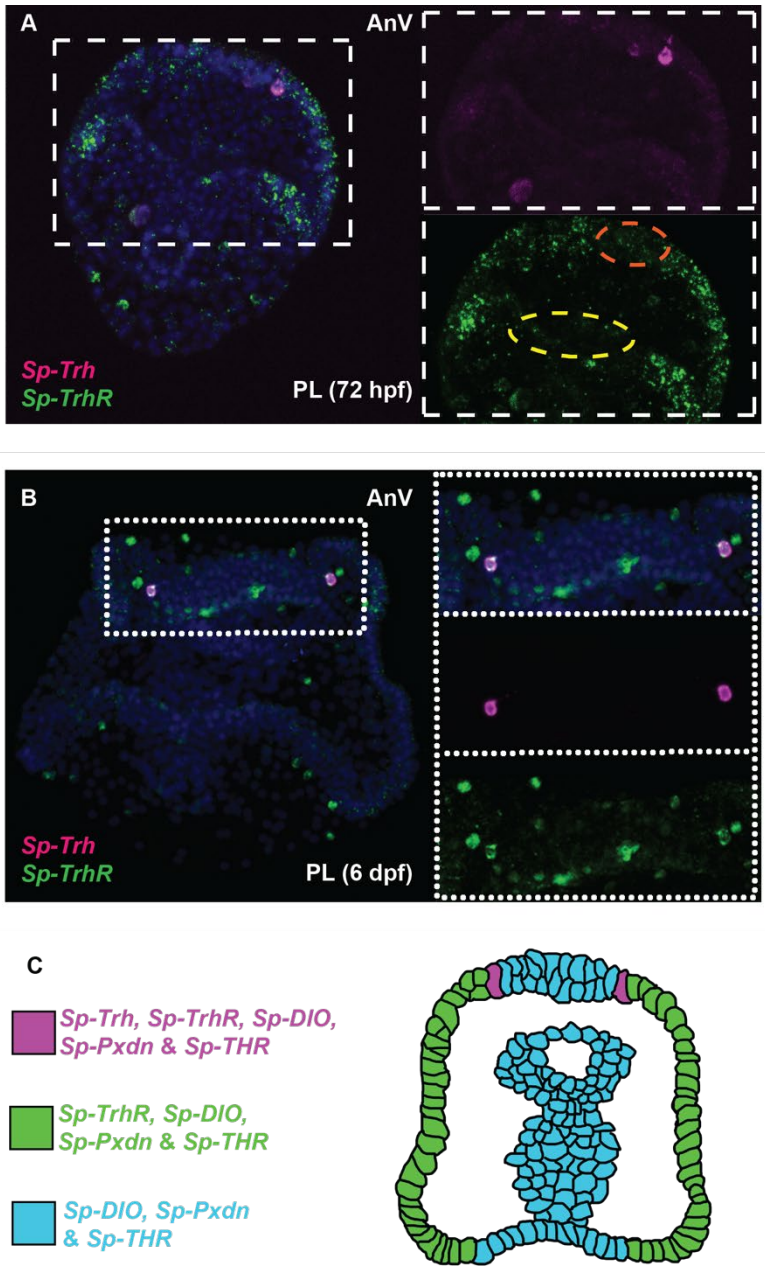

Figure 6.11 Combinatorial gene expression studies of *Sp-TRH* and *Sp-TRHR* reveal co-expression in two neuronal cells

(A-B) Merged and single channel confocal images of pluteus larvae labelled using double fluorescent ISH are shown. *Sp-TRH* (magenta) and *Sp-TRHR* (green) are co-expressed in two cells. (A) 72 hpf pluteus larvae. *Sp-TRHR* is expressed in the ciliary band except the region between post oral arms (yellow dotted circle) and signal is reduced from apical organ (orange dotted circle). (B) 6dpf late larvae. DAPI (blue) stain the nuclei. Top-right corner indicates the Anal View (AnV) orientation of the larvae. Bottom-right corner indicates the larval stage in hours/days post fertilisation. Dotted white boxes highlight the magnified region shown to right. C) Cartoon pluteus larvae (oral view) mapping the expression of TH signalling associated genes from Figure 6.10 and Figure 6.11A-B, showing that all genes are likely co-expressed in these two oral distal neurons.

6.6 Immunohistochemical localisation of Sp-TRH in *S. purpuratus* larvae

To complement the ISH expression analysis of TRH NP signalling genes, immunohistochemistry (IHC) was also performed with antibodies to Sp-TRH (gifted by the Arnone lab). The antibodies against Sp-TRH were generated by immunising rabbits with an antigen comprising the peptide CQYPG-NH_2 conjugated to the carrier protein KLH. IHC confirmed that Sp-TRH immunoreactivity is located in two neuronal cells on either side of the apical organ, consistent with the ISH analysis of *Sp-TRH* expression (Figure 6.12A-B;

Figure 3.8C; Figure 3.12H). IHC also revealed immunostaining in a few cells around the larval mouth (Figure 6.12A and C), but ISH analysis did not reveal *Sp-TRH* mRNA expression in this location (Figure 3.8C; Figure 3.12H).

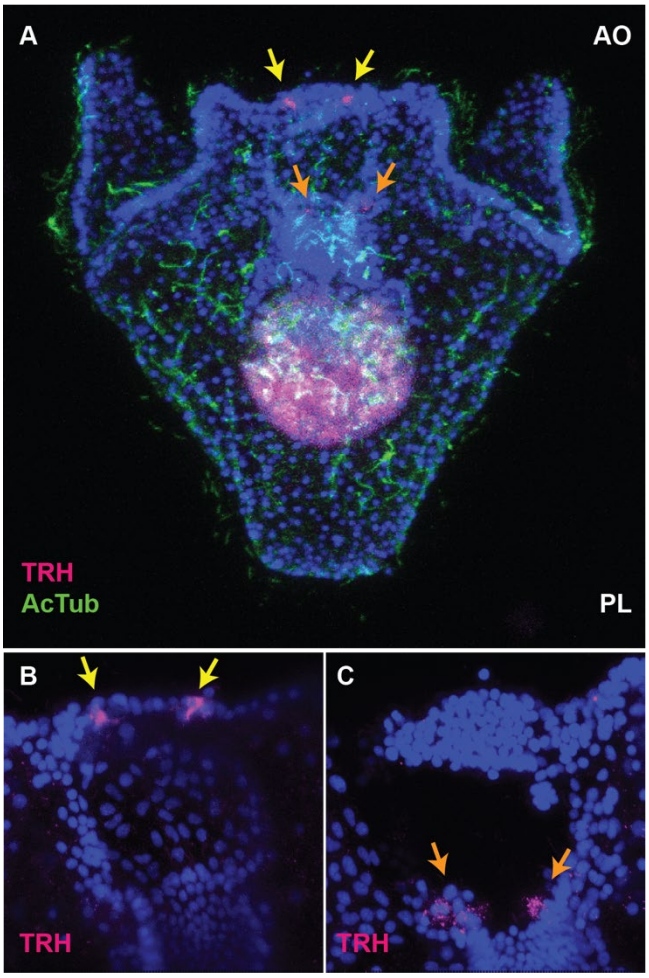

Figure 6.12 Immunohistochemistry reveals Sp-TRH immunoreactivity in two oral-distal neuronal cells and two-three cells around the mouth in *S. purpuratus* larvae

Maximum projection and z slices of confocal images of four-arm pluteus larvae labelled with antibodies to Sp-TRH and acetylated tubulin (AcTub) and stained with DAPI (blue) as a marker for nuclei. (A) Maximum projection revealing immunostaining in two oral distal neuronal cells (yellow arrows) and two cells around the mouth (orange arrows). Top-right corner indicates the Apical Organ (AO) orientation of the larva. (B-C) The same larva, as shown in (A) but magnified images of the apical organ and mouth region in different z-slices. (B) High-magnification image of the two oral distal neuronal cells (yellow) labelled with anti-Sp-TRH. Z-slices 95-115 out of 164 total z-slices were used for this image. (C) High magnification image of two-three cells around the mouth (orange) labelled with anti-Sp-TRH. Z-slices 62-89 out of 164 total z-slices were used for this image. Abbreviated label PL refers to pluteus larva.

It is unusual for a protein to be detected in cells where the mRNA encoding that protein is not detected. There are two possible explanations for this scenario; a) the mRNA is transcribed in the mouth cells also, but at such low levels that it is not detectable by chromogenic ISH; or b) the mature Sp-TRH peptide is only produced in the OD neuronal cells and the immunostaining in the mouth cells is due to antibody cross-reactivity with another peptide or protein.

A simple test can be performed to determine if an antibody is binding to a particular peptide or protein. An enzyme-linked immunosorbent assay (ELISA) was performed to check the specificity of the Sp-TRH antibodies for the synthetic Sp-TRH peptide. Two TRH peptides were available, pQYPG-NH_2 and CQYPG-NH_2. The first synthetic peptide, is the same sequence as the most frequent predicted mature peptide derived from the Sp-TRH precursor protein. The second, is the peptide that was used for antibody production, with a C-terminal cysteine modification to enable coupling to a carrier protein. I tested the affinity of four different Sp-TRH antibody fractions at 1:400 dilution (in 5% goat serum/PBS) against the two synthetic Sp-TRH peptides at 1 µM. Different fractions were tested as the antibodies can vary in specificity. Immunoreactivity was detected with the modified TRH peptide, but not with the unmodified peptide (Figure 6.13A).

To check the specificity of the antibody fraction for detection of the modified TRH peptide (1 µM) and the peptide Sp-GnRH (1 µM), which shares C-terminal sequence similarity with Sp-TRH, they were incubated with different amounts of affinity purified anti-Sp-TRH (fraction final purification 9, FP9) ranging from 1:4,000,000 to

1:40 diluted in 5 % GS/PBS. A concentration-dependent signal was detected with the modified TRH peptide and some immunoreactivity was detected with the Sp-GnRH peptide, but only with the highest concentration of the anti-Sp-TRH tested (Figure 6.13B). Pre-immune serum was used as a negative control, and as expected no immunoreactivity with Sp-TRH peptide was detected (Figure 6.13B). To investigate if some anti-Sp-TRH antibody fractions were more specific than others, I tested the immunoreactivity of Sp-GnRH peptide with two different anti-Sp-TRH antibody fractions - FP9 and FP3. Sp-GnRH exhibited stronger immunoreactivity with the anti-Sp-TRH antibody fraction FP3 than the FP9 fraction with Sp-GnRH at a concentration of 1:400 dilution, suggesting that fraction 3 has less specific antibodies than fraction 9 (Figure 6.13C). Antibodies to the starfish (*A. rubens*) neuropeptide Ar-GnRH were tested with the Sp-GnRH peptide but no immunoreactivity was detected. A positive control was used where the binding of anti-Ar-Calcitonin (Ar-CT) (1:500 diluted in 5% GS/PBS) to Ar-CT peptide (1 µM) was observed, as reported previously (Cai *et al.,* 2018).

Collectively, these data indicate that the anti-Sp-TRH antibodies recognise the modified Sp-TRH peptide CQYPG-NH_2 when tested using ELISA. However, these antibodies also exhibit some cross-reactivity with SpGnRH peptide *in vitro,* suggesting this may also be the case *in vivo*.

However, analysis of the temporal expression of the *Sp-GnRH* gene using QPCR was barely detected in embryonic and larval stages (Figure 3.1), and therefore the immunostaining in mouth cells may be due to antibody cross-reactivity with another as yet unidentified peptide or protein.

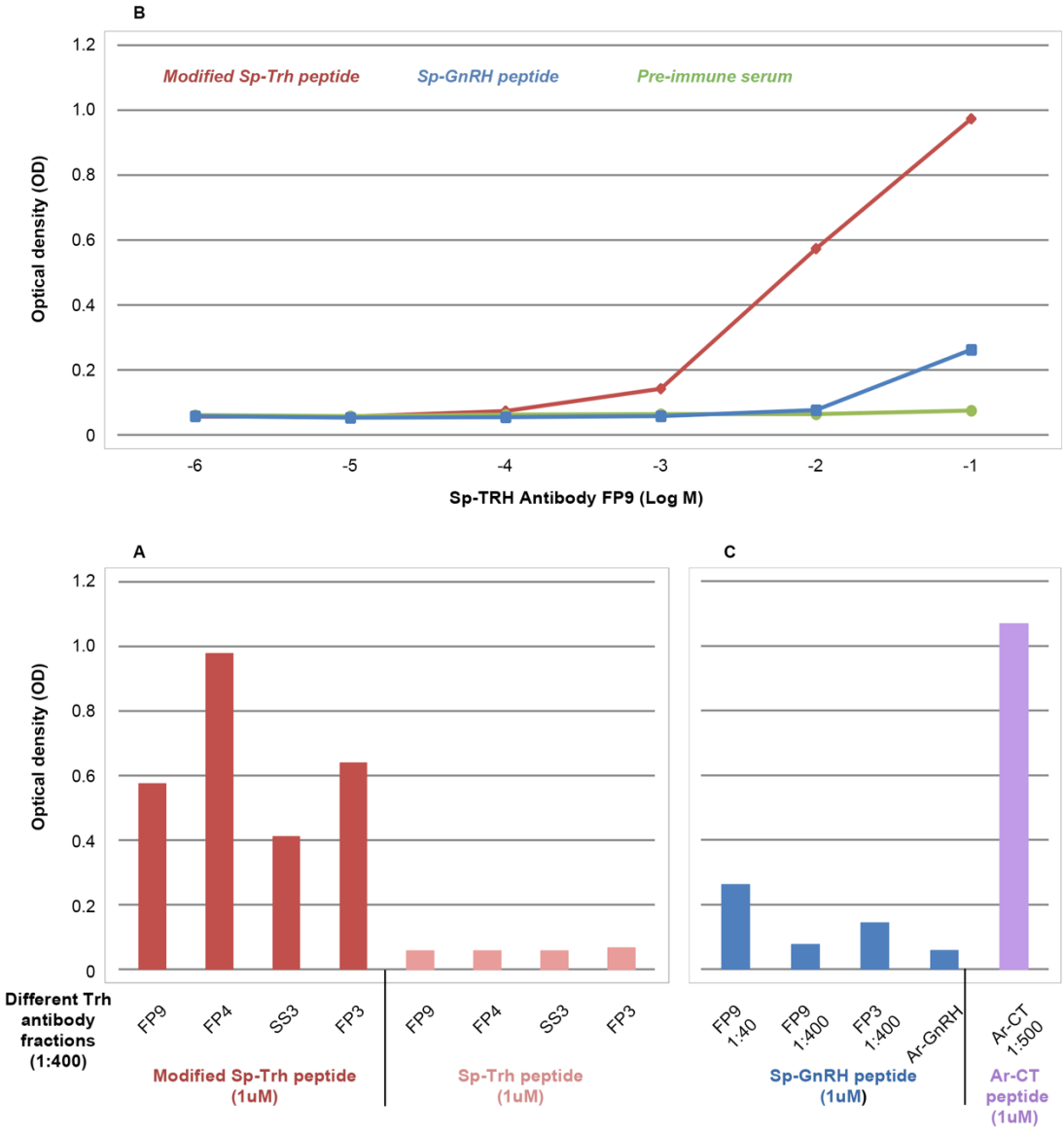

Figure 6.13 Characterisation of rabbit antibodies to a Sp-TRH peptide antigen using an enzyme-linked immunosorbent assay (ELISA)

A) Bar chart plotting the absorbance measurements (OD) for two synthetic Sp-TRH peptides (1 µM), a modified Sp-TRH peptide (red) and Sp-TRH peptide (pink) incubated with different fractions of anti-Sp-TRH antibodies (1:400 diluted in 5% goat serum/PBS) revealing that the modified Sp-TRH synthetic peptide is detected with all antibody fractions. However, the signal strength varies between antibody fractions and the strongest signal is detected with final purification (FP) 4. B) Modified Sp-TRH peptide (red) and Sp-GnRH peptide (blue) were tested against anti-Sp-TRH fraction FP9 at concentrations from 4 x 10^{-6} M to 4 x 10^{-1} M. Modified Sp-TRH peptide was also tested with pre-immune serum (green; negative control). Line graph reveals a concentration-dependent signal with both peptides, but with a stronger signal for the modified Sp-TRH peptide than the Sp-GnRH. No signal is observed with pre-immune serum (negative control). C) Bar chart comparing the immunoreactivity of Sp-GnRH peptide (blue) with different Sp-TRH antibody fractions, FP9 and FP3 and at two

dilutions, 1:400 and 1:40. FP3 exhibits stronger reactivity than FP9 with Sp-GnRH peptide (10^{-6} M) when tested at a dilution of 1:400. Sp-GnRH exhibits no immunoreactivity with anti-Ar-GnRH antibodies. A positive control was included where the known binding of Ar-Calcitonin (Ar-CT) antiserum (1:500) to Ar-CT peptide (10^{-6} M) was observed (Cai *et al.,* 2018). Data points are mean values determined from one experiment, performed in triplicate.

6.7 CRISPR/Cas9 knockouts and MO knockdowns of *Sp-TRH* and *Sp-TRHR* causes a short and/or abnormal skeleton in *S. purpuratus* pluteus larvae

The temporal and spatial analysis of genes associated with TH signalling, coupled with the effect of iodide FASW on growth provided a basis for the hypothesis that TH signalling may regulate skeleton growth in *S. purpuratus* larvae. To test this hypothesis, CRISPR/Cas9 and translational-blocking Morpholino Oligonucleotides (MO) were used to knockout or knockdown expression of *Sp-TRH* and *Sp-TRHR*. I designed sgRNA against *Sp-TRH* and ordered MO's against *Sp-TRH* and *Sp-TRHR* as described in methods sections 2.3.1 and 2.4.10, respectively. sgRNA targeting the coding sequence in exons 2 and 3 were picked, while translational-blocking MO's were designed, as is conventional, across the start codon.

Five sgRNA (total 40 ng/µl) targeting *Sp-TRH* combined with Cas9 mRNA (90 ng/ µl) were injected into fertilised eggs. Injected embryos had wild type-like development until pluteus larval stage (72 hpf) (Figure 6.14). However, at the pluteus stage approximately 50% of larvae appeared to have a shorter and/or abnormal skeleton (Figure 6.14A and Biv). The mutant larvae had phenotypes of varying degrees of severity, 20% had an abnormal skeleton, 25% had a short skeleton and 5% had a short and abnormal skeleton (Figure 6.14A). In comparison, 90% of the uninjected larvae had typical wild type phenotypes (Figure 6.14A and Bi). The specificity of the sgRNA against *Sp-TRH* was assessed by injecting sgRNA against the pigment-producing gene, *Sp-PKS1* (Oulhen and Wessel, 2016). As already shown in Chapter 5, sgRNA against *Sp-PKS1* produces albino larvae, revealing an easy visual detection method of CRISPR/Cas9 efficiency (Figure 5.3). sgRNA targeting *Sp-PKS1* combined with Cas9 mRNA gave approximately 90% albino larvae that were otherwise wild type, with approximately 5% of larvae having an abnormal/short skeleton and 5% having a pigmented wild type phenotype (Figure 6.14A and Bii).

To further assess the specificity and efficiency of the CRISPR/Cas9 system in the sea urchin, I compared the CRISPR/Cas9 results to MO knockdowns of *Sp-TRH* and *Sp-TRHR.* Interestingly, larvae injected with 200 µM *Sp-TRH* MO or 200µM *Sp-TRHR* MO gave the same short and/or abnormal skeleton phenotype as the CRISPR/Cas9 *Sp-*

TRH knockouts (compare Figure 6.14 Biv with Bv and Bvi). *Sp-TRH* MO had a similar efficiency to *Sp-TRH* CRISPR/Cas9 with 40% of MO larvae having an abnormal and/or short skeleton (Figure 6.14A). *Sp-TRHR* MO had the highest efficiency with 60% of larvae having a skeletal phenotype (Figure 6.14A). Control MOs were also injected into larvae as a negative control and as expected 85% were wild-type, similar to uninjected larvae (Figure 6.14A, Bi and Bii).

To summarise, CRISPR/Cas9 knockouts and MO knockdowns of *Sp-TRH* and *Sp-TRHR* give the same abnormal and/or short skeletal phenotype in pluteus larvae, providing strong evidence that this NP ligand-receptor pair have a role in regulation of skeleton growth in sea urchin larvae.

If TRH NP signalling regulates the production of thyroid hormones in sea urchins, we can also infer a role of TH in sea urchin larval skeleton growth. The evolutionary implications of this would suggest a conserved role of TRH regulating TH signalling to affect growth across deuterostomes. In addition, TRH NP signalling has been shown to have a role in regulation of growth in protostomian invertebrate, the nematode *C. elegans* (Sinay *et al.,* 2017b), suggesting that TRH-type NP signalling involvement in the regulation of growth may have been present in Urbilateria.

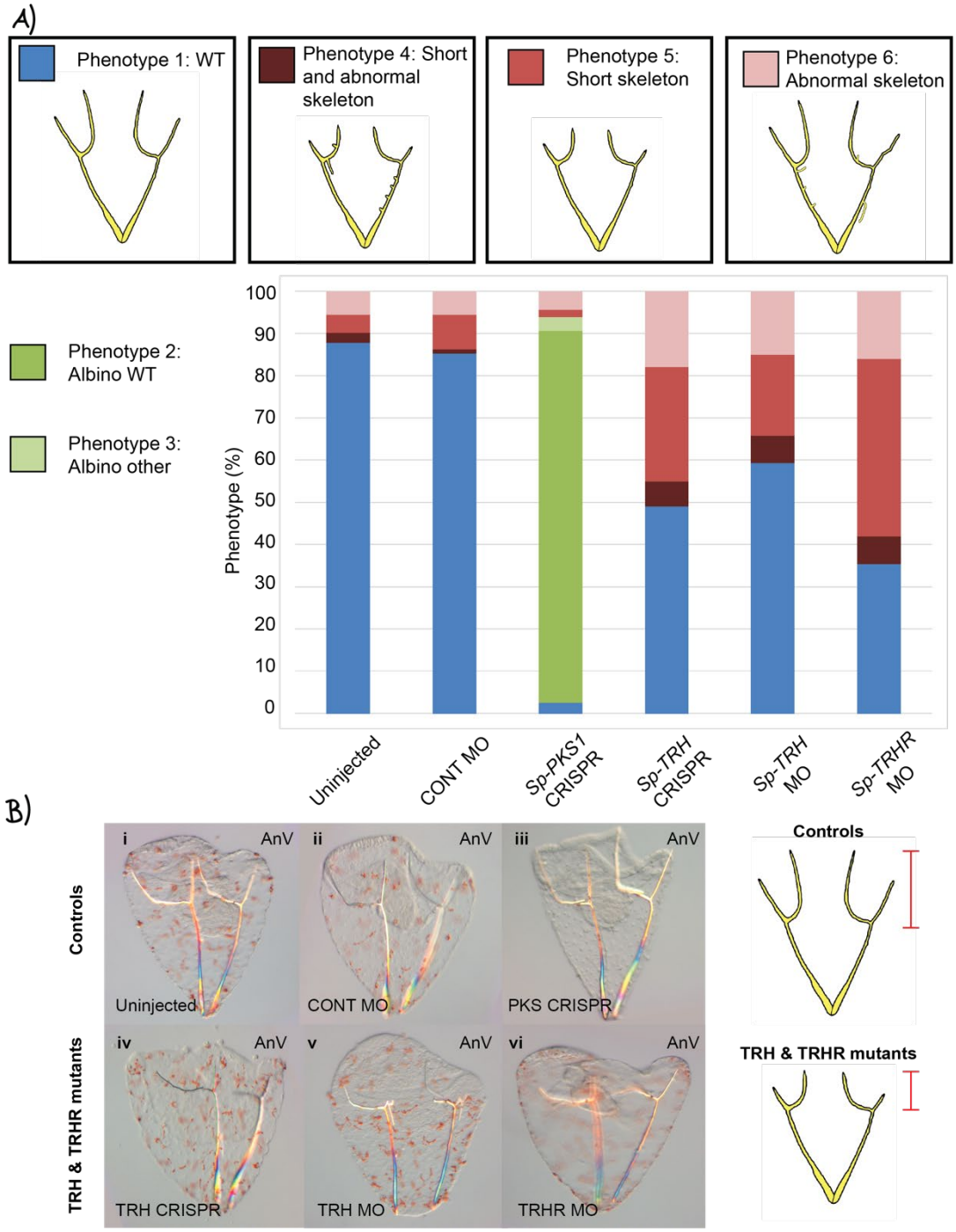

Figure 6.14 Knockdown and knockout of *Sp-TRH* and *Sp-TRHR* gives a short and/or abnormal skeleton in the pluteus larva of *S. purpuratus*

A) Bar graph showing the percentage of different phenotypes with different treatments: uninjected, CONT MO, *Sp-PKS1* CRISPR/Cas9, *Sp-TRH* CRISPR/Cas9, *Sp-TRH* MO and *Sp-TRHR* MO. There are six phenotypes: Wild type (blue), albino wild type (green), albino other (light green), short and abnormal skeleton (dark red), short skeleton (red) and abnormal skeleton (light red). Larvae were injected with *Sp-PKS1* CRISPR/Cas9 as a positive control. Larvae were injected with a control MO as a

negative control. Approximately 90% of uninjected, CONT MO and *Sp-PKS1* CRISPR larvae are wild type for the skeleton development. Short and/or abnormal larvae are seen in 50%, 40% and 60% of *Sp-TRH* CRISPR, *Sp-TRH* MO and *Sp-TRHR* MO injected larvae, respectively. Ba-f) Live images of pluteus larvae with the six treatments different treatments. Data were collected across 3-4 independent replicates. Top-right corner indicates the anal view (AnV) orientation of the larvae. The total number of individuals counted per treatment are as follows: 257 (uninjected), 110 (CONT MO), 118 (*Sp-PKS1* CRISPR), 118 (*Sp-TRH* CRISPR), 229 (*Sp-TRH* MO) and 169 (*Sp-TRHR* MO).

6.8 Inhibiting VEGF and FGF signalling pathways results in a short skeleton in the *S. purpuratus* pluteus larvae

Functional characterisation of *Sp-TRH* NP gene and its receptor *Sp-TRHR* has revealed that this NP pair are important for larval skeleton growth. But how does TRH NP signalling in the ciliary band transmit signalling information to the skeletogenic mesodermal cells (SM) to affect skeleton growth. To address this issue, known expression patterns for canonical signalling pathways, including vascular endothelial growth factor (VEGF) and fibroblast growth factor (FGF) signalling were examined. VEGF signalling in the larval sea urchin of *Paracentrous lividus* has ligand expression in the ciliary band at the arm tips, in a similar location to *Sp-TRH* positive oral-distal neuronal cells. Furthermore and interestingly, the VEGF receptor is expressed in SM cells at the oral-distal and post-oral arm tips (Duloquin *et al.,* 2007). In addition, FGF signalling in *P. lividus* has *Pl-FGFA* (*Pl-FGF9/16/20*) ligand expression in the ciliary band and SM at arm tips, with its receptor *Pl-FGFR2* expressed in SM cells at the arm tips. Unpublished data from the Oliveri laboratory (Lerner, 2013) has shown that *Sp-FGF9/16/20* and a novel ligand *Sp-FGF8/17/18* is expressed in the ciliary band and tip SM cells in *S. purpuratus* larvae. Taken together, the location of FGF and VEGF signalling in sea urchin larval species make them good candidates to connect ciliary band TRH NP signalling to skeletal cells. To investigate if VEGF and FGF signalling affects late developmental skeleton extension and thus could be the connecting signals between the ciliary band and SM cells, I added SU5402 (an inhibitor of FGF signalling) and Axitibin (an inhibitor of VEGF signalling) at a late gastrula stage (48 hpf) and imaged at the pluteus larval stage (72 hpf). Inhibitors were added at 48 hpf when TRH signalling starts to be expressed, but not before to avoid disrupting earlier developmental processes. Live imaging in the pluteus larvae revealed that both SU5402 and Axitibin inhibitor treated embryos had shorter skeletons than FASW and dimethyl sulfoxide (DMSO)-treated controls (Figure 6.15), remarkably similar to the phenotype of larvae with impaired TRH signalling. This suggests that VEGF and FGF signalling could be modulated by TRH NP signalling to regulate pluteus larval skeletal arm growth.

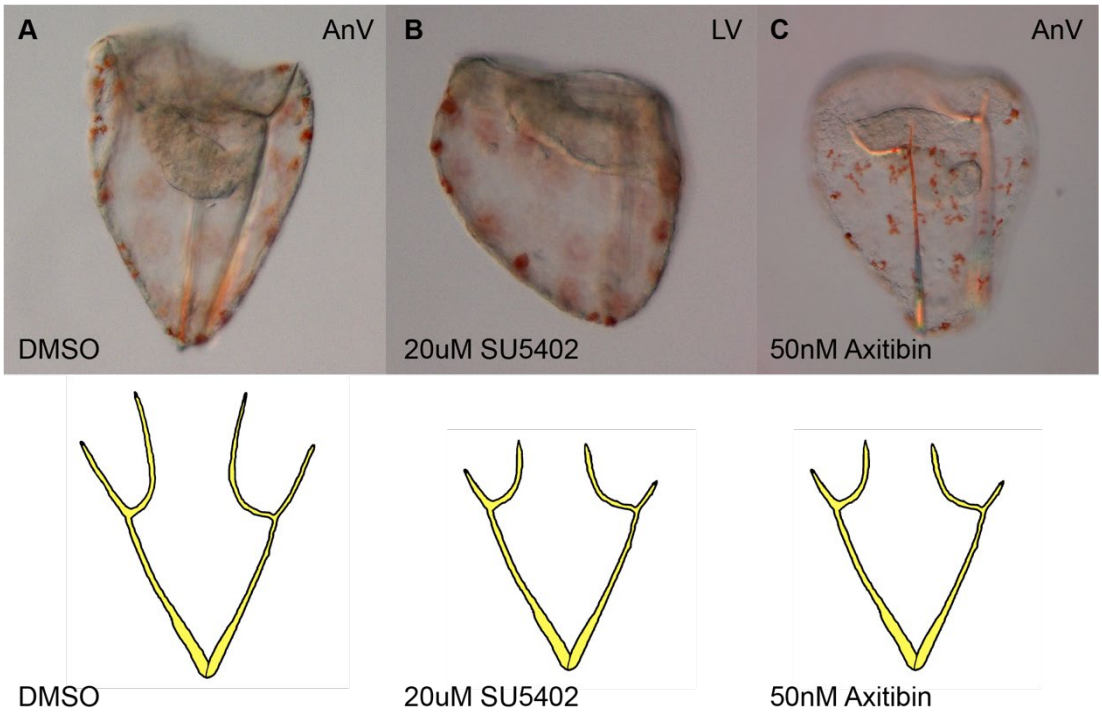

Figure 6.15 Inhibition of VEGF and FGF signalling at gastrula stage causes a short arm phenotype in the pluteus stage

A-C) Live images of pluteus larvae stage in different conditions: A) DMSO (negative control). Top-right corner indicates the anal view (AnV) or lateral view (LV) orientation of the larvae. B) 20µM SU5402 (an inhibitor of FGF signalling) and C) 50nM Axitibin (an inhibitor of VEGF signalling). Cartoons of the pluteus larval stage skeleton phenotypes for different conditions are shown below, revealing the shorter skeletons with both inhibitor treatments.

6.9 Identifying genes downstream of TRH-type signalling in *S. purpuratus* larvae

To identify genes downstream of TRH NP signalling I performed quantitative real-time PCR (QPCR) and chromogenic ISH on *Sp-TRH* CRISPR/Cas9, *Sp-TRH* MO and *Sp-TRHR* MO injected pluteus larvae. QPCR reveals quantitative changes in gene expression in whole mutated larvae, in comparison to controls (uninjected, control MO and Sp-PKS1 CRISPR/Cas9), while ISH reveals spatial changes in gene expression in the mutated larvae. I first undertook QPCR analysis on a large set of putative downstream genes, with the intention of picking only genes that showed an up- or down-regulation by QPCR for a detailed ISH spatial analysis.

I picked putative downstream genes of TRH NP signalling, including FGF and VEGF ligands and receptors (*Sp-FGF8*, *Sp-FGF9*, *Sp-FGFR1*, *Sp-FGFR2*, *Sp-VEGF (Sp-VEGF3)* and *Sp-VEGFR*), and other TH signalling genes (*Sp-TRH*, *Sp-TRHR*, *Sp-THR*, *Sp-TSHR*, *Sp-Pxdn* and *Sp-DIO*) that are known to be downstream of TRH NP signalling in vertebrates (Bassett and Williams, 2016b). In addition, I picked transcription factors (*Sp-Pax258*, *Sp-FoxG*, *Sp-Hnf6, Sp-pea3* and *Sp-FoxJ1*) and signalling molecules (*Sp-sprouty*) that were known to be expressed in the ciliary band (Otim *et al.,* 2004; Röttinger *et al.,* 2007; Tu *et al.,* 2006) and skeletogenic genes (*Sp-alx1, Sp-net7, Sp-p58, Sp-can1* and *Sp-sm30*) (Sun and Ettensohn, 2014). Changes in gene expression were quantified by normalising to an internal control and then calculating the fold changes between injected and uninjected larvae (see methods section 2.5.4 for details). *Sp-TRH* and *Sp-TRHR* genes were disregarded from further analysis because higher amplification was detected in the water negative control. A fold change of ± 1.6, a 3-fold change is considered significant.

No gene analysed showed a consistent fold change in gene expression (Figure 6.16). However, there seemed to be several issues with the data. Firstly, there was often no consistent change in fold expression between independent replicates (for example see *Sp-Net7* on Figure 6.16, compare batch A and C with batch B). Secondly, there was often a significant fold change (greater than ± 1.6) in CONT MO or *Sp-PKS1* CRISPR/Cas9 negative controls (for example see *Sp-Pax258* on Figure 6.16). Thirdly, the CONT MO often has a greater fold change than the *Sp-TRH* or *Sp-TRHR* MO

morphants (for example see *Sp-FGF8* batch B on Figure 6.16). Fourthly, the fold change in a *Sp-TRH*/*Sp-TRHR* treatment was often not significant (for example see *Sp-foxg* on Figure 6.16). In addition, nine genes only had one independent replicate and so I couldn't make comparisons between independent experiments (see those genes with an asterisk on Figure 6.16).

Taken together, the inconsistent changes in gene expression, coupled with an often greater change in expression seen in the negative controls suggests that QPCR is not a good technique for detecting gene expression changes in a few cells. Importantly, most of our putative downstream genes have a wider expression domain than our few *Sp-TRH* positive cells or SM cells of interest. I am unlikely to see a significant fold change in gene expression if we are expecting a reduction or loss in gene expression in only a few cells, and not the many total cells where a gene is expressed.

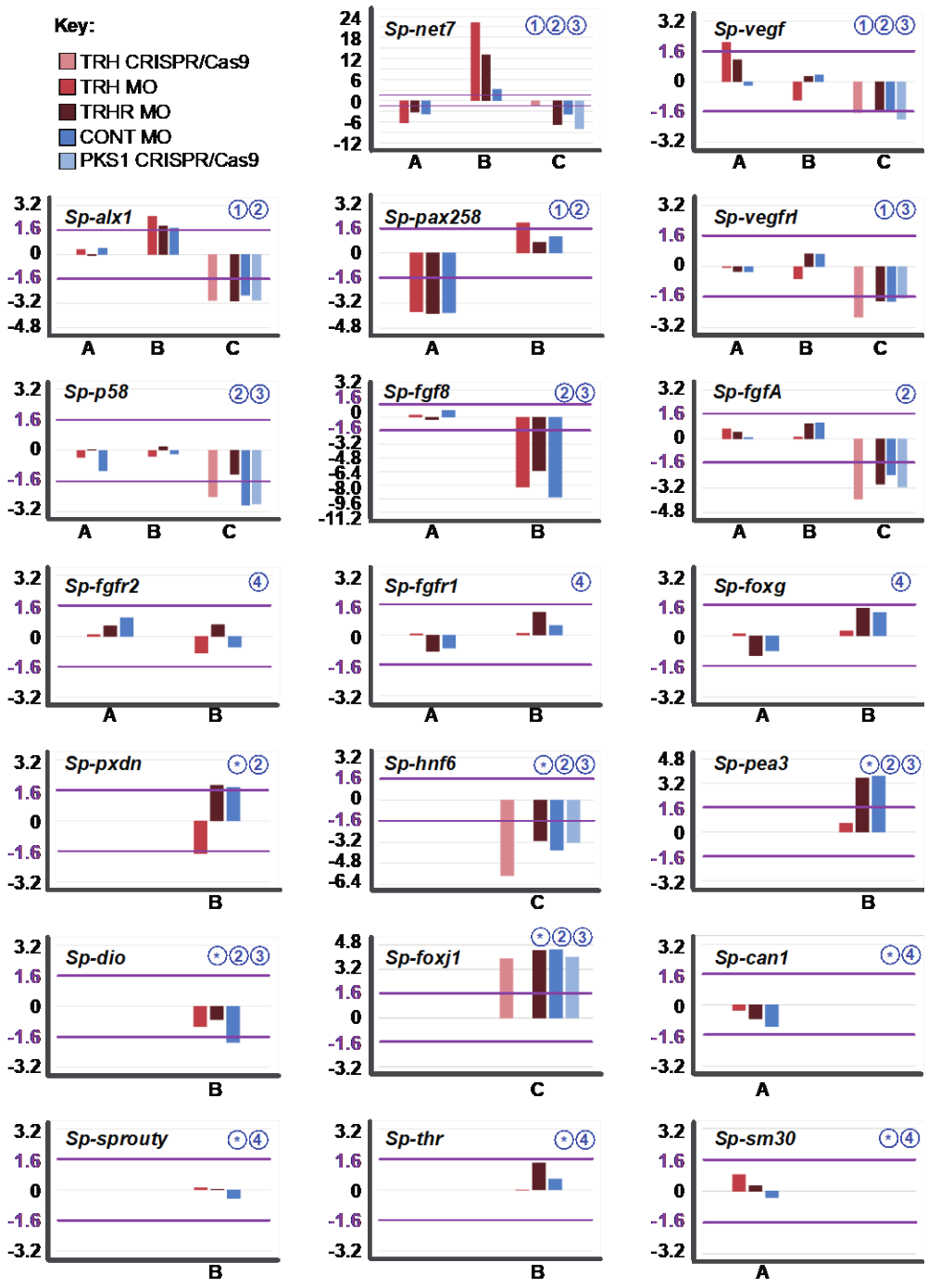

Figure 6.16 QPCR analysis of putative downstream genes in *Sp-TRH* and *Sp-TRHR* mutant larvae does not show consistent changes in changes expression

A bar graph is shown for each gene analysed by QPCR. The y-axes shows fold change and ± 1.6 significant fold change is marked by purple lines. The x-axes plots different treatments across different independent replicates (A, B and/or C). The different treatments are as follows: *Sp-TRH* CRISPR/Cas9 (light pink), *Sp-TRH* MO (pink), *Sp-TRHR* MO (dark pink), CONT MO (blue) and *Sp-PKS1* CRISPR/Cas9 (light blue). A number and/or asterisk is included in the top right corner of each graph. These illustrate the following inconsistencies between a particular gene; 1) There was no consistent change in fold expression between independent replicates; 2) There was

a significant fold change in CONT MO or CRISPR Sp-PKS1 negative controls; 3) The CONT MO has a greater fold change than the *Sp-TRH* or *Sp-TRHR* MO morphant and; 4) The fold change in a Sp-TRH/Sp-TRHR MO morphants was not significant.

To better identify downstream genes of TRH NP signalling I performed chromogenic ISH on MO *Sp-TRH* and *Sp-TRHR* injected larvae where I should be able to visualize small spatial changes in gene expression. Chromogenic ISH of *Sp-VEGF* and *Sp-FGF9/16/20* revealed a reduction in gene expression in the ciliary band and SM cells at the arm tips in the *Sp-TRH* MO and *Sp-TRHR* MO injected larvae (Figure 6.17). Thus, TRH NP signalling is likely upstream of VEGF and FGF signalling.

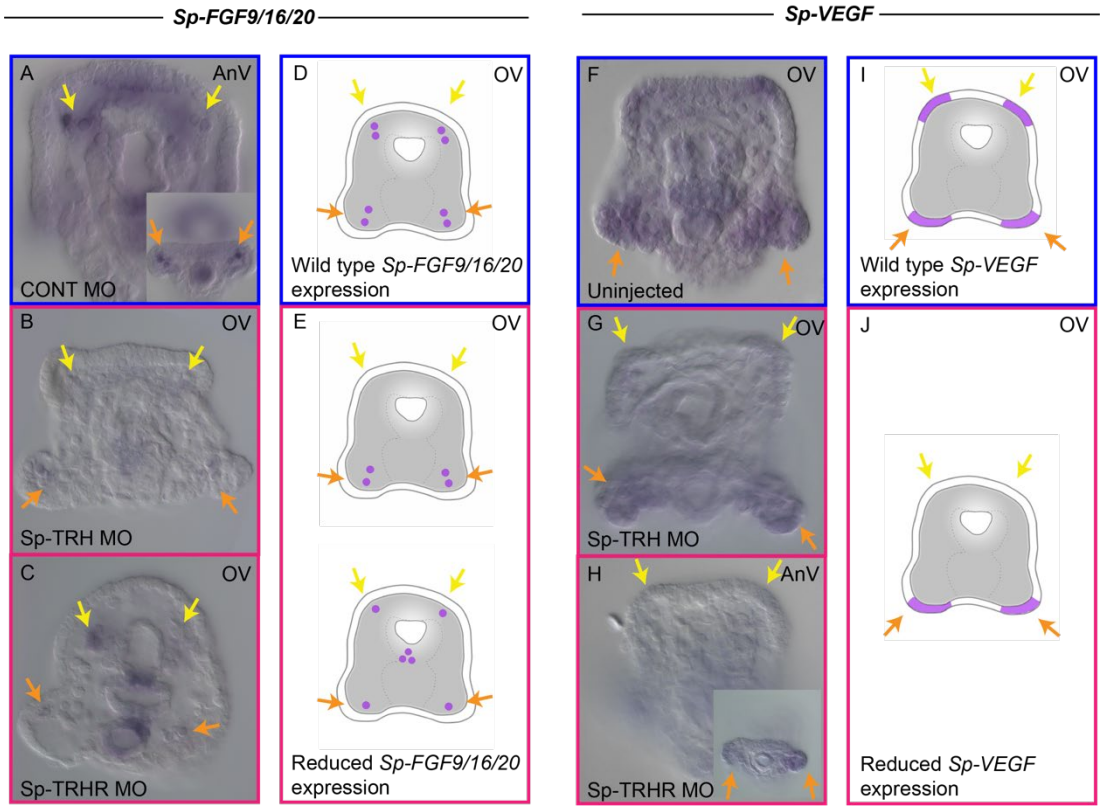

Figure 6.17 Reduction of *Sp-FGF9/16/20* and *Sp-VEGF expression* in *Sp-TRH* and *Sp-TRHR* MO morphants

Spatial expression analysis of *Sp-FGF9/16/20* (A-C) and *Sp-VEGF* (F-H) is revealed by chromogenic ISH. Yellow arrows point to oral distal (OD) ciliary band or SM cells and orange arrows point to post oral (PO) ciliary band or SM cells. (A) CONT MO larvae have expression of *Sp-FGF9/16/20* in OD and PO SM cells in 17/18 larvae. (B) *Sp-TRH* MO larvae have a loss of Sp-*FGF9/16/20* in OD SM cells and a reduction in PO SM cells in 3/7 larvae. (C) *Sp-TRHR* MO larvae have a reduction in *Sp-FGF9/16/20* in both the OD and PO SM cells in 14/23 larvae. (F) Uninjected larvae have *Sp-VEGF* expression in ciliary band cells of all four arm tips in 11/15 larvae. (G-H) *Sp-TRH* and *Sp-TRHR* MO

larvae has a loss of *Sp-VEGF* in ciliary band cells in OD arms in 3/6 and 13/18 larvae, respectively. Cartoons of *Sp-FGF9/16/20* and *Sp-VEGF* gene expression change in (D and I) control larvae and (E and J) MO injected larvae. For each probe, different samples were stained for the same amount of time. Individual larvae were counted across 1-2 independent replicates. Top-right corner indicates the orientation of the larva, oral view (OV) or anal view (AnV).

I next looked at the expression of a spicule matrix protein *Sp-sm30* in larvae with perturbed TRH, FGF or VEGF signalling. *Sp-Sm30* is a gene which is involved in depositing the calcium carbonate skeleton. Chromogenic ISH in control larvae revealed wild type *Sp-sm30* probe staining in SM cells at the tips of both oral distal and post oral skeletal arms (Figure 6.18 A, B, D, G and J) (Sun and Ettensohn, 2014), while a reduction in *Sp-sm30* staining was seen in oral distal and/or post oral SM cells of all injected and inhibitor-treated larvae (Figure 6.18 C, E-F, H-I and K).

Finally, I investigated if VEGF and/or FGF signalling can regulate TRH signalling by analysing the expression of *Sp-TRH* in SU5402- and Axitibin- treated larvae. Chromogenic ISH revealed the usual variable *Sp-TRH* expression in 0, 1 or 2 oral distal neurons in the uninjected and DMSO controls (Figure 6.19; Table 8.8). Two concentrations of SU5402 were tested, at the 10 µM lower concentration there was hardly any difference from the control larvae, but at the 20 µM concentration 90% of larvae had no *Sp-TRH* probe detection (approximately 20% more than DMSO larvae), suggesting that FGF signalling may positively regulate *Sp-TRH*. In addition, there was a 25% increase in the number of larvae that had *Sp-TRH* staining on both oral distal arms when treated with 50nM Axitibin, indicating that VEGF signalling may negatively regulate *Sp-TRH* expression.

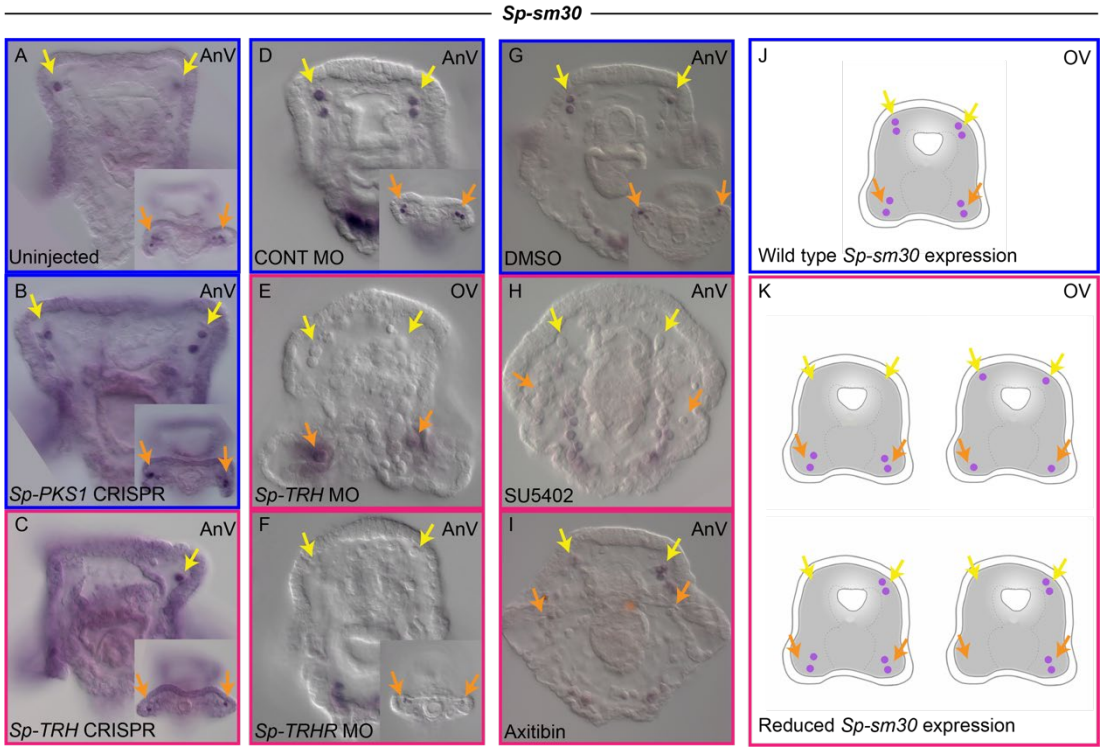

Figure 6.18 Reduction of *Sp-sm30* in CRISPR/Cas9 and MO injected and inhibitor-treated larvae.

Spatial expression analysis of *Sp-sm30* as revealed by chromogenic ISH. Yellow arrows point to oral distal SM cells and orange arrows point to post oral SM cells. Control larvae (A, D, G) had wild type *Sp-Sm30* expression of (typically 2 SM cells) in each oral distal and post oral arm in 7/11, 3/11 and 20/22 larvae, respectively. (C) Sp-TRH CRISPR/Cas9 injected larvae have a reduction of *Sp-Sm30* in oral distal and post oral SM cells in 10/33 larvae. (E-F) MO injected larvae have a loss of *Sp-Sm30* expression in oral distal SM cells and a reduction in post oral SM cells in (*Sp-TRH* MO) 1/7 and (*Sp-TRHR* MO) 17/18 larvae. (H) SU5403 inhibitor-treated larvae have a complete loss of *Sp-Sm30* expression in SM cells at all four arm tips in 11/26 larvae. (I) Axitibin inhibitor-treated larvae have a reduced *Sp-Sm30* expression in post oral, and to a lesser extent oral distal SM cells in 13/32 larvae. (J and K) Cartoons of *Sp-sm30* gene expression in SM cells in (J) control larvae and (K) *Sp-TRH* or *Sp-TRHR* perturbed larvae or inhibitor-treated larvae. Individual larvae were counted across one experiment. Top-right corner indicates the orientation of the larva, oral view (OV) or anal view (AnV).

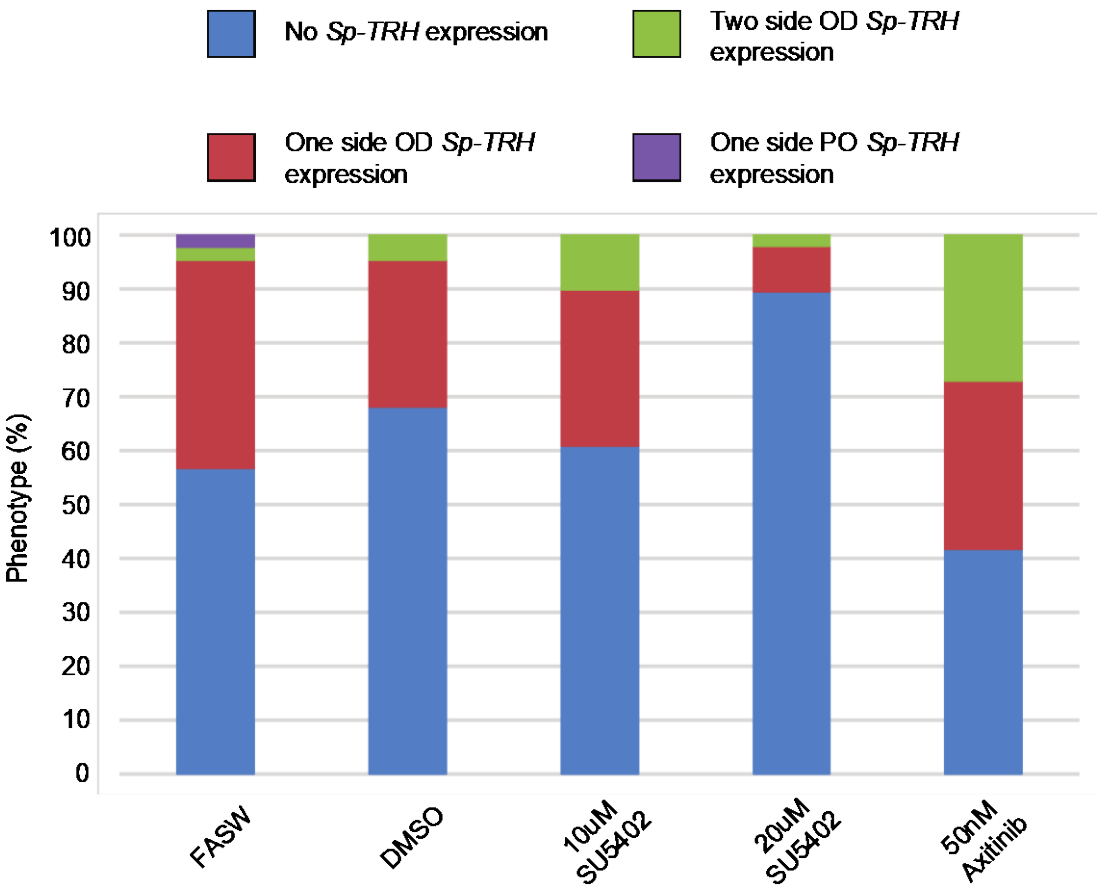

Figure 6.19 *Sp-TRH* is regulated by VEGF and FGF signalling

A bar graph is shown for the percent changes in *Sp-TRH* expression in five different treatments: FASW, DMSO, 10 µM SU5402, 20 µM SU5402 and 50nM Axitibin. Larvae cultured in FASW or DMSO (control conditions) mostly have *Sp-TRH* expression in one side (red) or have no *Sp-TRH* expression (blue) as previously shown in chapter 3. Only a small proportion of control larvae have *Sp-TRH* expression on two OD arms (green) or on one PO arm (purple). Larvae cultured in 10 µM SU5402 (FGF inhibitor) in DMSO have Sp-TRH expression in a similar proportion to control larvae. Interestingly, a larger proportion of larvae cultured in 20 µM SU5402 have no *Sp-TRH* expression (blue) and a larger proportion of larvae cultured with 50nM Axitibin (VEGF inhibitor) have more *Sp-TRH* expression on two OD arms (green). Data are from one experiment and the total number of individuals counted range from 44 to 96 larvae per treatment.

6.10 CRISPR/Cas9 knockouts of another neuropeptide, *Sp-FSALMFamide* causes a long skeleton in *S. purpuratus* pluteus larvae

Another neuropeptide, *Sp-FSALMFamide* (*Sp-FSALMFa*) is co-expressed with *Sp-TRH* in the OD neuronal cells and is also expressed in neuronal cells on the PO larval arms (Figure 3.12J; Figure 3.13B). To identify the function of *Sp-FSALMFa*, CRISPR/Cas9 was used to knockout the expression of the gene.

Four sgRNA (40 ng/µL) targeting *Sp-FSALMFa* combined with Cas9 mRNA (90 ng/µL) were injected into fertilised eggs. Injected embryos had wild type-like development until the pluteus larval stage (72 hpf) when larvae had longer larval arms (Figure 6.20A). The skeleton length was measured in injected and control uninjected larvae. Injected larvae had a longer post oral (a 97% increase) and oral distal (a 49% increase) arm tips when compared to uninjected larvae. No difference was observed in the length of the body rod or oral transverse skeletal parts between the two groups (Figure 6.20A). Intriguing, the phenotype observed in *Sp-FSALMFa* CRISPR/Cas9 injected larvae is opposite to the phenotype observed in larvae with a perturbed TRH signalling system.

To identify if there were any changes in *Sp-TRH* expression, chromogenic ISH was performed on *Sp-FSALMFa* CRISPR/Cas9 injected larvae. The *Sp-TRH* probe was detected as usual in the two OD neuronal cells in injected larvae and control uninjected larvae. Interestingly, in injected larvae the *Sp-TRH* probe was also detected in cells near the post oral arms (Figure 6.20B), in a similar location to *Sp-TRHR* and *Sp-FSALMFa* expression. This preliminary data (from one independent replicate) suggests that another neuropeptide, *Sp-FSALMFa* could be involved in regulating skeleton growth and may regulate TRH signalling.

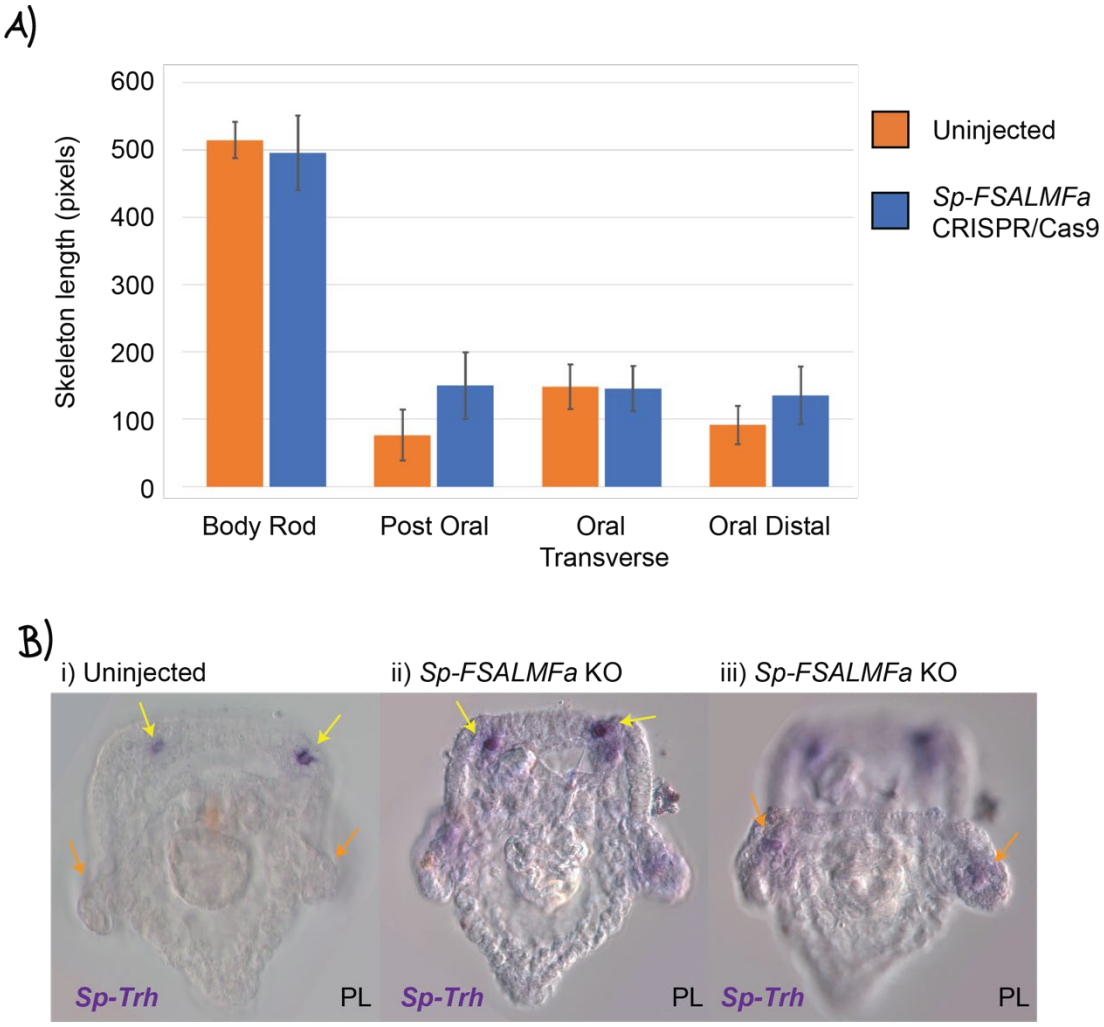

Figure 6.20 Knockout of *Sp-FSALMFa* accelerates skeleton growth

A) Bar graph plotting the length of skeleton (pixels) for the different skeletal parts in uninjected and *Sp-FSALMFa* CRISPR/Cas9 pluteus larvae. *Sp-FSALMFa* CRISPR/Cas9 injected larvae have longer post oral skeleton (97% increase) and oral distal skeleton (49% increase) and hardly any change in the body rod (4% decrease) and oral transverse (2% decrease). Error bars are shown as standard deviation. B) Chromogenic ISH of *Sp-TRH* expression. Bi) Wild-type expression in two oral distal neurons in an uninjected larva. Bii-iii) The same pluteus larva from two focal planes. *Sp-TRH* expression remains in the oral distal neurons and has expanded to the post oral arms in an *Sp-FSALMFa* CRISPR/Cas9 injected larva. Abbreviated label PL refers the pluteus larva and AO refers to the apical organ orientation of the larva. Experiment performed by Anne Ritoux.

6.11 Discussion

TRH-type signalling is found in all major clades of Bilateria except for Urochordata. Here I report the first functional study of TRH signalling in a marine invertebrate larvae. I have demonstrated experimentally the first TRH-type ligand-receptor pair in an invertebrate deuterostome and I have shown that this ligand-receptor pair are co-expressed in two oral distal (OD) neuronal cells. Furthermore, and most interestingly, I have shown that TRH neuropeptide signalling regulates skeleton growth in sea urchin larvae.

To investigate the function of TRH signalling in sea urchin larvae, I took a complementary approach using two perturbations techniques, CRISPR/Cas9 knockouts and MO knockdowns. Importantly, both approaches did specifically perturb TRH signalling to give sea urchin larvae with the same short skeletal arms and abnormal skeletons. More specifically, I discovered that TRH regulates the length of both sets of larval arms, the OD arms located near the Sp-TRH neuronal cells and intriguing the PO arms located further away from the Sp-TRH neuronal cells. Whilst, unsurprising given the expression of Sp-TRHR in ciliary band cells at the tips of all the larval arms (Figure 6.11; Figure 3.8 D-E), it is of interest in terms of understanding the molecular and cellular biology of TRH signalling. Sp-TRH seems to act on Sp-TRHR positive cells as an autocrine (on same cell) and paracrine hormone (on local cells) on the OD arms and as an endocrine hormone (on more distant cells) on the PO arms. This is consistent with known mammalian TRH signalling, where TRH acts on both local and distant cell- and tissue- types (Fröhlich and Wahl, 2019; Gershengorn and Osman, 1996; Miguel et al., 2005). Furthermore, no morphological changes were observed in perturbed larvae before the pluteus larval stage. This is consistent with both the peptide precursor and receptor being first expressed at the late gastrula stage, just before skeletal arm elongation. At earlier embryonic stages, only the *Sp-TRH* peptide precursor is expressed, and this is unlikely to be functional without the presence of a receptor. Moreover, it is unknown if the *Sp-TRH* gene is translated and processed into a functional mature peptide at early embryonic stages (here I have shown that the a functional Sp-TRH mature peptide is present at the pluteus larval

stage). In the future, an immunohistochemistry should be performed using the specific Sp-TRH antibody on the early embryonic stages.

Downstream of TRH signalling, I have shown the presence of VEGF and FGF signalling in the *S. purpuratus* larva. Previous studies in different sea urchin species has shown that VEGF3 and FGFA have roles in regulating larval skeleton development and growth. More specifically, several studies have shown that local ectodermal signals, FGFA and VEGF3, have a conserved role in regulating both PMC patterning in the embryo and biomineralization in the late gastrula and pluteus larvae in different sea urchin species (Adomako-Ankomah and Ettensohn, 2013; Duloquin et al., 2007; Röttinger et al., 2007). Interestingly, I have observed Sp-TRH and Sp-TRHR morphants with shortened skeletal arm rods and no obvious changes in the clustering or number of skeletogenic mesodermal (SM) cells. This phenotype is strikingly similar to the phenotype observed when FGF and VEGF signalling were inhibited later in development, after PMC migration, resulting in shortened skeletal arm rods and reduced expression of the biomineralization gene *Sp-sm30*. My findings show for the first time, that a neuropeptide signalling system, TRH, acts as a local ectodermal cue to regulate skeletogenesis. Furthermore, I show that TRH signalling, in the ectoderm, mediates FGF and VEGF effects on biomineralization (Figure 6.21), but not on earlier PMC patterning. Moreover, previous studies have shown that VEGF3, in the ectoderm regulates FGFA in SM cells in a different sea urchin species (Adomako-Ankomah and Ettensohn, 2013). Therefore, it would be worthwhile to investigate if TRH signalling regulates *Sp-VEGF3*, which in turn regulates *Sp-FGFA*, or whether TRH signalling directly regulates FGF and VEGF signalling. Additional analyses on the role of TRH signalling in other sea urchin species will be necessary to see if TRH acts similarly as an upstream regulator of FGF and VEGF across echinoids. I also show that FGF and VEGF may act upstream, as well as downstream of TRH signalling, however this needs further investigation as data comes from only one experimental repeat.

What are the intracellular signalling pathways that mediate TRH signalling, is another essential question. Neuropeptides exert their functions by interacting with specific receptors, typically of the G-protein coupled receptor (GPCR) class. These receptors on the cell surface couple to a range of intracellular G proteins, which then activate

different intracellular signalling pathways and regulates gene expression. Mammalian TRHRs have been shown to specifically couple to the G protein family, Gαq/Gα11, which typically activates the PLC-PKC pathway (Gershengorn and Osman, 1996; McCudden et al., 2005). In addition, studies looking at TRH regulation in rat cells have shown that TRHR activation can also stimulate the MAPK pathway (Gershengorn and Osman, 1996; Ohmichi et al., 1994; Sun et al., 2000). However, outside of mammals, it is unknown which G proteins couple to TRHR and which intracellular signalling pathways are stimulated. Interestingly, MAPK (ERK1/2) pathway studies in sea urchins have shown that inhibition/overexpression of MAPK genes produces embryos and larvae with skeletogenic defects and affects the expression of terminal differentiation genes, such as *Sp-Sm50* (Fernandez-Serra et al., 2004; Röttinger et al., 2004). These studies concluded that the MAPK pathway in sea urchins is required for various steps of skeletogenesis, including spicule growth. Moreover, Taylor and Heyland (Taylor and Heyland, 2018) recently showed that the addition of a synthetic thyroid hormone (TH), T4, can accelerate skeletogenesis, but the addition of a MAPK ERK1/2 inhibitor can prevent this. Therefore, they concluded that the TH signalling pathway likely acts via a MAPK signalling pathway to promote skeletogenesis (Taylor and Heyland, 2018). Additionally, there is evidence that FGF signalling may regulate skeletogenesis via the MAPK pathway (Röttinger et al., 2007). Taken together, there is strong evidence that the MAPK pathway is important for sea urchin larval skeletogenesis. Whether it is important to mediate TRH signalling, as well as FGF and T4 signalling, needs further investigation.

The discovery that TRH has such a prominent growth role in sea urchin larvae provides a basis to investigate if TRH signalling is similarly involved in regulating growth in other taxa. There Is currently little known about the physiological roles of TRH neuropeptides in other deuterostomian invertebrates. A recent study reported that the human TRH can promote oocyte proliferation in the sea cucumber *Holothuria scabra* (Chaiyamoon et al., 2020). However, it is unknown if the *H. scabra* peptide has a similar function in the sea cucumber. Moving to vertebrates, TRH neuropeptides are pleiotropic and are most widely known for their hypothalamic functions regulating growth, development and ossification (Fröhlich and Wahl, 2019;

Galas et al., 2009; Lovejoy, 2005). More specifically, the role of TRH neuropeptides and the TH pathway has been immensely studied in mammals in terms of the regulation of skeletal/ossification growth (Bassett and Williams, 2016a; Lovejoy, 2005). A considerable number of genetic mouse models have been generated, with mutations in genes related to the TH signalling pathway, producing mutant mice with skeletal phenotypes including delayed endochondral ossification, impaired chondrocyte differentiation and disorganisation of growth plates (Kim and Mohan, 2013). In addition, many TH signalling related mutations in human clinical studies have reported patients with skeletal phenotypes (Kim and Mohan, 2013). Furthermore, TRHR expression has been detected in rat bone marrow, suggesting that TRH signalling could directly act on skeletal cells in this species (Fukusumi et al., 1995). In summary, the TH pathway and the TRH neuropeptide have an important role in regulating growth in vertebrates. In the invertebrate protostomes, functional investigations of TRH signalling have only occurred in two taxa. Interestingly and comparable to mammals, TRH signalling regulates body size growth in the nematode *C. elegans* (Sinay et al., 2017). Conversely, in the hemipteran insect, *Pyrrhocoris apterus*, no obvious defects were detected in the CRISPR/Cas9 induced TRH null mutants (Kotwica-Rolinska et al., 2020). Taken together, the results provide further support that TRH signalling is an evolutionary ancient regulator of growth. Additional investigations are needed to see to what extent the ancient growth role of TRH signalling is conserved in different taxa.

As mentioned above, the TH pathway was been well studied in vertebrates and there is much evidence for a role of the TRH neuropeptide signalling system and the TH pathway in regulating vertebrate growth. *In silico* and chromogenic ISH analysis in this chapter provides further support for the presence of a TH signalling pathway in the invertebrate sea urchin *S. purpuratus* and therefore the ability of the sea urchin to endogenously produce thyroid hormones. Importantly, data from this chapter and previous studies supports the hypothesis that the TH pathway regulates growth in the sea urchin (Heyland, 2005; Heyland et al., 2006; Miller and Heyland, 2013; Taylor and Heyland, 2018; Wu et al., 2007). What is unknown and needs to be clarified in future research is whether the TRH neuropeptide signalling system regulates TH

production, similarly to mammals. Or if the two signalling pathways are acting independently to regulate larval growth. Also of interest, if how the TH pathway exerts it's affects in the sea urchin and other invertebrates: the classical genomic mode where thyroid hormones bind to nuclear thyroid hormone receptors, or a non-genomic mode where thyroid hormones bind to membrane receptors or extranuclear thyroid hormone receptors (Taylor and Heyland, 2017). The genomic mode directly regulates gene expression, while the non-genomic mode involves more rapid cellular changes, which can regulate gene expression indirectly.

To conclude, this chapter has revealed that TRH signalling has a conserved role in regulating growth in the sea urchin larval skeleton. The function of neuropeptides in the larvae of some marine invertebrates has been studied (Conzelmann et al., 2011; Thiel et al., 2017, 2019). For example, a CCHamide neuropeptide has been shown to regulate ciliary swimming in a nemertean larvae. Importantly, this is the first study to identify the function of TRH neuropeptides in a larva of a marine invertebrate. I discuss further the evolution and function of TRH signalling In Chapter 7.

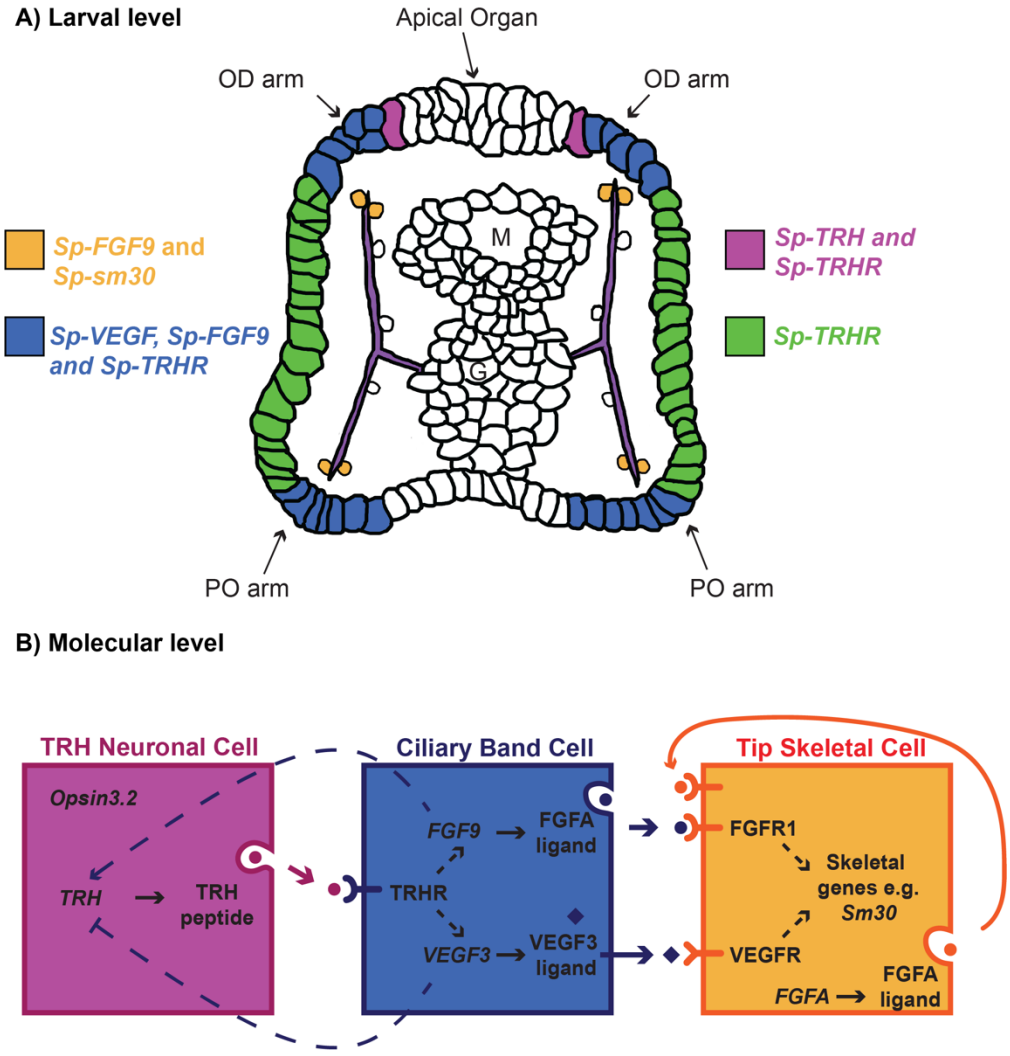

Figure 6.21 Proposed model for TRH NP signalling regulating larval skeleton growth

A) The expression patterns of *Sp-TRH*, *Sp-TRHR*, *Sp-VEGF*, *Sp-FGF9* and *Sp-Sm30* mapped onto a pluteus larval cartoon (oral view) in four cell/tissue-types (TRH neuronal cells (purple), ciliary band cells (blue), tip skeletal cells (orange) and other ciliary band cells (green). Only the co-expression of *Sp-TRH* and *Sp-TRHR* has been proven by double ISH, the overlapping expression of other genes is predicted based on the location of single chromogenic ISH data. Abbreviated labels refer to the OD (Oral Distal) arms, PO (Post Oral) arms, M (mouth) and G (gut). B) A summary of the proposed molecular interactions between the TRH neuronal cells (purple), the ciliary band cells (blue) and the tip skeletal cells (orange) supported by this chapter and previous studies (Adomako-Ankomah and Ettensohn, 2013; Duloquin et al., 2007; Röttinger et al., 2007; Sun and Ettensohn, 2014) . Solid lines refer to connections that are direct, while dashed lines refer to an unknown number of intermediate steps, which may be direct or indirect. At the end of the line, an arrow refers to upregulation and a solid line refers to downregulation. Ligands and their specific receptors are a specific colour and shape for the different signalling systems.

Chapter 7 Discussion

In this thesis I set out to provide new insight and understanding on the roles of neuropeptides in the development of the sea urchin, *S. purpuratus*. The first main objective of my thesis was to characterise the neuropeptide signalling systems in *S. purpuratus.* Here, temporal and spatial expression profiles showed that the majority of these neuropeptide signalling systems are expressed in different populations of cells in the larval nervous system (Chapter 3). In addition, we revealed that, surprisingly, some neuropeptides precursor genes showed early embryonic expression, which highlights a potential additional role (Chapter 4). The second main objective was to investigate the role(s) of neuropeptides in the *S. purpuratus* embryo and larvae. To start I optimised CRISPR/Cas9 genome-editing in the sea urchin and showed that CRISPR/Cas9 is a feasible perturbation tool in sea urchins, but the efficiency needs to be improved further. (Chapter 5). To this end, I used CRISPR/Cas9 and MOs to perturb the expression of *Sp-TRH* and *Sp-TRHR* genes and show that TRH NP signalling system regulates larval skeleton growth in *S. purpuratus.* Furthermore, I began to unravel the molecular mechanism for how TRH NPs signalling system regulates larval skeleton growth and found that it likely involves VEGF and FGF signalling pathways (Chapter 6).

In this chapter, I will present a discussion of the work presented in this thesis with three main themes that are all centred around NP signalling systems: 1) the identity of neuronal cell types, 2) the evolution and functions of TRH-type signalling, and 3) the evolution of neuronal cell types and nervous systems. Finally, I will provide some future directions and concluding remarks.

7.1 The identity of neuronal cell types

The work reported in this thesis on the analysis of NP signalling systems revealed at least nine populations of neuronal cells and one population of neuronal-like cells in the sea urchin pluteus larval nervous system. The genes that encode these NP signalling systems together with and other genes including neurotransmitters, receptors, ion channels, axon guidance molecules are used to define neuronal

identity and functionality. However ultimately, it is the combination of transcription factors in a given cell that regulates the particular signature of terminal effector or differentiation genes (Figure 1.8) (Arendt, 2008; Hobert, 2016a). It is important to uncover the regulatory states of these neuronal cell types for two reasons. Firstly, to understand how a sea urchin builds its nervous system. To do so we need to identify the regulatory state and ultimately the gene regulatory network of each neuronal cell type. Secondly, to make comparisons between different species and ultimately identifying homologous neuronal cell types. Since terminal selector transcription factors are more often conserved than terminal effector genes (Arendt *et al.,* 2016a, 2019; Davidson and Erwin, 2006; Peter and Davidson, 2011; Serrano-Saiz *et al.,* 2013), it may be easier to identify homologous cell types using transcription factors. Arendt and colleagues (2016) nicely illustrate that is the case for visceral smooth muscles and straited muscles in different bilaterian phyla. In fact, both vertebrates and the annelid *P. dumerilii* have visceral muscles that contain smooth myocytes that express the same set of transcription factors such as: *nk3.2* and *Foxj1*. Indeed, *Drosophila* also expresses those same transcription factors but in cells of striated muscle (Arendt *et al.,* 2016a; Brunet *et al.,* 2016), showing that the underlying regulation can be the same, while the phenotype (smooth or striated muscle) can be different.

Taking this into account, I gathered transcription factor spatial expression data from previously published datasets in *S. purpuratus*, *Lytechnius variegatus* and *Paracentrotus lividus* pluteus larvae. In Table 7.1 the expression of transcription factors expressed in differentiated neurons at the pluteus larva stage is summarised. These data reveal the unique regulatory states for the differentiated neuronal populations that were further established in this thesis (Chapter 3; Figure 3.17).

In addition, I can clearly see that some cell types including the: apical organ (AO) sensory neurons and oral distal (OD) neurons, are better molecularly characterized than others. In fact, the serotonergic sensory AO neurons can be characterised by the expression of 14 transcription factors including *Mox*, *z167*, *Lhx2* and *Mist*, while the *Sp-TRH* OD neurons can be characterised by the expression of 21 transcription factors, including *Tbx2/3*, *Nk2.1*, *Rx, otx* and *six3*. Much less is known about the

regulatory states of *Sp-AN* positive lateral ganglia neurons which are only expressing six transcription factors in these bilateral clusters (Table 7.1). There are even fewer transcription factors identified in the elusive other ciliary band neurons, which we define as neurons in the ciliary band that are not the OD, AO, post oral or lateral ganglia neurons. I am confident that these other ciliary band neurons will be divided into different neuronal populations, as the expression profiles of more genes are identified.

When looking at the distribution of transcription factors some evident patterns arise. Firstly, the distribution of transcription factors is generally quite restrictive; 45% of them are only expressed in a single neuronal cell type; 44% are expressed in two or three neuronal cell types; and only 11% (*SoxB2, Brn124, otp* and *islet*) are expressed in four or more neuronal cell types (Table 7.1).

If we compare our analysis in the sea urchin larvae to the molecular map of genes expressed in *C. elegans* neuronal cell types we can draw some similarities and differences. The nervous system of *C. elegans* consists of 302 neurons in the hermaphrodite and 385 neurons in the male, these are divided into at least 104 classes of sensory, interneuron and motor neurons (Hobert, 2016b). In a similar manner to what is observed in sea urchins, most *C. elegans* transcription factors operate in two to four neuronal cell types and are therefore quite restrictive. Indeed, Hobert and colleagues do not report how many transcription factors are expressed in only one neuronal cell type (Hobert, 2016b). Moreover, Hobert and colleagues show that as little as four transcription factors control the identity of a staggering 50 out of 100 distinct cell types (Hobert, 2016b).

Although the present study only confirms nine sub-populations of neuronal cells in the sea urchin larval nervous system, I predict that more cell types will be identified when additional transcription factors and effector genes are investigated. It would be interesting to see whether some of these transcription factors will control larger populations of cell types similarly to what we see in *C. elegans*. In particular, it will be intriguing to see if the pan-neuronal identity can be genetically separated from the neuron-type specific identity. More specifically, can we identify a distinct set of

transcription factors that control generic neuronal identity? Or in similar manner to *C. elegans* is generic neuronal identity controlled by diverse redundant regulatory inputs (Stefanakis *et al.,* 2015). From the data have available so far, it would suggest the latter option, as we only have one gene, *SoxB2* expressed in all sub-populations.

Another theme in *C. elegans* nervous system regulation is that homeobox genes are frequently involved in specifying neuronal cell type identity, whether by directly or indirectly specifying terminal effector genes (Hobert, 2016b). Of the data we gathered in the sea urchin, 39% of transcription factors involved in specifying neuronal identity are homeobox genes (Table 7.1) and homeobox transcription factors making up 34% of all the transcription factors in the *S. purpuratus* genome (Howard-Ashby *et al.,* 2006c, 2006b). This shows that, in contrast to *C. elegans,* homeobox genes seem to not be used more frequently than other transcription factor families.

To summarise we have identified the regulatory states of seven out of nine neuronal cell types in the sea urchin pluteus larva. There are likely many more transcription factors involved in each of these cell types that have not been identified yet. Furthermore, we have no information of the transcription factors that specify the cell identities of 1) the serotonergic interneurons that do not express any neuropeptides investigated so far; and 2) the two populations of neurons around the mouth, which express distinct combinations of neuropeptides (Figure 3.17; Table 8.16). A lot more work needs to be done to build a comprehensive molecular map of the sea urchin larval nervous system. We could definitely take advantage of single cell sequencing to provide a detailed molecular fingerprint of each cell type. For example, a recent study investigating Drosophila optic lobes revealed 52 clusters of transcriptionally distinct single cells. They also used a "random forest model" to predict the transcription factors that are responsible for the regulation of downstream effector genes. Using this model they were able to predict the transcription factors responsible for generating four neurotransmitter identities in the optic lobe and then knock down these transcription factors and show downregulation of specific neurotransmitters (Konstantinides *et al.,* 2018). This study gives one example of the many techniques that could be employed in the sea urchin larval nervous system, to

determine which transcription factors are specifying which terminal effector genes. From there, we can begin to make informed inferences about neuronal cell type evolution by comparing with the molecular maps of *C. elegans*, *P. dumerii, D. melanogaster*, vertebrates, and hopefully in the future other systems (Achim *et al.,* 2015; Hobert, 2016a; Konstantinides *et al.,* 2018; Tosches *et al.,* 2018; Zeisel *et al.,* 2018).

TF	Gene family	OD	PO	AO	LG	Mouth	Foregut	Other CB
Hnf6	ONECUT	1	1	1	0	0	0	0
FoxG	Forkhead	1	1	1	0	0	0	0
FoxJ1	Forkhead	1	?	0	0	0	0	0
ets1/2	ETS	?	0	0	0	0	0	0
Hlf	PAR bZIP	?	0	0	0	0	0	0
Tbx2/3	T-box	?	?	0	0	?	0	0
Zic	Zinc finger	?	0	0	0	0	0	0
Nk2.1	Homeobox	1	0	1	0	?	0	0
Rx	Homeobox	1	0	0	0	0	0	0
Otx	Homeobox	1	0	0	0	?	?	0
hbn	Homeobox	1	0	0	0	?	0	0
six3	Homeobox	1	0	0	0	?	?	0
awh	Homeobox	1	?	0	0	0	0	0
Islet	Homeobox	0	0	?	?	?	?	0
NeuroD	bHLH	0	0	?	0	0	?	0
Neurogenin	bHLH	0	0	?	1	0	0	1
Otp	Homeobox	?	?	0	0	?	0	1
Brn1/2/4	Homeobox	0	0	?	1	?	?	0
Mist	bHLH	0	0	1	1	0	0	0
Mox	Homeobox	0	0	1	0	0	0	0
z167	Zinc finger	0	0	1	0	0	0	0
z166	Zinc finger	?	?	0	0	0	0	0
Lhx2	Lim	0	0	?	0	0	0	0
dmrt	DM domain	0	0	0	0	0	1	0
mbx	Homeobox	0	0	0	0	0	1	0
prox	Homeobox	?	0	0	0	0	0	0
scratch	Snail	0	?	?	0	0	0	0
ese	ETS	0	?	?	0	0	0	1
elk	ETS	?	0	0	0	0	0	0
egr	Zinc finger	?	0	0	0	0	0	1
AsSc	bHLH	1	1	1	0	-	0	0
Hey	bHLH	1	0	0	0	0	0	0
Lox	Homeobox	0	0	0	1	0	0	0
Nk3.2	Homeobox	0	0	0	0	0	1	0
FoxA/B	Forkhead	0	0	0	0	1	0	0
SoxB2	HMG box	1	1	1	1	1	1	1

Table 7.1 Transcription factors expressed in pluteus larval neuronal cell types

The regulatory states of seven neuronal cell types in the sea urchin pluteus larva. The presence/absence of a transcription factor in a given cell type is illustrated by the following; (1) the presence of the TF has been proved by double expression; (?) cells in the same area express the TF in a similar expression pattern, but no double expression experiment has been done to prove co-expression; (0) there is no co-expression; and (-) there is no information. The last cell type, the other ciliary band neurons are defined as neurons in the ciliary band that are identified by synaptotagmin, but do not express any NP genes that are expressed in the first four categories. Data were obtained from personal communication with Periklis Paganos (Arnone Lab) and the following (Annunziata *et al.,* 2014a; Burke *et al.,* 2006a; Di Bernardo *et al.,* 1999; Howard-Ashby *et al.,* 2006b; Lerner, 2013; Otim *et al.,* 2004; Perillo, 2013; Perillo *et al.,* 2018; Royo *et al.,* 2011; Slota *et al.,* 2019; Slota and Mcclay, 2018; Takacs *et al.,* 2004; Tu *et al.,* 2006; Valencia *et al.,* 2019; Wei *et al.,* 2011).

7.2 The function of *Sp-TRH* expressing neuronal cells

Chapter 6 of this thesis focused on two *Sp-TRH* positive oral distal (OD) neuronal cells. The molecular identity of these neurons is well understood (Figure 3.16; Table 7.1; Table 8.16) and gene perturbation of *Sp-TRH* and *Sp-TRHR* demonstrates that these neurons regulate larval skeleton growth. Interestingly, another neuropeptide *Sp-FSALMFa* is co-expressed with *Sp-TRH* in the OD neuronal cell (Figure 3.17; Table 8.16) and preliminary data has shown that gene perturbation of *Sp-FSALMFa* accelerates skeleton growth and upregulates *Sp-TRH* (Figure 6.20). This data reveals that these two NP signalling systems are likely acting in an opposing manner to regulate skeleton growth. Thus, we have one NP signalling inhibitor (*Sp-FSALMFa*) and one activator (*Sp-TRH*) of skeleton growth (Figure 7.1). It would be extremely interesting to clarify whether *Sp-FSALMFa* is upregulated when the *Sp-TRH* gene is mutated, which will tell us if they are in a negative interaction, to control normal skeleton growth. Interestingly, the role of *Sp-FSALMFa* as an inhibitory signal is consistent with previously reported actions of SALMFamides in echinoderms. An example in seen with the SALMFamide S1 which has been shown to cause inhibition of a relaxin-like gonad-stimulating peptide (RGP) from radial nerves in the starfish *Asterina pectinifera* (Mita et al., 2004). The PO neurons, similar to the OD neurons, express *Sp-FSALMFa* and likely also *Sp-TRHR* (Figure 3.17; Table 8.16). The location of the PO neurons at the tips of the PO larval arms, coupled with the change in PO larval arm length when TRH or FSALMFa signalling is perturbed, suggests that both TRH and FSALMFa signalling systems act as local ectodermal cues, to regulate larval skeleton growth through the PO neurons, as well as the OD neurons (Figure 7.1).

In addition, the wider expression pattern of *Sp-TRHR* in the other ciliary band neurons implies that there are many more additional cells that respond to TRH NP signalling. It remains to be seen if these cells use the same molecular mechanism to signal to the skeleton, or if they have other functions. The presence of *Sp-VEGF* in many ectodermal cells of the arm tips, and the reduction in *Sp-VEGF* expression when *Sp-TRH* and *Sp-TRHR* expression is perturbed (Figure 6.17), does suggest that at least these cells are responding to TRH NP signalling. Furthermore, at present no *Sp-*

FSALMFa receptor has been reported, but if it is identified it would be interesting to see if it is co-expressed with *Sp-TRHR* in the OD, PO and/or other ciliary band neurons.

The OD and PO neurons have additional molecular signatures that can provide further inference on the roles of these neurons and the factors that might regulate these neurons/neuropeptides. *Sp-TRH* was previously reported to be co-expressed with *Sp-Opsin3.2* in photoreceptive neurons (Petrone, 2015) (Figure 1.12E). The co-expression of the neuropeptide TRH with a an opsin suggests that light could play a part in regulating the Sp-TRH OD neuronal cells (Figure 7.1). Interestingly, there are other examples of neuropeptides being regulated by light, for example the maturation inducing hormone (MIHs) in Clytia (Artigas et al., 2020; Quiroga Artigas et al., 2018). In these studies, opsin-expressing gonad cells were found to stimulate the release of MIH, which activates MIHR and triggers oocyte maturation (Artigas et al., 2020; Quiroga Artigas et al., 2018).

As well as light, there are other environmental factors that animals can respond to, including food availability, pH level and predation threat. For example, in the nematode *C. elegans*, the muscles that express *Ce-TRHR* are a subset of pharyngeal muscles that are involved in food intake, leading the authors to suggest that TRH may regulate growth via feeding in this species (Sinay et al., 2017). Intriguing, when *S. purpuratus* larvae are cultured in starving conditions (with no algae) they have longer larval arms in comparison to larvae cultured with algae (Adams et al., 2011), showing that sea urchin larvae regulate skeletal growth in response to food availability. Feeding rate has been investigated across many marine larvae and it is generally found that it increases with the total ciliary band length (Strathmann, 1971). In the sea urchin, a ciliary band is located around the larval mouth and as the larval skeleton grows the ciliary band length increases. Strathmann (1975) described that the ciliated bands anterior and posterior to echinoderm larval mouths creates a current which helps draw particles toward the mouth. Adams and colleagues suggested the longer PO skeleton increases the larva's ability to catch food (Adams *et al.,* 2011). Although they do no report whether the length of the OD arms are affected in starving/feeding conditions, I would predict that larvae likely have a higher feeding rate if both sets of larval arms are longer. In addition, Adams and colleagues showed that the

neurotransmitter, dopamine, mediates larval arm length in response to food availability. The dopaminergic neurons that respond to algal levels are found at the tips of the PO larval arms, at close proximity to the skeletal producing cells (Adams et al., 2011). Most excitingly, these dopaminergic neurons are in a similar location to the *Sp-TRHR* positive ciliary band cells and *Sp-FSALMFa* positive PO neurons (Figure 3.17; Table 8.16).

Taken together, the OD and PO neurons seem to regulate larval sea urchin skeletogenesis by a complex interaction of environmental stimuli, neurotransmitters and neuropeptides.

Aside from this well characterised function of TRH signalling in the pluteus larval stage, could TRH and FSALMFa signalling have important functions at other developmental times of life cycle stages? At later larval stages, the skeleton and other tissue types continue to grow and then the juvenile builds a new tissue, implying that genes important for growth of structures in the larva may also be important for growth of similar structures in the adult. In chapter 3, I showed that *Sp-TRH* and *Sp-FSALMFa* have higher relative expression in the juvenile in comparison to the early pluteus larval stage (70 hpf). This could suggest that these neuropeptide signalling systems also have important growth functions in juvenile and/or adult sea urchins.

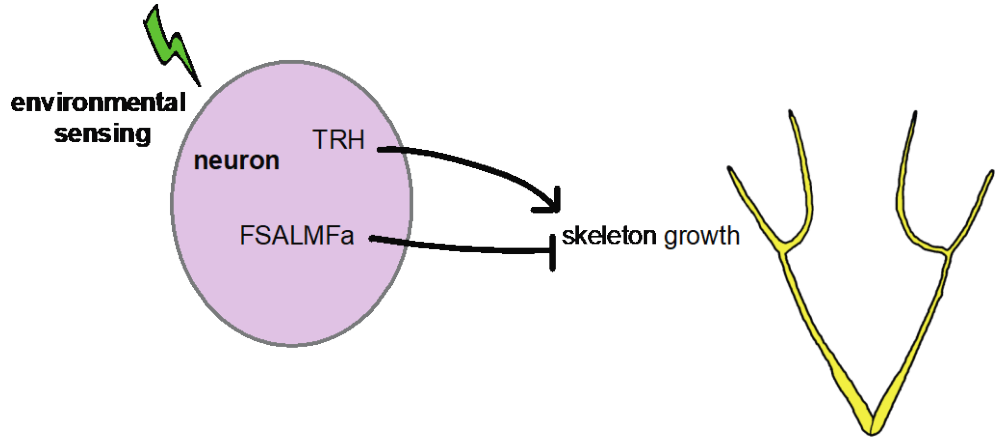

Figure 7.1 A diagram showing the proposed opposing NP signalling systems regulating larval skeleton growth

Environmental factors (such as light and food) send signals to neuronal cells. These cells express two neuropeptide signalling systems, TRH and FSALMFamide which acts as an activator and inhibitor of sea urchin larval skeleton growth, respectively.

7.3 Implications on neuronal cell-type and nervous systems evolution

7.3.1 Neuronal cell type evolution

As mentioned in the introduction, when and where neuronal cell types originated are two extremely exciting questions in the field of neurobiology. Evolutionary developmental biologists have taken a molecular approach to answer these questions by unravelling regulatory states that underpin neuronal identity. Given this, I will now discuss my results in relation to neuronal cell type evolution by comparing the regulatory state of *TRH* positive neurons in sea urchins, to annelids, *C. elegans* and mammals.

Sp-TRH oral distal (OD) neurons have been previously identified as non-directional photoreceptors that express a Go-opsin, *Sp-Opsin3.2* (Valencia *et al.,* 2019; Valero-gracia *et al.,* 2016). Valencia and colleagues also demonstrated that these photoreceptor neurons express several transcription factors, including *otx*, *six3* and *Rx* (Valencia *et al.,* 2019) (Table 7.1), some of which are also expressed in ciliary photoreceptors of other species, including the annelid *P. dumerilii,* and vertebrates (Arendt *et al.,* 2004; Musser and Arendt, 2017; Vopalensky *et al.,* 2012). The ciliary photoreceptors of the annelid *P. dumerilii* and rods and cones of vertebrates have shared expression of *rx* and c-opsin and have been suggested to be homologous cell types (Arendt, 2003; Arendt *et al.,* 2004; Mathers *et al.,* 1997; Vopalensky *et al.,* 2012). Therefore, based on this shared expression, Valencia and colleagues conclude that the sea urchin photoreceptor neurons are likely homologous to the ciliary photoreceptors of other bilaterians. However, the terminal effector genes are different. The sea urchin oral photoreceptor neurons express a Go-opsin, while most other bilaterian ciliary photoreceptors express c-opsin (Arendt, 2003). Therefore, this suggests that the sea urchin photoreceptor neurons are a sister cell type to other bilaterian ciliary photoreceptor cells. These sister cell types likely arose by the splitting of an ancestral cell types into different descendent cells, via the process of individualisation (Arendt *et al.,* 2016a). In this thesis, I have also shown that these OD photoreceptors neurons express TRH NP signalling, which is present throughout

Bilateria (Figure 1.1; Figure 6.1). These OD photoreceptor neurons also express FSALMFa NP signalling, however FSALMFa is specific to the Echinodermata phylum (Elphick *et al.,* 1991a). Interestingly, it has been reported that TRH is present in mammalian retina (Eldred *et al.,* 2018; Lexow, 1996). Furthermore, the nuclear receptors thyroid hormone receptor B (THRB) and retoinic X receptor (RXR) have also been shown to regulate opsin in mammalian cones (Ng *et al.,* 2001) and are known to regulate TRH in mammals (Hollenberg *et al.,* 1995). In Chapter 6, I showed that a *Sp-THR is* strongly expressed in the ciliary band, in a pattern that would suggest it is also expressed in the oral distal ciliary photoreceptor neurons (Figure 6.10E). The expression of an *Sp-RXR* gene has been illustrated in the sea urchin gut and I cannot rule out expression also in the OD neurons without additional data (Annuziata, 2011). Taken together, it would be intriguing to see if TRH is expressed in the ciliary or rhabdomeric photoreceptors of other invertebrates and vertebrates, and thus if the presence of TRH in sea urchin ciliary photoreceptor neurons is a novelty or more widespread across bilaterians.

7.3.2 Defining nervous system complexity

The degree to which an animal can sense, detect and respond to an environmental stimulus is thought to depend on the complexity of its nervous system. As I mentioned in the introduction, the term centralisation is often used as a proxy for complexity.

Ciliated larvae of in-direct developers generally have a centralised/condensed apical organ and additional neurons in a ciliary band and in other tissues. In this thesis we have shown the peptidergic complexity of the whole sea urchin larval nervous system. Moreover, chemical complexity has been seen in many other larvae (Conzelmann *et al.,* 2013; Marlow *et al.,* 2014; McDougall *et al.,* 2006; Nakajima *et al.,* 2004a, 2004b). Thus, nervous system complexity is not solely defined by the number of constituent neurons but also by the combination of neurochemical phenotype of each neuron.

Consequently, when thinking about how complex nervous systems are, is the term centralisation the best proxy for complexity? I agree that using centralisation when referring to terms like nerve cord, nerve ring, and brain is useful when referring to questions of homology of specific character states. However, the degree of centralisation is continuous, and a single ganglion (as seen in larval AOs) is technically a centralisation. In addition, it has become apparent that much simpler less centralised, or decentralised nervous systems such as larval nervous systems can be chemically very complex.

Therefore, when thinking about the complexity of **diverse** nervous systems, it could instead be clearer to look at a multitude of factors, including but not limited: 1) chemical complexity; 2) complexity of genes expressed; 3) connectivity (i.e. number of synapses); 4) the number of neurons; and 5) the number of neuronal populations.

Using this multifaceted definition of complexity, we can therefore make better comparisons between different species and we can appreciate the diversity in nervous systems. A human brain is chemically complex, highly connective and has trillions of neurons, while a sea urchin larva is chemically complex but has only 40-50 neurons.

I think this approach will truly appreciate the simpler complex nervous system of many invertebrates and make it easier to compare nervous systems and make inferences and nervous system evolution.

7.4 Future directions

The work presented in the thesis provides a deeper understanding of the identity of neuronal cell types in the sea urchin larvae. These insights provide an initial foundation for establishing a complete regulatory state of each population of neuronal cells. This would then allow us to build a GRN for the larval nervous system and understand how a nervous system can be built. In this section, I discuss the next steps that need to be taken to build a nervous system GRN. In addition, I highlight some other interesting questions that have developed during this work and suggest some possible subsequent steps that should be taken.

7.4.1 Building a GRN for the sea urchin nervous system

I have mostly explored the molecular identity of neuronal cells using NP genes. Indeed, we did investigate a few GPCR genes, but for the majority of GPCR their identity is predicted. A large-scale deorphanisation of *S. purpuratus* NP signalling systems would reveal ligand-receptor pairs. From here, I would first spatially characterise proven GPCRs for the ligands expressed in neuronal cells to reveal the target cells. As discussed earlier, one particular interesting revelation will be the spatial expression of *Sp-FSALMFa-Receptor* and whether it is co-expressed with *Sp-TRHR* in the OD, PO and/or other ciliary band neurons. In addition, we should take a look at the spatial characterisation of other effector genes that contribute to neuronal identity such as: neurotransmitter receptors, axon guidance molecules, ion channels and transporters.

Moreover, a more complete analysis of neuronal terminal selector genes should be performed. I have shown at least 36 transcription factors expressed in different larval neuronal cells. Indeed, there are likely more reported in the literature, but preferable to a targeted analysis would be an unbiassed comprehensive analysis of neuronal cell type regulatory states. This could be achieved by whole larval single-cell sequencing or using BAC-recombinant technology to identify and isolate a homogenous population of neuronal cells and performing RNA-sequencing of these cells. Following on, double fluorescent ISH to spatially map this sequencing data should be performed. It will be particularly interesting to see how many neuronal cell

populations there are in the sea urchin larva. Also, other interesting questions that this will answer are: How many populations are in the other ciliary band neurons? What terminal selector genes identify these other ciliary band neurons?, On average, how many cells share the same molecular signature?

Furthermore, once we have a complete characterisation of the molecular state, we can use gene perturbation of regulatory genes and monitor the spatial-temporal effects of downstream genes, including terminal effector genes. This will reveal cause-effect linkages between regulatory genes and terminal effector genes, identifying which terminal selector genes are responsible for specify particular effector genes. To prove functional linkages, cis-regulatory modules need to be identified and experimental validated.

7.4.2 TRH regulating skeleton growth

One of the most interesting discoveries of this thesis was the ancient role of TRH and the intricate network that seems to regulate the growth of the larval skeleton. The positive and negative interactions between TRH, VEGF and FGF signalling need further validation. While we do have several independent experiments showing a reduction in VEGF and FGF in *Sp-TRH* mutated larvae, we need to validate the spatial expression of *Sp-TRH* on VEGF and FGF inhibited larvae. Unfortunately, we have shown that QPCR is not a good technique for detecting changes in gene expression in few cells. Instead, ISH characterisation for many other putative downstream genes should be performed on *Sp-TRH* and *Sp-TRHR* mutated larvae, and VEGF and FGF inhibited larvae. Genes include additional FGF and VEGF ligands/receptors, *Sp-THR*, and skeletogenic genes *Sp-net7*, *Sp-Can1*, and *Sp-p58* and *Sp-Alx1*. In addition, once we have cloned and determined the spatial-temporal expression of the thyrostimulin genes, *Sp-GPA2* and *Sp-GPB5* we may be able to add these to our putative downstream genes.

In regard to the perturbed TRH phenotype, a double-blind experiment should be performed where it is unknown which larvae are injected/uninjected until after the samples are analysed. This way I can ensure there is no bias when measuring the length of the larval skeletons. Moreover, additional experimental repeats should be

performed for the *Sp-FSALMFa* CRISPR/Cas9 knockouts to further elucidate the potential growth function and identify the complex interactions between environmental stimuli, neurotransmitters and neuropeptides that seem to regulate larval growth. Furthermore, there are over 30 other neuropeptide signalling systems in the sea urchin and a huge plethora of functions that need to be identified.

7.4.3 Further optimisation of CRISPR/Cas9

In Chapter 5 I showed that CRISPR/Cas9 is a feasible gene perturbation tool in sea urchin. We have tested 32 sgRNAs across seven different genes and we generally see expected phenotypes that are comparable to MO knockdowns. However, some issues have come to light. Firstly, we saw a variability in *in vivo* efficiency that could not be predicted *in vitro*. Secondly, there were only a handful of times where we detected non-mosaic knockouts.

To increase the efficiency of *in vivo* knockouts we can test different concentrations of sgRNA mRNA and some intermediate Cas9 mRNA concentrations, between 90ng/µl that worked well and 500ng/µl that seemed to be toxic. In addition, we had two promising results that increased the efficiency of *in vivo* knockouts that should be further investigated: 1) We saw that Cas9 protein (PNA BIO) increased the efficiency of *Sp-TPH* knockouts, in comparison to Cas9 mRNA and 2) when we slowed down the cleavage stages we saw an increase in the number of homozygous *Sp-TPH* knockouts. Therefore, I think that further experiments using this Cas9 protein (PNA BIO) and slowing down early development will give some exciting results.

With regards to the variable sgRNA efficiency there are many things that can be done. One approach, which we have used, was to inject combinations of sgRNA in the hope that one or more will edit the genome. Another more directed tactic is to try and tackle the reason for this variability. Is it a problem with particular sgRNA sequences? Or is it an issue with particular sections of the genome? Or something else?

There have been many studies investigating the efficiency of the CRIPSR/Cas9 system and the problems with sgRNA on-target efficiency are generally suggested to come from nucleotide composition, secondary structure of sgRNA and chromatin

accessibility (Doench *et al.,* 2014; Hinz *et al.,* 2015; Horlbeck *et al.,* 2016; Knight *et al.,* 2015; Liu *et al.,* 2016, 2019). For example, some have demonstrated that the nucleotide composition proximal to the PAM sequence is important for sgRNA activity, while others have found that the nucleotide composition distal to PAM sequence is also important (Doench *et al.,* 2014; Liu *et al.,* 2016). In addition, there has also been conflicting evidence over the 'ideal' GC content of sgRNA (Gagnon *et al.,* 2014; Liu *et al.,* 2016).

Given that I have developed a working CRISPR/Cas9 system with 32 sgRNAs already designed, I think the best approach forward would be to first identify any correlations between efficient sgRNA, and the nucleotide composition, and then use these efficient sgRNAs with the PNA BIO Cas9 protein and a longer first cleavage step.

Finally, the attention should move to genotyping to better identify on-target mutations. One potential method is high resolution melting (HRM) analysis, which is a relatively fast and cheap method for detecting small variation in DNA. The target region of interest is first amplified, and then dsDNA-binding dyes are used with a real-time PCR machine that will detect small differences in PCR melting curves. This could be a good method to screen large numbers of embryos/larvae and then the known mutants can be selective sent for sequencing.

7.4.4 Non-neuronal role of neuropeptides

Another aspect of the thesis has been the putative non-neuronal role of some NP signalling systems. We identified some NP genes and GPCR genes that are expressed in early embryonic development. We now need functional data to determine what other role(s) they may have.

Future investigations should first focus on the general machinery used to syntheses and process neuropeptides, including the signal peptidases, prohormone convertases and secretory machinery. Perturbation of genes that encode proteins necessary to make and release functional mature neuropeptides, would be a good first step to testing the hypothesis that any neuropeptide has a role in early embryonic development. Additional investigations can then focus on molecularly (for

example, performing mass spectrometry for a proteomics analysis of early versus later embryonic and larval stages) and functionally characterising specific neuropeptide signalling systems and identifying how many (if any) of these systems have a non-neuronal role in early embryonic development. Importantly, functional investigations should include a combination of genetic, physiological and behavioural assays to have a comprehensive understanding of the roles of these signalling systems.

7.5 Concluding remarks

The molecular identity of cells is of central importance to understanding cell function and evolution. The set of terminal effector genes that are expressed in a given differentiated cell define cellular identity and functionality.

I have investigated the NP signalling systems expressed in neuronal cells in the sea urchin larva, which are a huge component of the molecular identity of neuronal cells. I have shown that combinations of these NP genes and some GPCR genes are expressed in at least nine populations of neuronal cells, revealing that the sea urchin larval nervous system is more complex than previously thought. This is all supported by the diverse combinations of transcription factors that are expressed in these populations of cells. Early expression of some NP genes is also seen in specified but undifferentiated ectodermal and endodermal cells, suggesting that these particular NP genes can function as regulatory genes as well as terminal effector genes.

In addition, we have revealed that one population of neurons (OD) are involved in larval skeleton growth and that this population of neurons and potentially more (PO and other CB) use a combination of signalling systems to regulate skeleton growth. Moreover, the TRH NP signalling system seems to have a conserved ancient role in growth throughout Bilateria. There is so much molecular/chemical complexity in just two neuronal cell types, and so it will be a thrilling task to molecularly and functionally characterise all the neurons and reveal the complexity of this 40-50 neuron sea urchin pluteus larva.

References

Abel, E. D., Ahima, R. S., Boers, M. E., Elmquist, J. K., and Wondisford, F. E. (2001). Critical role for thyroid hormone receptor B2 in the regulation of paraventricular thyrotropin-releasing hormone neurons. *J. Clin. Invest.* 107, 1017–1023.

Achim, K., Pettit, J. B., Saraiva, L. R., Gavriouchkina, D., Larsson, T., Arendt, D., et al. (2015). High-throughput spatial mapping of single-cell RNA-seq data to tissue of origin. *Nat. Biotechnol.* 33, 503–509. doi:10.1038/nbt.3209.

Adams, D. K., Sewell, M. A., Angerer, R. C., and Angerer, L. M. (2011). Rapid adaptation to food availability by a dopamine-mediated morphogenetic response. *Nat. Commun.* 2, 1–7. doi:10.1038/ncomms1603.

Adomako-Ankomah, A., and Ettensohn, C. A. (2013). Growth factor-mediated mesodermal cell guidance and skeletogenesis during sea urchin gastrulation. *Dev.* 140, 4214–4225. doi:10.1242/dev.100479.

Altschup, S. F., Gish, W., Pennsylvania, T., and Park, U. (1990). Altschul-1990-Basic Local Alignmen.pdf. 403–410.

Anctil, M. (2009). Chemical transmission in the sea anemone Nematostella vectensis: A genomic perspective. *Comp. Biochem. Physiol. - Part D Genomics Proteomics* 4, 268–289. doi:10.1016/j.cbd.2009.07.001.

Andrikou, C., Iovene, E., Rizzo, F., Oliveri, P., and Arnone, M. I. (2013). Myogenesis in the sea urchin embryo: the molecular fingerprint of the myoblast precursors. *Evodevo* 4, 1–16. doi:10.1186/2041-9139-4-33.

Angerer, L. M., and Angerer, R. C. (2004). Disruption of Gene Function Using Antisense Morpholinos Disruption of Gene Function Using Antisense Morpholinos. *Methods Cell Biol.* 74, 699–711. doi:10.1016/S0091-679X(04)74028-5.

Angerer, L. M., Oleksyn, D. W., Levine, A. M., Li, X., Klein, W. H., and Angerer, R. C. (2001). Sea urchin goosecoid function links fate specification along the animal-

vegetal and oral-aboral embryonic axes. *Development* 128, 4393–4404.

Angerer, L. M., Yaguchi, S., Angerer, R. C., and Burke, R. D. (2011). The evolution of nervous system patterning : insights from sea urchin development. *Development* 138, 3613–3623. doi:10.1242/dev.058172.

Annunziata, R., Andrikou, C., Perillo, M., Cuomo, C., and Arnone, M. I. (2019). Development and evolution of gut structures : from molecules to function.

Annunziata, R., Perillo, M., Andrikou, C., Cole, A. G., Martinez, P., and Arnone, M. I. (2014a). Pattern and Process During Sea Urchin Gut Morphogenesis : The Regulatory Landscape. *genesis* 52, 251–268. doi:10.1002/dvg.22738.

Annunziata, R., Perillo, M., Andrikou, C., Cole, A. G., Martinez, P., and Arnone, M. I. (2014b). Pattern and process during sea urchin gut morphogenesis: The regulatory landscape. *Genesis* 52, 251–268. doi:10.1002/dvg.22738.

Annuziata, R. (2011). Evolution of a Gene Regulatory Network that controls gut development, differentiation and functioning. *PhD Diss.*

Arendt, D. (2003). Evolution of eyes and photoreceptor cell types. *Int. J. Dev. Biol.* 47, 563–571.

Arendt, D. (2005). Genes and homology in nervous system evolution: Comparing gene functions, expression patterns, and cell type molecular fingerprints. *Theory Biosci.* 124, 185–197. doi:10.1016/j.thbio.2005.08.002.

Arendt, D. (2008). The evolution of cell types in animals: Emerging principles from molecular studies. *Nat. Rev. Genet.* 9, 868–882. doi:10.1038/nrg2416.

Arendt, D., Bertucci, P. Y., Achim, K., and Musser, J. M. (2019). Evolution of neuronal types and families. *Curr. Opin. Neurobiol.* 56, 144–152. doi:10.1016/j.conb.2019.01.022.

Arendt, D., Denes, A. S., Jékely, G., and Tessmar-Raible, K. (2008). The evolution of nervous system centralization. *Philos. Trans. R. Soc. B Biol. Sci.* 363, 1523–1528.

doi:10.1098/rstb.2007.2242.

Arendt, D., Musser, J. M., Baker, C. V. H., Bergman, A., Cepko, C., Erwin, D. H., et al. (2016a). The origin and evolution of cell types. *Nat. Rev. Genet.* 17, 744–757. doi:10.1038/nrg.2016.127.

Arendt, D., and Nübler-Jung, K. (1999). Comparison of early nerve cord development in insects and vertebrates. *Development* 126, 2309–2325.

Arendt, D., Tessmar-Raible, K., Snyman, H., Dorresteijn, A. W., and Wittbrodf, J. (2004). Ciliary photoreceptors with a vertebrate-type opsin in an invertebrate brain. *Science (80-.).* 306, 869–871. doi:10.1126/science.1099955.

Arendt, D., Tosches, M. A., and Marlow, H. (2016b). From nerve net to nerve ring, nerve cord and brain - evolution of the nervous system. *Nat. Rev. Neurosci.* 17, 61–72. doi:10.1038/nrn.2015.15.

Artigas, G. Q., Lapébie, P., Leclère, L., Bauknecht, P., Uveira, J., Chevalier, S., et al. (2020). A G protein-coupled receptor mediates neuropeptide-induced oocyte maturation in the jellyfish Clytia. *PLoS Biol.* 18, 1–25. doi:10.1371/journal.pbio.3000614.

Bartolomucci, A., Possenti, R., Mahata, S. K., Fischer-Colbrie, R., Loh, Y. P., and Salton, S. R. J. (2011). The Extended Granin Family: Structure, Function, and Biomedical Implications. *Endocr. Rev.* 32, 755–797. doi:10.1210/er.2010-0027.

Bassett, J. H. D., and Williams, G. R. (2016a). Role of Thyroid Hormones in Skeletal Development. *Endocr. Rev.* 37, 135–187. doi:10.1210/er.2015-1106.

Bassett, J. H. D., and Williams, G. R. (2016b). Role of Thyroid Hormones in Skeletal Development and Bone Maintenance. *Endocr. Rev.* 37, 135–187. doi:10.1210/er.2015-1106.

Baubet, V., Le Mouellic, H., Campbell, A. K., Lucas-Meunier, E., Fossier, P., and Brûlet, P. (2000). Chimeric green fluorescent protein-aequorin as bioluminescent Ca2+ reporters at the single-cell level. *Proc. Natl. Acad. Sci. U. S. A.* 97, 7260–7265.

doi:10.1073/pnas.97.13.7260.

Bauknecht, P., and Jékely, G. (2015). Large-scale combinatorial deorphanization of platynereis neuropeptide GPCRs. *Cell Rep.* 12, 684–693. doi:10.1016/j.celrep.2015.06.052.

Beer, A., Moss, C., and Thorndyke, M. (2001). Development of Serotonin-like and SALMFamide-like Immunoreactivity in the Nervous System of the Sea Urchin Psammechinus miliaris. *Biol. Bull.* 200, 268–280.

Beets, I., Janssen, T., Meelkop, E., Temmerman, L., Suetens, N., Rademakers, S., et al. (2012). Vasopressin/oxytocin-related signaling regulates gustatory associative learning in C. elegans. *Science (80-.).* 338, 543–545. doi:10.1126/science.1226860.

Bendtsen, J. D., Nielsen, H., Heijne, G. Von, and Brunak, S. (2004). Improved prediction of signal peptides — SignalP 3.0. *J. Mol. Biol.*, 1–22.

Bernstein, M. H. (1962). Normal and Reactive Morphology of Sea Urchin Spermatozoa. *Exp. Cell Res.* 27.

Bianco, A. C., Salvatore, D., Gereben, B., Berry, M. J., and Larsen, P. R. (2002). Biochemistry, cellular and molecular biology, and physiological roles of the iodothyronine selenodeiodinases. *Endocr. Rev.* 23, 38–89. doi:10.1210/edrv.23.1.0455.

Bisgrove, B. W., and Burke, R. D. (1986). Development of Serotonergic Neurons in Embryos of the Sea Urchin, Strongylocentrotus purpuratus. *Dev. Growth Differ.* 28, 569–574. doi:10.1111/j.1440-169X.1986.00569.x.

Bisgrove, B. W., and Burke, R. D. (1987). Development of the nervous system of the pluteus larva of Strongylocentrotus droebachiensis. *Cell Tissue Res.* 248, 335–343. doi:10.1007/BF00218200.

Britten, R. J., and Davidson, E. H. (1969). Gene Regulation for Higher Cells : A Theory. 165, 349–357.

Brunet, T., Fischer, A. H. L., Steinmetz, P. R. H., Lauri, A., Bertucci, P., and Arendt, D. (2016). The evolutionary origin of bilaterian smooth and striated myocytes. *Elife* 5, 1–24. doi:10.7554/eLife.19607.

Budelamnn, B. U. (1995). "The cephalopod nervous system: What evolution has made of the molluscan design," in *The Nervous Systems of Invertebrates: An Evolutionary and Comparative Approach*.

Burke, R. D. (1978). The Structure of the Nervous System of the Pluteus Larva of Strongylocentrotus purpuratus. *Cell Tissue Res.* 191, 233–247. doi:10.1007/BF00222422.

Burke, R. D. (2011). Deuterostome neuroanatomy and the body plan paradox. *Evol. Dev.* 13, 110–115. doi:10.1111/j.1525-142X.2010.00460.x.

Burke, R. D., Angerer, L. M., Elphick, M. R., Humphrey, G. W., Yaguchi, S., Kiyama, T., et al. (2006a). A genomic view of the sea urchin nervous system. *Dev. Biol.* 300, 434–460. doi:10.1016/j.ydbio.2006.08.007.

Burke, R. D., Moller, D. J., Krupke, O. A., and Taylor, V. J. (2014). Sea Urchin Neural Development and the Metazoan Paradigm of Neurogenesis. *Genesis* 52, 208–221. doi:10.1002/dvg.22750.

Burke, R. D., Osborne, L., Wang, D., Murabe, N., Yaguchi, S., and Nakajima, Y. (2006b). Neuron-Specific Expression of a Synaptotagmin Gene in the Sea Urchin Strongylocentrotus purpuratus. *J. Comp. Neurol.* 496, 244–251. doi:10.1002/cne.20939.

Burrows, M. (1996). *Neurotransmitters, neuromodulators and neurohormones Neurotransmitters, neuromodulators and neurohormones*. doi:10.1093/acprof.

Byrne, M., and Cisternas, P. (2006). Development and Distribution of the Peptidergic System in Larval and Adult Patiriella : Comparison of Sea Star. 114, 101–114. doi:10.1002/cne.10315.

Byrne, M., Nakajima, Y., Chee, F. C., and Burke, R. D. (2007). Apical organs in

echinoderm larvae: Insights into larval evolution in the Ambulacraria. *Evol. Dev.* 9, 432–445. doi:10.1111/j.1525-142X.2007.00189.x.

Cai, W., Kim, C. H., Go, H. J., Egertová, M., Zampronio, C. G., Jones, A. M., et al. (2018). Biochemical, anatomical, and pharmacological characterization of Calcitonin-type neuropeptides in Starfish: Discovery of an ancient role as muscle relaxants. *Front. Neurosci.* 12, 1–24. doi:10.3389/fnins.2018.00382.

Cameron, R. A., and Hinegardner, R. T. (1974). Initiation of Metamorphosis in laboratory cultured sea urchins. *Biol. Bull.* 146, 335–342.

Cameron, R. A., Hough-evans, B. R., Britten, R. J., and Davidson, E. H. (1987). Lineage and fate of each blastomere of the eight-cell sea urchin embryo. *Genes Dev.* 1, 75–84.

Cameron, R. A., Samanta, M., Yuan, A., He, D., and Davidson, E. (2009). SpBase : the sea urchin genome database and web site. *Nucleic Acids Res.* 37, 750–754. doi:10.1093/nar/gkn887.

Cary, G. A., Wolff, A., Zueva, O., Pattinato, J., and Hinman, V. F. (2019). Analysis of sea star larval regeneration reveals conserved processes of whole-body regeneration across the metazoa. *BMC Biol.* 17, 1–19. doi:10.1186/s12915-019-0633-9.

Chaiyamoon, A., Tinikul, R., Nontunha, N., Chaichotranunt, S., Poomtong, T., Sobhon, P., et al. (2020). Characterization of TRH/GnRH-like peptides in the sea cucumber, Holothuria scabra, and their effects on oocyte maturation. *Aquaculture* 518, 734814. doi:10.1016/j.aquaculture.2019.734814.

Chubb, J. R., Trcek, T., Shenoy, S. M., and Singer, R. H. (2006). Transcriptional Pulsing of a Developmental Gene. *Curr. Biol.* 16, 1018–1025. doi:10.1016/j.cub.2006.03.092.

Cobb, J. L. . (1987). *Neurobiology of the Echinodermata. In: Ali M.A. (eds) Nervous Systems in Invertebrates.*

Coffman, J. A., Dickey-Sims, C., Haug, J. S., McCarthy, J. J., and Robertson, A. A. (2004). Evaluation of developmental phenotypes produced by morpholino antisense targeting of a sea urchin Runx gene. *BMC Biol.* 2, 1–9. doi:10.1186/1741-7007-2-6.

Cole, A. G., Rizzo, F., Martinez, P., Fernandez-Serra, M., and Arnone, M. I. (2009). Two ParaHox genes , SpLox and SpCdx , interact to partition the posterior endoderm in the formation of a functional gut. *Development* 136, 541–549. doi:10.1242/dev.029959.

Consortium, S. U. G. S. (2006). The Genome of the Sea Urchin. *Science (80-.).* 314, 941–952. doi:10.1126/science.1133609.

Conzelmann, M., Offenburger, S. L., Asadulina, A., Keller, T., Münch, T. A., and Jékely, G. (2011). Neuropeptides regulate swimming depth of Platynereis larvae. *Proc. Natl. Acad. Sci. U. S. A.* 108. doi:10.1073/pnas.1109085108.

Conzelmann, M., Williams, E. A., Krug, K., Franz-Wachtel, M., Macek, B., and Jékely, G. (2013). The neuropeptide complement of the marine annelid Platynereis dumerilii. *BMC Genomics* 14, 906. doi:10.1186/1471-2164-14-906.

Cornelia I., B. (1998). Neurobiology of the Caenorhabditis elegans genome. *Science (80-.).* 282, 2028–2033.

Croce, J. C., and McClay, D. R. (2010). Dynamics of Delta/Notch signaling on endomesoderm segregation in the sea urchin embryo. *Development* 137, 83–91. doi:10.1242/dev.044149.

Davidson, E. H. (1989). Lineage-specific gene expression and the regulative capacities of the sea urchin embryo: a proposed mechanism. *Development* 105, 421–45. Available at: http://www.ncbi.nlm.nih.gov/pubmed/2693035.

Davidson, E. H., Cameron, R. A., and Ransick, A. (1998). Specification of cell fate in the sea urchin embryo: Summary and some proposed mechanisms. *Development* 125, 3269–3290.

Davidson, E. H., and Erwin, D. H. (2006). Gene Regulatory Networks and the Evolution of Animal Body Plans". *Science (80-.).* 313, 761c-761c. doi:10.1126/science.1126765.

Davidson, E. H., Rast, J. P., Oliveri, Paola, Ransick, Andrew, Calestani, C., Yuh, C.-H., et al. (2002a). A Genomic Regulatory Network for Development. *Science (80-.).* 295, 1669–1678.

Davidson, E. H., Rast, J. P., Oliveri, P., Ransick, A., Calestani, C., Yuh, C. H., et al. (2002b). A provisional regulatory gene network for specification of endomesoderm in the sea urchin embryo. *Dev. Biol.* 246, 162–190. doi:10.1006/dbio.2002.0635.

De Lange, R. P. J., Van Golen, F. A., and Van Minnen, J. (1997). Diversity in cell specific co-expression of four neuropeptide genes involved in control of male copulation behaviour in Lymnaea stagnalis. *Neuroscience* 78, 289–299. doi:10.1016/S0306-4522(96)00576-3.

De Velasco, B., Shen, J., Go, S., and Hartenstein, V. (2004). Embryonic development of the Drosophila corpus cardiacum, a neuroendocrine gland with similarity to the vertebrate pituitary, is controlled by sine oculis and glass. *Dev. Biol.* 274, 280–294. doi:10.1016/j.ydbio.2004.07.015.

Degnan, B. M., Adamska, M., Rochards, G. s, Larroux, C., Leininger, S., Bergum, B., et al. (2015). “Porifera,” in *Evolutionary Developmental Biology of Invertebrates 1: Introduction, Non-Bilateria, Acoelomorpha, Xenoturbellida, Chaetognatha*, 1–240. doi:10.1007/978-3-7091-1862-7.

Denes, A. S., Jékely, G., Steinmetz, P. R. H., Raible, F., Snyman, H., Prud’homme, B., et al. (2007). Molecular Architecture of Annelid Nerve Cord Supports Common Origin of Nervous System Centralization in Bilateria. *Cell* 129, 277–288. doi:10.1016/j.cell.2007.02.040.

Di Bernardo, M., Castagnetti, S., Bellomonte, D., Oliveri, P., Melfi, R., Palla, F., et al. (1999). Spatially restricted expression of PlOtp, a Paracentrotus lividus

orthopedia-related homeobox gene, is correlated with oral ectodermal patterning and skeletal morphogenesis in late-cleavage sea urchin embryos. *Development* 126, 2171–9. Available at: http://www.ncbi.nlm.nih.gov/pubmed/10207142.

Díaz-Balzac, C. A., Lázaro-Peña, M. I., Vázquez-Figueroa, L. D., Díaz-Balzac, R. J., and García-Arrarás, J. E. (2016). Holothurian Nervous System Diversity Revealed by Neuroanatomical Analysis. *PLoS One* 11, e0151129. doi:10.1371/journal.pone.0151129.

Doench, J. G., Hartenian, E., Graham, D. B., Tothova, Z., Hegde, M., Smith, I., et al. (2014). Rational design of highly active sgRNAs for CRISPR-Cas9-mediated gene inactivation. *Nat. Biotechnol.* 32, 1262–1267. doi:10.1038/nbt.3026.

Douglass, J., Civelli, O., and Herbert, E. (1984). Polyprotein gene expression: Generation of Diversity of Neuroendocrine Peptides. *Ann. Rev. Biochem.* 53, 665–715.

Duboc, V., Rottinger, E., Besnardeau, L., and Lepage, T. (2004). Nodal and BMP2 / 4 Signaling Organizes the Oral-Aboral Axis of the Sea Urchin Embryo. *Dev. Cell* 6, 397–410.

Duloquin, L., Lhomond, G., and Gache, C. (2007). Localized VEFG singaling from ectoderm to mesenchyme cells control morphogenesis of the sea urchin embryo skeleton. *Development* 134, 2293–2302. doi:10.1242/dev.005108.

Dylus, D. V., Czarkwiani, A., Stångberg, J., Ortega-Martinez, O., Dupont, S., and Oliveri, P. (2016). Large-scale gene expression study in the ophiuroid Amphiura filiformis provides insights into evolution of gene regulatory networks. *Evodevo* 7. doi:10.1186/s13227-015-0039-x.

Dylus, D. V., Czarkwiani, A., Blowes, L. M., Elphick, M. R., and Oliveri, P. (2018). Developmental transcriptomics of the brittle star Amphiura filiformis reveals gene regulatory network rewiring in echinoderm larval skeleton evolution. *Genome Biol.* 19, 1–17. doi:10.1186/s13059-018-1402-8.

Eakin, R. M. (1979). Evolutionary Significance of Photoreceptors: In Retrospect. *Am. Zool.* 653, 647–653.

Edgar, R. C. (2004). MUSCLE: Multiple sequence alignment with high accuracy and high throughput. *Nucleic Acids Res.* 32, 1792–1797. doi:10.1093/nar/gkh340.

Eipper, B. A., Stoffers, D. A., and Mains, R. E. (1992). The Biosynthesis of Neuropeptides: Peptide a-Amidation. *Annu. Rev. Neurosci.*

Eldred, K. C., Hadyniak, S., Hussey, K., Brennerman, B., Zhnag, P., Chamling, X., et al. (2018). Thyroid hormone signaling specifies cone subtypes in human retinal organoids. *J. Chem. Inf. Model.* 53, 1689–1699. doi:10.1017/CBO9781107415324.004.

Elphick, M. R., and Mirabeau, O. (2014). The evolution and variety of RFamide-type neuropeptides: Insights from deuterostomian invertebrates. *Front. Endocrinol. (Lausanne).* 5, 1–11. doi:10.3389/fendo.2014.00093.

Elphick, M. R., Mirabeau, O., and Larhammar, D. (2018). Evolution of neuropeptide signalling systems. *J. Exp. Biol.* 221, jeb151092. doi:10.1242/jeb.151092.

Elphick, M. R., Price, D. A., Lee, T. D., and Thorndyke, M. C. (1991a). The SALMFamides : a new family of neuropeptides isolated from an echinoderm. *Proc. R. Soc. London* 243, 121–127.

Elphick, M. R., Reeve JR, J. R., Burke, R. D., and Thorndyke, M. C. (1991b). Isolation of the Neuropeptide SALMFamide-1 From Starfish Using a New Antiserum. *Peptides* 12, 455–459.

Elphick, M. R., and Rowe, M. L. (2009). NGFFFamide and echinotocin: structurally unrelated myoactive neuropeptides derived from neurophysin-containing precursors in sea urchins. *J. Exp. Biol.* 212, 1067–1077. doi:10.1242/jeb.027599.

Elphick, M. R., Semmens, D. C., Blowes, L. M., Levine, J., Lowe, C. J., Arnone, M. I., et al. (2015). Reconstructing SALMFamide neuropeptide precursor evolution in the phylum Echinodermata: Ophiuroid and crinoid sequence data provide new

insights. *Front. Endocrinol. (Lausanne).* 6, 1–10. doi:10.3389/fendo.2015.00002.

Erclik, T., Hartenstein, V., McInnes, R. R., and Lipshitz, H. D. (2009). Eye evolution at high resolution: The neuron as a unit of homology. *Dev. Biol.* 332, 70–79. doi:10.1016/j.ydbio.2009.05.565.

Erhardt, N. M., Fradinger, E. A., Cervini, L. A., Rivier, J. E., and Sherwood, N. M. (2001). Early Expression of Pituitary Adenylate Cyclase-Activating Polypeptide and Activation of its Receptor in Chick Neuroblasts *. *Endocrinology* 142, 1616–1625.

Eskandari, S., Loo, D. D. F., Dai, G., Levy, O., Wright, E. M., and Carrasco, N. (1997). Thyroid Na + /I − Symporter . *J. Biol. Chem.* 272, 27230–27238. doi:10.1074/jbc.272.43.27230.

Fernandez-Serra, M., Consales, C., Livigni, A., and Arnone, M. I. (2004). Role of the ERK-mediated signaling pathway in mesenchyme formation and differentiation in the sea urchin embryo. *Dev. Biol.* 268, 384–402. doi:10.1016/j.ydbio.2003.12.029.

Fire, A., Xu, S., Montgomery, M. K., Kostas, S. A., Driver, S. E., and Mello, C. C. (1998). 35888. *Nature* 391, 806–811.

Fredriksson, R., Lagerström, M. C., Lundin, L.-G., and Schiöth, H. B. (2003). The G-Protein-Coupled Receptors in the Human Genome Form Five Main Families. Phylogenetic Analysis, Paralogon Groups, and Fingerprints. *Mol. Pharmacol.* 63, 1256 LP – 1272. doi:10.1124/mol.63.6.1256.

Fröhlich, E., and Wahl, R. (2019). The forgotten effects of thyrotropin-releasing hormone: Metabolic functions and medical applications. *Front. Neuroendocrinol.* 52, 29–43. doi:10.1016/j.yfrne.2018.06.006.

Fuge, R., and Johnson, C. C. (1986). The geochemistry of iodine. *Environ. Geochem. Health* 8, 31–54. doi:10.1007/BF00146712.

Fukusumi, S., Ogi, K., Onda, H., and Hinuma, S. (1995). Distribution of thyrotropin-releasing hormone receptor mRNA in rat peripheral tissues. *Regul. Pept.* 57,

115–121. doi:10.1016/0167-0115(95)00026-8.

Gagnon, J. A., Valen, E., Thyme, S. B., Huang, P., Ahkmetova, L., Pauli, A., et al. (2014). Efficient mutagenesis by Cas9 protein-mediated oligonucleotide insertion and large-scale assessment of single-guide RNAs. *PLoS One* 9, 5–12. doi:10.1371/journal.pone.0098186.

Galas, L., Raoult, E., Tonon, M. C., Okada, R., Jenks, B. G., Castaño, J. P., et al. (2009). TRH acts as a multifunctional hypophysiotropic factor in vertebrates. *Gen. Comp. Endocrinol.* 164, 40–50. doi:10.1016/j.ygcen.2009.05.003.

Garner, S., Zysk, I., Byrne, G., Kramer, M., Moller, D., Taylor, V., et al. (2016). Neurogenesis in sea urchin embryos and the diversity of deuterostome neurogenic mechanisms. *Development* 143, 286–297. doi:10.1242/dev.124503.

Gershengorn, M. C., and Osman, R. (1996). Molecular and cellular biology of thyrotropin-releasing hormone receptors. *Physiol. Rev.* 76, 175–191. doi:10.1152/physrev.1996.76.1.175.

Gilbert, S. F. (2000). *Developmental biology*. 6th ed.

Glover, J. C., and Fritzsch, B. (2009). Brains of primitive chordates. *Encycl. Neurosci.*, 439–448. doi:10.1016/B978-008045046-9.00945-1.

Hall, J. D., and Lloyd, P. E. (1990). Involvement of pedal peptide in locomotion in Aplysia: Modulation of foot muscle contractions. *J. Neurobiol.* 21, 858–868. doi:10.1002/neu.480210604.

Hall, M. R., Kocot, K. M., Baughman, Kenneth, W., Fernandez-Valverde, S. L., Gauthier, M. E. A., Hatleberg, W. L., et al. (2017). The crown-of-thorns starfish genome as a guide for biocontrol of this coral reef pest. *Nature* 544, 231–234. doi:10.1038/nature22033.

Hamdoun, A., and Foltz, K. R. (2019). “Echinoderms, Part B,” in *Methods in Cell Biology*, 2–256.

Hansen, G. N., Williamson, M., and Grimmelikhuijzen, C. J. P. (2002). A new case of neuropeptide coexpression (RGamide and LWamides) in Hydra, found by whole-mount, two-color double-labeling in situ hybridization. *Cell Tissue Res.* 308, 157–165. doi:10.1007/s00441-002-0534-y.

Hartline, D. K. (2011). The evolutionary origins of glia. *Glia* 59, 1215–1236. doi:10.1002/glia.21149.

Herget, U., and Ryu, S. (2015). Coexpression analysis of nine neuropeptides in the neurosecretory preoptic area of larval zebrafish. *Front. Neuroanat.* 9, 1–11. doi:10.3389/fnana.2015.00002.

Hertwig, O. (1876). Beitragezurkenntniss der bildung, befruchtung und' theilung des thierischeneies. *Morph. Jb.* 1, 347–432.

Heyland, A. (2005). Cross-kingdom hormonal signaling: an insight from thyroid hormone functions in marine larvae. *J. Exp. Biol.* 208, 4355–4361. doi:10.1242/jeb.01877.

Heyland, A., Price, D. A., Bodnarova-Buganova, M., and Moroz, L. L. (2006). Thyroid Hormone Metabolism and Peroxidase Function in Two Non-choradate Animals. *J. Exp. Zool. (Mol Dev Evol)* 566, 642–654. doi:10.1002/jez.b.

Hinman, V. F., and Burke, R. D. (2018). Embryonic neurogenesis in echinoderms. *Wiley Interdiscip. Rev. Dev. Biol.* e316, 1–15. doi:10.1002/wdev.316.

Hinz, J. M., Laughery, M. F., and Wyrick, J. J. (2015). Nucleosomes Inhibit Cas9 Endonuclease Activity in Vitro. *Biochemistry* 54, 7063–7066. doi:10.1021/acs.biochem.5b01108.

Hirth, F., Kammermeier, L., Frei, E., Walldorf, U., Noll, M., and Reichert, H. (2003). An urbilaterian origin of the tripartite brain: Developmental genetic insights from Drosophila. *Development* 130, 2365–2373. doi:10.1242/dev.00438.

Hobert, O. (2010). Neurogenesis in the Nematode Caenorhabditis elegans. *WormBook.org*, 609–626. doi:10.1016/B978-0-12-397265-1.00115-5.

Hobert, O. (2016a). A map of terminal regulators of neuronal identity in Caenorhabditis elegans. *Wiley Interdiscip. Rev. Dev. Biol.* 5, 474–498. doi:10.1002/wdev.233.

Hobert, O. (2016b). A map of terminal regulators of neuronal identity in Caenorhabditis elegans. *WIREs Dev Biol* 5, 474–498. doi:10.1002/wdev.233.

Hobert, O., Carrera, I., and Stefanakis, N. (2010). The molecular and gene regulatory signature of a neuron. *Trends Neurosci.* 33, 435–445. doi:10.1016/j.tins.2010.05.006.

Hoekstra, L. A., Moroz, L. L., and Heyland, A. (2012). Novel Insights into the Echinoderm Nervous System from Histaminergic and FMRFaminergic-Like Cells in the Sea Cucumber Leptosynapta clarki. *PLoS One* 7. doi:10.1371/journal.pone.0044220.

Holland, L. Z. (2015). Evolution of basal deuterostome nervous systems. *J. Exp. Biol.* 218, 637–645. doi:10.1242/jeb.109108.

Holland, L. Z., Carvalho, J. E., Escriva, H., Laudet, V., Schubert, M., Shimeld, S. M., et al. (2013). Evolution of bilaterian central nervous systems: A single origin? *Evodevo* 4, 1–20. doi:10.1186/2041-9139-4-27.

Hollenberg, A. N., Monden, T., Flynn, T. R., Boers, M. E., Cohen, O., and Wondisford, F. E. (1995). The human thyrotropin-releasing hormone gene is regulated by thyroid hormone through two distinct classes of negative thyroid hormone response elements. *Mol. Endocrinol.* 9, 540–550. doi:10.1210/mend.9.5.7565802.

Hopkins, E. J., Layfield, S., Ferraro, T., Bathgate, R. A. D., and Gooley, P. R. (2007). The NMR solution structure of the relaxin (RXFP1) receptor lipoprotein receptor class A module and identification of key residues in the N-terminal region of the module that mediate receptor activation. *J. Biol. Chem.* 282, 4172–4184. doi:10.1074/jbc.M609526200.

Horlbeck, M. A., Witkowsky, L. B., Guglielmi, B., Replogle, J. M., Gilbert, L. A., Villalta, J. E., et al. (2016). Nucleosomes impede cas9 access to DNA in vivo and in vitro. *Elife* 5, 1–21. doi:10.7554/eLife.12677.

Hosoi, S., Sakuma, T., Sakamoto, N., and Yamamoto, T. (2014). Targeted mutagenesis in sea urchin embryos using TALENs. *Dev. Growth Differ.* 56, 92–97. doi:10.1111/dgd.12099.

Howard-Ashby, M., Materna, S. C., Brown, C. T., Chen, L., Cameron, R. A., and Davidson, E. H. (2006a). Gene families encoding transcription factors expressed in early development of Strongylocentrotus purpuratus. *Dev. Biol.* 300, 90–107. doi:10.1016/j.ydbio.2006.08.033.

Howard-Ashby, M., Materna, S. C., Brown, C. T., Chen, L., Cameron, R. A., and Davidson, E. H. (2006b). Identification and characterization of homeobox transcription factor genes in Strongylocentrotus purpuratus, and their expression in embryonic development. *Dev. Biol.* 300, 74–89. doi:10.1016/j.ydbio.2006.08.039.

Howard-Ashby, M., Materna, S. C., Brown, C. T., Tu, Q., Oliveri, P., Cameron, R. A., et al. (2006c). High regulatory gene use in sea urchin embryogenesis: Implications for bilaterian development and evolution. *Dev. Biol.* 300, 27–34. doi:10.1016/j.ydbio.2006.10.016.

Jager, M., Chiori, R., Alié, A., Dayraud, C., Quéinnec, E., and Manuel, M. (2011). New insights on ctenophore neural anatomy: Immunofluorescence study in Pleurobrachia pileus (Müller, 1776). *J. Exp. Zool. Part B Mol. Dev. Evol.* 316 B, 171–187. doi:10.1002/jez.b.21386.

Jagersten, G. (1972). *Evoluton of Metazoan Life Cycle. A Comprehensive Theory*.

Jékely, G. (2013). Global view of the evolution and diversity of metazoan neuropeptide signaling. *Proc. Natl. Acad. Sci. U. S. A.* 110, 8702–8707. doi:10.1073/pnas.1221833110.

Jékely, G., Paps, J., and Nielsen, C. (2015). The phylogenetic position of ctenophores and the origin(s) of nervous systems. *Evodevo* 6, 1. doi:10.1186/2041-9139-6-1.

Johnson, Z. V., and Young, L. J. (2017). Oxytocin and vasopressin neural networks: Implications for social behavioral diversity and translational neuroscience. *Neurosci. Biobehav. Rev.* 76, 87–98. doi:10.1016/j.neubiorev.2017.01.034.

Kim, H. Y., and Mohan, S. (2013). Role and Mechanisms of Actions of Thyroid Hormone on the Skeletal Development. *Bone Res.* 1, 146–161. doi:10.4248/BR201302004.

Kleinstiver, B. P., Pattanayak, V., Prew, M. S., Tasi, S. Q., Nguyen, N. T., Zheng, Z., et al. (2016). High-fidelity CRISPR-Cas9 nucleases with no detectable genome-wide off-target effects. *Nature* 529, 490–495. doi:10.1038/nature16526.

Knight, S. C., Xie, L., Deng, W., Guglielmi, B., Witkowsky, L. B., Bosanac, L., et al. (2015). Dynamics of CRISPR-Cas9 genome interrogation in living cells. *Science (80-.).* 350, 823–826. doi:10.1126/science.aac6572.

Koizumi, O., Hamada, S., Minobe, S., Hamaguchi-Hamada, K., Kurumata-Shigeto, M., Nakamura, M., et al. (2015). The nerve ring in cnidarians: Its presence and structure in hydrozoan medusae. *Zoology* 118, 79–88. doi:10.1016/j.zool.2014.10.001.

Konstantinides, N., Kapuralin, K., Fadil, C., Barboza, L., Satija, R., and Desplan, C. (2018). Phenotypic Convergence: Distinct Transcription Factors Regulate Common Terminal Features. *Cell* 174, 622-635.e13. doi:10.1016/j.cell.2018.05.021.

Kotwica-Rolinska, J., Krištofová, L., Chvalová, D., Pauchová, L., Provazník, J., Hejníková, M., et al. (2020). Functional analysis and localisation of a thyrotropin-releasing hormone-type neuropeptide (EFLa) in hemipteran insects: EFLa in Hemiptera. *Insect Biochem. Mol. Biol.* 122, 103376. doi:10.1016/j.ibmb.2020.103376.

Krishnan, A., and Schiöth, H. B. (2015). The role of G protein-coupled receptors in the early evolution of neurotransmission and the nervous system. *J. Exp. Biol.* 218, 562–571. doi:10.1242/jeb.110312.

Kudtarkar, P., and Cameron, R. A. (2017). Database update Echinobase : an expanding resource for echinoderm genomic information. *Database*, 1–9. doi:10.1093/database/bax074.

Kumar, S., Stecher, G., and Tamura, K. (2016). MEGA7: Molecular Evolutionary Genetics Analysis Version 7.0 for Bigger Datasets. *Mol. Biol. Evol.* 33, 1870–1874. doi:10.1093/molbev/msw054.

Lacalli, T. C. (1994). Apical Organs, Epithelial Domains, and the Origin of the Chordate Central Nervous System 1. 541, 533–541.

Lagerström, M. C., Fredriksson, R., Bjarnadóttir, T. K., Fridmanis, D., Holmquist, T., Andersson, J., et al. (2005). Origin of the prolactin-releasing hormone (PRLH) receptors: Evidence of coevolution between PRLH and a redundant neuropeptide Y receptor during vertebrate evolution. *Genomics* 85, 688–703. doi:10.1016/j.ygeno.2005.02.007.

Lagorce, J. F., Thomes, J. C., Catanzano, G., Buxeraud, J., Raby, M., and Raby, C. (1991). Formation of molecular iodine during oxidation of iodide by the peroxidase/H2O2 system. Implications for antithyroid therapy. *Biochem. Pharmacol.* 42, 0–3. doi:10.1016/0006-2952(91)90396-M.

Lapraz, F., Besnardeau, L., and Lepage, T. (2009). Patterning of the dorsal-ventral axis in echinoderms: Insights into the evolution of the BMP-chordin signaling network. *PLoS Biol.* 7. doi:10.1371/journal.pbio.1000248.

Leahy, P. S. (1986). Laboratory Culture of Strongylocentrotus Purpuratus Adults, Embryos, and Larvae. *Methods Cell Biol.* 27, 1–13.

Lerner, A. (2013). Development of sea urchin apical organ: cellular mappung of gene expression and FGF signalling. *PhD Diss.*

Lexow, N. (1996). Localisation and expression of Thyrotropin releasing hormone in rat and cat retina.

Leys, S. P. (2015). Elements of a “nervous system” in sponges. *J. Exp. Biol.* 218, 581–591. doi:10.1242/jeb.110817.

Leys, S. P., and Degnan, B. M. (2005). Embryogenesis and metamorphosis in a haplosclerid demosponge: gastrulation and transdifferentiation of larval ciliated cells to choanocytes. *Invertebr. Biol.* 121, 171–189. doi:10.1111/j.1744-7410.2002.tb00058.x.

Lin, C., and Su, Y. (2015). Genome editing in sea urchin embryos by using a CRISPR/Cas9 system. *Dev. Biol.* 409, 420–428. doi:10.1017/CBO9781107415324.004.

Lin, M., Egertov, M., Alexandra, G. Z., and Elphick, M. R. (2018). Functional characterization of a second pedal peptide / orcokinin-type neuropeptide signaling system in the starfish Asterias rubens. 858–876. doi:10.1002/cne.24371.

Lin, M., Egertová, M., Zampronio, C. G., Jones, A. M., and Elphick, M. R. (2017). Pedal peptide/orcokinin-type neuropeptide signaling in a deuterostome: The anatomy and pharmacology of starfish myorelaxant peptide in Asterias rubens. *J. Comp. Neurol.* 525, 3890–3917. doi:10.1002/cne.24309.

Lin, Y. T., and Chen, J. C. (2019). Neuropeptide ff modulates neuroendocrine and energy homeostasis through hypothalamic signaling. *Chin. J. Physiol.* 62, 47–52. doi:10.4103/CJP.CJP_23_19.

Liu, G., Yin, K., Zhang, Q., Gao, C., and Qiu, J.-L. (2019). Modulating chromatin accessibility by transactivation and targeting proximal dsgRNAs enhances Cas9 editing efficiency in vivo. *Genome Biol.* 20, 1–11. doi:10.1186/s13059-019-1762-8.

Liu, X., Homma, A., Sayadi, J., Yang, S., Ohashi, J., and Takumi, T. (2016). Sequence

features associated with the cleavage efficiency of CRISPR/Cas9 system. *Sci. Rep.* 6, 1–9. doi:10.1038/srep19675.

Lovejoy, D. A. (2005). *Neuroendocrinology: An Integrated Approach*. doi:10.1002/0470027878.

Lovejoy, D. A., and Balment, R. J. (1999). Evolution and physiology of the corticotropin-releasing factor (CRF) family of neuropeptides in vertebrates. *Gen. Comp. Endocrinol.* 115, 1–22. doi:10.1006/gcen.1999.7298.

Lovejoy, D. A., Chang, B. S. W., Lovejoy, N. R., and del Castillo, J. (2014). Molecular evolution of GPCRs: CRH/CRH receptors. *J. Mol. Endocrinol.* 52. doi:10.1530/JME-13-0238.

Lowe, C. J., Wu, M., Salic, A., Evans, L., Lander, E., Stange-Thomann, N., et al. (2003). Anteroposterior patterning in hemichordates and the origins of the chordate nervous system. *Cell* 113, 853–865. doi:10.1016/S0092-8674(03)00469-0.

Mackie, G. O. (2004). Central Neural Circuitry in the Jellyfish Aglantha: A Model "Simple Nervous System." *NeuroSignals* 13, 5–19. doi:10.1159/000076155.

Mali, P., Yang, L., Esvelt, K. M., Aach, J., Guell, M., DiCarlo, J. E., et al. (2013). RNA-guided human genome engineering via Cas9. *Science (80-.).* 339, 823–826. doi:10.1126/science.1232033.

Marlow, H. Q., Srivastava, M., Matus, D. Q., Rokhsar, D., and Martindale, M. Q. (2009). Anatomy and development of the nervous system of Nematostella vectensis, an anthozoan cnidarian. *Dev. Neurobiol.* 69, 235–254. doi:10.1002/dneu.20698.

Marlow, H., Tosches, M. A., Tomer, R., Steinmetz, P. R., Lauri, A., Larsson, T., et al. (2014). Larval body patterning and apical organs are conserved in animal evolution. 1–17.

Mashanov, V. S., Zueva, O. R., Heinzeller, T., Aschauer, B., and Dolmatov, I. Y. (2007). Developmental origin of the adult nervous system in a holothurian: An attempt

to unravel the enigma of neurogenesis in echinoderms. *Evol. Dev.* 9, 244–256. doi:10.1111/j.1525-142X.2007.00157.x.

Mashanov, V. S., Zueva, O. R., Heinzeller, T., Aschauer, B., Naumann, W. W., Grondona, J. M., et al. (2009). The central nervous system of sea cucumbers (Echinodermata: Holothuroidea) shows positive immunostaining for a chordate glial secretion. *Front. Zool.* 6, 1–15. doi:10.1186/1742-9994-6-11.

Mashanov, V. S., Zueva, O. R., Heinzeller, T., and Dolmatov, I. Y. (2006). Ultrastructure of the circumoral nerve ring and the radial nerve cords in holothurians (Echinodermata). *Zoomorphology* 125, 27–38. doi:10.1007/s00435-005-0010-9.

Mashanov, V., and Zueva, O. (2018). Radial Glia in Echinoderms. *Dev. Neurobiol.* 79, 396–405. doi:10.1002/dneu.22659.

Masland, R. H. (2004). Neuronal cell types. *Curr. Biol.* 14, 497–500.

Materna, S. C., and Oliveri, P. (2008). A protocol for unraveling gene regulatory networks. *Nat. Protoc.* 3, 1876–1887. doi:10.1038/nprot.2008.187.

Mathers, P. H., Grinberg, A., Mahon, K. A., and Jamrich, M. (1997). The Rx homeobox gene is essential for vertebrate eye development. *Nature* 387, 603–607. doi:10.1038/42475.

Mayorova, T. D., Tian, S., Cai, W., Semmens, D. C., Odekunle, E. A., Zandawala, M., et al. (2016). Localization of Neuropeptide Gene Expression in Larvae of an Echinoderm, the Starfish Asterias rubens. *Front. Neurosci.* 10, 1–18. doi:10.3389/fnins.2016.00553.

Mcclay, D. R., Miranda, E., and Feinberg, S. L. (2018). Neurogenesis in the sea urchin embryo is initiated uniquely in three domains. *Development*. doi:10.1242/dev.167742.

McCudden, C. R., Hains, M. D., Kimple, R. J., Siderovski, D. P., and Willard, F. S. (2005). G-protein signaling: Back to the future. *Cell. Mol. Life Sci.* 62, 551–577. doi:10.1007/s00018-004-4462-3.

McDougall, C., Chen, W. C., Shimeld, S. M., and Ferrier, D. E. K. (2006). The development of the larval nervous system, musculature and ciliary bands of Pomatoceros lamarckii (Annelida): Heterochrony in polychaetes. *Front. Zool.* 3, 1–14. doi:10.1186/1742-9994-3-16.

Meinertzhagen, I. A. (2019). *Morphology of Invertebrate Neurons and Synapses*. doi:10.1093/oxfordhb/9780190456757.013.9.

Mellott, D. O., Thisdelle, J., and Burke, R. D. (2017). Notch signalling patterns neurogenic ectoderm and regulates the asymmetric division of neural progenitors in sea urchin embryos. *Development*, 3602–3611. doi:10.1242/dev.151720.

Menschaert, G., Vandekerckhove, T. T. M., Baggerman, G., Landuyt, B., Sweedler, J. V, Schoofs, L., et al. (2010). A Hybrid , de Novo Based , Genome-Wide Database Search Approach Applied to the Sea Urchin Neuropeptidome. *J. Proteome Res.* 9, 990–996.

Miguel, M. De, Utrilla, J. C., Borrero, J., Conde, E., and Guerrero, J. M. (2005). Thyrotropin-releasing hormone receptor expression in thyroid follicular cells : a new paracrine role of C-cells ? 713–718.

Miller, A. E. M., and Heyland, A. (2013). Iodine accumulation in sea urchin larvae is dependent on peroxide. *J. Exp. Biol.* 216, 915–926. doi:10.1242/jeb.077958.

Minokawa, T., Rast, J. P., Arenas-mena, C., Franco, C. B., and Davidson, E. H. (2004). Expression patterns of four different regulatory genes that function during sea urchin development. *Gene Expr. Patterns* 4, 449–456. doi:10.1016/j.modgep.2004.01.009.

Mirabeau, O., and Joly, J.-S. (2013). Molecular evolution of peptidergic signaling systems in bilaterians. *PNAS* 110, E2028-37. doi:10.1073/pnas.1219956110.

Mita, M., Oka, H., Thorndyke, M. C., Shibata, Y., Yoshikuni, M., and Nagahama, Y. (2004). Inhibitory Effect of a SALMFamide Neuropeptide on Secretion of Gonad-

Stimulating Substance from Radial Nerves in the Starfish Asterina pectinifera. *Zoolog. Sci.* 21, 299–303. doi:10.2108/zsj.21.299.

Molina, M. D., de Crozé, N., Haillot, E., and Lepage, T. (2013). Nodal: Master And Commander Of The Dorsal-Ventral And Left-Right Axes In The Sea Urchin Embryo. *Curr. Opin. Genet. Dev.* 23, 445–453. doi:10.1016/j.gde.2013.04.010.

Monroe, E. B., Annangudi, S. P., Wadhams, A. A., Richmond, T. A., Yang, N., Southey, B. R., et al. (2018). Exploring the Sea Urchin Neuropeptide Landscape by Mass Spectrometry. *J. Am. Soc. Mass. Spectrom.* 29, 923–934. doi:10.1007/s13361-018-1898-x.

Moroz, L. L. (2009). On the independent origins of complex brains and neurons. *Brain. Behav. Evol.* 74, 177–190. doi:10.1159/000258665.

Moroz, L. L., Kocot, K. M., Citarella, M. R., Dosung, S., Norekian, T. P., Povolotskaya, I. S., et al. (2014). The ctenophore genome and the evolutionary origins of neural systems. *Nature* 510, 109–114. doi:10.1038/nature13400.

Musser, J. M., and Arendt, D. (2017). Loss and gain of cone types in vertebrate ciliary photoreceptor evolution. *Dev. Biol.* 431, 26–35. doi:10.1016/j.ydbio.2017.08.038.

Nakabayashi, K., Matsumi, H., Bhalla, A., Bae, J., Mosselman, S., Yu Hsu, S., et al. (2002). Thyrostimulin, a heterodimer of two new hunan glycoprotein hormone subunits, actiovates the thyroid-stimulaing hormone receptor. *J. Clin. Invest.* 109, 1445–1452. doi:10.1172/JCI200214340.Introduction.

Nakajima, Y., Humphreys, T., Kaneko, H., and Tagawa, K. (2004a). Development and Neural Organization of the Tornaria Larva of the Hawaiian Hemichordate, Ptychodera flava. *Zoolog. Sci.* 21, 69–78. doi:10.2108/zsj.21.69.

Nakajima, Y., Kaneko, H., Murray, G., and Burke, R. D. (2004b). Divergent patterns of neural development in larval echinoids and asteroids. *Evol. Dev.* 6, 95–104.

Nakanishi, N., Martindale, M. Q., and States, U. (2018). CRISPR knockouts reveal an

endogenous role for ancient neuropeptides in regulating developmental timing in a sea anemone. *Elife*, 1–16. doi:10.7554/eLife.39742.

Nemer, M., Rondinelli, E., Infante, D., and Infante, A. A. (1991). Polyubiquitin RNA Characteristics and Conditional Induction in Sea Urchin Embryos. *Dev. Biol.* 145, 255–265.

Nezlin, L. P., and Yushin, V. V. (2004). Structure of the nervous system in the tornaria larva of Balanoglossus proterogonius (Hemichordata: Enteropneusta) and its phylogenetic implicationa. *Zoomorphology*, 1–13.

Ng, L., Hurley, J. B., Dierks, B., Srinivas, M., Saltó, C., Vennström, B., et al. (2001). A thyroid hormone receptor that is required for the development of green cone photoreceptors. *Nat. Genet.* 27, 94–98. doi:10.1038/83829.

Nielsen, C. (1999). Origin of the chordate central nervous system and the origin of chordates. *Dev. Genes Evol.* 209, 198–205. doi:10.1007/s004270050244.

Nielsen, C. (2012). How to make a protostome. *Invertebr. Syst.* 26, 25–40. doi:10.1071/IS11041.

Nielsen, C. (2015). Larval nervous systems: true larval and precocious adult. *J. Exp. Biol.* 218, 629–636. doi:10.1242/jeb.109603.

Nikitin, M. (2015). Bioinformatic prediction of Trichoplax adhaerens regulatory peptides. *Gen. Comp. Endocrinol.* 212, 145–155. doi:10.1016/j.ygcen.2014.03.049.

Niven, J. E., Graham, C. M., and Burrows, M. (2008). Diversity and Evolution of the Insect Ventral Nerve Cord. *Annu. Rev. Entomol.* 53, 253–271. doi:10.1146/annurev.ento.52.110405.091322.

O'Connor, C., and Adams, J. U. (2010). *Essentials of Cell Biology*. Cambridge: NPG Education.

Ochiai, H., Fujita, K., Suzuki, K. I., Nishikawa, M., Shibata, T., Sakamoto, N., et al.

(2010). Targeted mutagenesis in the sea urchin embryo using zinc-finger nucleases. *Genes to Cells* 15, 875–885. doi:10.1111/j.1365-2443.2010.01425.x.

Odekunle, E. A., Semmens, D. C., Martynyuk, N., Tinoco, A. B., Garewal, A. K., Patel, R. R., et al. (2019). Ancient role of vasopressin / oxytocin-type neuropeptides as regulators of feeding revealed in an echinoderm. 1–23.

Ohmichi, M., Sawada, T., Kanda, Y., Koike, K., Hirota, K., Miyake, A., et al. (1994). Thyrotropin-releasing hormone stimulates MAP kinase activity in GH3 cells by divergent pathways. Evidence of a role for early tyrosine phosphorylation. *J. Biol. Chem.* 269, 3783–3788.

Oliveri, P., and Davidson, E. H. (2004). Gene Regulatory Network Analysis in Sea Urchin Embryos. *Methods Cell Biol.* 74, 775–794.

Oliveri, P., Tu, Q., and Davidson, E. H. (2008). Global regulatory logic for specification of an embryonic cell lineage. *PNAS* 105, 5955–5962.

Oliveri, P., Walton, K. D., Davidson, E. H., and Mcclay, D. R. (2006). Repression of mesodermal fate by foxa , a key endoderm regulator of the sea urchin embryo. *Development* 133, 4173–4181. doi:10.1242/dev.02577.

Omasits, U., Ahrens, C. H., Müller, S., and Wollscheid, B. (2014). Protter: Interactive protein feature visualization and integration with experimental proteomic data. *Bioinformatics* 30, 884–886. doi:10.1093/bioinformatics/btt607.

Otim, O., Amore, G., Minokawa, T., Mcclay, D. R., and Davidson, E. H. (2004). SpHnf6 , a transcription factor that executes multiple functions in sea urchin embryogenesis. 273, 226–243. doi:10.1016/j.ydbio.2004.05.033.

Oulhen, N., and Wessel, G. M. (2016). Albinism as a visual, in vivo guide for CRISPR/Cas9 functionality in the sea urchin embryo. *Mol. Reprod. Dev.* doi:10.1002/mrd.22757.

Perillo, M. (2013). Evolutionary Origin and Diversification of Pancreatic Cell Types.

Perillo, M., and Arnone, M. I. (2014). Characterization of insulin-like peptides (ILPs) in the sea urchin Strongylocentrotus purpuratus: Insights on the evolution of the insulin family. *Gen. Comp. Endocrinol.* 205, 68–79. doi:10.1016/j.ygcen.2014.06.014.

Perillo, M., Paganos, P., Cocurullo, M., Mattiello, T., Oliveri, P., and Arnone, M. I. (2018). New neuronal subtypes with a pancreatic-like signature in the sea urchin Stongylocentrotus purpuratus. *Front. Endocrinol. (Lausanne).*

Perillo, M., Wang, Y. J., Leach, S. D., and Arnone, M. I. (2016). A pancreatic exocrine-like cell regulatory circuit operating in the upper stomach of the sea urchin Strongylocentrotus purpuratus larva. *BMC Evol. Biol.* 16, 1–15. doi:10.1186/s12862-016-0686-0.

Peter, I. S., and Davidson, E. H. (2011). Evolution of gene regulatory networks controlling body plan development. *Cell* 144, 970–985. doi:10.1016/j.cell.2011.02.017.

Petrone, L. (2015). Circadian clock and light input system in the sea urchin larva. *PhD Diss.*

Pfleger, J., Gresham, K., and Koch, W. J. (2019). G protein-coupled receptor kinases as therapeutic targets in the heart. *Nat. Rev. Cardiol.* 16, 612–622. doi:10.1038/s41569-019-0220-3.

Power, D. M., Elias, N. P., Richardson, S. J., Mendes, J., Soares, C. M., and Santos, C. R. A. (2000). Evolution of the thyroid hormone-binding protein, transthyretin. *Gen. Comp. Endocrinol.* 119, 241–255. doi:10.1006/gcen.2000.7520.

Quiroga Artigas, G., Lapébie, P., Leclère, L., Takeda, N., Deguchi, R., Jékely, G., et al. (2018). A gonad-expressed opsin mediates light-induced spawning in the jellyfish clytia. *Elife* 7. doi:10.7554/eLife.29555.

Raff, R. A., and Byrne, M. (2006). The active evolutionary lives of echinoderm larvae. *Heredity (Edinb).* 97, 244–252. doi:10.1038/sj.hdy.6800866.

Raible, F., Tessmar-Raible, K., Arboleda, E., Kaller, T., Bork, P., Arendt, D., et al. (2006). Opsins and clusters of sensory G-protein-coupled receptors in the sea urchin genome. *Dev. Biol.* 300, 461–475. doi:10.1016/j.ydbio.2006.08.070.

Ransick, A., Rast, J. P., Minokawa, T., Calestani, C., and Davidson, E. H. (2002). New Early Zygotic Regulators Expressed in Endomesoderm of Sea Urchin Embryos Discovered by Differential Array Hybridization. *Dev. Biol.* 246, 132–147.

Rast, J. P., Amore, G., Calestani, C., Livi, C. B., Ransick, A., and Davidson, E. H. (2000). Recovery of Developmentally Define Gene Sets from High-Density cDNA Macroarrays. *Dev. Biol.* 228, 270–286.

Re, R. N., and Cook, J. L. (2006). The intracrine hypothesis: An update. *Regul. Pept.* 133, 1–9. doi:10.1016/j.regpep.2005.09.012.

Reich, A., Dunn, C., Akasaka, K., and Wessel, G. (2015). Phylogenomic analyses of echinodermata support the sister groups of Asterozoa and Echinozoa. *PLoS One* 10, 1–11. doi:10.1371/journal.pone.0119627.

Reichert, H., and Simeone, A. (2001). Developmental genetic evidence for a monophyletic origin of the bilaterian brain. *Philos. Trans. R. Soc. B Biol. Sci.* 356, 1533–1544. doi:10.1098/rstb.2001.0972.

Richter, S., Brenneis, G., Fritsch, M., Møller, O. S., Stegner, M. E. J., Loesel, R., et al. (2010). Invertebrate neurophylogeny: Suggested terms and definitions for a neuroanatomical glossary. *Front. Zool.* 7, 1–49. doi:10.1186/1742-9994-7-29.

Roch, G. J., Busby, E. R., and Sherwood, N. M. (2011). Evolution of GnRH: Diving deeper. *Gen. Comp. Endocrinol.* 171, 1–16. doi:10.1016/j.ygcen.2010.12.014.

Roch, G. J., and Sherwood, N. M. (2014). Glycoprotein Hormones and Their Receptors Emerged at the Origin of Metazoans. *Genome Biol. Evol.* 6, 1466–1479. doi:10.1093/gbe/evu118.

Röttinger, E., Besnardeau, L., and Lepage, T. (2004). A Raf/MEK/ERK signaling pathway is required for development of the sea urchin embryo micromere

lineage through phosphorylation of the transcription factor Ets. *Development* 131, 1075–1087. doi:10.1242/dev.01000.

Röttinger, E., Saudemont, A., Duboc, V., Besnardeau, L., Mcclay, D., Lepage, T., et al. (2007). FGF signals guide migration of mesenchymal cells, controlskeletal morphogenesis of the skeleton and regulategastrulation during sea urchin development. 785, 1–14. doi:10.1242/dev.020016.

Rowe, M. L., Achhala, S., and Elphick, M. R. (2014). Neuropeptides and polypeptide hormones in echinoderms: New insights from analysis of the transcriptome of the sea cucumber Apostichopus japonicus. *Gen. Comp. Endocrinol.* 197, 43–55. doi:10.1016/j.ygcen.2013.12.002.

Rowe, M. L., and Elphick, M. R. (2010). Discovery of a second SALMFamide gene in the sea urchin Strongylocentrotus purpuratus reveals that L-type and F-type SALMFamide neuropeptides coexist in an echinoderm species. *Mar. Genomics* 3, 91–97. doi:10.1016/j.margen.2010.08.003.

Rowe, M. L., and Elphick, M. R. (2012). The neuropeptide transcriptome of a model echinoderm, the sea urchin Strongylocentrotus purpuratus. Elsevier Inc. doi:10.1016/j.ygcen.2012.09.009.

Royo, J. L., Maeso, I., Irimia, M., Gao, F., Peter, I. S., Lopes, C. S., et al. (2011). Transphyletic conservation of developmental regulatory state in animal evolution. *Proc. Natl. Acad. Sci. U. S. A.* 108, 14186–14191. doi:10.1073/pnas.1109037108.

Rozen, S., and Skaletsky, H. (1999). “Primer3 on the WWW for General Users and for Biologist Programmers,” in *Bioinformatics Methods and Protocols*, eds. S. Misener and S. A. Krawetz (Totowa, NJ: Humana Press), 365–386. doi:10.1385/1-59259-192-2:365.

Ryan, J. F. (2014). Did the ctenophore nervous system evolve independently? *Zoology* 117, 225–226. doi:10.1016/j.zool.2014.06.001.

Ryan, J. F., Pang, K., Schnitzler, C. E., Nguyen, A. D., Moreland, R. T., Simmons, D. K., et al. (2013). The genome of the ctenophore Mnemiopsis leidyi and its implications for cell type evolution. *Science (80-.).* 342. doi:10.1126/science.1242592.

Samanta, M. P. (2006). The transcriptome of the sea urchin embryo. *Science (80-.).* 314, 960–962. Available at: http://dx.doi.org/10.1126/science.1131898.

Schafer, W. (2016). Nematode nervous systems. *Curr. Biol.* 26, R955–R959. doi:10.1016/j.cub.2016.07.044.

Scott, D. J., Wilkinson, T., Tregear, G. W., and Bathgate, R. A. D. (2003). The relaxin peptide family and their novel G-protein coupled receptors. *Lett. Pept. Sci.* 10, 393–400. doi:10.1007/BF02442569.

Semmens, D. C., Beets, I., Rowe, M. L. M., Blowes, L. M. L., Oliveri, P., and Elphick, M. R. M. (2015). Discovery of sea urchin NGFFFamide receptor unites a bilaterian neuropeptide family. *Open Biol.* 5, 150030. doi:10.1098/rsob.150030.

Semmens, D. C., Mirabeau, O., Moghul, I., Pancholi, M. R., Wurm, Y., and Elphick, M. R. M. (2016). Transcriptomic identification of starfish neuropeptide precursors yields new insights into neuropeptide evolution. *Open Biol.* 6. doi:10.1098/rsob.150224.

Senatore, A., Reese, T. S., and Smith, C. L. (2017). Neuropeptidergic integration of behavior in Trichoplax adhaerens , an animal without synapses. *J. Exp. Biol.* 220, 3381–3390. doi:10.1242/jeb.162396.

Serrano-Saiz, E., Poole, R. J., Felton, T., Zhang, F., De La Cruz, E. D., and Hobert, O. (2013). XModular control of glutamatergic neuronal identity in C. elegans by distinct homeodomain proteins. *Cell* 155, 659. doi:10.1016/j.cell.2013.09.052.

Shashikant, T., Khor, J. M., and Ettensohn, C. A. (2018). Global analysis of primary mesenchyme cell cis-regulatory modules by chromatin accessibility profiling. *BMC Genomics* 19, 1–18. doi:10.1186/s12864-018-4542-z.

Shea Yu Hsu, Kudo, M., Chen, T., Nakabayashi, K., Bhalla, A., Van der Spek, P. J., et al. (2000). The three subfamilies of leucine-rich repeat-containing G protein-coupled receptors (LGR): Identification of LGR6 and LGR7 and the signaling mechanism for LGR7. *Mol. Endocrinol.* 14, 1257–1271. doi:10.1210/me.14.8.1257.

Shen, B., Zhang, J., Wu, H., Wang, J., Ma, K., Li, Z., et al. (2013). Generation of gene-modified mice via Cas9/RNA-mediated gene targeting. *Cell Res.* 23, 720–723. doi:10.1038/cr.2013.46.

Sherwood, N. M., and Wu, S. (2005). Developmental role of GnRH and PACAP in a zebrafish model. *Gen. Comp. Endocrinol.* 142, 74–80. doi:10.1016/j.ygcen.2005.02.007.

Shevidi, S., Uchida, A., Schudrowitz, N., Wessel, G. M., and Yajima, M. (2017). Single Nucleotide Editing Without DNA Cleavage Using CRISPR/Cas9-deaminase in the Sea Urchin Embryo. *Dev. Dyn.* 246, 1036–1046. doi:10.1002/dvdy.24586.

Shigeno, S., Andrews, P. L. R., Ponte, G., and Fiorito, G. (2018). Cephalopod brains: An overview of current knowledge to facilitate comparison with vertebrates. *Front. Physiol.* 9, 1–16. doi:10.3389/fphys.2018.00952.

Sinay, E. Van, Mirabeau, O., Depuydt, G., Boris, M., Hiel, V., Peymen, K., et al. (2017). Evolutionarily conserved TRH neuropeptide pathway regulates growth in Caenorhabditis elegans. *PNAS*, 4065–4074. doi:10.1073/pnas.1617392114.

Skinner, J. A., Campbell, E. J., Dayas, C. V., Garg, M. L., and Burrows, T. L. (2019). The relationship between oxytocin, dietary intake and feeding: A systematic review and meta-analysis of studies in mice and rats. *Front. Neuroendocrinol.* 52, 65–78. doi:10.1016/j.yfrne.2018.09.002.

Slota, L. A., and Mcclay, D. R. (2018). Identi fi cation of neural transcription factors required for the di ff erentiation of three neuronal subtypes in the sea urchin embryo. *Dev. Biol.* 435, 138–149. doi:10.1016/j.ydbio.2017.12.015.

Slota, L. A., Miranda, E. M., and McClay, D. R. (2019). Spatial and temporal patterns of gene expression during neurogenesis in the sea urchin Lytechinus variegatus. *Evodevo* 10, 1–16. doi:10.1186/s13227-019-0115-8.

Smarandache-Wellmann, C. R. (2016). Arthropod neurons and nervous system. *Curr. Biol.* 26, R960–R965. doi:10.1016/j.cub.2016.07.063.

Smith, C. L., Kittelmann, M., Azzam, R. N., Cooper, B., Winters, C. A., Eitel, M., et al. (2014). Article Novel Cell Types , Neurosecretory Cells , and Body Plan of the Early-Diverging Metazoan Trichoplax adhaerens. 1565–1572. doi:10.1016/j.cub.2014.05.046.

Smith, M. M., Smith, L. C., Cameron, R. A., and Urry, L. A. (2008). The larval stages of the sea urchin, Strongylocentrotus purpuratus. *J. Morphol.* 269, 713–733. doi:10.1002/jmor.10618.

Sodergren, E., Martinez, P., Materna, S. C., Nam, J., Oliveri, P., Rizzo, F., et al. (2006). The Genome of the Sea Urchin Strongylocentrotus purpuratus. *Science (80-.).* 314, 941–952. doi:10.1126/science.1133609.The.

Spetter, M. S., and Hallschmid, M. (2017). Current findings on the role of oxytocin in the regulation of food intake. *Physiol. Behav.* 176, 31–39. doi:10.1016/j.physbeh.2017.03.007.

Srivastava, M., Begovic, E., Chapman, J., Putnam, N. H., Hellsten, U., Kawashima, T., et al. (2008). The Trichoplax genome and the nature of placozoans. doi:10.1038/nature07191.

Stefanakis, N., Carrera, I., and Hobert, O. (2015). Regulatory logic of pan-neuronal gene expression in C. elegans. *Neuron* 84, 733–750. doi:10.1016/j.physbeh.2017.03.040.

Steiner, D. F. (1998). The proprotein convertases. *Curr. Opin. Chem. Biol.* 2, 31–39. doi:10.1016/S1367-5931(98)80033-1.

Strathmann, R. R. (1971). The feeding behaviour of planktotrophic echinoderm

larvae: mechanisms, regulation and rates of suspension-feeding. *J. exp. mar. Biol. Ecol* 6, 109–160. doi:10.1063/1.5066465.

Su, Y. H., Li, E., Geiss, G. K., Longabaugh, W. J. R., Krämer, A., and Davidson, E. H. (2009). A perturbation model of the gene regulatory network for oral and aboral ectoderm specification in the sea urchin embryo. *Dev. Biol.* 329, 410–421. doi:10.1016/j.ydbio.2009.02.029.

Sudo, S., Kuwabara, Y., Park, J. Il, Sheau, Y. H., and Hsueh, A. J. W. (2005). Heterodimeric fly glycoprotein hormone-α2 (GPA2) and glycoprotein hormone-β5 (GPB5) activate fly leucine-rich repeat-containing G protein-coupled receptor-1 (DLGR1) and stimulation of human thyrotropin receptors by chimeric fly GPA2 and human GPB5. *Endocrinology* 146, 3596–3604. doi:10.1210/en.2005-0317.

Summerton, J. (2007). Morpholino, siRNA, and S-DNA Compared: Impact of Structure and Mechanism of Action on Off-Target Effects and Sequence Specificity. *Curr. Top. Med. Chem.* 7, 651–660. doi:10.2174/156802607780487740.

Sun, Y., Lu, X., and Gershengorn, M. C. (2000). G PROTEIN-COUPLED RECEPTOR SIGNALLING IN NEUROENDOCRINE SYSTEMS Thyrotropin-releasing hormone receptors – similarities and differences. *J. Mol. Endocrinol.*, 87–90.

Sun, Z., and Ettensohn, C. A. (2014). Signal-dependent regulation of the sea urchin skeletogenic gene regulatory network. *Gene Expr. Patterns* 16, 93–103. doi:10.1016/j.gep.2014.10.002.

Swanson, L. W. (2012). Basic Plan of the Nervous System. Iconoclast To Icon. *Fundam. Neurosci. Fourth Ed.*, 15–38. doi:10.1016/B978-0-12-385870-2.00002-0.

Takacs, C. M., Amore, G., Oliveri, P., Poustka, A. J., Wang, D., Burke, R. D., et al. (2004). Expression of an NK2 homeodomain gene in the apical ectoderm defines a new territory in the early sea urchin embryo. *Dev. Biol.* 269, 152–164. doi:10.1016/j.ydbio.2004.01.023.

Takahashi, T., and Holland, P. W. H. (2004). Amphioxus and ascidian Dmbx homeobox genes give clues to the vertebrate origins of midbrain development. *Development* 131, 3285–3294. doi:10.1242/dev.01201.

Talbot, J. C., and Amacher, S. L. (2014). A streamlined CRISPR pipeline to reliably generate zebrafish frameshifting alleles. *Zebrafish* 11, 583–585. doi:10.1089/zeb.2014.1047.

Taupenot, L., Harper, K. L., and O'Connor, D. T. (2003). The Chromogranin–Secretogranin Family. *N. Engl. J. Med.* 348, 1134–1149.

Taylor, E., and Heyland, A. (2017). Evolution of thyroid hormone signaling in animals: Non-genomic and genomic modes of action. *Mol. Cell. Endocrinol.* 459, 14–20. doi:10.1016/j.mce.2017.05.019.

Taylor, E., and Heyland, A. (2018). Thyroid Hormones Accelerate Initiation of Skeletogenesis via MAPK (ERK1/2) in Larval Sea Urchins (Strongylocentrotus purpuratus). *Front. Endocrinol. (Lausanne).* 9, 1–16. doi:10.3389/fendo.2018.00439.

Telford, M. J., Lowe, C. J., Cameron, C. B., Ortega-martinez, O., Aronowicz, J., Oliveri, P., et al. (2014). Phylogenomic analysis of echinoderm class relationships supports Asterozoa. *Proc. R. Soc. B* 281.

Temereva, E., and Wanninger, A. (2012). Development of the nervous system in Phoronopsis harmeri (Lophotrochozoa, Phoronida) reveals both deuterostome- and trochozoan-like features. *BMC Evol. Biol.* 12. doi:10.1186/1471-2148-12-121.

Thiel, D., Bauknecht, P., Jeákely, G., and Hejnol, A. (2017). An ancient FMRFamide-related peptide-receptor pair induces defence behaviour in a brachiopod larva. *Open Biol.* 7. doi:10.1098/rsob.170136.

Thiel, D., Bauknecht, P., Jékely, G., and Hejnol, A. (2019). A nemertean excitatory peptide/CCHamide regulates ciliary swimming in the larvae of Lineus

longissimus. *Front. Zool.* 16, 1–24. doi:10.1186/s12983-019-0326-9.

Tian, S., Egertová, M., and Elphick, M. R. (2017). Functional characterization of paralogous gonadotropin-releasing hormone-type and corazonin-type neuropeptides in an echinoderm. *Front. Endocrinol. (Lausanne).* 8. doi:10.3389/fendo.2017.00259.

Tosches, M. A., Yamawaki, T. M., Naumann, R. K., Jacobi, A. A., Tushev, G., and Laurent, G. (2018). Evolution of pallium, hippocampus, and cortical cell types revealed by single-cell transcriptomics in reptiles. *Science (80-.).* 360, 881–888. doi:10.1126/science.aar4237.

Trifinopoulos, J., Nguyen, L. T., von Haeseler, A., and Minh, B. Q. (2016). W-IQ-TREE: a fast online phylogenetic tool for maximum likelihood analysis. *Nucleic Acids Res.* 44, W232–W235. doi:10.1093/nar/gkw256.

Tu, Q., Brown, C. T., Davidson, E. H., and Oliveri, P. (2006). Sea urchin Forkhead gene family : Phylogeny and embryonic expression. 300, 49–62. doi:10.1016/j.ydbio.2006.09.031.

Tu, Q., Cameron, R. A., and Davidson, E. H. (2014a). Quantitative developmental transcriptomes of the sea urchin Strongylocentrotus purpuratus. *Dev. Biol.* 385, 160–167. doi:10.1016/j.ydbio.2013.11.019.

Tu, Q., Cameron, R. A., Worley, K. C., Gibbs, R. A., and Davidson, E. H. (2012). Gene structure in the sea urchin Strongylocentrotus purpuratus based on transcriptome analysis. *Genome Res.* 22, 2079–2087. doi:10.1101/gr.139170.112.

Tu, Q., R. Cameron, A., and Davidson, and E. H. (2014b). Quantitative developmental transcriptomes of the sea urchin Strongylocentrotus purpuratus. *Dev Biol* 385, 160–167. doi:10.1016/j.ydbio.2013.11.019.Quantitative.

Vacquier, V. D., and Moy, G. W. (1977). Isolation of bindin: The protein responsible for adhesion of sperm to sea urchin eggs. *Proc. Natl. Acad. Sci. U. S. A.* 74, 2456–

2460. doi:10.1073/pnas.74.6.2456.

Valencia, J. E., Feuda, R., Mellott, D. O., and Burke, R. D. (2019). Ciliary photoreceptors in sea urchin larvae indicate pan-deuterostome cell type conservation. *bioRxiv Prepr.*

Valero-gracia, A., Petrone, L., Oliveri, P., Nilsson, D.-E., and Arnone, M. I. (2016). Non-directional Photoreceptors in the Pluteus of Strongylocentrotus purpuratus. *Froniers Ecol. Evol.* 4, 1–12. doi:10.3389/fevo.2016.00127.

Van Hiel, M. B., Vandersmissen, H. P., Van Loy, T., and Vanden Broeck, J. (2012). An evolutionary comparison of leucine-rich repeat containing G protein-coupled receptors reveals a novel LGR subtype. *Peptides* 34, 193–200. doi:10.1016/j.peptides.2011.11.004.

Van Sinay, E., Mirabeau, O., Depuydt, G., Van Hiel, M. B., Peymen, K., Watteyne, J., et al. (2017). Evolutionarily conserved TRH neuropeptide pathway regulates growth in Caenorhabditis elegans *Proc. Natl. Acad. Sci.*, 201617392. doi:10.1073/pnas.1617392114.

Veenstra, J. A., and Šimo, L. (2020). The TRH-ortholog EFLamide in the migratory locust. *Insect Biochem. Mol. Biol.* 116. doi:10.1016/j.ibmb.2019.103281.

Verasztó, C., Ueda, N., Bezares-Calderón, L. A., Panzera, A., Williams, E. A., Shahidi, R., et al. (2017). Ciliomotor circuitry underlying whole-body coordination of ciliary activity in the platynereis larva. *Elife* 6, 1–25. doi:10.7554/eLife.26000.

Vopalensky, P., Pergner, J., Liegertova, M., Benito-Gutierrez, E., Arendt, D., and Kozmik, Z. (2012). Molecular analysis of the amphioxus frontal eye unravels the evolutionary origin of the retina and pigment cells of the vertebrate eye. *Proc. Natl. Acad. Sci. U. S. A.* 109, 15383–15388. doi:10.1073/pnas.1207580109.

Wei, Z., Angerer, R. C., and Angerer, L. M. (2011). Direct development of neurons within foregut endoderm of sea urchin embryos. *Proc. Natl. Acad. Sci. U. S. A.* 108, 9143–9147. doi:10.1073/pnas.1018513108.

Wei, Z., Yaguchi, J., Yaguchi, S., Angerer, R. C., and Angerer, L. M. (2009). The sea urchin animal pole domain is a Six3-dependent neurogenic patterning center. *Development* 136, 1583–1583. doi:10.1242/dev.037002.

Wilber, J. F., Yamada, M., Kim, U. J., Feng, P., and Carnell, N. E. (1992). The human prepro thyrotropin-releasing hormone (TRH) gene: cloning, characterization, hormonal regulation, and gene localization. *Trans. Am. Clin. Climatol. Assoc.* 103, 111–119.

Williams, E. A., Verasztó, C., Jasek, S., Conzelmann, M., Shahidi, R., Bauknecht, P., et al. (2017). Synaptic and peptidergic connectome of a neurosecretory center in the annelid brain. *Elife* 6, 1–22. doi:10.7554/eLife.26349.

Willows, A. O., Pavlova, G. A., and Phillips, N. E. (1997). Modulation of ciliary beat frequency by neuropeptides from identified molluscan neurons. *J. Exp. Biol.* 200, 1433–9. Available at: http://www.ncbi.nlm.nih.gov/pubmed/9192496.

Wood, N. J., Mattiello, T., Rowe, M. L., Ward, L., Perillo, M., Arnone, M. I., et al. (2018). Neuropeptidergic Systems in Pluteus Larvae of the Sea Urchin Strongylocentrotus purpuratus: Neurochemical Complexity in a "Simple" Nervous System. *Front. Endocrinol. (Lausanne).* 9, 1–13. doi:10.3389/fendo.2018.00628.

Wu, W., Niles, E. G., and LoVerde, P. T. (2007). Thyroid hormone receptor orthologues from invertebrate species with emphasis on Schistosoma mansoni. *BMC Evol. Biol.* 7. doi:10.1186/1471-2148-7-150.

Yaguchi, S., Yaguchi, J., Angerer, R. C., Angerer, L. M., and Burke, R. D. (2010). TGFB signaling positions the ciliary band and patterns neurons in the sea urchin embryo. *Dev. Biol.* 347, 71–81. doi:10.1016/j.ydbio.2010.08.009.

Yan, X. C., Chen, Z. F., Sun, J., Matsumura, K., Wu, R. S. S., and Qian, P. Y. (2012). Transcriptomic Analysis of Neuropeptides and Peptide Hormones in the Barnacle Balanus amphitrite: Evidence of Roles in Larval Settlement. *PLoS One* 7. doi:10.1371/journal.pone.0046513.

Yañez-Guerra, L. A., Delroisse, J., Barreiro-Iglesias, A., Slade, S. E., Scrivens, J. H., and Elphick, M. R. (2018). Discovery and functional characterisation of a luqin-type neuropeptide signalling system in a deuterostome. *Sci. Rep.* 8, 1–14. doi:10.1038/s41598-018-25606-2.

Yañez-Guerra, L. A., Zhong, X., Moghul, I., Butts, T., Zampronio, C. G., Jones, A. M., et al. (2019). Urbilaterian origin and evolution of sNPF-type neuropeptide signalling. *bioRxiv*, 712687. doi:10.1101/712687.

York, J. R., Yuan, T., Zehnder, K., and McCauley, D. W. (2017). Lamprey neural crest migration is Snail-dependent and occurs without a differential shift in cadherin expression. *Dev. Biol.* 428, 176–187. doi:10.1016/j.ydbio.2017.06.002.

Yoshida, M. A., Ogura, A., Ikeo, K., Shigeno, S., Moritaki, T., Winters, G. C., et al. (2015). Molecular Evidence for Convergence and Parallelism in Evolution of Complex Brains of Cephalopod Molluscs: Insights from Visual Systems. *Integr. Comp. Biol.* 55, 1070–1083. doi:10.1093/icb/icv049.

Zandawala, M., Moghul, I., Alfonso Yanez Guerra, L., Delroisse, J., Abylkassimova, N., Hugall, A. F., et al. (2017a). Discovery of novel representatives of bilaterian neuropeptide families and reconstruction of neuropeptide precursor evolution in ophiuroid echinoderms. *Open Biol.* 7, 1–20.

Zandawala, M., Moghul, I., Yanez Guerra, L. A., Delroisse, J., Abylkassimova, N., Hugall, A. F., et al. (2017b). Discovery of novel representatives of bilaterian neuropeptide families and reconstruction of neuropeptide precursor evolution in ophiuroid echinoderms. *Open Biol.* 7.

Zeisel, A., Hochgerner, H., Lönnerberg, P., Johnsson, A., Memic, F., van der Zwan, J., et al. (2018). Molecular Architecture of the Mouse Nervous System. *Cell* 174, 999-1014.e22. doi:10.1016/j.cell.2018.06.021.

Zeng, H., and Sanes, J. R. (2017). Neuronal cell-type classification: Challenges, opportunities and the path forward. *Nat. Rev. Neurosci.* 18, 530–546. doi:10.1038/nrn.2017.85.

Zhu, X., and Birnbaumer, L. (1996). G protein subunits and the stimulation of phospholipase C by Gs-and Gi-coupled receptors: Lack of receptor selectivity of Gα16 and evidence for a synergic interaction between Gβγ and the a subunit of a receptor-activated G protein. *Proc. Natl. Acad. Sci. U. S. A.* 93, 2827–2831. doi:10.1073/pnas.93.7.2827.

Chapter 8 Appendix

Presented below are additional experimental details. I first provide a full conversion table for bilaterian peptide gene names, and *S. purpuratus* gene identification numbers, QPCR and cloning primers. I include a list of recipes used in this thesis. I include transcriptome (Echinobase) and QPCR data for genes investigated in this thesis, and quantitative counts of spatial data for Sp-TRH and serotonin. In addition, I include a list of sgRNA designed for CRISPR/Cas9 perturbation experiments, MO targeting sequences and genotyping primers. I also include a list of sequence IDs for the orthologous genes identified in this thesis and the sequences used to make the TRH-type signalling phylogenetic tree. Additional details for the deorphanisation assay and a table of terminal effector genes mapped to sea urchin larval neuronal cells.

Chapter 3 is based on the paper published in *Frontiers in Endocrinology* (Wood *et al.,* 2018). I have included the original paper at the end of the appendix.

8.1 Conversion tables

Table 8.1 Bilaterian full and abbreviated peptide names

For peptide names with no known abbreviated names, n/a is written.

Peptide name	Abbreviated peptide name
Uncharacterised neuropeptide precursor	NP
G-Protein Coupled Receptor	GPCR
Vasopressin	VP
Oxytocin	OT
Tachykinin	TK
Gonadotropin-Releasing Hormone	GnRH
Adipokinetic Hormone	AKH
Corazonin	CRZ
Cholecystokinin	CCK
Sulfakinin	SK
Neuromedin U	NMU
Capability	CAPA
Pyrokinin	PK
Pheromone Biosynthesis Activatin Neuropeptide	PBAN
Neuropeptide Y	NPY
Neuropeptide F	NPF
Corticotropin-Releasing Hormone	CRH
Diuretic Hormone 44	DH44
Egg-Laying Hormone	ELH
Calcitonin	Calc
Diuretic Hormone 31	DH31
Orexin	Ox
Allatotropin	AT
Neuropeptide S	NPS
Crustacean Cardioactive Peptide	CCAP
Neuropeptide FF	NPFF
SIFamide	SIFa
Gastrin-Releasing Peptide	GRP
CCHamide	CCHa
Galanin	Gal
Allostatin A	AstA
Allostatin B	AstB
Thyrotropin-Releasing Hormone	TRH
Fulicin	n/a
Kisspeptin	Kiss/Kp
Ox26/RF-amide family 26 amino acid Peptide	QRFP
Parathyroid Hormone	PTH
Glucagon	GCG

Pituitary Adenylate Cyclase-Activating Peptide	PACAP
Leucokinin	LK
Ecdysis-Triggering Hormone	ETH
RWamide	RWa
RYamide	RYa
RFamide	RFa
Luqin	Lq
Pigment-Dispersing Factor	PDF
Myoinhibitory Peptide	MIP
Proctolin	Prct
Achatin	Acha
Thyroid-Stimulating Hormone	TSH
Leucine-Rich Repeat	LR
Prolactin-Releasing Hormone	PRH
Growth Hormone Secretagogue	GHS
Ghrelin	Gh
Neuromedin B	NMB
Echinotocin	n/a
NGFFFamide	NGFFFa
Nesfatin	Nesf
Insulin-Like Peptide	ILP
SALMFamide	SALMFa

Table 8.2 *S. purpuratus* gene names, abbreviated names, identification and QPCR primer sequence for the genes investigated in this thesis neuropeptides, GPCRs, thyroid synthesis gene and putative downstream targets

Genes include those encoding neuropeptides, GPCRs, TH synthesis and other putative downstream genes. Genes with an * after their appreciated names were removed from the analysis of at least one QPCR experiment, because they technically didn't work as the negative control (water) had a lower Ct value (higher expression) when compared with the un-injected sample. Gene identification numbers are from Echinobase (SPU or WHL numbers) or NCBI (XM or XR numbers). Some genes have n/a instead of QPCR primer sequences because only transcriptome data.

Gene name	Abbreviated gene name	Gene Id.	Forward QPCR primer (5'-3')	Reverse QPCR primer (5'-3')
Sp-Neuropeptide precursor 13	*Sp-Np13*	XM_001176371.3	GTCACTTCCG GCCAATCTTG	GTCTAATGTG GTGGGTGGCT
Sp-Neuropeptide precursor 8	*Sp-Np8*	XR_143667.2	CCCTCGCCTTT ATCGTCTCT	GTGCCTTTATC GGGTAGTGC
Sp-Neuropeptide precursor 9	*Sp-Np9*	XR_143632.2	TTTAGCCGTTC TCCTCCTCG	CCTTGCATTGT TTCCGCTGT
Sp-Corazonin	*(Sp-CRZ) (previously Sp-GnRH2)*	XR_971124.1	CGGCTCAGCG GTAGATACT	TGTGGAAGGT CAGGTCGTAC
Sp-Melanin-concentrating hormone	*Sp-MCH*	GI: 115958765	GTCACATGAT CGACGGTTTA	TCTACCCGATC TGCTCCTCT
Sp-Eclosion hormone 2	*Sp-EH2*	XR_972749.1	GATGACGTCT TCTCCCGATT	GCAGTTTCCG AGCTTGTAGG
Sp-Somatostatin 2	*Sp-SS2*	XM_001176809.3	GCCTGTCATG GAACTGCAAG	GTCTACGGCT TGGTCCATCT
Sp-Somatostatin 1	*Sp-SS1*	XP_001176669.1	GGGAACTTGG AGACGCAGAT	TCGAATCCTCT TGAGGTGGC
Sp-Pigment-dispersing factor	*Sp-PDF*	XP_001192435.1	ACGTGGGATG ATGCAGAAGA	CTTGAGCGCT TTCCTGCTTT
Sp-Orexin1	*Sp-Ox1*	XM_011677444.1	GACAGACACA GCAGAAACCG	TATGGTGATG GCCCTGTGTT
Sp-Orexin2	*Sp-Ox2*	XR_973664.1	TGCAACCTCA GAAGCGATTG	AGTGATGCCA ACTCCGCTAT

Sp-Neuropeptide precursor 17	*Sp-Np17*	XM_001177757.3	CGATATGTGTCCACCAAGCC	TTCAATACGCCTGTCCTCCA
Sp-Echinotocin	*Sp-Echinotocin*	SPU_006899	AACTCCCAGGAAACCCTTGT	TAACCCGGAGGTCTTTCCTC
Sp-Ftype SALMFamide	*Sp-FSALMFa**	SPU_021555	AAACGTACGACTGGGTCCAC	CATCTCTGCGTTTCGTTGAA
Sp-Ltype SALMFamide	*Sp-LSALMFa*	XR_973850.1	AGTTGCATATGCCCAAGAGG	GAATGCTGCCCATGTTCTTT
Sp-NGFFFamide	*Sp-NGFFFa*	SPU_030074	CCATCATCACGAAGCAGAA	TCCCTGGGTGAGTTTACAGC
Sp-Gonadotropin-releasing hormone	*Sp-GnRH*	SPU_019680	CGCAGAAGTCAACTCGAACA	ATTCGATGTCGCATCATTCA
Sp-Thyrotropin-releasing hormone	*Sp-TRH**	SPU_008352	GCCAGTACCCAGGTGGTAAA	CGTAGCTCAGGCGATGGTAT
Sp-AN	*n/a*	SPU_018666	GTGACGATTTCGGTGATGAA	TCCTCTGAAGTAGTTCGCTCTC
Sp-Calcitonin	*Sp-Calc*	XR_972762.1	CCAACAGAGACGGACTCTCA	CACTCGGTTCTTTGCCACTT
Sp-Neuropeptide precursor 10	*Sp-Np10*	XR_971715.1	GGAGAGGTGCAGCTGAGAAC	TTGCCGCTGTTCAGAAGATT
Sp-Adam/Tsl6	n/a	SPU_003170.4a	ACGTAAACGCCCTCACATTC	CTTGTGGGCTTCTGATCTCC
Sp-Neuropeptide precursor 18	*Sp-Np18*	XM_001175944.3	CACAAGCCGTTTGCAGTCTA	AAGCACTTCTTTGCGCAGTT
Sp-Neuropeptide precursor 11	*Sp-Np11*	XR_973214.1	ACGAAGATGCAATGGACCTC	ATACACTCCGGCATCGTCAT
Sp-Cholecystokinin	*Sp-CCK*	WHL22.619425.0	GAACTATGACCCGCAACCAT	GCCGAGTTCACCGTAGAGTC
Sp-Pedal peptide-like neuropeptide 2	*Sp-PPLN2*	SPU_024381	TGGACACTACCGATTGAGGA	TTGCATCGGTTCCATGTTTA
Sp-Glycoprotein hormone 3	*Sp-GPH3*	SPU_011451	CAGGTCCCATCGCTTCTTAC	AAGTGAAGGTCGGGTCAATG
Sp-Kisspeptin	*Sp-Kp*	WHL22.176298.0	n/a	n/a

Sp-Neuropeptide precursor 20	*Sp-Np20*	SPU_014142	n/a	n/a
Sp-Nesfatin	*Sp-Nesf*	WHL22.529220	n/a	n/a
Sp-Thymosin		WHL22.736516.0	n/a	n/a
Sp-Luqin		WHL22.555906.0	n/a	n/a
Sp-Secretogranin V	*Sp-SecV*	SPU_015798	AACCCAATCC CTGAGGTTTC	TCACATGCAC ACACCTGATG
Sp-Glycoprotein hormone 1/2	*Sp-GPH1/2*	SPU_004405 / SPU_005842	AAGTCTTCGC ACCACGAGAT	GTTTCGGCAT TTGCAACTCT
Sp-Buriscon alpha-like	*Sp-Burs□*	SPU_003984	GTTGATGTTG GCCCTGATTC	CCTACCGAGT CCAAGGTGAC
Sp-Buriscon beta-like	*Sp-Burs□*	SPU_017707	AACCAATGCG AGGGTAAATG	TGTGATTCCTA GGGCGTGAT
Sp-Ubquitin	*Sp-Ubq*	SPU_021496	CACAGGCAAG ACCATCACAC	GAGAGAGTGC GACCATCCTC
Sp-18S-rRNA	*Sp-18S*	L28055	CAGGGTTCGA TTCCGTAGAG	CCTCCAGTGG ATCCTCGTTA
Sp-Pedal peptide-like neuropeptide	*Sp-PPLN1*	SPU_003108	GAGCTTTCCTC GTCGTCAAC	TCTGCGTTGTC AATCACCTC
Sp-Thyrotropin-releasing hormone Receptor	*Sp-TRHR**	SPU_010167	CCTTATCGGA TGCTTGTCGT	GTAGAGGATC GGGTTGACCA
Sp-Calcitonin-like Receptor	*Sp-CalcR*	SPU_018314	TGCTCCAAATT TCAGCACAG	CCATGAGTTC TCGCAGCATA
Sp-Cholecystokinin-like Receptor	*Sp-CCKR*	SPU_026458	AGGCATTAAT GGACGACAGC	TGACGAGAAC GAGCAACATC
Sp-Echinotocin-like Receptor	*Sp-EchinotocinR*	SPU_021290	GCTCGTGTGG GACATTACCT	TTCGTGTAGT CACCGCGTAG
Sp-NGFFFamide Receptor	*Sp-NGFFFaR*	SPU_021291	GCACCAATGT CTGCAAAGAA	TTGAATTCCGT CGTGTGTGT
*Sp-Can1**	*Sp-Can1**	SPU_012518	CGGTAGGAAA CAGTCACCCA	CAGTTGAATC CACTGCCACC
Sp-Net7	*Sp-Net7*	SPU_025068	ACGGCTGTCT TCAATCTCCA	AGCCGTAACC TCGTGAGTTA

Sp-Paired box homeobox 258	*Sp-Pax258*	SPU_014539	CCAAAGGTGG TGTCGAAGAT	ATCGAGCTGA CACTGGGAAC
Sp-Thyroid hormone receptor	*Sp-THR*	XM_003731865.2 / XM_011669640.1	GTGTGTAGTA TGCGGAGATG C	GTGCCATGCC CACGTTAAG
Sp-Thyrotropin stimulating hormone Receptor	*Sp-TSHR**	SPU_027375	ATACCGGGAC AGAAACCACC	ACGTCCGAGT AATCCGTTGT
Sp-Pea3	*Sp-Pea3*	SPU_014576	TCAAACACGG TTCAGGGAGA	TCATCATAGA ACGCCCTGCC
Sp-Peroxidase	*Sp-Pxdn*	SPU_013889	GGATCATCTA GAGGGCGGTC	GGTTCACCCG GTCTATGGAA
Sp-Deiodinase	*Sp-DIO*	SPU_002251	AAGATGCCAC CAACGTTTCC	TCCCGTCTGTT GAGTCCATT
Sp-vascular endotheliak growth factor-like	Sp-vegfrl	WHL22.240520.0	AGTCTGTGCC AGCTTAGAGG	CGGTAACCTT GCTGATGTCG
Sp-Aristaless-like homebox 1	Sp-alx1	WHL22.731056.1	CAGTGCAGCT TTACGTGGAC	TTAAGTCTCG GCACGACAAA
Sp-p58	Sp-p58	WHL22.23776.1	TTTTGAGCAG GCGATCTTTT	CTTCCACAGG GCTGGAGTAA
Sp-Fibroblast growth factor a / 9/16/20	Sp-fgfa / 9/16/20	WHL22.343932.0	CGTGTTGCTG CACAATCTCT	CGTCGACGAA GACGATGTAA
Sp-Fibroblast growth factor receptor 2	Sp-fgfr2*	WHL22.147868.1	AATGGCGGTG TCTACCAAAG	ACACCAGGGT ACGGGTATGA
Sp-vascular endothelial growth factor	Sp-vegf	SPU_030148	CACCGTCGTG AGACACTCCT	TGGTAATGCG TCATGTGTGA
Sp-Fibroblast growth factor receptor 1	Sp-fgfr1	SPU_020677	CCTTCGGACA AACCAGACAT	TGATCCTGAG TGGGAGTTCC
Sp-Fibroblast growth factor 8	Sp-fgf8	WHL22.213412.2	AAGGGTAGAC GCCAAAGGTT	TATTTATGCGT CAACGGCAA
Sp-hepatocyte nuclear factor 6	Sp-hnf6*	WHL22.288683.1	TGCAGCTTCTC TGCATACCA	ACTCCAACAT GCCTCCAAAC
Sp-Forkhead box g	Sp-foxg*	WHL22.389872.0	CGCTCGAGTC CAGAGAAAG	TGTCGAGGGA CTTTCACAAA

Sp-sprouty	*Sp-spry*	WHL22.244716.0	GGTTCTTCCAGCGAGTCATC	GGCTGGCTGTGTAAGGATGT
Sp-spicule matrix protein 50	Sp-sm50*	WHL22.742398.0	TAGCCTTTGCTACGGGTCAA	CTGAGGCGACGAAACTGAA
Sp-spicule matrix protein 30	Sp-sm30*	SPU_000825	GTTCTCCGGTAGGCAAACA	ACATTTTGGGGCAAATGAAA
Sp-Forkhead box J1	Sp-FoxJ1*	WHL22.468365.0	ATTCCATCCGTCATAATCTCTCA	TCTCTTCTTGAAGACACCATTCTC
Sp-gatac*	Sp-gatac*	WHL22.660411.0	CAGGGACATCATGTGCAAAC	CCGTGTTTGAATGCCTTCTT
Sp-receptor for egg jelly 5	Sp-rej5*	WHL22.684298.0	ATCGCAGCTTGCTCTGGTAT	CTTCCTGCTCCTCAGGTGTC

Table 8.3 Clone and probe information for genes used in this thesis that I cloned

Genes include those encoding for neuropeptides, GPCRs, TH synthesis and other putative downstream genes. For each gene the following information is provided: a) gene name, b)) forward and reverse cloning primers and c) length of probe. For *Sp-TRHR,* two sets of cloning primers are shown, one amplified a partially sequence and was used for *in situ* hybridisation, the second amplified a full length ORF and the primers include restriction enzyme sites (in bold) for directional cloning into the pcDNA3.1+ vector for the deorphanisation assay.

Gene name	Forward cloning primer	Reverse cloning primer	Probe length
Sp-TRHR	CGAAGGGCTGCTAAGATCAC	CGCTAATTGGCCGCAGTAG	1360
Sp-TRHR	GCT**GATATC**GACTTATTGTT GACCATTGCACT	GC**TCTAGA**TGATGCGCGCTTTG TTTAGA	n/a
Sp-NGFFFa-R	clone gifted from Maurice Elphick	clone gifted from Maurice Elphick	1355
Sp-ILP2	GACCCATCTCATCGTTTCGG	TCCTTCTTTCGCGTTGCATT	1123
Sp-Np20	TGTCTAAGCCTCCAATCCGG	CGAATAAGGTGCCACTCCCT	1323
Sp-Kp	CCACCGCACTATCATTTGACC	CCTTCTCCCATCCCATTTGTAAT	1210
Sp-Kp	CCACCGCACTATCATTTGACC	CCTTCTCCCATCCCATTTGTAAT	1410
Sp-SynB	GAACAAGATAAGCGACGTG ATG	TGTCAACCAACCTGATAGTCCA	1017
Sp-Nesf	TAGTGCATGTAGCCCAGCAG	GAAGCAGCCTCCATGAACTC	955
Sp-Np13	ACGACCAACCCAGTACTCAG	CAGAAGGCCATCATTCGTCA	1387
Sp-Np8	CAAACAGACAACTCCTCGCC	TGGTATTAGGTCGTCGCCAT	1124
Sp-Np9	AGCCTGAGTTTAGCCGTTCT	GCGATTGACACCACCTCTTC	940
Sp-MCH	CCGTTCCAATAGCGTGAAAG T	TGTCGTCTGCTTTATCCCGT	677
Sp-SS2	CCCTGACATCGGCATTGAAG	TGTCCGGTTACAGCATACGA	2460
Sp-Np17	TCTAGGCGCGAATCTACAGG	GCCAGAGAGCTCCGATAACT	1666
Sp-SS1	GGTCCTATTGAACCACCGGA	CAAACTACAACAGCTGCCGT	860
Sp-PDF	TGCAGTCGTCACTAGTCGTT	GCGGCACTGACTCTTTAACA	1124
Sp-Ox1	TGACACAGGTGCGGTAGAAT	GCCATCGAGTCATCTTCCCT	1703
Sp-Ox2	TGATCTTATGTGCCAGGCCA	GGTCACGTTAGCATGCAACA	1760
Sp-Echino	AAAGGAAACCAACGCGCAA A	TTTCCTCTCGACTCATCTGC	675
Sp-THR	CAAGCAAGGGAAACTGTCG G	ATACAGCAGCTAGTAGGGCC	1569
Sp-DIO	GTCTCGATTCGACGCATTCC	CATTACTACGCTGTTGGGCC	2053
Sp-Pxdn	AGGGCAGCACTGTAGAACTT	GGTTCACCCGGTCTATGGAA	2520

Table 8.4 Clone and probe information for genes used in this thesis that were obtained from a Radial nerve cDNA library

Genes include those encoding for neuropeptides and GPCRs. For each gene, the RNSP-clone identification number is provided and the length of the probe (nucleotides).

Gene name	RNSP -clone identification number	Probe length
Sp-TRH	9P21	3900
Sp-NGFFFa	5L15	1650-2000
Sp-PPLN1	9e2	1300
Sp-PPLN2	5B10	3700
Sp-FSALMFa	5H7	2000
Sp-AN	5K1	2155
Sp-Np18	9L6	1650
Sp-SecV	9I5	900
Sp-CRZ	5E18	3546

8.2 Recipes

In this section I include a list of recipes which for solutions used when performing experiments described in the chapter 2, materials and methods.

8.2.1 Molecular cloning

1% TBE gel	
agarose	0.5 g
Tris Borate EDTA	50 mL
Total Volume	50 mL

LB plates	
LB agar	8 g
NaCl	2 g
MilliQ-H_20	400 mL
Total Volume	400 mL
After autoclaving, plate out and add 100 µL/mL ampicillin and 50 µL/mL X-gal	

Luria Broth (LB)	
Tryptone (pancreatic digest of casein)	5 g
Yeast extract	2.5 g
NaCl	2.5 g
MilliQ water	500 mL
Total Volume	500 mL

8.2.2 Embryological techniques

Artificial sea water (ASW)	
NaCl	28.32 g
KCL	0.77 g
$MgCl_2.6H_2O$	5.41 g
$MgSO_4.7H_2O$	7.13 g
$CaCl_2$	1.18 g
$NaHCO_3$	0.2 g
MilliQ water	1 L
Total Volume	1 L

Fixative 1	
16% PFA	10 mL
1M MOPS	4 mL
5M NaCl	4 mL
DEPC H_2O	22 mL
Total Volume	40 mL

Fixative 2	
16% PFA	10 mL
DEPC Artificial sea water	13 mL
1M MOPS	1.3 mL
5M NaCl	2.6 mL
DEPC H_2O	13.1 mL
Total Volume	40 mL

MOPS buffer	
1M MOPS	10 mL
5M NaCl	10 mL
Tween 20	100 µL
DEPC H_2O	80 mL
Total Volume	100 mL

TBST	
2M Tris pH 7.5	15 mL
5M NaCll	4.5 mL
10% Tween-20	1.5 mL
Deionised H_20	129 mL
Total Volume	150 mL

Perkin Elmer blocking buffer	
MABT	50 mL
Perkin Elmer Blocking Reagent II	0.5 g
Total Volume	50 mL

Glycine solution	
Glycine	0.75 g
Deionised water (adjust pH to 2.2 with HCL)	40 mL
10% Tween-20	50 µL
Total Volume	50 mL

1 X Maleic acid Buffer (MABT)	
0.1M Maleic Acid (MA) pH 7.5	50 mL
0.15M NaCl	15 mL
0.1% Tween-20	5 mL
DEPC H2O	395 mL
Total Volume	500 mL

Hybridization buffer	
Deionized formamide	500 µL
50% PEG	200 µL
5M NaCl	120 µL
2M Tris pH7.5	10 µL
20mg/ml yeast RNA	25 µL
10% Tween-20	10 µL
0.5M EDTA	10 µL
DEPC H_2O	105 µL
50X Denhardst	20 µL
Total Volume	1 mL

Blocking buffer	
MABT	1.9mL
Sheep/goat serum	0.1mL
Total Volume	2mL

Alkaline Phosphatase Buffer (AP)	
1M Tris pH 9.5	0.5 mL
5M NaCl	100 µL
1M $MgCl_2$	0.25 mL
10% Tween-20	50 µL
dH_2O	4.05 mL
100mM Levamisole	50 µL
Total Volume	5 mL

Staining Solution [purple]	
AP buffer	890 µL
Dimethylformamide (DMF)	100 µL
NBT/BCIP Mix (Roche)	10 µL
Total Volume	1 mL

4% PFA in PBS	
16% Paraformaldehyde	250 µL
Phosphate-buffered saline (PBS)	750 µL
Total Volume	1 mL

4% PFA in PBST (0.02% Tween-20)	
16% Paraformaldehyde	250 µL
Phosphate-buffered saline (PBS)	749.5 µL
Tween-20	0.5 µL
Total Volume	1 mL

PEM (pH 6.8)	
100mM PIPES	30.24 g
5mM EGTA	1.899 g
2mM $MgCl_2$	0.411 g
0.2% Triton X-1000	2 mL
Water	748 mL
16% PFA	250 mL
Total Volume	1 L

PBSTx (0.1% Triton X-100	
Phosphate-buffered saline (PBS)	998.5µL
Tween-20	0.5µL
Triton X-100	1 µL
Total Volume	1mL

8.3 Temporal expression data

Table 8.5 High-resolution expression of NP genes, GPCRs and *Sp-SecV* across development from fertilisation (0 hpf) to pluteus larval stage (70 hpf) as determined by Quantitative PCR (QPCR)

Data indicated as number of transcripts per embryo. *Sp-CRZ has previously been referred to as Sp-GnRH2

	Developmental time (hpf)																
NP gene	**0**	**5**	**7**	**9**	**12**	**15**	**18**	**21**	**24**	**27**	**30**	**33**	**40**	**45**	**48**	**52**	**70**
Sp-Np13	3	7	10	23	11	5	7	12	34	38	11		14	31	45	137	222
Sp-Np8	1	1		1	25	2	60	51	68	78	80		180	240	123	142	195
Sp-Np9	33	21	53	35	142	95	52	52	70	62	34		88	204	284	641	2690
Sp-CRZ			4	1		29	151	210	202	212	12		9	19	49	121	957
Sp-MCH	823	263	206	273	384	330	384	182	161	154	19		7	15	33	186	356
Sp-EH2	2		4	3	95	9	15	6	6	17	1		11	7	8	21	73
Sp-SS2	3	6	21	19	14	12	4	7	16	47	5		18	6	14	53	1272
Sp-SS1	1	6	8	14	6	101	290	267	321	279	141	140	139	77	68	88	134
Sp-PDF	20	22	18	73	58	36	18	15	8	8	12	1	20	37	56	65	623
Sp-Ox1	4	9	3	15	11	176	490	365	359	316	575	241	241	689	1255	2610	6405
Sp-Ox2	2	5	8	32	68	33	56	89	288	477	343	75	40	46	52	107	517
Sp-Np17	6	15	27	23	18	11	11	7	19	94	14	31	14	22	31	87	209
Sp-Echino	5	0		6	17	9			68		34		96		200		64
Sp-FSALMFa	9	4		43	67	26			64		128		164		346		2167

Sp-LSALMFa	0	0		0	0	3			7		5		0		11		257
Sp-NGFFFa	7	28		206	262	127			34		11		33		19		108
Sp-GnRH	0	0		0	0	0			0		0		0		0		0
Sp-TRH	3	4		19	52	178			618		250		210		82		426
Sp-AN	18	8		9	33	23			26		7		120		655		9377
Sp-Calc	4	0		1	2	4	14		28		8		31		6		39
Sp-Np10	2	0		15	3	8	10		25		39		114		63		71
Sp-Adam/Tsl6	1	5		2	2	3	5		4		44		32		73		11
Sp-Np18	30	62		145	56	179	71		220		196		317		485		4943
Sp-Np11	6	1		72	88	52	22		1		1		27		23		122
Sp-CCK	1	16		8	48	28	27		105		156		601		391		1695
Sp-PPLN2	0	4		0	0	2	9		62		79		430		830		451
Sp-GPH3	0	3		7	16	10	4		9		19		432		1476		3262
Sp-SecV	173	58					64			104	111	211	1664	6497	13471		70876
Sp-GPH1/2					446		68		239	364	690	604	1415	3717	10450		42529
Sp-Burs□					181				90				813	1958	5652		9011
Sp-Burs□									137	144	122		155	464	853		3750
Sp-PPLN1	48	37		77	79	433	4197		11114		13536		17023		16253		10281
Sp-EchinoR	19	6		13	18	18	1		0		0		55		14		40
Sp-NGFFFaR	309	73		75	83	69	90		18		13		9		14		241
Sp-TRHR	227	173		175	185	92	34		266		452		989		1256		3386
Sp-CCKR	0	204		117	160	2	3		0		1		14		6		60
Sp-Calc R	3	208		1255	231	150	46		217		346		627		228		156

Table 8.6 Expression of NP genes and GPCRs across development from fertilisation (0 hpf) to pluteus larval stage (72 hpf) as determined by transcriptome sequencing (Echinobase)

Transcriptome sequencing from publicly available database (Echinobase; URL://www.echinobase.org/Echinobase/). Data indicated as number of transcripts per embryo.

Gene name	Developmental time (hpf)									
	0	**10**	**18**	**24**	**30**	**40**	**48**	**56**	**64**	**72**
Sp-Kp	0	6	784	14	13	16	44	23	137	205
Sp-ILP1	2,207	1,878	121	0	7	19	4	8	8	8
Sp-ILP2	841	313	162	414	590	591	552	477	491	400
Sp-Np20	42,563	37544	66891	60547	44078	29780	18304	22102	15777	15940
Sp-Nesf	16,434	15986	16443	16702	10949	6568	5199	4371	5363	4564
Sp-Thymosin	0	0	5	9	13	6	0	0	0	7
Sp-Luqin	0	20	0	9	22	10	238	149	857	930
Sp-DIO	0	5	24	19	12	38	10576	2864	3081	380
Sp-Pxdn	9,074	3,134	5,366	3696	4586	3378	3620	3138	3131	2593
Sp-THR	892	1094	395	1682	1679	1473	1987	1482	2799	2294
Sp-GPA2	0	0	0	9	23	40	445	312	761	1,241
Sp-GPB5	0	0	0	7	0	42	239	182	595	972
Sp-TSHR	14	0	0	9	7	29	119	72	303	242
Sp-VP/OT/GnRH-R	0	0	18	0	16	7	25	0	77	107
Sp-NGFFFaR	141	94	273	0	12	15	13	3	71	142
Sp-EchinoR	63	45	9	0	6	5	30	24	15	18
Sp-GRP/NMB-R	0	4	0	3	0	0	0	0	0	12

Sp-GRP/NMB-R	0	3	0	3	0	7	0	4	7	11
Sp-GRP/NMB-R	95	132	25	70	123	36	23	47	11	51
Sp-NMU/GH/Gh-likeR	0	0	0	0	0	25	0	0	9	0
Sp-NMU/GH/Gh-likeR	0	7	0	12	0	0	64	77	107	171
Sp-CCKR	3	4	0	9	0	4	30	24	38	70
Sp-OxR	0	90	9	0	64	182	115	243	136	92
Sp-TRHR	218	77	99	257	325	359	703	723	666	857
Sp-RFaR	0	0	0	0	0	0	0	0	0	11
Sp-RFaR	0	7	6	0	0	11	76	70	42	61
Sp-RFaR	465	877	56	48	38	113	155	183	149	77
Sp-RFaR	0	0	9	68	0	0	0	7	0	0
Sp-PRHR	3	3	0	3	0	19	562	263	915	904
Sp-LGR1	22	593	174	492	973	715	581	559	598	461
Sp-LGR2	3	4	16	58	194	233	150	203	138	115
Sp-LGR3	0	0	9	109	204	227	137	116	95	124
Sp-TSHR	14	0	0	9	7	29	119	72	303	242
Sp-GnRHR	158	179	27	1	0	17	11	1	26	16
Sp-GnRHR	341	262	27	15	24	13	15	17	21	25
Sp-CalcR	314	233	82	448	645	329	328	229	448	516
Sp-CRHR	168	146	48	58	21	107	303	292	545	551
Sp-CRHR	55	110	28	13	46	40	33	9	48	46
Sp-CRHR	64	69	227	39	81	29	64	44	91	62
Sp-GnRHR	0	0	0	0	0	0	23	12	19	39

Table 8.7 Expression of 16 NP genes during larval and juvenile development

Data indicated as the relative expression (individual maximum expression) for 70 hpf, 5 weeks post fertilsation (wpf) and juvenile stage.

	Developmental time		
NP gene	**70 hpf**	**5 wpf**	**Juvenile**
Sp-Np13	0.02371858	0.10131153	1
Sp-Np8	0.01366149	0.11122428	1
Sp-Np9	0.08060814	0.10280544	1
Sp-CRZ	0.28977156	0.11685176	1
Sp-MCH	0.27288881	0.00862537	1
Sp-EH2	1	0.03895619	0.35636706
Sp-SS2	0.24273597	0.00713382	1
Sp-SS1	0.0409494	0.0976186	1
Sp-PDF	0.18371394	0.07857701	1
Sp-Ox1	0.29105348	0.1687522	1
Sp-Ox2	0.28376764	0.12352741	1
Sp-Np17	0.11674842	0.13117141	1
Sp-Echino	0.00372839	0.06630062	1
Sp-FSALMFa	0.57652326	0.57488247	1
Sp-LSALMFa	0.07630607	0.42142967	1
Sp-NGFFFa	0.04330869	0.59059288	1
Sp-GnRH	0.00511301	0.71111863	1
Sp-TRH	0.14404645	0.8736893	1
Sp-AN	0.75832663	0.62634399	1
Sp-Calc	0.00718127	0.47603659	1
Sp-Np10	0.00479285	0.50050079	1
Sp-Adam/Tsl6	0.00052381	0.31856497	1
Sp-Np18	0.4678527	0.34813253	1
Sp-Np11	0.07654822	0.34587632	1
Sp-CCK	0.01648378	0.30434047	1
Sp-PPLN2	0.09607691	0.5939407	1
Sp-GPH3	1	0.17780457	0.19260849

8.4 Spatial expression data

Table 8.8 Frequency of individuals expression of *Sp-TRH* positive cells

Data indicates the frequency of differential *Sp-TRH* positive cells in the ciliary band of a population of larvae. 116 larvae were counted.

Number of TRH positive cells	Number of larvae	Percentage of larvae
0	46	40%
1 cell on 1 side	44	38%
(2 + cells) on one side	8	7%
(2 cells) 1 cell on each side	11	9%
(4 + cells) 2 cells on each side	7	6%

Table 8.9 Frequency of individuals expression of serotonergic positive neurons

Data indicates the frequency of differential serotonergic positive neurons in the apical organ of populations of larvae with different treatments: A) Uninjected (n = 75), B) Cas9 mRNA and TPH sgRNA (n = 34), C) Cas9 protein (PNA BIO) and TPH sgRNA when incubated at 16°C (n = 48) and D) Cas9 protein (PNA BIO) and TPH sgRNA when incubated at 12°C (n = 20). N = number of individuals counted across 1-3 independent experiments. Experiment carried out by Anne Ritoux.

	Treatments			
Number of serotonergic neurons	**Uninjected**	**Cas9 mRNA and TPH sgRNA**	**Cas9 protein (PNA BIO) and TPH sgRNA at 16°C**	**Cas9 protein (PNA BIO) and TPH sgRNA at 12°C**
0	0	0	1	3
1	0	0	3	1
2	1	0	5	1
3	1	3	5	5
4	6	6	16	3
5	14	14	11	4
6	20	9	4	2
7	19	1	3	1
8	7	0	0	0
9	2	1	0	0
10	4	0	0	0
11	1	0	0	0

8.5 CRISPR/Cas9 and MO components

Table 8.10 Constant primers used for sgRNA synthesis

Guide-oligos are synthetic DNA strands, which are used to generate templates for sgRNA synthesis. Guide-oligos are made of three main parts: a T7 promoter (green) a variable targeting sequences (bold, underlined and italic), and a Cas9 binding scaffold (purple). A short clamp (orange) is provided to stabilize the 5' end of the double-stranded sequence. A PCR fusion was performed with four primers to make a guide-oligo. Three of these primers are constant for each sgRNA: 1) a 79 nucleotide constant scaffold, which overlaps with the variable sgRNA primer, b) a 21bp constant forward primer at 5' end of the guide-oligo, and c) a 21bp constant reverse primer at the 3' end of the guide-oligo.

Primer name	Primer sequence
gRNA_constant_forward	GCGTAATACGACTCACTATAG
gRNA_constant_reverse	AAAGCACCGACTCGGTGCCAC
gRNA constant scaffold_RC	AAAGCACCGACTCGGTGCCACTTTTTCAAGTTGATAACGGACTAGCC TTATTTTAACTTGCTATTTCTAGCTCTAAAAC

Table 8.11 Gene specific primers used for sgRNA synthesis

A list of the variable 61 nucleotide sgRNA primers targeting three genes: a) *Sp-PKS1*, *Sp-TPH* and *Sp-TRH.* The main parts of the guide-oligo and coloured and formatted as follows: short clamp (orange), T7 promoter (green), variable targeting sequence (bold, italic and underlined) and Cas9 binding scaffold (purple). The red "g" nucleotides of the variable sequence indicate changes made from the target sequence for optimal T7 transcription.

Primer name	Primer sequence
gRNA2_PKS1	GGCGTAATACGACTCACTATA***GgTGAGGGGTTTGAGGACA A***GTTTTAGAGCTAGAAATAGC
gRNA3_PKS1	GGCGTAATACGACTCACTATA***ggAGAGGGTTGTCTTTGGT G***GTTTTAGAGCTAGAAATAGC
gRNA1_TPH	GCGTAATACGACTCACTATA***gGGGCCGAGGTGCTGGAAG A***GTTTTAGAGCTAGAAATAGC
gRNA2_TPH	GCGTAATACGACTCACTATA***GGAAGACGGGGTCATAACCT***GTTTTAGAGCTAGAAATAGC
gRNA3_TPH	GCGTAATACGACTCACTATA***GGCTCACATGAGCTCGGAGC***GTTTTAGAGCTAGAAATAGC
gRNA4_TPH	GCGTAATACGACTCACTATA***ggCGTCGTGCCTTGTTAAGA***GTTTTAGAGCTAGAAATAGC
gRNA5_TPH	GCGTAATACGACTCACTATA***GgCCCCGTCTTCCAGCACCT***GTTTTAGAGCTAGAAATAGC
gRNA6_TPH	GCGTAATACGACTCACTATA***GgTGTTGGCGTGGTTCATGT***GTTTTAGAGCTAGAAATAGC
gRNA1_TRH	GGCGTAATACGACTCACTATA***ggCGTCCTTAGTGAGAACG A***GTTTTAGAGCTAGAAATAGC
gRNA2_TRH	GGCGTAATACGACTCACTATA***GgATTCTGGGATACGTCAC A***GTTTTAGAGCTAGAAATAGC
gRNA3_TRH	GGCGTAATACGACTCACTATA***ggGGGATACGTCACATGGG G***GTTTTAGAGCTAGAAATAGC
gRNA4_TRH	GGCGTAATACGACTCACTATA***gGCTGACTGGGTGCAAGGA A***GTTTTAGAGCTAGAAATAGC
gRNA5_TRH	GGCGTAATACGACTCACTATA***ggGGCCCATCGTTCTCACT A***GTTTTAGAGCTAGAAATAGC

Table 8.12 Morpholino Oligonucleotide (MO) target sequences

MO name	MO sequence
TRH MO	5'GCCCTCTTGCTAAGTCCTCTTGCTA
TRHR MO	5'TACACCAACCGTGACTCCCGCCATG

Table 8.13 Genotyping primers

Primer name	Primer sequence
SpPKS1_NW40_F	GACGAGGACCAGACAAGACA
SpPKS1_NW41_ex3_R	TGAGGCCAATGATGTGCTTG
Sp-Jun Cloning 4- 26	TGGCTGAGCAAGAAGAAATG
Sp-Jun Cloning 4- 27	CTTGACATCCGCTCTTCACA
SpPmar1b qCPR-C- B5 R	CGATGAAGGCATCGTTGAAT
SpPmar1b qPCR-A-G1 F	CATCAATCGCGTTCCAACTA
Sp-TPH_NW44_F	TCGACGTCCTACTCTGTCAC
Sp_TPH_NW45_R	CGGGTGATCTGCGTCTAACT
Sp_Trh_NW46_F	AGGTACCCGAAAGTCATCCG
Sp_Trh_NW47_R	AAATGCCGTTTCCCTTCCAG
Sp_Trh_NW50_F	GTGGGACTTAGCAAGAGGACT
Sp_Trh_NW51_F	ACGGAGCAGTTTAGGTAGCC
Sp_Trh_NW52_F	ACCAACGAAATAACCCACGC
Sp_PPLN1_NW42_F	CGAGCCGTTATTCCTTCCAG
Sp_PPLN1_NW43_R	CCCCACTGTTGATCCCTTCT
Sp_PPLN1_NW48_R	TGACTCGGAGGGGTAGTACG
Sp_PPLN1_NW53_R	TCATCCACGTCTCTCGTCTTT
Sp_PPLN1_NW54_F	CCCTTATTACCCTCCGTCCA
Sp_PPLN1_NW55_R	AATGTCCCCAAATCGCTCAG

8.6 Gene details

Table 8.14 Orthologous genes identified by best reciprocal blast hit

Species	Gene name	Gene ID.
Strongylocentrotus purpuratus	*Sp-THRB*	SPU_018861
Strongylocentrotus purpuratus	*Sp-DIO*	SPU_002251
Strongylocentrotus purpuratus	*Sp-TSHR*	SPU_027375
Strongylocentrotus purpuratus	*Sp-Pxdn*	SPU_013889
Strongylocentrotus purpuratus	*Sp-GPA2*	SPU_015344
Strongylocentrotus purpuratus	*Sp-GPB5*	SPU_005842/SPU_004405
Amphuira filiformis,	*Afi-TrhR*	id151584.tr199124
Apostichopus japonicus	*Aja-TrhR*	PIK53909.1
Antedon mediterranea	*Ame-TrhR*	scaffold42678_Locus_247202
Bermisia tabaci	*Bta-TrhR*	XP_018902557.1
Penaeus vannamei	*Pva-TrhR*	XP_027211847.1
Hyalella azteca	*Haz-TrhR*	XP_018023390.1 (partial)
Armadillidium vulgare	*Avu-TrhR*	RXG59615.1
Bermisia tabaci	*Bta-Trh*	XP_018902557.1
Limulus polyphemus	*Lpo-Trh*	XP_022248620.1
Daphnia pulex	*Dpu-Trh*	EFX70415.1
P. vannamei	*Pva-Trh*	ROT85541.1
H. azteca	*Haz-Trh*	XP_018019133.1

Table 8.15 TRHR-type receptor and outgroup receptor (NMU and Orexin-type) sequences used in to make the phylogenetic tree

Species	Receptor	Gene ID.
Homo sapien	TRHR	NP_003292.1
Gallus gallus	TRHR	NP_990261.1/ QCU72305.1
Petromyzon marinus	TRHR	ALG00050.1
Callorhinchus milii	TRHR	XP_007887760.1/XP_007883694.1/XP_007900908.1
Branchiostoma belcheri	TRHR	XP_019618161.1
Saccoglossus kowalevskii	TRHR	XP_002730943.1
Strongylocentrotus purpuratus	TRHR	SPU_010167
Antedon mediterranea	TRHR	scaffold42678_Locus_247202
Amphiura filiformis	TRHR	id151584.tr199124
Pomacea canaliculata	TRHR	XP_025076289.1
Crassostrea gigas	TRHR	XP_011445673.1
Lobatus gigas	TRHR	XP_009058286.1
Capitella teleta	TRHR	ELT88781.1
Platyneresis dumerilii	TRHR	AKQ63029.1
Priapulus caudatus	TRHR	XP_014667677.1/XP_014663378.1
Limulus polyphemus	TRHR	XP_013780050.1/XP_013780778.1
Daphnia pulex	TRHR	ADZ15312.1
Penaeus vannamei	TRHR	ROT64141.1
Hyalella azteca	TRHR	XP_018023390.1
Armadillidium vulgare	TRHR	RXG59615.1
Bemisia tabaci	TRHR	XP_018902557.1
Ancylostoma caninum	TRHR	RCN50537.1 7
Caenorhabditis elegans	TRHR	CCD66234.1
Caenorhabditis briggsae	TRHR	XP_002639359.1
Trichinella spiralis	TRHR	XP_003374352.1

Petromyzon marinus	NMUR	ALG00034.1
Branchiostoma belcheri	NMUR	XP_019623728.1
Callorhinchus milii	NMUR	XP_007900680.1
Gallus gallus	NMUR	NP_001305365.1/NP_001305366.1
Homo Sapien	NMUR	AAH16938.1
Saccoglossus kowalevskii	NMUR	P_006812467.1
Mmus	OxR	NP_945197.2
Hsap	OxR	NP_001516.2
Danio rerio	OxR	NP_001073337.1
Acanthaster planci	OxR	XP_022107462.1/XP_022089610.1
Strongylocentrotus purpuratus	OxR	XP_789606.2

8.7 Receptor deorphanisation assay

Figure 8.1 pcDNA3.1+ vector map

pcDNA3.1+ vector from addgene (CAT no. V790-20). *Sp-TRHR* gene was subcloned into the eukaryotic expression vector pcDNA3.1 + cut with EcoRV and Xbal restriction endonucleases using the oligos 5”-gctGATATCgacttattgttgaccattgcact-3’ and 5’ gcTCTAGAtgatgcgcgctttgtttaga-3.

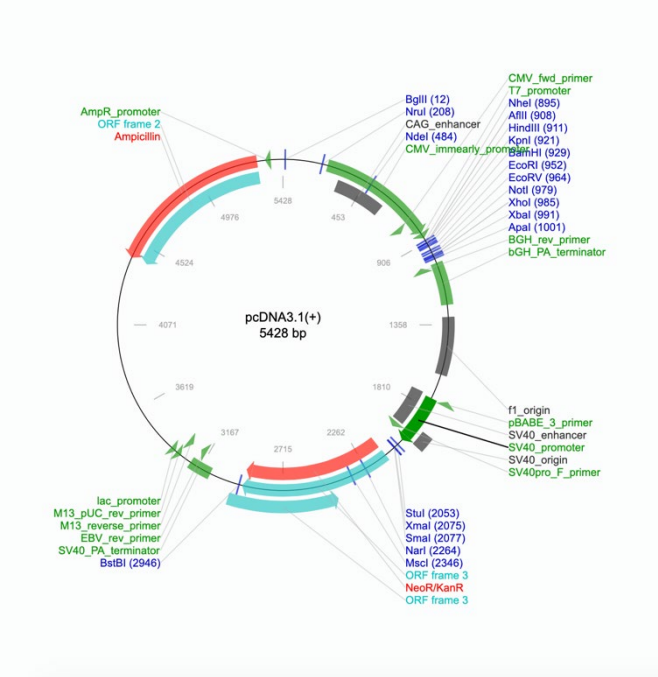

>*Sp-TRHR*_ XM_011684235.1_sequenced

GGTGGAATTCTGCAGATATCGACTTATTGTTGACCATTGCACTTCGAGTATCTGAAATTTGAAAATT
CAATCTACAGCCATGGCGGGAGTCACGGTTGGTGTAGTTCCTACCGTGGTCACAGAAGTGAACGT
TTATCAAACAGAATTTTTCGACGTAACTCCAAACATGTCGCTTGCATCACCAAATGCCACTAGAGAT
TTACCCGAGCTGGAATTCTACAACCTCGATTACAAGATCATAGCGACGATATTCTACCTGCTCTTG
GGTGCAGCGGCCATCATCGGTAACGCGATGGTGATCATCGTCGTTCTCAGAGTGGCTCACATGC
GAACTCCGACGAACTGTTACCTGGTGAGTCTGGCAGTGGCCGACTCTATGGTCGGAGCAATAACC
ATCATGATGCATTCCGTACCGGAGAACCTGCTGCCGAAGAACGCGTTCATCTACGGCGCCACCG
GCTGCTACTCCATCATTGCTCTCGAGTATCTGTCCTTCAACGTATCCGCGCTGTCCATTACCGCTT
TCACAATCGAACGCTACATCGCCATATGTCACCCCATGAAGGCCCACATCATGTGCTCCGTGTCG
AGGGCCACCAAAATCATAATCACTCTCTGGGTCTTCGAAATCATCTACTGCTCACAGTGGTGCTTC
TTGCTCGAGTACAGCGAGGAAGAGTATGCAGGTGGACATGCCTTTGGACGTTGCTGGTATCGTAT
GGACAAAGTGGCCTACATCAATGCGGTCTATTTAGTGGACTGTTTCTTATATTACATTGTTCCGGTT
GGTGTCTCTATTCCTCTTTATGCTATCATCGGACGGGTTCTCTTCCGAAGTACCATGTCACAAAAT
GGCATTAGGAGAGGTTACGAGGTCGGTTCGAAGGGGAAGGAAAATGGGAACACGACGCGGTTGC
GACTCATGAAGTCGAGCGAAGGCAGTGACGGAAGTAACTCACCAAGACGGTGCAAAGATTCAGG
AAGCACAGCTGTATCATCGAGAAAACAGGTAATAAAGATGCTGGTAATAGTGGTAGCCCTCTTTGG
TATCCTTTGGGCACCTTATCGGATGCTTGTCGTCTTCAACTGGTTCAACACACCATCCAAGCAGTA
CCACAACGAGTGGTTCCTCTTCTTCTGTCGCGCCTGCCTCTATCTGAACAGTGTGGTCAACCCGA
TCCTCTACAACTTCATGTCCATCAAGTTCCGACGGGCCTTCATCAAACTCTGCTCCTGCCGCGGT
GTGGACCGGCGCCACAATCAGTTCACCTGGGTATCTACCAATGACCCTGACAATACGGCCACCAC
CAAGGCCATCCGCATGAGCTCCACTGCGGGCCACTTCGAGTCGATCAGGAAACACTGCGGTCAT
TACAACGCCAATCACAACACGTCAGCTATCTAAACAAAGCGCGC

8.8 *S. purpuratus* embryonic axes

Figure 8.2 Embryonic axes for *S. purpuratus* embryonic and larval stages

Depending on the cell- or tissue-type of interest, images of *S. purpuratus* embryos and larvae are shown from different views. To assist readers in understanding the morphology of the live and fixed samples, the embryonic axes (Animal-Vegetal (A-V), Aboral-Oral (Ab-O) and Left-Right (L-R)) for four keys stages of *S. purpuratus* development (Blastula, Mesenchyme Blastula, Gastrula and Pluteus Larval stages) are shown. For each development stage, the embryonic axis for the lateral view is shown on a cartoon diagram and then the embryonic axes for different views (Lateral View, Oral View, Animal View and Vegetal View) are shown on representative images. At the Blastula and Mesenchyme Blastula stages, there are few morphological features that can be used to identify the embryonic axes, often only the A-V axis is identified by the thickened vegetal plate, small micromeres (dark purple) and ingression of PMCs (red). Only when cell- or tissue- specific probes or antibodies are used (for example the *Sp-PPLN1* probe detected in aboral ectodermal cells of the Mesenchyme Blastula embryo) can additional embryonic axes (Ab-O and L-R) be identified. At Gastrula and Pluteus Larval stages morphological features can be used to identify all embryonic axes. At the Pluteus Larval stage the Animal View (AV) is also referred to as the Apical Organ (AO) OR Abanal View (AbV), and the Vegetal View (VV) is referred to as the Anal View (AnV).

	Blastula	Mesenchyme Blastula
Cartoon Lateral View (LV)	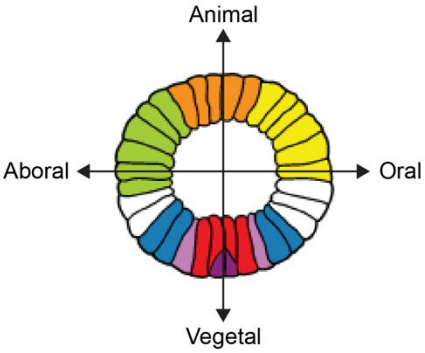	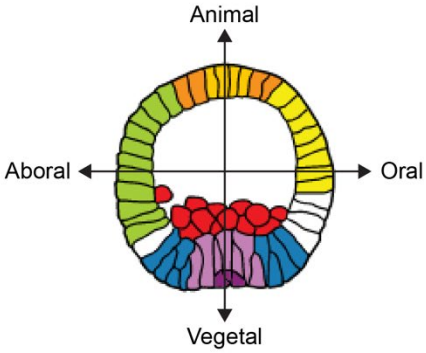
Lateral View (LV)	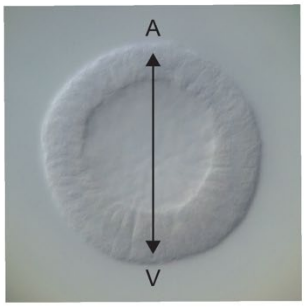	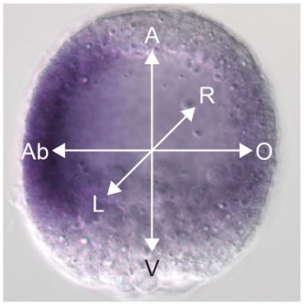
Ventral View (VV)	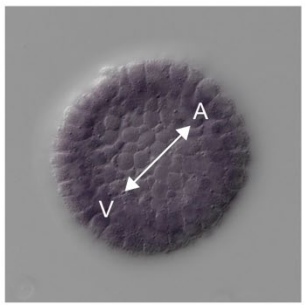	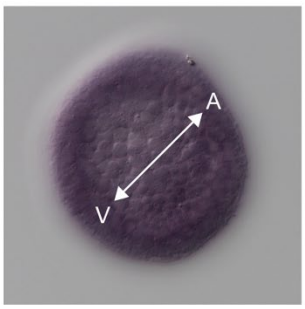

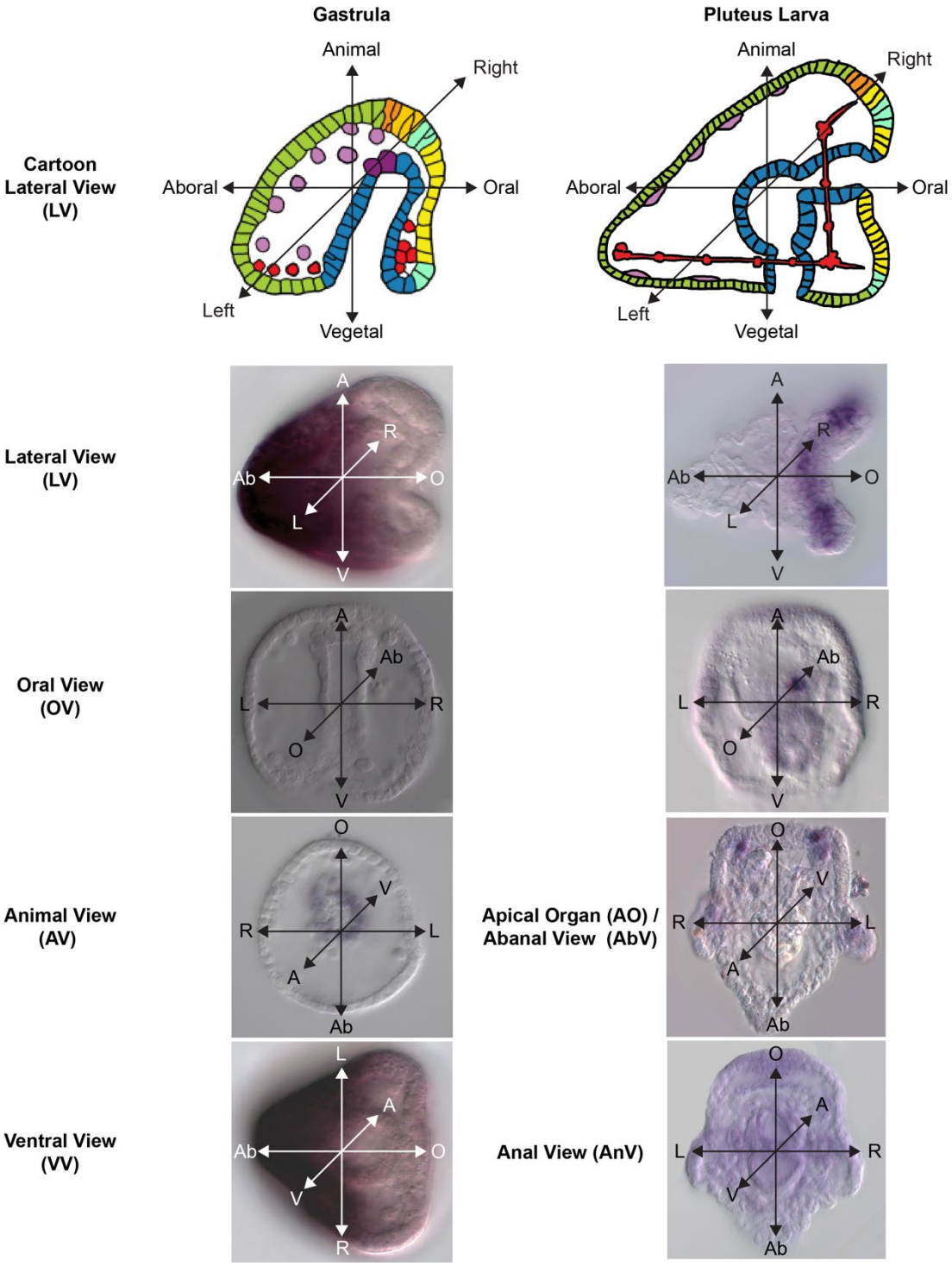
Gastrula
Pluteus Larva
Cartoon Lateral View (LV)
Animal
Right
Aboral
Oral
Left
Vegetal
Lateral View (LV)
Oral View (OV)
Animal View (AV)
Ventral View (VV)
Apical Organ (AO) / Abanal View (AbV)
Anal View (AnV)
A
R
Ab
O
L
V

Table 8.16 Terminal effector identity in pluteus larval neuronal cell types

A summary of terminal effector genes that control cell identity. Neuropeptides, GPCRs and *Sp-SecV* data are from this thesis (also summarized in a diagram Figure 3.16) and neurotransmitter and *Sp-SynB* data were previously published (Bisgrove and Burke, 1987; Burke *et al.,* 2006b).

Family	Terminal effector gene	OD neurons	PO neurons	AO sensory neurons	Lateral ganglion neurons	Mouth neurons 1	Mouth neurons 2	Foregut neurons	Other ciliary band neurons
Membrane trafficking	SynB	1	1	1	?	?	?	?	1
Neurotransmitters	Serotonin	0	0	1	0	0	0	0	0
	Dopamine	0	?	0	0	1	1	0	0
	GABA	0	0	0	0	0	0	1	0
Granin	SecV	0	0	1	1	0	0	0	0
Neuropeptides	Np18	0	0	1	0	0	1	0	0
	AN	0	0	1	1	0	1	0	0
	PPLN2	0	0	1	0	0	1	0	0
	TRH	1	0	0	0	0	0	0	0
	FSALMFa	1	1	0	0	1	0	0	0
	NGFFFa	0	0	0	0	1	0	0	0
	Np20	0	0	0	0	0	0	?	0
	Kp	0	0	0	0	0	0	?	0
	ILP2	0	0	0	0	0	0	1	0
	PPLN1	0	0	0	0	0	0	0	0
GPCRs	TRHR	1	?	0	0	0	0	0	?
	NGFFFaR	1	1	1	1	1	1	1	1

8.9 Published paper

Wood *et al.,* 2018 “Neuropeptidergic Systems in Pluteus Larvae of the Sea Urchin Strongylocentrotus purpuratus: Neurochemical Complexity in a Simple Nervous System”

Chapter 3 is based on this published paper.

frontiers in Endocrinology

ORIGINAL RESEARCH
published: 25 October 2018
doi: 10.3389/fendo.2018.00628

Neuropeptidergic Systems in Pluteus Larvae of the Sea Urchin *Strongylocentrotus purpuratus*: Neurochemical Complexity in a "Simple" Nervous System

Natalie J. Wood[1†], *Teresa Mattiello*[1,2†], *Matthew L. Rowe*[1,3], *Lizzy Ward*[1,4‡], *Margherita Perillo*[2], *Maria Ina Arnone*[2], *Maurice R. Elphick*[3*] and *Paola Oliveri*[1*]

[1] Centre for Life's Origins and Evolution, Research Department of Genetics, Evolution and Environment, University College London, London, United Kingdom, [2] Stazione Zoologica Anton Dohrn, Naples, Italy, [3] School of Biological and Chemical Sciences, Queen Mary University of London, London, United Kingdom, [4] Research Department of Cell and Developmental Biology, University College London, London, United Kingdom

The nervous system of the free-living planktonic larvae of sea urchins is relatively "simple," but sufficiently complex to enable sensing of the environment and control of swimming and feeding behaviors. At the pluteus stage of development, the nervous system comprises a central ganglion of serotonergic neurons located in the apical organ and sensory and motor neurons associated with the ciliary band and the gut. Neuropeptides are key mediators of neuronal signaling in nervous systems but currently little is known about neuropeptidergic systems in sea urchin larvae. Analysis of the genome sequence of the sea urchin *Strongylocentrotus purpuratus* has enabled the identification of 38 genes encoding neuropeptide precursors (NP) in this species. Here we characterize for the first time the expression of nine of these NP genes in *S. purpuratus* larvae, providing a basis for a functional understanding of the neurochemical organization of the larval nervous system. In order to accomplish this we used single and double *in situ* hybridization, coupled with immunohistochemistry, to investigate NP gene expression in comparison with known markers (e.g., the neurotransmitter serotonin). Several sub-populations of cells that express one or more NP genes were identified, which are located in the apica organ, at the base of the arms, around the mouth, in the ciliary band and in the mid- and fore-gut. Furthermore, high levels of cell proliferation were observed in neurogenic territories, consistent with an increase in the number of neuropeptidergic cells at late larval stages. This study has revealed that the sea urchin larval nervous system is far more complex at a neurochemical level than was previously known. Our NP gene expression map provides the basis for future work, aimed at understanding the role of diverse neuropeptides in control of various aspects of embryonic and larval behavior.

Keywords: neuron, co-expression, neuropeptide, echinoderm, embryo, serotonin

OPEN ACCESS

Edited by:
Takayoshi Ubuka,
Monash University Malaysia, Malaysia

Reviewed by:
Pedro Martinez,
University of Barcelona, Spain
Ryota Matsuo,
Fukuoka Women's University, Japan

***Correspondence:**
Paola Oliveri
p.oliveri@ucl.ac.uk
Maurice R. Elphick
m.r.elphick@qmul.ac.uk

[†]These authors have contributed equally to this work

[‡]Present Address:
Lizzy Ward,
Division of Cell Matrix Biology and Regenerative Medicine, School of Biological Sciences, Faculty of Biology, Medicine and Health, University of Manchester, Manchester, United Kingdom

Specialty section:
This article was submitted to Experimental Endocrinology, a section of the journal Frontiers in Endocrinology

Received: *24 July 2018*
Accepted: *02 October 2018*
Published: *25 October 2018*

Citation:
Wood NJ, Mattiello T, Rowe ML, Ward L, Perillo M, Arnone MI, Elphick MR and Oliveri P (2018) Neuropeptidergic Systems in Pluteus Larvae of the Sea Urchin Strongylocentrotus purpuratus: Neurochemical Complexity in a "Simple" Nervous System. Front. Endocrinol. 9:628. doi: 10.3389/fendo.2018.00628

INTRODUCTION

The evolution of neuronal cell types and nervous systems is a hotly debated topic (1, 2), reflecting the diversity in nervous system organization found in animals. Understanding the complexity and organization of neuronal cell types in less studied taxa may help to provide new insights into neural evolution. As invertebrate deuterostomes, the echinoderms (sea urchins, sea stars, brittle stars, sea cucumbers, and feather stars) are a key phylum for evolutionary studies because they "bridge the gap" between the intensely studied vertebrates and protostomian model invertebrates such as *Drosophila* and *C. elegans*.

Echinoderm embryos develop into free-living planktonic larvae equipped with a relatively "simple" nervous system, typified by the sea urchin pluteus larva, that allows them to sense the environment and to control swimming and feeding behaviors. The larval nervous system of sea urchins is thought to be completely independent of the adult nervous system, which develops in the larval rudiment (3). The sea urchin larva, therefore, offers opportunities to observe the complete development and function of a nervous system in a small and tractable organism. The larval nervous system is the "product" of neurogenic processes that have been studied using immunostaining for neural markers and analysis of the expression of pro-neuronal genes, as reviewed in Hinman and Burke (4). However, the diversity of neuronal sub-types in sea urchin larvae has not been characterized in detail.

Neurogenic capacity in the sea urchin embryo is initially present throughout the entire ectoderm, but later it becomes restricted to the anterior neuroectoderm (ANE) and the ciliary band neuroectoderm (CBE), under the control of Wnt-dependent pathways that regulate Nodal and bone morphogenetic protein (BMP) signaling (5). The first neurons, sensory serotonergic neurons, appear in the apical plate at the gastrula stage (48 hours post-fertilization (hpf) in *S. purpuratus*), along with two cells in the oral ectoderm that will develop into the post-oral neurons (6). From here onwards, the nervous system continues to grow and become increasingly complex as the larva increases in size from a four-arm pluteus to an eight-arm competent larva (6–8). Pioneering electron microscopy (EM) studies and more recent use of pan-neural markers (e.g. synaptotagmin) have provided a detailed picture of the number of neurons and the organization of the larval nervous system in the apical organ, which is considered the central nervous system of the larva, whereas the ciliary band and the lateral ganglia are considered the peripheral nervous system (3, 4, 6, 9)]. Populations of neurons, formed from neuro-endoderm precursor cells, have also been identified in the pharynx (10). The identification of sub-populations of larval neurons has thus far been largely restricted to the analysis of the neurotransmitters serotonin, dopamine and GABA (6). In the early four-arm larva, Bisgrove and Burke identified serotonin-positive neurons in apical organ cells, dopamine-positive neurons in the lower lip and post-oral cells, and GABA-positive neurons in the esophagus.

A major class of neuromodulators in the nervous system are neuropeptides, which are ancient intercellular signaling molecules that act through specific G protein-coupled receptors (GPCRs) to mediate neuronal regulation of many physiological and behavioral processes. Neuropeptides are present across the Eumetazoa, suggesting that these ancient molecules play a key role in the function and evolution of nervous systems (11, 12). The first neuropeptides to be identified in echinoderms were the starfish SALMFamides S1 and S2 (13, 14). Using antibodies to S1 and S2, Beer and collaborators produced the first description of a neuropeptidergic component of the larval sea urchin nervous system (8). However, the molecular identity of the immunoreactive molecules was unknown. Sequencing of the sea urchin genome has enabled the identification of genes encoding candidate secreted peptides in *S. purpuratus* (15), including genes encoding two types of SALMFamides - F-type SALMFamides, which have the C-terminal motif Phe-X-Phe-NH_2, and L-type SALMFamides, which like S1 and S2 have the C-terminal motif (Leu/lle)-X-Phe-NH_2 and which are presumably the neuropeptides that are recognized by antibodies to S1 and S2. Other neuropeptide precursor (NP) genes identified in the genome of *S. purpuratus* include genes encoding paralogous precursors of the vasopressin/oxytocin-type neuropeptide echinotocin and the neuropeptide NGFFFamide (15–17). Furthermore, a detailed analysis of cDNAs derived from a radial nerve cDNA library enabled the identification of 20 putative NP genes in *S. purpuratus*, including seven that share sequence similarity with known neuropeptides and 13 that were not found to share sequence similarity with known neuropeptides (18, 19). Six additional putative NP genes were identified in *S. purpuratus*, in parallel with the discovery of homologs in other echinoderms (starfish *Asterias rubens*, brittle stars *Ophionotus victoriae*, *Amphiura filiformis,* and *Ophiopsila aranea*) and also through phylogenomic studies (20–23). Mass spectrometry has also been used to determine the structures of some of the neuropeptides encoded by NP genes in *S. purpuratus* (16, 18, 24, 25). Furthermore, characterization of neuropeptides and neuropeptide receptors in *S. purpuratus* and other echinoderms has provided important insights into the evolution of neuropeptide signaling. For example, discovery of the receptor for the neuropeptide NGFFFamide in *S. purpuratus* facilitated the reconstruction of the common evolutionary history of neuropeptide-S-type signaling in vertebrates and crustacean cardioactive peptide (CCAP)-type signaling in protostomes (16). Secreted peptide signaling molecules have also been identified in association with the larval sea urchin gut. Perillo and Arnone (26) reported specific cells in the anterior region of the gut that express a *Sp-Insulin-like peptide 1* (*Sp-ILP1*) NP gene together with other molecular markers typical of pancreatic exocrine-like cell types. Furthermore, expression of *Sp-ILP1* in the gut is affected by different feeding regimes (26), highlighting an ancient deuterostome role of ILP secreted peptides and the power of echinoderms in helping resolve evolutionary questions. Against this background, there now exists the opportunity to investigate the expression of multiple NP genes in populations of neurons in larval sea urchins, and to correlate findings with existing knowledge of the larval nervous system.

Recently, the first multi-gene analysis of NP gene expression in echinoderm larvae was reported, with mRNA *in situ* hybridization employed to analyse the expression of eight NP genes in the starfish *Asterias rubens* (27). Here we describe the complement of NP genes in the *S. purpuratus* genome, the temporal expression of 31 NP genes and the spatial expression of nine NP genes during larval development of the sea urchin *S. purpuratus,* using Quantitative PCR (QPCR) and mRNA *in situ* hybridization (ISH), respectively. Then having compared the patterns of expression, we have used double-labeling techniques to investigate NP gene expression in comparison with markers for other neurotransmitters (e.g., serotonin). The identification of specific populations of cells, neurons, and gut cells expressing NP genes enriches our understanding of the diversity of neuronal cell types in sea urchin larvae and the complexity of the larval nervous system.

METHODS

Animal Husbandry and Embryonic and Larval Culture

Adult specimens of the purple sea urchin *Strongylocentrotus purpuratus* were obtained from Patrick Leahy (Kerchoff Marine Laboratory, California Institute of Technology, Pasadena, CA, USA) and housed in closed seawater aquaria at University College London and Stazione Zoologica Anton Dohrn of Naples at 14°C. Gametes and embryos were obtained from *S. purpuratus* and cultured as previously described (28). Filtered artificial seawater (FASW; 34.6ppt salinity) containing the antibiotics streptomycin (50 μg/mL) and penicillin (20 U/mL) was used as an alternative to seawater for maintenance of embryos.

Isolation of cDNAs Encoding NPs

Clones of cDNAs encoding NP genes were obtained from an *S. purpuratus* radial nerve arrayed cDNA library (Caltech; LIBEST_019872). Fragments of cDNAs encoding *Sp-Kp*, *Sp-Np20* and *Sp-Nesf* were amplified from cDNA obtained from embryos/larvae at 18, 21, and 27 hpf, and 1-week, and then cloned in a pGEM-T® easy vector system (Promega) according to the manufacturer's instructions. Antisense probes were synthesized after sequencing. Primers and probe information are presented in **Supplementary Table 1**.

In situ Hybridization (ISH)

Embryo and larvae were fixed as previously described (29). For single fluorescent or chromogenic whole-mount ISH, antisense probes were transcribed from isolated cDNA fragments and labeled using 10X DIG RNA labeling mix (Roche). For double fluorescent ISH, digoxigenin-11-UTP (Roche), and Label IT® DNP (Mirus, MIR3800) antisense probes were synthesized, according to the manufacturer's protocol. For both single and double fluorescent ISH experiments, probes were used at a final concentration of 0.03–0.05 ng/μL.

For a detailed ISH procedure, see **Supplementary Material**. Nuclei were stained in 2.5 μg/mL DAPI in PBST. At least three embryos were imaged in detail by confocal microscopy and others by fluorescent microscopy using three-channel fluorescence and DIC images were generated using a Zeiss 510 Meta Light Microscope or a Leica TCS SPE2. Image analysis was done using FIJI and Adobe Photoshop software. A developmental stage that was known not to express a particular gene was used as a negative control. For chromogenic ISH *Sp-FoxA* was used as a positive control as the spatial expression pattern is well characterized across development (30). Single chromogenic ISH was first completed for all genes later analyzed using double fluorescent ISH.

Immunostaining

Embryo and larvae were fixed in 4% paraformaldehyde. Rabbit polyclonal anti-serotonin (Sigma) and mouse anti-acetylated tubulin (Sigma), mouse anti-synaptotagminB (SynB/1E11) (31) were used. Secondary antibodies Alexa 488 goat anti-rabbit, Alexa 633 donkey anti-mouse and Alexa 488 goat anti-mouse (Thermo Scientifics) were used at a dilution of 1:250. For a detailed protocol, see **Supplementary Material**.

EdU Labeling

Larvae at 4 days of development were incubated in ethynyl deoxyuridine (EdU) for 2 h using the Click-iT™ EdU Alexa Fluor™ 555 Imaging Kit (ThermoFisher), according to the manufacturer's instructions (for details see **Supplementary Material**).

Quantitative PCR (QPCR)

Total RNA was isolated from batches of embryos at different stages of development. The RNA was extracted using the RNAeasy Micro Kit (Qiagen), according to the manufacturer's instructions. First-strand cDNA was synthesized using a maximum of 1 μg of total RNA and the iScript™ cDNA synthesis kit (Bio-Rad), as described by the manufacturer. The cDNA was diluted to 2.8 ng/μl and used directly for quantitative PCR (QPCR) analysis. QPCR was conducted as previously described (32) and each sample was run in quadruplicate technical replicas. For QPCR experiments, the data from each cDNA sample (0–72 hpf) were normalized against ubiquitin mRNA levels, which are known to remain relatively constant during development (33–35). cDNA samples from 5 week old larvae and juveniles were normalized against 18S rRNA and compared using relative expression (individual maximum expression). cDNA was substituted with water for negative control experiments. The primers used can be found in **Supplementary Table 2**.

RESULTS

The Complexity of the Neuropeptidome in the Developing Sea Urchin Larvae

To obtain a detailed overview of NP gene expression in the developing nervous system of the sea urchin embryo and larva, we first analyzed *S. purpuratus* genome sequence data to characterize the complexity of the neuropeptidome in this species. Previous studies (18, 20, 21, 24) have identified 34 NP genes belonging to over 20 different families. Of these genes, 14 NPs were found not to share sequence similarity with known NPs from other species (18). The availability of genome

(36) and transcriptome (22, 23) sequence data from other echinoderms enabled the identification of a total of 38 NP genes, including the previously identified genes. The latest version of the *S. purpuratus* genome (Echinobase, v 4.2; http://www.echinobase.org/Echinobase/) was analyzed using newly identified echinoderm NP sequences as queries for BlastP searches and SignalP (http://www.cbs.dtu.dk/services/SignalP-3.0/; (37)) was used to determine the presence of a signal peptide, which is a characteristic feature of neuropeptide precursors and other secreted proteins. This analysis enabled identification of *S. purpuratus* NP genes that have been reported previously as well as the *Sp-Kp* gene. These findings were confirmed independently (22, 23).

Once the complement of NP genes present in the sea urchin genome was established, we studied their temporal expression during the development of the sea urchin nervous system: from the appearance of the first neuronal precursor cells at mesenchyme blastula (24 hpf), through embryonic development to the early larval stage (72 hpf) when several types of neurons are differentiated (6, 9, 38, 39). For this we used the available data from a *S. purpuratus* quantitative developmental transcriptome [http://www.echinobase.org/Echinobase/; (40)]and we also carried out quantitative real-time PCR (QPCR) measurements for all the NP genes not annotated in the latest *S. purpuratus* genome (Echinobase, v4.2), but predicted by NCBI or transcriptome studies. To be directly comparable to the transcriptome data, QPCR time points were chosen only up to end of development (70 hpf). We also studied the expression of 27 NP genes randomly choosen in two postembryonic stages: 5-week-old larvae and the juvenile stage. Generally, NP transcripts are present at very low levels throughout mesenchyme blastula and early gastrula stages (**Figure 1**; **Supplementary Table 3**; **Supplementary Figure 4B**), with the total number of transcripts ranging between 50 and 300 transcripts per embryo. Transcript levels then steadily increase throughout the prism and pluteus stages (48–70 hpf), with the total number of transcripts ranging between 300 and 42,000 transcripts per embryo (**Figure 1**; **Supplementary Table 3**). There are three exceptions to this pattern: (i) The *Sp-Orexin 1* (*Sp-Ox1)* and *Sp-Orexin 2* (*Sp-Ox2)* genes have a high number of transcripts (>300 transcripts per embryo) during mesenchyme blastula or early gastrula stages (**Figure 1B**). (ii) The *Sp-Thyrotropin-releasing hormone* (*Sp-Trh*) gene has a high number of transcripts (>300 transcripts per embryo) during mesenchyme blastula and then has a reduction in expression during gastrula and prism stages, before the number of transcripts increase to 426 transcripts per embryo at 70 hpf (**Figure 1D**). (iii) The *Sp-Somatostatin 1* (*Sp-SS1*) gene has a peak in expression at the mesenchyme blastula stage (>300 transcripts per embryo) followed by a gradual decrease in transcript levels for the remaining embryonic stages (**Figure 1A**). The QPCR data were in agreement with transcriptome data available from Echinobase (40) (**Supplementary Figure 4**). Furthermore, these two techniques quantified gene expression in different batches of embryos, thus validating the overall expression trends and the absolute number of transcripts per embryos. The increase in expression at 48 hpf, seen in most NP genes (23 out of 31), is coincident with the onset of neural differentiation (31, 41). Increase in expression at subsequent stages might reflect the increased number of neuronal precursors/neurons expressing NP genes.

Of the 38 NP genes identified in the sea urchin genome, 27 were analyzed for their expression: at a very early larval stage (70 hpf) when only the larval nervous system is present, which was used as a positive control; at the juvenile stage, when only the adult nervous system is present; and a late larval stage at 5 weeks (advanced rudiment stage), when both the larval and juvenile nervous systems are present. The temporal patterns of NP gene expression during post-embryonic stages are quite diverse (**Supplementary Figure 5**). The majority of NP genes, including *Sp-Trh* and *Sp-L-SALMFa*, among others (**Supplementary Figures 5A,C**), exhibit an increase in relative expression as larval development proceeds, with maximum expression at the juvenile stage. This trend correlates with an increase in the number of neuronal cells during the larval and juvenile stages. One group of NP genes, including *Sp-AN*, [containing an N-terminal alanine (A)/asparagine (N) (AN) motif] (**Supplementary Figure 5B**) also show a maximum expression at the juvenile stage, but have higher expression at the end of embryogenesis (70 hpf, pluteus stage) than in the 5 week old larvae. In contrast, *Sp-Glycoprotein hormone 3* (*Sp- GPH3)* and *Sp-Eclosion hormone 2 (Sp-EH2)* (**Supplementary Figure 5D**) have higher expression at the end of embryogenesis (70hpf, pluteus stage) and then their expression steadily decreases in later larval and juvenile stages. Collectively, these data show that NP gene expression largely correlates with the development of the sea urchin larval nervous system and the increased complexity in post-embryonic stages, suggesting that these genes are expressed in neurons.

Early Expression of Neuropeptide Precursors in Neural Precursor Cells

To obtain more detailed insights into the expression of NP genes in the developing nervous system of sea urchin larvae, we next examined their spatial expression patterns at the gastrula stage (48 hpf) when the first neuronal precursor cells are detected and an overall increase in NP gene expression is evident (**Figure 1**) (39, 41). Two populations of neural precursor cells are present by the 48 hpf gastrula stage: serotonergic neural precursors in the apical plate and post-oral precursors in the oral ectoderm (39, 41). Double fluorescent ISH analysis was undertaken to determine the expression pattern of eight NP genes in the larval nervous system, relative to serotonin, a marker for apical plate neurons, and synaptotagmin, a pan-neuronal marker. In this work, for simplicity, we will refer to **neurons** if the co-expression of a NP gene with one or both of these two neuronal markers is reported, while we will refer to **neuron-like** cells, when the position and the shape of the NP-positive cell(s) is consistent with previously described neurons, but no expression with a neuronal differentiation marker is reported.

Out of the eight probes tested, five show clear staining at this stage, consistent with QPCR and transcriptome data at 48 hpf (**Figures 1C,D**; **Supplementary Table 3**). Indeed only

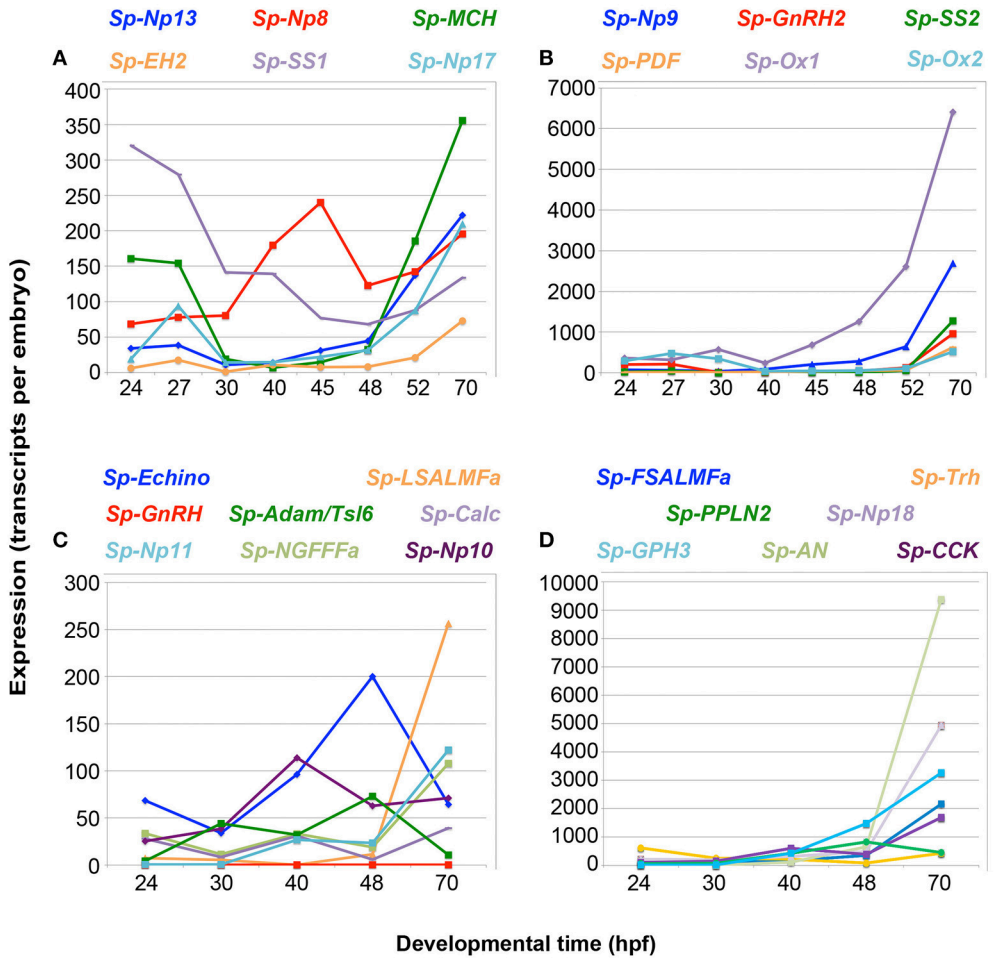

FIGURE 1 | Quantitative PCR (QPCR) reveals that NP gene expression correlates with an increase in the complexity of the larval nervous system. NP gene expression (transcripts per embryo) is shown from the appearance of the first neuronal precursor cells at mesenchyme blastula stage [24 h post-fertilization (hpf)], through embryonic development to the early larval stage (70 hpf) when several types of neurons are differentiated. An increase in expression is seen for most NP genes from 48 to 70 hpf, when the first serotonergic neurons differentiate. The line graphs depict different levels of gene expression for 27 NP genes, with lower expression in graphs **(A,C)** and higher expression in graphs **(B,D)**. The color of the NP gene name above each graph reflects the line color in the corresponding graph.

the genes with expression levels above 300 transcripts/embryo are detected by ISH at this stage (**Supplementary Table 3**), while *Sp-Trh* and *Sp-Kisspeptin* (*Sp-Kp*), which both have <100 transcripts/embryo at 48 hpf, are not detected by this technique (data not shown). Transcriptome data available from Echinobase reveals that the *Sp-Kp* and *Sp-Np20* NP genes have low relative expression at 48 hpf (**Supplementary Figure 3**). This limit of detection is also supported by the absence of staining in WMISH experiments conducted with the same probes at stages with little or no expression (negative controls) and it is in agreement with published data (40). The exception is the *Sp-NGFFFamide* (*Sp-NGFFFa*) NP gene which has only 19 transcripts per embryo by our QPCR analysis and 47 transcripts per embryo by transcriptome quantification [**Figure 1D**; **Supplementary Table 3**; **Supplementary Figure 4**; (40)] and shows expression detectable by ISH. This could be explained by an under estimation of the level of expression of these quantitative techniques, or the highly localized expression in just a few cells.

Co-expression of three NP genes, *Sp-AN*, *Sp-Np18,* and *Sp-Pedal peptide-like neuropeptide 2* (*Sp-PPLN2),* is detected in two cells in the apical domain, which are also positive for serotonin and *Sp-SynB* (**Figures 2A–C**; **Supplementary Figure 6A**), whereas expression of the *Sp-FSALMFamide* (*Sp-FSALMFa*), *Sp-NGFFFa* and *Sp-PPLN2* NP genes is detected in one or two cells bilaterally arrayed in the oral ectoderm, in a position consistent with post-oral neuronal precursors [**Figures 2A,D,E**; (39, 41)].

In summary, spatial expression data revealed that various NP genes are expressed before the neurons are fully differentiated. Furthermore, distinct combinations of NP genes are co-expressed in specific populations of neuronal precursors at the gastrula stage.

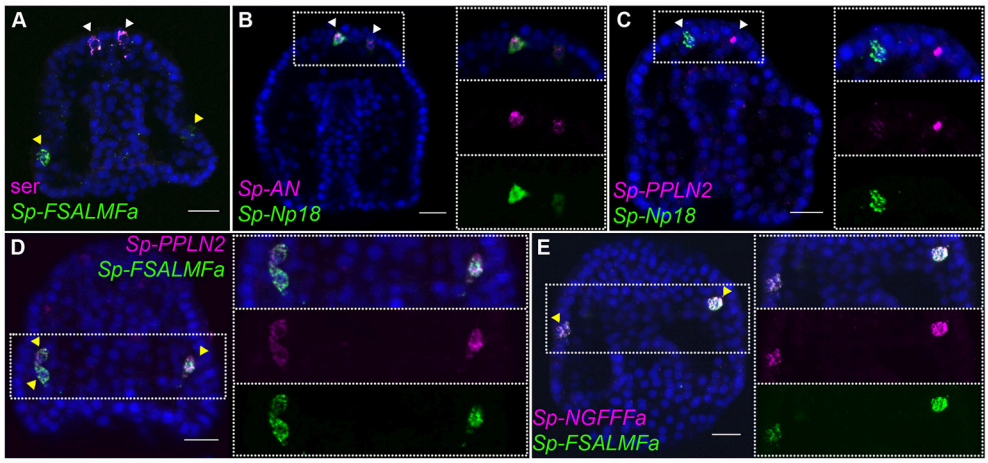

FIGURE 2 | Expression of NP genes in the apical plate and post-oral neuron-like precursor cells of the gastrula embryo. Merged and single channel confocal images of 48 hpf embryos labeled using double fluorescent ISH are shown. **(A)** Expression of serotonin and *Sp-FSALMFa* highlights two populations present at 48 hpf, the serotonergic (white arrowheads) and post-oral (yellow arrowheads) neuron-like precursor cells, respectively. **(B,C)** Co-expression of three NP genes in the apical plate sensory precursors. **(D,E)** Co-expression of three NP genes in two-three post-oral neuron-like precursor cells. Bottom-left/Top-right corner indicates the probe or antibody used. Dotted white boxes highlight the magnified region shown to the right. Scale bars: 20 μm.

Expression of Neuropeptide Precursors in the Larval Nervous System

During post-gastrula development the number of neurons and neuronal precursor cells increases dramatically, consistent with the high level of proliferation detected by EdU staining, mainly in neurogenic tissues of the pluteus stage, such as the apical organ, ciliary band, and oral ectoderm (41). At the end of development, the simple nervous system of the pluteus larva (72 hpf) is composed of 40–50 neurons, which have differentiated in the apical organ [containing eight to nine serotonergic neurons (42)], ciliary band, lateral ganglia, post-oral, lip, and gut regions (6, 9, 10, 15, 38, 39, 41). The number of neurons and the complexity of the nervous system continues to increase during postembryonic larval development (6), consistent with the large number of proliferative cells identified by EdU staining located almost exclusively in neurogenic tissues of the pluteus (**Figure 3A**). To gain more detailed insights into the expression of NP genes relative to the known neuronal structures and the complexity of the larval nervous system, we studied the spatial expression of genes that have high levels of expression (**Figure 1**) using single probe chromogenic and double probe fluorescent ISH. Furthermore, we analyzed the expression of an ortholog of the human *SecretograninV (7B2L)* gene, *Sp-SecV*, a marker of neuroendocrine cells (43).

Central and Peripheral Nervous System

At the pluteus stage (72 hpf), the number of serotonergic neurons in the apical organ has increased and will continue to increase during larval development, consistent with the findings from EdU labeling, which illustrate a high rate of cell proliferation in the apical plate, ciliary band, lip, and foregut tissues (41) (**Figure 3A**). Furthermore, EdU labeling coupled with immunohistochemistry with the pan-neuronal marker SynB [1E11; (31)] revealed that neurons in the ciliary band are both mitotic ($SynB^+/Edu^+$) or post-mitotic ($SynB^+/EdU$) (**Supplementary Figure 6B**). This is important to explain the different number of NP gene expressing cells identified in pluteus larvae.

The apical organ, considered the central nervous system of the sea urchin larva, consists of two types of serotonergic neurons: bottle shaped primary sensory neurons associated with long cilia of the apical tuft (**Figure 3B**) and small interconnected serotonergic neurons that form a ganglion (**Figure 3**), along with support cells (4). Fluorescent ISH (FISH) analysis of the expression of neuroendocrine marker *Sp-SecV* only labeled the primary sensory serotonergic neurons in the apical organ (**Figure 3C**), indicating a neuroendocrine role for these cells. Furthermore, various probe combinations in FISH experiments revealed that the *Sp-Np18*, *Sp-AN*, and *Sp-PPLN2* NP genes continue to be co-expressed in 2-5 cells with a morphology typical of sensory neurons that also express *Sp-SecV* and serotonin (**Figures 3C–G**; **Supplementary Figure 6H**). On either side, next to the serotonergic central neuronal system, two neuron-like cells at the base the oral distal arms (**Figures 3H–J**) were identified by the expression of the *Sp-Trh* and *Sp-FSALMFa* NP genes (**Figures 3H–J**). These cells are associated with the ciliary band and send projections toward the apical ganglion and their fibers intermingle with the fibers of the serotonergic interneurons, which is most clearly seen in 1-week old larvae (**Supplementary Figure 6C**). The cells do not express serotonin or *Sp-SecV*, suggesting they are a different population of neurons that communicate with the serotonergic central ganglion.

The peripheral nervous system of the sea urchin larva is composed of neurons in the ciliary band, post-oral neurons, and lateral ganglion. *Sp-FSALMFa* is expressed in two single cells in the ciliary band at the base of the post-oral arms

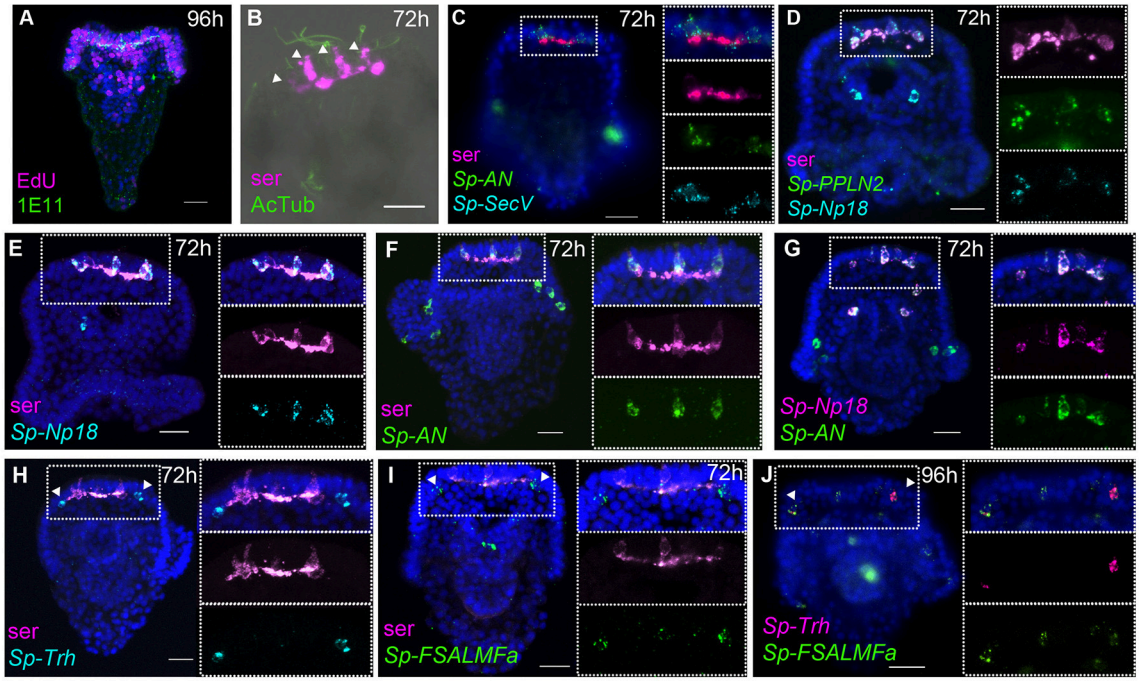

FIGURE 3 | Expression of NP genes in the apical plate serotonergic neurons and ciliary band neuron-like cells. Merged and single channel confocal images of pluteus larvae labeled using double fluorescent ISH and immunohistochemistry are shown. **(A)** EdU-and SynB (1E11) labeling experiment showing a high rate of cell proliferation in the neurogenic territories (apical plate and ciliary band, lip and foregut). **(B,C)** Labeling of the larval nervous system using antibodies to serotonin and to acetylated tubulin (AcTub) and using *Sp-SecV* ISH. **(B–G)** NP gene expression in the apical plate serotonergic neurons. **(H–J)** *Sp-Trh* and *Sp-FSALMFa* co-expressed in the ciliary band, at the base of the oral distal arms, adjacent to the apical plate. Bottom-left corner indicates the probe or antibody used. Top-right corner indicates the larval stage in hours' post-fertilization; bottom-left corner indicates the probe or antibody used. Dotted white boxes highlight the magnified region shown to the right. Scale bars: 20 μm.

(**Supplementary Figure 6D**). The location is consistent with the expression of *Sp-FSALMFa* NP gene in the presumptive dopaminergic post-oral neurons (6, 44), and with the expression of this gene at the gastrula stage (**Figures 2A,D,E**). Interestingly, the expression of no other NP gene analyzed in this study was detected in these cells at the pluteus stage (**Supplementary Figures 6A–E**). The lateral ganglion neurons consist of two clusters of two-three neurons on the left and right side of the larva (3, 15) and are associated with the ciliary band. This population of neurons has been described as dopaminergic (6). At 72 hpf the hybridization signal associated with *Sp-SecV* and *Sp-AN* NP expression is specifically revealed in two groups of cells bilaterally arranged in a manner that resembles the lateral ganglia neurons (**Figures 4A,B**). The expression of *Sp-SecV* and *Sp-AN* NP gene suggests a neurosecretory role of these cells. Finally, a probe against the *Sp-Nesf* NP gene shows a diffuse signal in the ciliary band, not restricted to any particular subpopulation of cells (**Supplementary Figure 6E**).

Taken together our data revealed that several NP genes are expressed in single or groups of cells and identifies several neuronal and neuronal-like sub-types in both the central and peripheral nervous system of sea urchin larvae. Each subtype of cells is characterized by a specific combination of expressed NP genes.

Mouth and Gut Cell Systems

Several neurons expressing GABA or dopamine have been described in the mouth and in the esophagus of the sea urchin larva (6). At the early pluteus stage (72 hpf), approximately four to six neurons appear in the lip and these have been described as dopaminergic neurons (6), while a few neurons of endodermal origin differentiate in the esophagus (10). Single and double whole-mount ISH experiments show that *Sp-FSALMFa*, *Sp-NGFFFa, Sp-Np18*, *Sp-PPLN2,* and *Sp-AN* NP genes are all expressed in two to four isolated and bilaterally arranged cells around the mouth (**Figures 5A–F**) in the 72 hpf larvae. Although there is variation in the number of cells and the degree of co-expression of NP genes around the mouth, signals associated with *Sp-PPLN2, Sp-AN,* and *Sp-Np18* expression are largely co-localized in two to four cells in the larval lip, as they are co-localized in the apical domain (**Figures 3D,G**, **5A,B**). The *Sp-FSALMFa* and *Sp-NGFFFa* NP genes are mostly co-expressed in another population of cells around the mouth of the larva (**Figure 5D**), which rarely coincide with the cells expressing *Sp-PPLN2* (**Figure 5C**). Even the cells expressing the *Sp-FSALMFa* and *Sp-NGFFFa* NP genes around the mouth show a high degree of variability of co-expression (compare **Figure 5D** with **Figure 5E** and **Supplementary Table 4**). The number and type of neurons around the mouth increase in the larva, as well

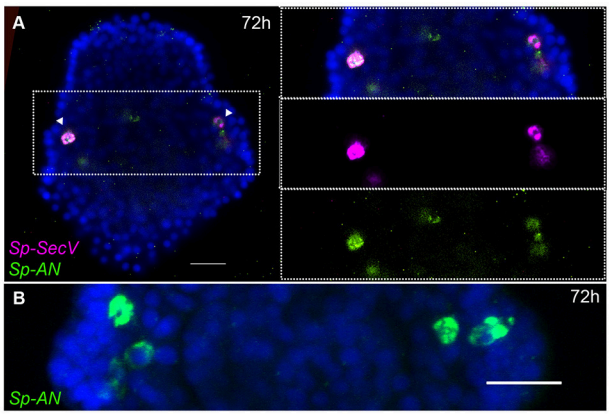

FIGURE 4 | Expression of NP genes in two clusters of two-three lateral ganglia neuron-like cells. Merged confocal images of pluteus larvae labeled using single and double FISH are shown. **(A)** *Sp-SecV* and *Sp-AN* NP gene expression in lateral ganglia neuron-like cells. **(B)** Magnification of *Sp-AN* NP gene expression in the lateral ganglia neuron-like cells. Bottom-left corner indicates the probe used. Top-right corner indicates the larval stage in hours' post-fertilization. Dotted white boxes highlight the magnified region shown to the right. Scale bars: 20 μm.

as the number of NP gene-expressing cells, as shown by the expression of *Sp-FSALMFa* (**Figure 5F**) in 1 week old larvae, which is consistent with the EdU staining shown in **Figure 3A**. To better understand the variation in NP genes expressed in various cells we analyzed several ($N > 7$, with exception of *Sp-FSALMFa* and *Sp-Np18* NP genes where $N > 2$) larvae in each experiment. **Supplementary Table 4** summarizes the results and shows that the single cells surrounding the mouth never express *Sp-Trh* or *Sp-SecV* (**Figures 3C,H**). *Four* double fluorescent ISH experiments are analyzed in the 72 hpf and 1 week old larval mouth. The co-expression of *Sp-Np18* with either *Sp-AN* or *Sp-PPLN2* shows a high degree of variability when several embryos are analyzed. In contrast, *Sp-FSALMFa* with *Sp-NGFFFa* fluorescent ISH experiments generally show a more consistent co-expression in the cells around the mouth (**Supplementary Table 4**).

Two to three GABAnergic neurons have been identified in the early pluteus foregut (6). Chromogenic ISH hybridization reveals the expression of two NP genes, *Sp-Np20,* and *Sp-Kp*, with a diffuse pattern in the foregut and not only in individual neurons (**Figures 5G,H**). Indeed, these two NP genes are also expressed in the entire midgut. Later in larval development, at 1 week-old, *Sp-FSALMFa*, *Sp-NGFFFa* (**Supplementary Figures 6F,G**) and *Sp-PPLN2* are co-expressed in two to three isolated cells in the midgut (**Figures 5F,I**). There is also variability in the expression of *Sp-FSALMFa* and *Sp-NGFFFa*—compare **Supplementary Figure 6F** with **Supplementary Figure 6G**. None of the other NP genes analyzed in this study were detected in these cells, not even in 1-week old larvae (**Figure 5I**; **Supplementary Figure 6C**). Neuronal cell types have so far not been described to be in association with the midgut, however other cell types with endocrine/digestive function are known to be present in the midgut (45). Our results reveal a similar situation as described for the central and peripheral nervous systems: several cell populations are identified by specific NP gene expression signatures. Furthermore, our fluorescent ISH analysis has revealed a variable pattern of NP gene expression in the neuron-like cells around the mouth and the presence of a specific population of cells in the midgut.

DISCUSSION

The early sea urchin larval nervous system is composed of 40–50 neurons, characterized by the expression of specific neurotransmitters (5, 6). Understanding the diversity and distribution of NP gene expression is essential for identification of the diverse neuronal subtypes in echinoderm larval nervous systems. Here we report the first multi-gene analysis of NP gene expression in larvae of a sea urchin species (**Figure 6**). *S. purpuratus* has at least 38 NP genes and expression of almost all NP genes analyzed here was detected in the developing sea urchin or larval stages. Spatial expression patterns of nine NP genes were revealed in the early pluteus larvae and the expression of five NP genes was detected already in the gastrula. The existence of diverse neuronal subtypes in the echinoderm larval nervous system has been revealed by immunocytochemical analysis of the neurotransmitters serotonin, dopamine and GABA (6). Localization of NP gene expression, as reported here, has revealed distinct sub-populations of neuropeptidergic cells, demonstrating that the sea urchin larval nervous system is far more complex than previously thought (**Figure 6**). Furthermore, QPCR analysis detected the expression of a few NP genes prior to the gastrula stage, suggesting that these signaling molecules also have a role during the early development of the sea urchin embryos. Our spatial analysis shows no evidence of localization to known neuronal precursor cells (data not shown) and therefore NPs may be involved in signaling associated with non-neural developmental processes.

Neuronal co-expression of multiple neuropeptide precursor genes and/or neuropeptides derived from different precursor proteins has been reported in a variety of taxa including, for example, cnidarians (46), molluscs (47), annelids (48), and vertebrates (49). Here we report this property of neuropeptide signaling systems for the first time in the larval nervous system of an echinoderm. Thus, our results show that consistent co-expression signatures were found for two different combinations of NP genes: (i) *Sp-FSALMFa* and *Sp-NGFFFa* and (ii) *Sp-AN*, *Sp-PPLN2,* and *Sp-Np18*. The former two genes are initially co-expressed in cells that resemble the precursor of postoral neurons in the gastrula and then in neuron-like cells around the mouth, while the latter three genes are expressed in the primary sensory neurons located in the apical organ. Their co-expression starts as soon as the precursor sensory cells express the serotonin marker at the gastrula stage (48 hpf) and then remains in these cells in all subsequent stages analyzed here. The same three genes are also co-expressed in neuron-like cells around the mouth at the pluteus stage (**Supplementary Table 4**). These co-expression signatures suggest similar regulation of these

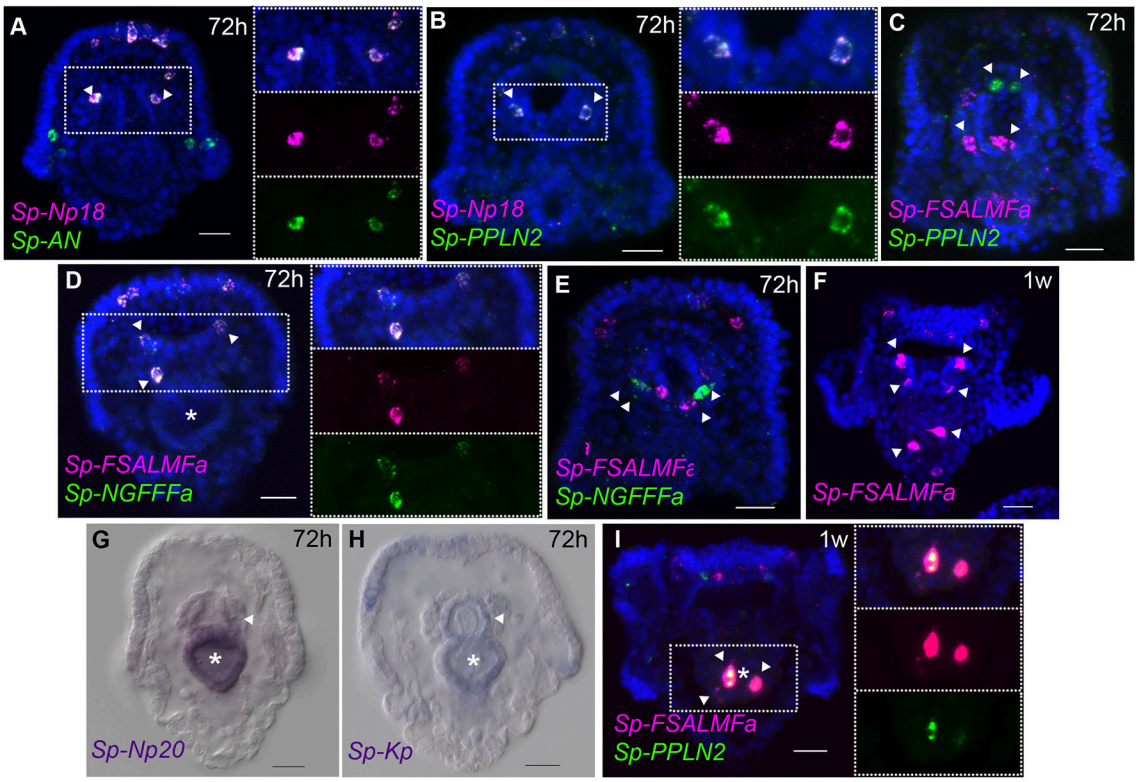

FIGURE 5 | Expression of NP genes in the mouth and gut cell systems. **(A–F,I)** Merged and single channel confocal images of pluteus larvae labeled using single and double fluorescent ISH. **(G,H)** Chromogenic whole-mount ISH of *Sp-Np20* and *Sp-Kp* NP gene expression in pluteus larvae. Bottom-left corner indicates the probe used. Top-right corner indicates the larval stage in hours or weeks post-fertilization. Dotted white boxes highlight the magnified region shown to the right. Asterisk indicates the midgut. Scale bars: 20 μm.

genes, possibly by a combination of transcription factors, which may work as terminal selector genes to control the differentiated state of post-mitotic neurons (50). Recent studies have shown the role of several transcription factors and signaling molecules in determining the identity of large sub-populations of neurons [for review see (4)], including, for example, *Ac-sc* regulation of the development of serotonergic neurons (51). However, none of the data so far published can explain the highly restricted expression pattern of NP genes that we have identified in this study. This suggests that more studies need to be done to investigate the regulation of neuronal subtypes. Accordingly, a paper by Perillo and collaborators in this issue (52), identifies for the first time a precise combination of transcription factors (*Lox, Brn1/2/4,* and *Islet-1*) that is consistent with the restricted expression of the *Sp-AN* NP gene in the lateral ganglia neurons.

A few distinct sub-populations of neurons and neuron-like cells have been identified in this study, which have not been described before. For instance, the isolated cells associated with the ciliary bands, at the base of the arms, the oral distal and the post-oral, all express *Sp-FSALMFa* while the oral distal cells also express *Sp-Trh*. Perillo et al. (52) also identified *Sp-AN* NP gene expression in the post-oral neurons. Two types of neurons have been recently described in the ciliary bands of sea urchin larvae: cholinergic neurons are widely distributed throughout this structure and dopaminergic neurons are concentrated in a post-oral location (51). Adams and collaborators identified the post-oral dopaminergic neurons to be involved in controlling arm length in response to food (53). *Sp-FSALMFa* is expressed in four cells, one at the base of each arm and so neuropeptides encoded by the *Sp-FSALMFa* gene may likewise have a role in controlling arm length or arm growth, possibly in response to an environmental signal. In comparison, the *Sp-Trh* NP gene is expressed only in two cells and these are at the base of the oral distal arms. Interestingly, TRH is known to have a role in growth in vertebrates and in the nematode *C. elegans* (54–56) and therefore it is plausible to hypothesize that TRH-type peptides may also affect arm growth in *S. purpuratus* larvae, perhaps asymmetrically. Furthermore, *Sp-Opsin3.2* has been detected in two cells, adjacent to the apical plate (57), in a similar position to the *Sp-Trh* positive cells. Double fluorescent ISH will reveal if these two genes are co-expressed, suggesting a light-sensing role of the cells expressing the *Sp-Trh* NP gene. Taken together, these observations suggest that neuropeptides expressed in the cells at the base of the arms may be involved in controlling arm length in response to food and/or light.

Neuropeptides derived from precursor proteins are packed in dense core vesicles (DCV). The maturation and release of functional neuropeptides is regulated by several factors, among

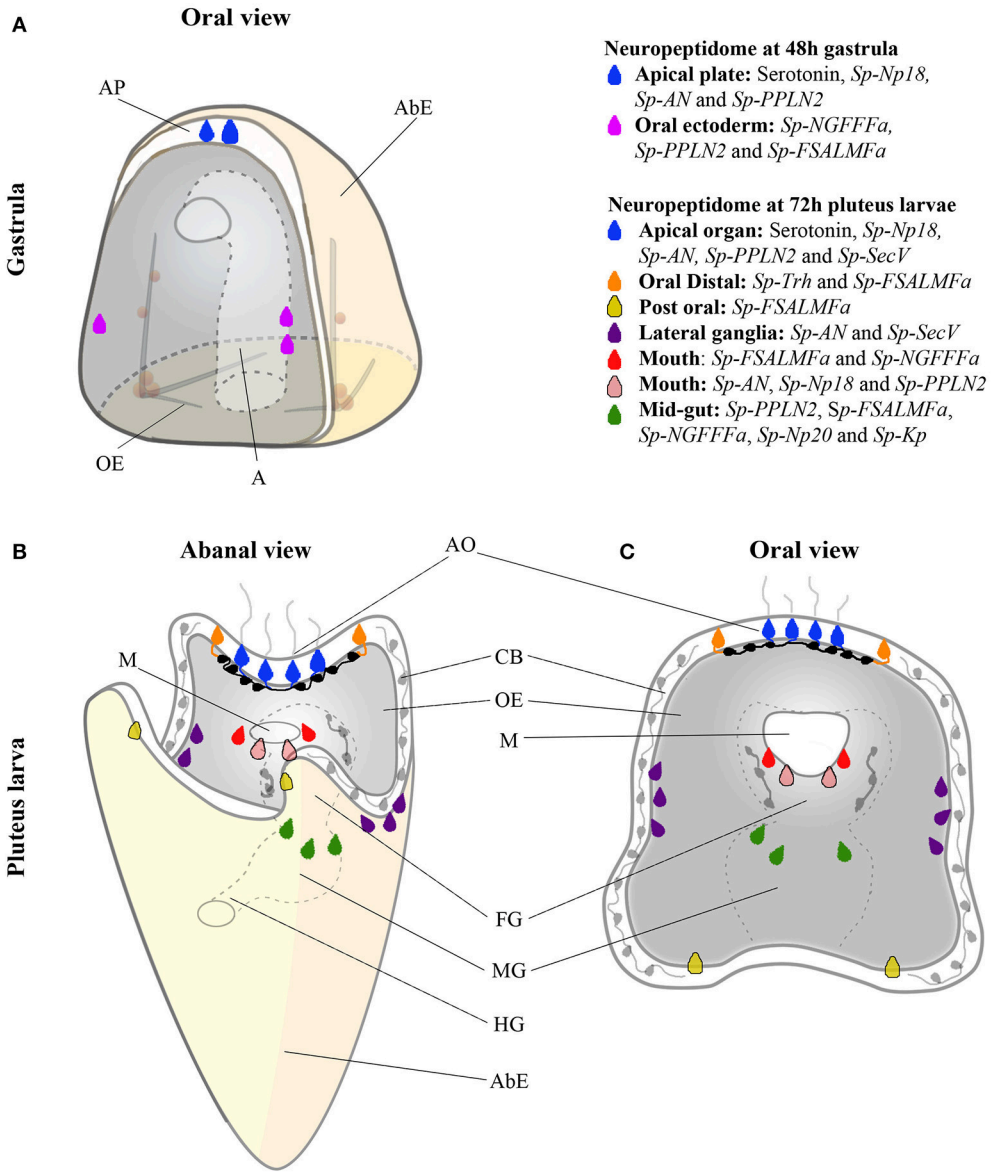

FIGURE 6 | Color coded cartoon map showing various combinations of NP gene and *Sp-SecV* expression at single cell resolution in the sea urchin at the gastrula stage and in pluteus larvae. **(A)** NP gene expression in two populations of cells at the gastrula stage. Serotonergic neuronal precursor cells (blue) and post-oral neuronal-like precursor cells in the oral ectoderm (magenta). **(B,C)** NP gene expression in eight different neuronal and presumed neuronal populations in the larval nervous system, shown from abanal and an oral view. Sensory serotonergic neurons (blue), lateral ganglion neurons (purple), presumed oral distal neurons (orange), presumed post-oral neurons (yellow), presumed lip neurons (red and pink), and mid-gut exocrine-like cells (dark green). Black and gray neurons (in foregut, ciliary band, and serotonergic interneurons) have been identified in previous studies but do not express any of the NP genes examined in this study. Abbreviated labels refers to the following, AP (Apical Plate), AbE (Aboral Ectoderm), OE (Oral Ectoderm), A (Archenteron), AO (Apical Organ), CB (Ciliary band), M (Mouth), FG (Foregut), MG (Midgut) and HG (Hindgut).

them the family of chromogranin/secretogranin proteins, which play a key role in the regulated secretory pathway (58). In this study we show the expression of *Sp-SecV,* previously identified in proteomic studies (25), specifically in the primary sensory neurons of the apical organ and in the pancreatic-like neurons of the lateral ganglia (52). Interestingly, human Secretogranin V (SGC5, Gene ID 6447) is specifically expressed in the brain, pancreas, adrenal and stomach, highlighting the conservation in deuterostomes of an ancient neuroendocrine molecular pathway.

Our quantitative analysis of the whole-mount ISH results (**Supplementary Tables 4, 5**) reveals variability of the NP gene combinations expressed during development and larval stages, suggesting a constant modulation of the expression of NP genes, in response to both developmental and possibly environmental cues. For instance, the post-oral neuron precursors seem to

exhibit a transient expression of NP genes between 48 and 72 hpf: at 48 hpf, they specifically express *Sp-FSALMFa*, *Sp-NGFFFa* and *Sp-PPLN2,* whereas only the *Sp-FSALMFa* precursor gene is expressed at 72hpf. A similar combination of NP genes is expressed in the lip and midgut cells at 72 hpf, suggesting that these newly formed neuronal or secretory cells might acquire a similar NP gene signature. Therefore, the two initial post-oral neuron-like cells (**Figure 6**) either turn off *Sp-NGFFFa* and *Sp-PPLN2* NP genes, or the cells at 72 hpf are actually newly differentiated, consistent with the constant production of neurons identified by EdU labeling (**Figure 3A**) (41). Cell-tracing experiments have not been performed on those cells, and so despite previous literature referring to both sets of neurons as "post-oral" we cannot be sure these are the same cells. In both situations, our analysis identifies a highly dynamic regulation of NP genes in the larvae, as already discussed for neuron-like cells associated with the mouth (**Supplementary Table 3**).

Figure 6 summarizes the expression of NP genes at the gastrula (48 hpf) and pluteus (72 hpf) stages. At the gastrula stage the first NPs genes are expressed in a pattern consistent with the appearance of post-mitotic precursors of serotonergic neurons and post-oral neurons (41). Furthermore, two distinct combinations of NP genes are expressed in each population of cells consistent with these neuronal precursors, overlapping only by the expression of *Sp-PPLN2,* suggesting they have diverse functions. In the early pluteus (72 hpf) the number of NP genes expressed (**Figure 1**) largely correlates with the increased complexity of the nervous and secretory systems in the apical plate, ciliary band, lateral ganglia, lip, and foregut. At the early pluteus stage, the NP genes are expressed in a pattern suggesting the apical plate and lip each have at least two distinct sub-populations of neurons and neuron-like cells. The expression of *Sp-FSALMFa* in the post-oral dopaminergic neuron-like cells and *Sp-FSALMFa* and *Sp-Trh* in the oral distal neuron-like cells identifies two distinct populations of cells, separate from rest of the ciliary band. Taken together, we propose the following populations of neuronal and/or secretory cells in the sea urchin pluteus (**Figure 6**): the apical plate is divided into: (1) primary sensory serotonergic neurons that express various NP genes and *Sp-SecV*; and (2) serotonergic interneurons that do not express any of the NP genes investigated; (3) the oral distal neuron-like cells in the ciliary band, adjacent to the apical plate, characterized by the expression of *Sp-Trh* and *Sp-FSALMFa* NP genes; (4) two post-oral neuron-like cells associated with the ciliary band, at the bases of the post-oral arms, identified by the expression of *Sp-FSALMFa*; (5) other ciliary band neurons generally identified by SynB neuronal markers (5) and expressing *Sp-Nesf*; (6) lateral ganglia neurons associated with the left and right ciliary bands and expressing *Sp-AN* (52) and *Sp-SecV* NP genes; (7) the larval neuron-like cells associated with the mouth, which are divided into at least two sub-types, each with a distinct combination of NP gene expression; (8) foregut GABAergic neurons described by Bisgrove and Burke (6) not expressing any of the NP genes studied here; and (9) midgut cells expressing NP genes.

In conclusion, our study has revealed that the sea urchin larval nervous system is far more complex at a neurochemical level than was previously known. Our NP gene expression map provides the basis for future work, aimed at understanding the regulation and function of diverse neuropeptides in the sea urchin larval nervous system.

AUTHOR CONTRIBUTIONS

PO and MRE originally conceived the study. NJW, TM, LW, MLR and MP contributed to the acquisition of data. NJW, TM, MIA, MRE and PO contributed to the interpretation of the data. NJW and PO wrote the first draft of the manuscript. All authors contributed to manuscript revision, read and approved the submitted version.

FUNDING

NJW was supported by the Biotechnology and Biological Sciences Research Council [grant number BB/M009513/1]. TM was supported by a FEBS short-term fellowship. The study received support from the UCL Centre for Ecology and Evolution to PO and MRE.

ACKNOWLEDGMENTS

The authors would like to thank Evgeniya Anishchenko for kindly providing the cartoon of the sea urchin embryo and larvae. We thank Pat Leahy (KML, Caltech, Pasadena, CA) for providing adult *S. purpuratus* and Wendy Hart (UCL) and Davide Caramiello (SZN) for animal maintenance. We thank Robert Burke for the gift of the 1E11 antibody used in **Figure 3** and **Supplementary Figure 6**. We would also like to thank Farrell MacKenzie for the cloning and probe synthesis of *Sp-Np20* and assistance with QPCR experiments.

SUPPLEMENTARY MATERIAL

The Supplementary Material for this article can be found online at: https://www.frontiersin.org/articles/10.3389/fendo.2018.00628/full#supplementary-material

REFERENCES

1. Arendt D, Tosches MA, Marlow H. From nerve net to nerve ring, nerve cord and brain - evolution of the nervous system. *Nat Rev Neurosci.* (2016) 17:61–72. doi: 10.1038/nrn.2015.15
2. Martín-Durán JM, Pang K, Børve A, Lê HS, Furu A, Cannon JT, et al. Convergent evolution of bilaterian nerve cords. *Nature* (2018) 553:45–50. doi: 10.1038/nature25030
3. Burke RD, Osborne L, Wang D, Murabe N, Yaguchi S, Nakajima Y. Neuron-specific expression of a synaptotagmin gene in the sea urchin *Strongylocentrotus purpuratus*. *J Comp Neurol.* (2006) 496:244–51. doi: 10.1002/cne.20939
4. Hinman VF, Burke RD. Embryonic neurogenesis in echinoderms. *Wiley Interdiscip Rev Dev Biol.* (2018) e316:1–15. doi: 10.1002/wdev.316

5. Angerer LM, Yaguchi S, Angerer RC, Burke RD. The evolution of nervous system patterning : insights from sea urchin development. *Development* (2011) 138:3613–23. doi: 10.1242/dev.058172
6. Bisgrove BW, Burke RD. Development of the nervous system of the pluteus larva of *Strongylocentrotus droebachiensis*. *Cell Tissue Res.* (1987) 248:335–43. doi: 10.1007/BF00218200
7. Smith MM, Smith LC, Cameron RA, Urry LA. The larval stages of the sea urchin, *Strongylocentrotus purpuratus*. *J Morphol.* (2008) 269:713–33. doi: 10.1002/jmor.10618
8. Beer A, Moss C, Thorndyke M. Development of serotonin-like and SALMFamide-like immunoreactivity in the nervous system of the sea urchin *Psammechinus miliaris*. *Biol Bull.* (2001) 200:268–80. doi: 10.2307/1543509
9. Burke RD. The structure of the nervous system of the pluteus larva of *Strongylocentrotus purpuratus*. *Cell Tissue Res.* (1978) 191:233–47. doi: 10.1007/BF00222422
10. Wei Z, Angerer RC, Angerer LM. Direct development of neurons within foregut endoderm of sea urchin embryos. *Proc Natl Acad Sci USA*. (2011) 108:9143–7. doi: 10.1073/pnas.1018513108
11. Elphick MR, Mirabeau O, Larhammar D. Evolution of neuropeptide signalling systems. *J Exp Biol.* (2018) 221:1–15. doi: 10.1242/jeb.151092
12. Jékely G, Melzer S, Beets I, Kadow ICG, Koene J, Haddad S, et al. The long and the short of it – a perspective on peptidergic regulation of circuits and behaviour. *J Exp Biol.* (2018) 221:jeb166710. doi: 10.1242/jeb.166710
13. Elphick MR, Reeve JR Jr, Burke RD, Thorndyke MC. Isolation of the neuropeptide SALMFamide-1 from starfish using a new antiserum. *Peptides* (1991) 12:455–9. doi: 10.1016/0196-9781(91)90083-2
14. Elphick MR, Price DA, Lee TD, Thorndyke MC. The SALMFamides : a new family of neuropeptides isolated from an echinoderm. *Proc R Soc Lond.* (1991) 243:121–7. doi: 10.1098/rspb.1991.0020
15. Burke RD, Angerer LM, Elphick MR, Humphrey GW, Yaguchi S, Kiyama T, et al. A genomic view of the sea urchin nervous system. *Dev Biol.* (2006) 300:434–60. doi: 10.1016/j.ydbio.2006.08.007
16. Semmens DC, Beets I, Rowe ML, Blowes LM, Oliveri P, Elphick MR. Discovery of sea urchin NGFFFamide receptor unites a bilaterian neuropeptide family. *Open Biol.* (2015) 5:150030. doi: 10.1098/rsob.150030
17. Elphick MR, Rowe ML. NGFFFamide and echinotocin: structurally unrelated myoactive neuropeptides derived from neurophysin-containing precursors in sea urchins. *J Exp Biol.* (2009) 212:1067–77. doi: 10.1242/jeb.027599
18. Rowe ML, Elphick MR. The neuropeptide transcriptome of a model echinoderm, the sea urchin *Strongylocentrotus purpuratus*. *Gen Comp Endocrinol.* (2012) 179:331–44. doi: 10.1016/j.ygcen.2012.09.009
19. Rowe ML, Elphick MR. Discovery of a second SALMFamide gene in the sea urchin *Strongylocentrotus purpuratus* reveals that L-type and F-type SALMFamide neuropeptides coexist in an echinoderm species. *Mar Genomics* (2010) 3:91–7. doi: 10.1016/j.margen.2010.08.003
20. Mirabeau O, Joly J. Molecular evolution of peptidergic signaling systems in bilaterians. *Proc. Acad Natl USA*. (2013). 110:E2028–37. doi: 10.1073/pnas.1219956110
21. Jékely G. Global view of the evolution and diversity of metazoan neuropeptide signaling. *Proc Natl Acad Sci USA*. (2013) 110:8702–7. doi: 10.1073/pnas.1221833110
22. Zandawala M, Moghul I, Alfonso Yanez Guerra L, Delroisse J, Abylkassimova N, Hugall AF, et al. Discovery of novel representatives of bilaterian neuropeptide families and reconstruction of neuropeptide precursor evolution in ophiuroid echinoderms. *Open Biol.* (2017) 7:1–20. doi: 10.1098/rsob.170129
23. Semmens DC, Mirabeau O, Moghul I, Pancholi MR, Wurm Y, Elphick MR. Transcriptomic identification of starfish neuropeptide precursors yields new insights into neuropeptide evolution. *Open Biol.* (2016) 6:150224. doi: 10.1098/rsob.150224
24. Menschaert G, Vandekerckhove TTM, Baggerman G, Landuyt B, Sweedler JV, Schoofs L, et al. A hybrid , de novo based , genome-wide database search approach applied to the sea urchin neuropeptidome. *J Proteome Res.* (2010) 9:990–6. doi: 10.1021/pr900885k
25. Monroe EB, Annangudi SP, Wadhams AA, Richmond TA, Yang N, Southey BR, et al. Exploring the sea urchin neuropeptide landscape by mass spectrometry. *J Am Soc Mass Spectrom*. (2018) 29:923–34. doi: 10.1007/s13361-018-1898-x
26. Perillo M, Arnone MI. Characterization of insulin-like peptides (ILPs) in the sea urchin *Strongylocentrotus purpuratus*: insights on the evolution of the insulin family. *Gen Comp Endocrinol.* (2014) 205:68–79. doi: 10.1016/j.ygcen.2014.06.014
27. Mayorova TD, Tian S, Cai W, Semmens DC, Odekunle EA, Zandawala M, et al. Localization of neuropeptide gene expression in larvae of an echinoderm, the starfish *Asterias rubens*. *Front Neurosci.* (2016) 10:553. doi: 10.3389/fnins.2016.00553
28. Leahy PS. Laboratory culture of *Strongylocentrotus purpuratus* adults, embryos, and larvae. *Methods Cell Biol.* (1986) 27:1–13.
29. Minokawa T, Rast JP, Arenas-mena C, Franco CB, Davidson EH. Expression patterns of four different regulatory genes that function during sea urchin development. *Gene Expr Patterns* (2004) 4:449–56. doi: 10.1016/j.modgep.2004.01.009
30. Oliveri P, Walton KD, Davidson EH, McClay DR. Repression of mesodermal fate by foxa , a key endoderm regulator of the sea urchin embryo. *Development* (2006) 133:4173–81. doi: 10.1242/dev.02577
31. Nakajima Y, Kaneko H, Murray G, Burke RD. Divergent patterns of neural development in larval echinoids and asteroids. *Evol Dev.* (2004) 6:95–104. doi: 10.1111/j.1525-142X.2004.04011.x
32. Rast JP, Amore G, Calestani C, Livi CB, Ransick A, Davidson EH. Recovery of developmentally defined gene sets from high-density cDNA macroarrays. *Dev Biol.* (2000) 228:270–86. doi: 10.1006/dbio.2000.9941
33. Nemer M, Rondinelli E, Infante D, Infante AA. Polyubiquitin RNA characteristics and conditional induction in sea urchin embryos. *Dev Biol.* (1991) 145:255–65. doi: 10.1016/0012-1606(91)90124-L
34. Oliveri P, Davidson EH. Gene regulatory network analysis in sea urchin embryos. *Methods Cell Biol.* (2004) 74:775–94. doi: 10.1016/S0091-679X(04)74032-7
35. Ransick A, Rast JP, Minokawa T, Calestani C, Davidson EH. New early zygotic regulators expressed in endomesoderm of sea urchin embryos discovered by differential array hybridization. *Dev Biol.* (2002) 246:132–47. doi: 10.1006/dbio.2002.0607
36. Hall MR, Kocot KM, Baughman KW, Fernandez-Valverde SL, Gauthier MEA, Hatleberg WL, et al. The crown-of-thorns starfish genome as a guide for biocontrol of this coral reef pest. *Nature* (2017) 544:231–4. doi: 10.1038/nature22033
37. Bendtsen JD, Nielsen H, Heijne G, von Heijne G, Brunak S. Improved prediction of signal peptides — signalP 3.0. *J Mol Biol.* (2004) 340:783–95. doi: 10.1016/j.jmb.2004.05.028
38. Bisgrove BW, Burke RD. Development of serotonergic neurons in embryos of the sea urchin, *Strongylocentrotus purpuratus*. *Dev Growth Differ.* (1986) 28:569–74. doi: 10.1111/j.1440-169X.1986.00569.x
39. Mellott DO, Thisdelle J, Burke RD. Notch signaling patterns neurogenic ectoderm and regulates the asymmetric division of neural progenitors in sea urchin embryos. *Development* (2017) 144:3602–11. doi: 10.1242/dev.151720
40. Tu Q, Cameron RA, Davidson EH. Quantitative developmental transcriptomes of the sea urchin *Strongylocentrotus purpuratus*. *Dev Biol.* (2014) 385:160–7. doi: 10.1016/j.ydbio.2013.11.019
41. Garner S, Zysk I, Byrne G, Kramer M, Moller D, Taylor V, et al. Neurogenesis in sea urchin embryos and the diversity of deuterostome neurogenic mechanisms. *Development* (2016) 143:286–97. doi: 10.1242/dev.124503
42. Byrne M, Nakajima Y, Chee FC, Burke RD. Apical organs in echinoderm larvae: insights into larval evolution in the Ambulacraria. *Evol Dev.* (2007) 9:432–45. doi: 10.1111/j.1525-142X.2007.00189.x
43. Bartolomucci A, Possenti R, Mahata SK, Fischer-Colbrie R, Loh YP, Salton SRJ. The extended granin family: structure, function, and biomedical implications. *Endocr Rev.* (2011) 32:755–97. doi: 10.1210/er.2010-0027
44. Burke RD, Moller DJ, Krupke OA, Taylor VJ. Sea urchin neural development and the metazoan paradigm of neurogenesis. *Genesis* (2014) 52:208–21. doi: 10.1002/dvg.22750
45. Perillo M, Wang YJ, Leach SD, Arnone MI. A pancreatic exocrine-like cell regulatory circuit operating in the upper stomach of the sea urchin *Strongylocentrotus purpuratus* larva. *BMC Evol Biol.* (2016) 16:117. doi: 10.1186/s12862-016-0686-0

46. Hansen GN, Williamson M, Grimmelikhuijzen CJP. A new case of neuropeptide coexpression (RGamide and LWamides) in Hydra, found by whole-mount, two-color double-labeling in situ hybridization. *Cell Tissue Res.* (2002) 308:157–65. doi: 10.1007/s00441-002-0534-y
47. De Lange RPJ, Van Golen FA, Van Minnen J. Diversity in cell specific co-expression of four neuropeptide genes involved in control of male copulation behaviour in *Lymnaea stagnalis*. *Neuroscience* (1997) 78:289–99. doi: 10.1016/S0306-4522(96)00576-3
48. Williams EA, Verasztó C, Jasek S, Conzelmann M, Shahidi R, Bauknecht P, et al. Synaptic and peptidergic connectome of a neurosecretory center in the annelid brain. *Elife* (2017) 6:1–22. doi: 10.7554/eLife.26349
49. Herget U, Ryu S. Coexpression analysis of nine neuropeptides in the neurosecretory preoptic area of larval zebrafish. *Front Neuroanat.* (2015) 9:2. doi: 10.3389/fnana.2015.00002
50. Hobert O. A map of terminal regulators of neuronal identity in *Caenorhabditis elegans*. *Wiley Interdiscip Rev Dev Biol.* (2016) 5:474–98. doi: 10.1002/wdev.233
51. Slota LA, McClay DR. Identification of neural transcription factors required for the differentiation of three neuronal subtypes in the sea urchin embryo. *Dev Biol.* (2018) 435:138–49. doi: 10.1016/j.ydbio.2017.12.015
52. Perillo M, Paganos P, Cocurullo M, Mattiello T, Oliveri P, Arnone MI. New neuronal subtypes with a "pre-pancreatic" signature in the sea urchin *Stongylocentrotus purpuratus*. *Front Endocrinol.* (in press) doi: 10.3389/fendo.2018.00650
53. Adams DK, Sewell MA, Angerer RC, Angerer LM. Rapid adaptation to food availability by a dopamine-mediated morphogenetic response. *Nat Commun.* (2011) 2:592. doi: 10.1038/ncomms1603
54. Duncan Bassett JH, Williams GR. Role of thyroid hormones in skeletal development and bone maintenance. *Endocr Rev.* (2016) 37:135–87. doi: 10.1210/er.2015-1106
55. Galas L, Raoult E, Tonon MC, Okada R, Jenks BG, Castaño JP, et al. TRH acts as a multifunctional hypophysiotropic factor in vertebrates. *Gen Comp Endocrinol.* (2009) 164:40–50. doi: 10.1016/j.ygcen.2009.05.003
56. Sinay EV, Mirabeau O, Depuydt G, Van Hiel MB, Peymen K, Watteyne J, et al. Evolutionarily conserved TRH neuropeptide pathway regulates growth in *Caenorhabditis elegans*. *Proc Natl Acad Sci USA.* (2017) 114:4065–74. doi: 10.1073/pnas.1617392114
57. Valero-gracia A, Petrone L, Oliveri P, Nilsson D-E, Arnone MI. Non-directional photoreceptors in the pluteus of *Strongylocentrotus purpuratus*. *Front Ecol Evol.* (2016) 4:127. doi: 10.3389/fevo.2016.00127
58. Taupenot L, Harper KL, O'Connor DT. The chromogranin–secretogranin family. *N Engl J Med.* (2003) 348:1134–49. doi: 10.1056/NEJMra021405

Conflict of Interest Statement: The authors declare that the research was conducted in the absence of any commercial or financial relationships that could be construed as a potential conflict of interest.